# DISCLAIMER NOTICE

THIS DOCUMENT IS BEST
QUALITY AVAILABLE. THE COPY
FURNISHED TO DTIC CONTAINED
A SIGNIFICANT NUMBER OF
PAGES WHICH DO NOT
REPRODUCE LEGIBLY.

Two-Phase Flow Instrumentation Review
Group Meeting; Proceedings of Meeting Held at
Silver Spring, Maryland on January 13-14, 1977

Nuclear Regulatory Commission, Washington, D.C.

| Accesion For | |
|---|---|
| NTIS CRA&I | ☑ |
| DTIC TAB | ☐ |
| Unannounced | ☐ |
| Justification | |
| By | |
| Distribution / | |
| Availability Codes | |
| Dist | Avail and / or Special |
| A-1 | |

Mar 78

**4. TITLE AND SUBTITLE** *(Add Volume No., if appropriate)*

Proceedings of 1977 Two Phase Flow Instrumentation Review Group Meeting

2. *(Leave blank)*

3. RECIPIENT'S ACCESSION NO.

**7. AUTHOR(S)**

Y. Y. Hsu (editor)

| 5. DATE REPORT COMPLETED | |
|---|---|
| MONTH | YEAR |
| September | 1977 |

**9. PERFORMING ORGANIZATION NAME AND MAILING ADDRESS** *(Include Zip Code)*

Reactor Safety Research
Office of Nuclear Regulatory Research
U.S. Nuclear Regulatory Commission
Washington, D.C. 20555

| DATE REPORT ISSUED | |
|---|---|
| MONTH | YEAR |
| March | 1978 |

6. *(Leave blank)*

8. *(Leave blank)*

**12. SPONSORING ORGANIZATION NAME AND MAILING ADDRESS** *(Include Zip Code)*

Same as 9. above.

10. PROJECT/TASK/WORK UNIT NO.

11. CONTRACT NO.

**13. TYPE OF REPORT**

Meeting Proceedings

PERIOD COVERED *(Inclusive dates)*

February 1976 - February 1977

**15. SUPPLEMENTARY NOTES**

14. *(Leave blank)*

**16. ABSTRACT** *(200 words or less)*

This report contains the progressed made by various NRC sponsored programs on two phase flow instrumentation. The topics discussed by the contributors are:

ORNL - Flow interaction with drag body; use of dispersers, flow modeling for DDT; adaptive cross correlation technique, advanced spool piece development.

RPI - Development of IR-probe, Z-probe, RF-probe, X-ray standard;

BNL - Derivative of constitutive equations, construction test facility and optical probe

SUNY - Stoney Brook-- Use of laser doppler effect to measure velocity and size distribution of droplets in air water flow,

INEL - Performance of DDT spool piece, turbine model analysis, upgrade of DDT, rake design and pilot tube data, full flow drag screen, transit time study, nuclear hardened densitometer.

MPR - Survey of calibration facilities.

**17. KEY WORDS AND DOCUMENT ANALYSIS**          17a. DESCRIPTORS

Two phase flow instrumentation
Drag Dise - Turbine
Spool piece
Densitometer/local probes

**17b. IDENTIFIERS/OPEN-ENDED TERMS**

**18. AVAILABILITY STATEMENT**

Unlimited availability.

| 19. SECURITY CLASS *(This report)* | 21. NO. OF PAGES |
|---|---|
| | 261 |
| 20. SECURITY CLASS *(This page)* | 22. PRICE |
| | PCA 12-A01 |

# TWO-PHASE FLOW INSTRUMENTATION
# REVIEW GROUP MEETING

## Proceedings of Meeting
## January 13-14, 1977

Y. Y. Hsu, Editor

## Foreword

On January 13-14, 1977 an Instrumentation Meeting was held in the
Silver Spring, Maryland offices of the U.S. Nuclear Regulatory
Commission.

In the meeting, the R/D progress of two-phase flow instrumentation made
by various NRC contractors was reported. An informal survey of the
state-of-art was made by experts in the field. Since many request were
made for copies of the proceedings of the meeting, it was decided that
the Meeting Minutes and the contractors' reports shoul  be published in
the form of a NUREG report for public dissemination.

> Yih-yun Hsu, Chairman
> Instrumentation Review Group
> Systems Engineering Branch
> Division of Reactor Safaty Research
> U.S. Nuclear Regulatory Commission

## MEETING MINUTES

## TWO-PHASE FLOW INSTRUMENTATION REVIEW GROUP

By

Y. Y. Hsu, USNRC

Date: January 13-14, 1977

Place: Room 150, Willste Building, USNRC

Attendees: See Attachment 1

Agenda: See Attachment 2

A full text of proceedings will be published as an NRC report in the near future. A summary is given below.

I. Progress Reports by NRC Contractors (January 13, AM)

1. ORNL, J. Sheppard - subjects reported are:

    a. Effect of drag body on flow pattern.
    b. Improvements of drag disk signal by the disperser screen.
    c. Test results using drag screen.
    d. Testing of ionization chamber as a detector.
    e. Modeling of turbine meter dynamic.
    f. Adaptive cross-correlation algorithm.
    g. Interpretation of flow measurements from spool piece.

2. RPI, R. Lahey - subjects reported are:

    a. Steam-air content measurements with I.R. technique - analysis and test facilities.
    b. Novel techniques
       (1) test facilities and electronics,
       (2) x-ray standard,
       (3) exploratory tests with I.R., R.F. and impedence probes.

3. BNL, O. C. Jones

   a. Description of test facility and probe.
   b. Present status of development of local optical probes.

4. SUNY Stoney Brook, R. Lee - reported development of Laser-Doppler anemonety, including:

   a. Operating principles and difficulties.
   b. Proposed scheme to determine number density of particles as function of velocity and particle size.
   c. Description of electronic package.
   d. Calibration method.
   e. Experimental data to demonstrate the feasibility of the method.

5. INEL, EG&G Staff

   a. DTT and densitometer in LOFT - R. Wesley
      (1) description of system,
      (2) uncertainty analysis,
      (3) results from LOFT tests,
      (4) comparison of density measurements from DTT and from $\gamma$-densitometer.
   b. Turbine model analysis - L. Goodrich
      (1) description of various models,
      (2) voltage vs free field velocity curves from WCL,
      (3) comparison of velocities of liquid and vapor based upon various model vs the true mass flux. Proposed "volumetric theory" model is shown to be more accurate than the Aya or Rouhani models.
   c. Upgraded drag disc turbine separate effects tests - R. Bearden
      (1) test results of bearing life,
      (2) description of single bearing and compound bearing turbine,
      (3) summary of single-phase tests of prototype DTT,
      (4) scope of model development at RPI,
      (5) development eddy current sensor.
   d. Rake design and pitot-tube data - R. Bearden and S. Banerjee
      (1) description of location and design requirement of 3-DTT rake for LOFT application,

         (2)  pitot tube rake developed by McMaster University,

         (3)  sample results of using pitot tube rake to measure two-phase flow.

   e.  Full flow drag screen - J. Colson, J. R. Fincke (presented by A. Arave)

         (1)  principle of drag on a blunt body discussed,

         (2)  present drag screen design (3-lever arm),

         (3)  air-water test results on round-wire screen (over a wide range of void fraction, capable to detect flow pattern).

   f.  Transit time flow meter - G. Lassahn

         (1)  discussion of error associated with transit time flow meter,

         (2)  presentation of calculated delay time as function of averaging time,

         (3)  presentation of sample signal correlation using thermocouples.

   g.  Nuclear hardened densitometer - A. Stephens

         (1)  present setup for testing in Adv. Testing Reactor,

         (2)  methods of removing background radiation

            (a)  shielding,

            (b)  background subtraction (in both digital and analog modes),

         (3)  chordal average density statistical error position and energy dependent.

II.  State-of-Art Review (January 13, PM)

   1.  Local probes - J. M. Delhaye, Grenoble

      a.  Theoretical prerequisites for local probe measurements were discussed, including

         (1)  speed of displacement of moving interface,

         (2)  phase density function,

         (3)  instantaneous space-averaging,

         (4)  local, time-averaging,

         (5)  commutativity of averaging operators.

      b.  Survey of recent work on local probes

         (1)  electrical probes - recent work at Karlsruhe was discussed,

         (2)  Laser-Doppler velocimetry - papers presented at LDA-symposium (including those by Durst and Zare and by Delhaye), at Osaka University and in AIChE Journal were discussed,

v

(3) hot film anemometry - work by Remke, Bremhorst
and Gilmore, and Lyon were discussed,

(4) film thickness measurements capabilities and
limitations of impedence probe and x-ray technique
were discussed,

(5) optical probe - current work at England and at
Grenoble (CENG and AID) were discussed. At Grenoble,
studies are being carried out on threshold adjustment;
on in-bundle void measurements; and on monofibre
probes for droplet flow.

2. Radioactive beams - S. Banerjee, McMaster University

Current work on attenuation and scattering methods were
discussed. Particular attention was given to multi-beam
γ-ray and to neutron scattering (by B&W, French and McMaster).
The neutron scattering technique is a promising technique for
density measurement, since it is independent of flow pattern.
Only difficulty is the low counting rate, thus not very good
for fast transient.

3. Drag body, turbine and other impact devices - L. Davis,
Measurement Inc. The presentation includes:

a. Parameters to be measured and sensor requirements.
b. Current sensors used.
c. Methods of combining sensor readings for flow parameters.
d. Current development to improve sensor - work is being
done at Semiscale, LOFT, Germany ("True Flow Meter"),
Battelle, M.I. and GE.
e. Check list for considerations for sensor applications.

4. Tracer techniques - P. Kehler, ANL
The presentation includes:

a. Outline of NRC-ANL tracer technique program.
b. Discussion of basic principles.
c. Lists of γ-emitting tracers for gas; for liquid;
commercially available radioisotope milking systems;
elements easily activated by thermal neutrons; and
those activated by fast neutrons.

5. Novel techniques - P. Griffith, MIT

a. Unresolved thermal-hydraulic measurements needs were
listed as:

(1)  code verification - subchannel void and flow
                         rate; channel or pipe void and flow rate,
                    (2)  diagnostic measurements - flow behavior in upper
                         and lower plena and subchannel flow distribution
                         in core.
          b.  Novel techniques to be used:
                    (1)  flow measurements
                         (a)  nuclear magnetic resonance (no disturbance
                              but need flow modeling),
                         (b)  Laser-Doppler anemomety (non-disturbing and
                              quick response, need clear line of sights,
                              may be good for reflood, but not very suitable
                              for integral tests).
                    (2)  void fraction
                         (a)  x-ray (flow regime dependent)
                         (b)  impedence device (flow regime dependent but
                              with good transient response)
                         (c)  acoustic method (flow regime and quality
                              dependent).
                    (3)  diagnostic
                         (a)  Storz lense (good viewing angle, needs light,
                              not good for high temperature, good diagnostic
                              tool).
          c.  Conclusion
                    (1)  none of the novel devices is really readily useful.
                         Impedence probe and Storz lense are worthwhile
                         development,
                    (2)  meanwhile, drag body-turbine, $\gamma$-densitometer is
                         still a good tool for pipe flow measurement,
                    (3)  for plena flow behavior, photographic methods are
                         the only ones that are useful.


III.  Open Discussions (January 14, AM)

      1.  Tracer technique -

          Participants were concerned about the following difficulties
          involved in tracer measurements:

          a.  Diffusion and spread of tracer.
          b.  Injection method.
          c.  Length of transient time vs transit time.
          d.  Presence of tracer material affecting other instrumentation.
          e.  Number and location of detectors.
          f.  Need of bench tests.

P. Kehler answered some of the concerns, such as a, b, c, and e, and took note of the various cautions.

Pertinent references produced are:

(1) P. Kehler, ANL-CT-76-17.
(2) Gopal, M.Sc. Thesis, Penn State Univ., 1967 .n N[16] flow meter.
(3) D. Rowe, BNWL-371-Pt. 3, 1969.
(4) Quant's work.
(5) McMaster's work.

2. Measurements of $\Delta P$ diametrically across core barrel - (brought up by W. Hodges, NRR)

Range of interest 200 psi, in 1 millisecond. This high frequency fluctuations are difficult to measure. Piezo-electric transducers were used in Semiscale but the potting deteriorates at 600°F. Diaphram is too thick for response. Strain gauge on the core barrel was proposed as one possible answer. It may need cooling to eliminate thermal effect. Brockett and Davis offered to help Hodges.

3. Transit time

Last year, INEL reported some inconclusive results based upon cross-correlation of thermocouple signatures. Raptis of ANL suggested that a more sophisticated approach is that of input-response function (Reference, Raptis - ANL-CT-76-39). The consensus is that while cross-correlation method should be continuously studied, people should also look into input-response function method.

IV. Two-Phase Flow Calibration (January 14, late AM, all PM)

1. State-of-art review - M. Stanley, INEL

   a. Statement of problems
      (1) definition of calibration,
      (2) parameters that can be measured,
      (3) parameters that are difficult to measure.
   b. Survey of existing facilities
      (1) Karlsruhe loop,
      (2) Cise loop,
      (3) WCL loop,

(4) French loops,
        (5) INEL steady state loop,
        (6) INEL transient flow.

        Characteristics and measurement capability of each
        facility was given.
    c.  Calibration methods currently used at INEL for Semiscale
        and LOFT was described.
    d.  Recommendations
        (1) establish a universal standard,
        (2) establish repeatable conditions,
        (3) for phase velocity, use tracer techrique and
            local probes,
        (4) for flow regime, use multibeam γ-densitometers
            and local probes,
        (5) for density distribution use multibeam γ-densitometer.

2.  Survey of facilities for two-phase instrumentation testing -
    H. Estrada, MPR

    Presentation includes:

    a.  Categories of testing
        (1) conventional calibration tests - to determine "meter
            factors" in each single phase,
        (2) prototype calibration - test in two-phase flow in
            conjunction with other related instrumentation to
            arrive at a set of flow parameters with the help
            of proper modeling.  This is the "calibration"
            generally referred in two-phase flow measurements
            community,
        (3) mechanical development and proof testing,
        (4) scaling tests,
        (5) transient tests.
    b.  Facility requirements
        (1) conventional calibration (metering factors) -
            single phase loops, full flow,
        (2) prototype calibration
            (a) gas-water loop,
            (b) geometry effect,
            (c) scaling.
        (3) proof testing - simulation of full range of conditions
            to test instrumentation survivability.  May be skipped
            if structurally strong.

(4) scaling test - large scaled gas-water system
properly instrumented, with visual observation.
Density ratio must be simulated.

(5) transient test facilities - need a known standard
fast response measuring device.

c. Facility survey
Salient finding is the need of a high-flow high momentum
flux air-water loop.

3. Discussion on standard calibration techniques and reference
instruments.

The discussion on this topic is lively and sometimes
controversial, many times, opposing views were voiced.
The following is a summary drawn up by G. D. Lassahn of
INEL, with additions/corrections made by Y. Y. Hsu.

## Discussion on Standard Calibration Techniques
## and Reference Instruments

### Summary Notes

The discussion addressed the general problem of calibrating instruments
for use in measuring steam-water flow parameters, with particular
attention to establishing a standardized system of calibration for
use throughout the industry.

## General Considerations

Instruments must be calibrated as integrated systems. It is usually
not acceptable to calibrate an instrument separated from its companion
instruments. Effects of environment should be checked. Upstream
flow perturbations and pipe size effects must be realistically
represented.

Reference instruments should perturb the fluid conditions as little
as possible.

There should be redundancy in the reference measurements.

The calibration facility should be readily accessible (physically
close).

x

## Steady State Calibration

<u>Concensus</u>:  Most calibration should be done in gas-water, with occasional checks in steam-water.

<u>Dissenting Opinion</u>:  For some instruments (drag bodies and some transit time flowmeters for example), there are qualitative or quantitative performance differences in steam-water and in gas-water.

<u>Comments</u>:

The main problem with steam-water loops is in knowing exactly what the flow conditions are.  Freon-water loops avoid condensation effects, but turbine bearings do not survive long in freon.

Air-water loops may be more expensive than steam-water loops with similar flow rates, depending on the particular installation.

An operating pressure of about 2.8 MPa (400 psi) in an air-water loop may be sufficient to simulate a 15 MPa (2200 psi) operating pressure in a steam-water loop.

Gas-water loops have the advantage that the gas and liquid flow rates can be measured separately.

There is no mass transfer between the phases in a gas-water loop; this is an advantage in that it simplifies a detailed study of the instrument performance, but it is a disadvantage in that it may give different calibration constants for some instruments (different from steam-water calibrations, due to difference in density ratios).

## Steady State Calibration of Full Flow or Global Measurements

<u>Consensus</u>:  Reference instruments could be a pair of full flow drag screens, for $\rho V^2$ and transit time measurements, a scanning gamma densitometer, for density average and perhaps density profile, and tracers as a backup, to measure either total mass flux or separate phase mass fluxes.

xi

<u>Dissenting Opinion</u>: A drag screen upstream from the test instrument tends to homogenize the flow so that the instrument does not see the full range of flow regimes; a drag screen downstream does not measure the momentum flux incident on the test instrument.

We cannot measure density profiles reliably with presently available scanning gamma densitometer.

Tracers (either injected or neutron activated) are reliable and meaningful global reference measurement, and should be used as the primary standard.

<u>Comments</u>:

Photographic techniques are a powerful tool in at least some applications.

Neutron activation and radioactive tracers are expensive and not universally available.

<u>Steady State Calibration of Local Measurements</u>

<u>Concensus</u>: The reference instruments could be retractable local probes (of unspecified type), checked by photographic techniques. Scanning gamma densitometers might also be useful.

<u>Dissenting Opinion</u>: Most local probes interfere with the flow. Paragraph photographic techniques are not useful in some flow regimes.

Local measurements should be used only as a diagnostic tool; accurate calibration is not necessary.

<u>Comments</u>:

Isokinetic probes do not work well for the gaseous phase, and they perturb the flow too much.

Laser-Doppler shift anemometry is useful in certain restricted flow regimes.

Two-color illumination photographic techniques help overcome the problems usually encountered with standard photographic techniques.

Flash radiography and gamma radiation Fresnel holography might have some potential.

Hot wires might be useful in determining the liquid phase local velocity.

Transit time flowmeters should be useful in local velocity measurements, although they might cause local velocity perturbations.

## Steady State Calibration of Rakes

**Concensus:** The separate probes of a rake can first be calibrated separately but the whole rake assembly must be calibrated with piping and flow conditions which realistically represent the intended application of the rake.

**Dissenting Opinion:** In some opinions, separate free field calibration of the individual probes of a rake is sufficient. But some others believe that the full rake calibration is the only meaningful method.

## Comments:

Full scale, realistic geometry tests are necessary to determine optimum rake geometry.

All flow regimes must be represented in calibrating a rake assembly.

Large rakes are being considered only for LOFT. In LOFT, flow regime effects are not important until the latter part of the blowdown, when the pressure is relatively low. It would be much easier to calibrate the whole rake assembly only at these lower pressures.

## Steady State Calibration Checks in Steam-Water

## Comments:

The total mass flux through the pipe is not affected by phase changes.

The steam and water should be near thermal equilibrium when they are injected into the mixer.

Scaling (pipe size) effects are probably different for steam-water and air-water.

## Transient Calibration

Concensus:  The major purpose of studying the transient response of an instrument is to know the magnitude of the error of the instrument readings (as calibrated in steady state) in transient flow.

It is very difficult to create a known fast transient in steam-water flow.  Because of this difficulty, transient performance experiments should be done in single-phase fluids or perhaps in air-water, even though the instrument performance may be different in air-water than in steam-water.  Good mathematical modeling is very important in studying the transient response of an instrument.

Comments:

If the transient response of a device is linear and independent of flow conditions, then the transient response expression can be inverted to obtain the real flow parameter from the instrument readings. Turbine flowmeters, for example, do not meet these requirements.

The only reliable calibration check we have in transient flow is the total mass transport during the transient.

## Scaling or Pipe Size Effects

Concensus:  Some full-flow instruments (a full flow drag screen, for example) must be calibrated in a full-sized pipe.  For free flow rake, full-size pipe is not necessary, provided flow pattern and flow profiles are properly modeled and measured.

To assess pipe size effect which has been observed in several experiments calibration should be done with increasing pipe size until pipe size effect levels off.  Full-sizes pipe and realistic simulation of upstream geometry are necessary in at least some calibration work.  It is important to stress that, whether for calibration or for actual measurement application, the upstream geometry effect should be properly modeled and accounted for.  To achieve this objective, the selection of instruments; their location; deployment; and alignment; should be carefully done with the help of knowledge in flow pattern and flow distribution.

## General Conclusions

This problem of standardizing calibration techniques is important and needs further study. Dr. Y. Y. Hsu will establish a task force to work on this problem.

## ATTENDEES

| Name | Organization |
|------|--------------|
| A. G. Stephens | EG&G Idaho, Inc. |
| L. D. Goodrich | EG&G Idaho, Inc. |
| R. S. L. Lee | SUNY-Stony Brook |
| J. Srinivasan | SUNY-Stony Brook |
| O. C. Jones | BNL |
| D. E. Dukler | Univ. of Houston |
| N. Zuber | NRC/RSR |
| S. Banerjee | McMaster Uni·./Canada |
| W. W. Bixby | NRC/RSR |
| M. McCoy | NRC/DSS |
| D. Cain | EPRI |
| P. A. Schlosser | Ohio State |
| F. A. Kulacki | Ohio State |
| G. D. McPherson | NRC/RSR |
| W. H. Woodward | MTI |
| J. M. Googe | Union Carbide (ORNL) |
| G. D. Lassahn | EG&G Idaho, Inc. |
| W. L. Riebold | EURATOM-J.R.C.-Ispra |
| H. J. Casper | GRS-Cologne-Germany |
| C. A. McMonegle | PNL |
| C. Solbrig | EG&G Idaho, Inc. |
| S. G. Bankoff | Northwestern Univ. |
| R. S. Tankin | Northwestern Univ. |
| R. J. Simoneau | NASA Lewis |
| W. H. Leavell | ORNL |
| H. W. Wahle | B&W, Ohio |
| R. K. Kim | B&W, Ohio |
| J. G. MacKinnon | B&W, Ohio |
| A. R. Barber | B&W, Ohio |
| A. C. Raptis | ANL |
| P. Kehler | ANL |
| M. W. Hodges | NRC/DSS |
| O. Pinleus | MTI |
| J. B. Colson | EG&G Idaho, Inc. |
| D. E. Solberg | NRC/RSR |
| E. H. Davidson | NRC/RSR |
| R. G. Bearden | EG&G Idaho, Inc. |
| H. N. Guerrero | CE |

| | |
|---|---|
| R. Antoun | Univ. of Maryland |
| J. Saltvoid | AECL, Canada |
| H. Breed | RPI |
| D. Kreid | PNL |
| G. Sozzi | GE |
| J. Creer | PNL |
| T. Sutey | PNL |
| M. Vince | RPI |
| G. Krycuk | RPI |
| D. Taylor | EG&G Idaho, Inc. |
| M. Stanley | EG&G Idaho, Inc. |
| P. Kosky | Lehigh Univ. |
| R. W. Wright | NRC/RES |
| J. M. Delhaye | Grenoble, France |
| R. D. Wesley | EG&G Idaho, Inc. |
| T. C. Piper | EG&G Idaho, Inc. |
| L. J. Flanigan | BCL |
| B. G. Eads | ORNL |
| P. Griffith | MIT |
| L. L. Davis | Measurements, Inc. |
| R. T. Lahey | RPI |
| G. F. Brockett | ITI |
| A. E. Arave | EG&G Idaho, Inc. |
| E. R. Rosal | W |
| H. Estrada | MPR |
| F. Volpe | ERDA-HQ |
| Y. Y. Hsu | NRC/RSR |

## AGENDA

### January 13, 1977, Thursday

AM - Progress Reports by NRC Contractors

8:30   -   Welcome and Introduction, Y. Y. Hsu

8:35   -   Progress Report by ORNL, J. Sheppard

9:15   -   Progress Report by RPI (IR, RF, X-ray), R. Lahey

9:45   -   Progress Report by BNL (local probes), O. Jones

10:05   -   Progress Report by SUNY (LDV), R. Lee

10:25   -   Break

10:35   -   Progress Report by INEL, Staff of EG&G

12:40   -   LUNCH

PM - State-of-art Survey by Invited Rapporteurs - (Significant
     development in design, operation, modeling and interpretation
     of two-phase instrumentations: with emphasis in progress in
     1976 - 30 minute presentation, 10 minutes discussion, each)

1:30   -   Local probes, (hot-wire anemometer, impedence probes,
           optical probes, microthermocouple, etc.), J. M. Delhaye,
           Grenoble

2:10   -   Radioactive beams (attenuation or scattering),
           S. Benerjee, McMaster University

2:50   -   Break

3:00   -   Drag body, turbine and other impact-activated devices,
           L. Davis, Measurement, Inc.

3:40   -   Tracer technique, P. Kehler, ANL

4:20   -   Novel techniques (acoustic, NMR, IR, RF, X-ray,
           Auburn, fluidic, Storz lense, LDV, etc.), P. Griffith,
           Massachusett Institute of Technology

5:00   -   Adjourn

## January 14, 1977, Friday

AM - Discussion and Presentations -

8:30 - Discussion on papers presented January 13, 1977

10:00 - Break

10:10 - State-of-art report on calibration techniques and procedures, M. Stanley, EG&G

11:10 - MPR report on requirements and procedures for calibration, (MPR report will be mailed to the addresses prior to the meeting to serve as frameowrk for discussion in the afternoon), H. Estrada, MPR

12:00 - LUNCH

PM - Discussion on Calibration Procedures and Techniques -

1:00 - Discussion - Following questions will be discussed

    1) How to calibrate full-field, air-water, steady state instruments in small channel?

    2) How to calibrate free-field instrumentation?

    3) How to scale up?

    4) Is it necessary to calibrate in transient conditions? If so, any difficulties?

    5) Is it necessary to calibrate in steam-water mixutre? If so, any difficulties?

    6) Should (items 3, 4) (items 4, 5) (items 3, 5) be combined?

    7) Should items 3, 4, 5 be all combined, i.e., is it necessary to calibrate instruments in transient, steam-water, large loop?

4:30 - Summary

5:00 - Adjourn

## AGENDA

<u>January 13, 1977, Thursday</u>

AM - Progress Reports by NRC Contractors

8:30  - Welcome and Introduction, Y. Y. Hsu

8:35  - Progress Report by ORNL, J. Sheppard

9:15  - Progress Report by RPI (IR, RF, X-ray), R. Lahey

9:45  - Progress Report by BNL (local probes), O. Jones

10:05 - Progress Report by SUNY (LDV), R. Lee

10:25 - Break

10:35 - Progress Report by INEL, Staff of EG&G

12:40 - LUNCH

PM - State-of-art Survey by Invited Rapporteurs - (Significant
     development in design, operation, modeling and interpretation
     of two-phase instrumentations; with emphasis in progress in
     1976 - 30 minute presentation, 10 minutes discussion, each)

1:30  - Local probes, (hot-wire anemometer, impedence probes,
        optical probes, microthermocouple, etc.), J. M. Delhaye,
        Grenoble

2:10  - Radioactive beams (attenuation or scattering),
        S. Benerjee, McMaster University

2:50  - Break

3:00  - Drag body, turbine and other impact-activated devices,
        L. Davis, Measurement, Inc.

3:40  - Tracer technique, P. Kehler, ANL

4:20  - Novel techniques (acoustic, NMR, IR, RF, X-ray,
        Auburn, fluidic, Storz lense, LDV, etc.), P. Griffith,
        Massachusett Institute of Technology

5:00  - Adjourn

January 14, 1977, Friday

AM - Discussion and Presentations -

8:30   -  Discussion on papers presented January 13, 1977

10:00  -  Break

10:10  -  State-of-art report on calibration techniques and
          procedures, M. Stanley, EG&G

11:10  -  MPR report on requirements and procedures for calibration.
          (MPR report will be mailed to the addresses prior to the
          meeting to serve as frameowrk for discussion in the
          afternoon), H. Estrada, MPR

12:00  -  LUNCH

PM - Discussion on Calibration Procedures and Techniques -

1:00   -  Discussion - Following questions will be discussed

          1)  How to calibrate full-field, air-water, steady
              state instruments in small channel?

          2)  How to calibrate free-field instrumentation?

          3)  How to scale up?

          4)  Is it necessary to calibrate in transient conditions?
              If so, any difficulties?

          5)  Is it necessary to calibrate in steam-water mixutre?
              If so, any difficulties?

          6)  Should (items 3, 4) (items 4, 5) (items 3, 5) be
              combined?

          7)  Should items 3, 4, 5 be all combined, i.e., is it
              necessary to calibrate instruments in transient,
              steam-water, large loop?

4:30   -  Summary

5:00   -  Adjourn

xxii

# PROGRESS REPORT ON ADVANCED TWO-PHASE INSTRUMENTATION

J. D. Sheppard
W. H. Leavell    F. Shahrokhi
M. C. Wynn

## ABSTRACT

A Venturi meter was tested as a two-phase momentum moni-
toring device in the ORNL air-water, two-phase flow facility.
Void fraction was monitored at the Venturi inlet with a ro-
tating electric field, conductance meter, and Venturi pressure
drop was correlated with mixture momentum determined by a
separated-flow model.

A computer algorithm was developed to apply cross-corre-
lation techniques to the measurement of nonstationary two-
phase velocities. The algorithm was tested with computer-
generated, two-phase velocity transients. Preliminary results
show good agreement between algorithm estimates and the known
velocities.

## 1. ADVANCED SPOOL PIECE STUDIES

J. D. Sheppard    M. C. Wynn

The determination of transient, two-phase mass flow rates during
blowdown heat transfer experiments generally requires the combination
of two or more characteristic fluid parameters (e.g., velocity and
density) with appropriate two-phase flow models. For measurements in
the primary piping of experimental loops, flow-monitoring instruments
have been concentrated in piping spool pieces located at selected sites
in the loop. Spool pieces at the ORNL Thermal-Hydraulic Test Facility
(THTF)[1] and the INEL Semiscale Facility[2] utilize full pipe turbine
meters for mixture velocity measurement, gamma densitometers for
mixture density, drag disks for mixture momentum, and temperature and
pressure transducers for determinations of liquid and vapor phase states.

The scope of the Advanced Two-Phase Instrumentation Program includes consideration of new or alternative instruments, or combinations thereof, for what is referred to as an advanced spool piece in order to improve the accuracy and precision of transient mass flow rate determinations.

## 1.1 Two-Phase Momentum

Many nuclear reactor safety studies in this country utilize drag disks (target flowmeters) for two-phase momentum measurements. Drag disks are capable of indicating direction as well as magnitude of momentum (i.e., bidirectional); however, they have the undesirable characteristic of sampling a relatively small fraction of the flow cross-sectional area. One solution to this problem is to eliminate the disk target and utilize a screen target[3] that samples more of the flow area. However, other momentum measurement techniques are applicable and should be considered. For example, t\ phase momentum has been related to the pressure drop of resistance currents such as woven wire and perforated plate screens.[4] This report presents some preliminary results of steady-state, air-water studies with a Venturi meter and the application of a separated-flow model to data correlation.

Steady-state, two-phase flow tests were conducted in the air-water loop with a Venturi meter installed for vertical upflow. The Venturi had a major inside diameter of 7.62 cm (3.0 in.) and a 3.81-cm (1.5-in.) throat diameter; the total angle of convergence upstream of the throat was 21°, and the total angle of divergence downstream of the throat was 7°. The pressure drop was measured with differential-pressure transducers. Due to the fluctuating character of the transducer signal during

two-phase testing, an integrating digital voltmeter was used to average the signal for periods of approximately 1 min.

Volume-average void fraction was monitored immediately upstream of the Venturi by a rotating electric field conductance meter[5] (Auburn International, Inc., model 1080). Further, a two-phase flow disperser consisting of a stack of four, 20-mesh woven wire screens was located at the upstream flange of the void fraction meter to minimize radial variations in the two-phase velocity distribution.

Venturi pressure drop and void fraction were monitored as a function of air and water flow rates. Axial separation of the vertically oriented pressure taps was 10.2 cm (4 in.), so the measured pressure drop included gravitational effects ($\rho gh$) which were considered in the data reduction. For the tests with water only, the gravitational term was 1 kN/m$^2$ (0.14 psi).

Figure 1.1 shows the pressure drop, corrected for the gravitational term, as a function of air flows from 0 to 0.24 m$^3$/sec (0 to 512 scfm) and water flows from $6.3 \times 10^{-4}$ to $2.5 \times 10^{-2}$ m$^3$/sec (10 to 400 gpm). As shown in the figure, the gravitational effects were of the same magnitude as the Bernoulli effects only at the lower water and air flows. At the highest air flows (0.24 m$^3$/sec), the water flow rate was limited to $\sim 3 \times 10^{-3}$ m$^3$/sec; at higher water flows the total system pressure drop was too high to maintain critical flow in the air meters. Venturi pressure drop ranged from $\sim 1$ to 200 kN/m$^2$.

A separated-flow model was used by Collins and Gacesa[6] and modified by Fouda and Rhodes[7] to determine two-phase quality from Venturi $\Delta P$, mass flow, and Venturi geometry. While their model assumes no slip between

I.1-3
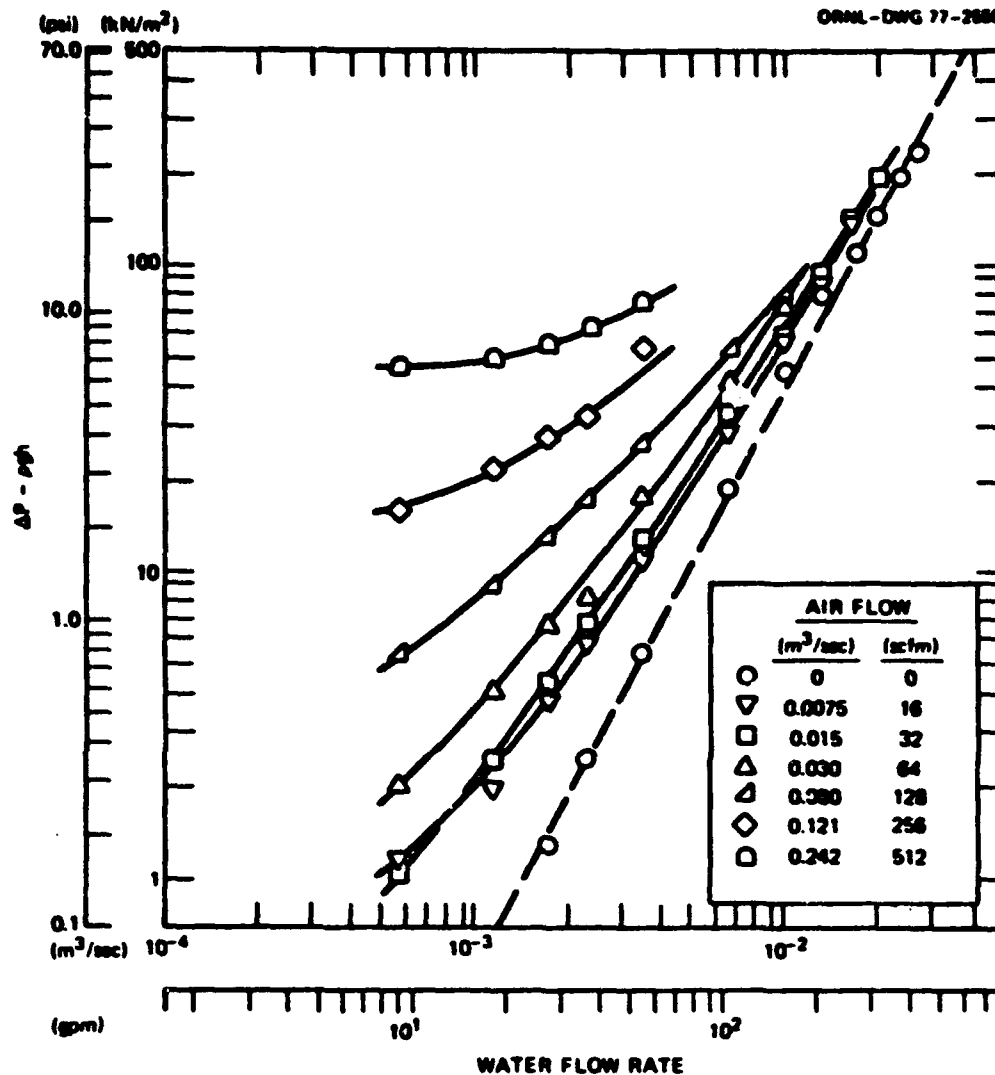
Fig. 1.1. Venturi pressure as a function of air and water rates in two-phase flow facility (7.2-cm Venturi, 3.8-cm-throat; 4-20 flow disperser located 30.5 cm upstream of Venturi).

phases, it considers such effects as the difference in incompressible and compressible flow through the Venturi. The Aya[8] separated-flow model considers the effects of slip by assuming that each of the two phases can be represented with a characteristic velocity, $V_g$ or $V_l$, and a given instrument reading is the response of the instrument to each phase of the fluid mixture. This model has resulted in distinct improvement over more common homogeneous models in determining mass flow from THTF spool piece instrument readings.[9]

According to the Aya model, two-phase momentum is given by

$$\overline{\rho V^2}_{sf} = C_1 \alpha \rho_g V_g^2 + C_2 (1 - \alpha) \rho_l V_l^2 \ ,$$ (1.1)

where $V_g$ and $V_l$ are mean velocities of the vapor and liquid phases, respectively, $\rho_g$ and $\rho_l$ are phase densities, and $\alpha$ is void fraction.

For the data shown in Fig. 1.1, void fraction was measured near the Venturi, and individual phases were metered into the system; therefore, phase-continuity relationships permit the calculation of the phase velocities, $V_g$ and $V_l$, entering the Venturi. That is,

$$\dot{m}_g = \alpha \rho_g V_g$$ (1.2)

and

$$\dot{m}_l = (1 - \alpha) \rho_l V_l \ ,$$ (1.3)

where $\dot{m}_g$ and $\dot{m}_l$ are the mass flows of air and water, respectively. After solving for the phase velocities, the mixture momentum can be calculated from Eq. (1.1).

I.1-5

Figure 1.2 shows the Venturi pressure drop as a function of the fluid momentum determined by Eqs. (1.1) through (1.3), along with void fraction and phase mass flow rate data. The family of curves shown in Fig. 1.1 reduced to a single band of data, with $(\Delta P - \rho gh)$ varying linearly with $\overline{\rho V_{sf}^2}$ for nearly three orders of magnitude. The width of the scatter band, ±30%, can probably be significantly reduced by improved void fraction measurements since the void fraction meter is sensitive to flow regime.

Figure 1.2 and Eq. (1.1) give the relationship between pressure drop and mixture momentum for this Venturi as

$$\Delta P - \rho_a gh = C[\alpha\rho_g V_g^2 + (1 - \alpha)\rho_\ell V_\ell^2] , \tag{1.4}$$

where C is a constant. Rewriting Eq. (1.4) gives

$$\Delta P - \rho_a gh = C\alpha V_\ell^2[\rho_g S^2 + \rho_\ell(1 - \alpha)/\alpha] , \tag{1.5}$$

where S is the slip ratio, $V_g/V_\ell$. If the Venturi reading is combined with turbine meter and gamma densitometer data, mass flow and quality can be calculated from the Aya model. However, if only Venturi pressure drop and void fraction data are available, an assumption of the value of the slip ratio is required to give mass flow rates. Due to the fact that $\rho_g$ is much less than $\rho_\ell$ for air-water and steam-water mixtures, the actual value of the slip ratio is not important in Eq. (1.5) except at very high values of void fraction. For example, for air and water at ambient conditions, $\rho_g = 0.07$ $lb_m/ft^3$ and $\rho_\ell = 62$ $lb_m/ft^3$. If the void fraction were as high as 95%, the slip ratio would have to be nearly 50 for the gas-phase effects to be of the same magnitude as the liquid-phase effects. As discussed above, Fouda and Rhodes[7] assumed unit slip and achieved good correlation for a wide range of steam-water flows.

I.1-6
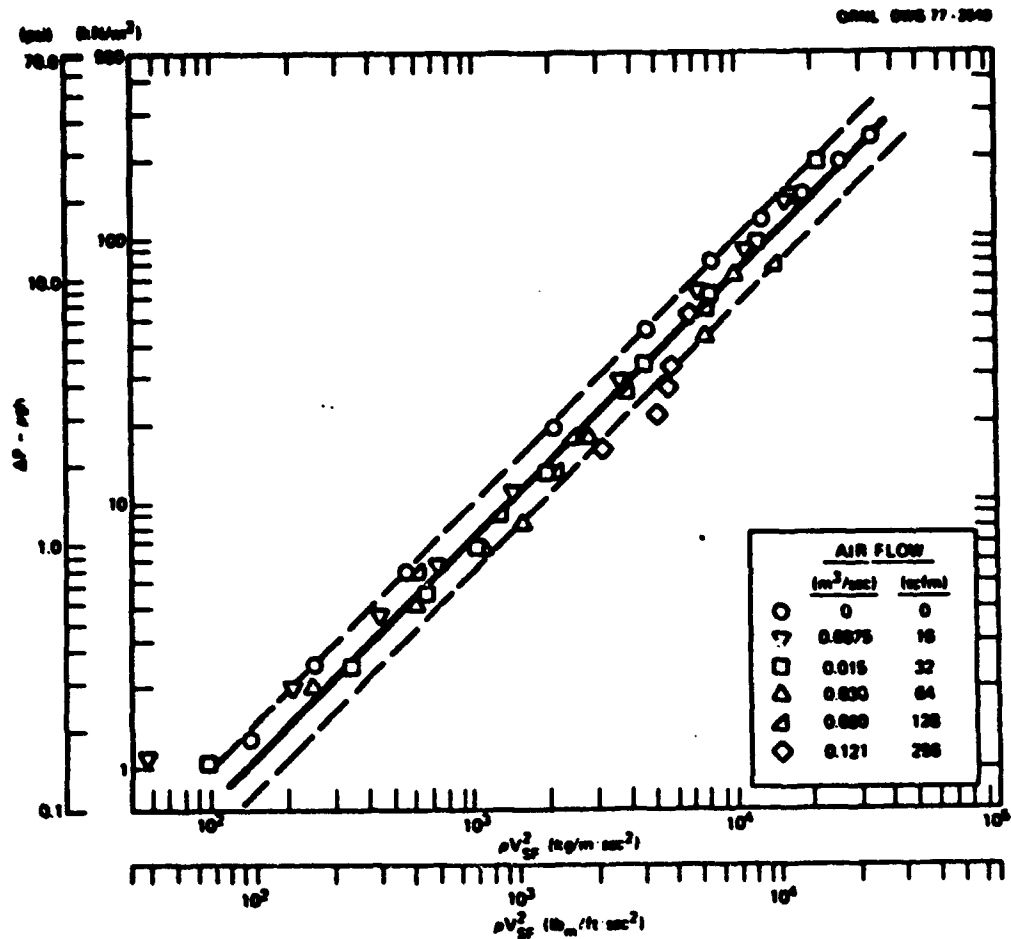
Fig. 1.2. Venturi pressure drop as a function of two-phase momentum as determined by a separated-flow model (7.6-cm Venturi, 3.8-cm-throat; void fraction determined by Auburn meter; 4-20 flow disperser located 30.5 cm upstream of Venturi).

Two-phase Venturi studies will continue with emphasis on optimum throat design for two-phase flow and the use of void fraction data determined from a triple-beam gamma densitometer. Further, many blowdown experiments include flow reversals, and Venturi designs that will accommodate flow reversal will be considered.

## 1.2 Fluidics

A subcontract has been initiated with Harry Diamond Laboratories (HDL), Department of the Army, to investigate the application of fluidics technology to two-phase flow measurement problems. The scope of the work to be performed by HDL includes (1) a study of the feasibility of using fluidics technology to monitor mass flow rate, mixture quality, and other key transient two-phase flow parameters; and (2) the fabrication of devices demonstrating the application of fluidics principles to the measurement of (1) two-phase momentum, (2) temperature, and (3) pressure drop. These devices will be tested in ORNL two-phase flow facilities.

### References

1. *Project Description — ORNL PWR Blowdown Heat Transfer Separate-Effects Program — Thermal Hydraulic Test Facility (THTF)*, ORNL/NUREG/TM-2 (February 1976).

2. E. M. Feldman and D. J. Olson, *Semiscale MOD-1 Program and System Description for the Blowdown Heat Transfer Tests (Test Series 2)*, ANCR-1230 (August 1975).

3. D. G. Thomas et al., *Quarterly Progress Report on Blowdown Heat Transfer Separate-Effects Program for July–September 1976*, ORNL/NUREG/TM-61 (January 1977).

4. *Quarterly Progress Report on Reactor Safety Programs Sponsored by the Division of Reactor Safety Research for July–September 1974*, Vol. I, *Light-Water-Reactor Safety*, ORNL/TM-4729, Vol. I (December 1974).

5.  M. Merilo, R. L. Dechene, and W. M. Cichowlas, "Void Fraction Measurement with a Rotating Electric Field Conductance Gauge," submitted for publication November 1976.

6.  D. B. Collins and M. Gacesa, "Measurement of Steam Quality in Two-Phase Upflow with Venturi Meters and Orifice Plates," *J. Basic Eng.* 93, p. 11 (March 1971).

7.  A. E. Fouda and E. Rhodes, "Total Mass Flow and Quality Measurement in Gas-Liquid Flow," submitted for publication September 1976.

8.  I. Aya, *A Model to Calculate Mass Flow Rate and Other Quantities of Two Phase Flow in a Pipe with a Densitometer, a Drag Disk, and a Turbine Meter*, ORNL/TM-4759 (November 1975).

9.  J. D. Sheppard, P. H. Hayes, and M. C. Wynn, "An Experimental Study of Flow Monitoring Instruments in Air-Water, Two-Phase Downflow," paper presented at CREST Specialists Meeting on Transient Two-Phase Flow, Toronto, Canada, Aug. 3-4, 1976.

## 2. NONSTATIONARY SIGNAL CORRELATION

W. H. Leavell[*]  F. Shahrokhi[*]

### 2.1 Theory

One technique of fluid velocity measurement is to directly measure the transit time of a quantity between two points A and B, fixed a distance D apart in space, and then divide the distance D by the transit time to calculate the velocity. If the measured process is random, the statistical technique of cross-correlation is often used to measure transit time. Using this technique, signals A(t) and B(t) are measured for T seconds at points A and B, respectively, and their cross-correlation function is approximated using the following general expression:

$$R_{AB}(\tau) = \frac{1}{T} \int_0^T A(t)\ B(t + \tau)\ dt \quad , \tag{2.1}$$

where $\tau$ is the value of time delay between points A and B. The transit time between points A and B of the measured process will correspond to a unique value, $\tau_{AB}$, of $\tau$ that maximizes the cross-correlation function given in Eq. (2.1).[1] If the measured signals A(t) and B(t) are contaminated by additive noise, time-averaging of $R_{AB}(\tau)$ will improve the signal-to-noise ratio if the noise is uncorrelated because the cross products between the noise and the signals in Eq. (2.1) will average zero. An important assumption of this averaging process is that the fluid velocity being measured is constant throughout the time-averaging interval. If the fluid velocity of the process is not constant, as in the case of a blowdown test, conventional cross-correlation analysis

---

[*]Instrumentation and Controls Division.

is no longer applicable to the problem and a modified procedure is required.

If the measurement procedures were not altered for a nonstationary fluid velocity, what would be the expected results if the cross-correlation function [Eq. (2.1)] were calculated? First, assume for simplicity that the fluid velocity decreases with time at a constant rate (in practice, the algorithm does not require that this assumption be true) and that the measurement at points A and B of the random process proceeds for T seconds. During those T seconds, the fluid velocity has changed from a maximum value at $t = 0$ to a minimum value at $t = T$. If the cross-correlation function $R_{AB}(\tau)$ [Eq. (2.1)] were not computed over the entire T seconds of data and examined, the peak value of $R_{AB}(\tau)$ corresponding to the unique transit time $\tau_{AB}$ in the constant-velocity case would appear broadened to include the range of transit times that were momentarily present during the period T; the minimum transit time would correspond to the maximum velocity at $t = 0$, and the maximum transit time would correspond to the minimum velocity at $t = T$. However, if the measurement time T could be made sufficiently small so that the flow velocity could be considered constant (to first order) over the interval 0 to T, then the velocity could be tracked as it decreases on a longer time scale by continually readjusting T so as to resolve each new minimum transit time $\tau_{AB}$ corresponding to the changing velocity. Such stepwise alteration of the measurement time T forms the basis of a modified cross-correlation algorithm, which is presented next.

## 2.2 Nonstationary Cross-Correlation Algorithm

The cross-correlation algorithm that has been developed to track a nonstationary flow velocity can be divided into four main parts (see Fig. 2.1): initializing, partitioning, averaging, and data shifting. The assumptions made in the algorithm are (1) the maximum number of data points operated on by the algorithm during any one iteration is 1024 (this is only a limitation of the particular computer core size used and not a basic limitation of the algorithm); (2) the distance $D$ between the two measuring points is fixed; and (3) the initial fluid velocity $V(0)$ is known.

The initialization portion of the algorithm (see Fig. 2.1) consists of three tasks: (1) choosing an initial sampling rate $f_s$; (2) choosing an initial partition $P$ of the measurement time $T$; and (3) sampling the signal $A(t)$ at point A and the signal $B(t)$ at point B in the fluid medium. In choosing the initial sampling rate $f_s$, the measurement time $T$ is fixed since $1/f_s = \Delta t$, the time interval between sampled data points, and the number of data points is fixed at 1024; thus,

$$T = 1024\Delta t = 1024/f_s \quad . \tag{2.2}$$

Further, the resolution of transit times between points A and B is limited to $\pm\Delta t$ seconds. The sampling rate is chosen based on two criteria which are functions of the initial velocity $V(0)$. The time interval $\Delta t$ must be smaller than the initial transit time between points A and B, $\tau_{AB}(0) = D/V(0)$; thus, the first criterion is that $f_s$ must be greater than $1/\tau_{AB}(0)$. The second criterion states that the minimum total measurement time $T$ must be sufficiently large that $\tau_{AB}(0)$ can be adequately

I.1-12

Fig. 2.1. Flow chart of adaptive cross-correlation algorithm.
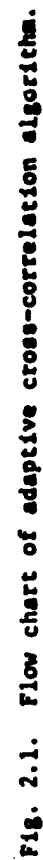
resolved using the cross-correlation algorithm. This is accomplished by defining T as some multiple of $\tau_{AB}(0)$ that can be resolved using the first 256 data points of the total 1024 points sampled. Therefore the minimum T has to be equal to or greater than $4\tau_{AB}(0)$ seconds, and according to Eq. (2.1),

$$f_s \leq 1024/4\tau_{AB}(0) \quad . \tag{2.3}$$

Thus the upper and lower bounds of $f_s$ are

$$1/\tau_{AB}(0) < f_s \leq 256/\tau_{AB}(0) \quad . \tag{2.4}$$

Although the selection of $f_s$ is based on the assumption that $V(0)$ is the maximum velocity measured during the T seconds, this does not prevent velocities greater than V(0) to be resolved if they occur during the T seconds, since T seconds is more time than is necessary to resolve higher velocities than V(0). As an initial selection, $f_s$ is normally set at one-half the maximum sampling rate, or $128/\tau_{AB}(0)$. Since the sampling rate is fixed for the entire set of 1024 data points, variation of the measurement time T to resolve the minimum transit time is accomplished by taking fractions of the total time T and using these to calculate each transit time $\tau_{AB}(t_i)$ from the set of transit times covered by the total time T.

The second task accomplished during initialization is the selection of an initial partition P, which is typically set equal to the first 512 data points, since the sampling rate is one-half the maximum sampling rate. Having selected $f_s$ and P, the algorithm samples sensors A and B for T seconds, yielding

$$A = \{a_1, a_2, \ldots, a_{1024}\} \tag{2.5}$$

and

$$B = \{b_1, b_2, \ldots, b_{1024}\} \ , \tag{2.6}$$

where $a_i$ and $b_i$ are sampled values of $A(t)$ and $B(t)$, the sensor signals.
The partitions of A and B have the form

$$P(A) = \{a_1, a_2, \ldots, a_{512}\} \tag{2.7}$$

and

$$P(B) = \{b_1, b_2, \ldots, b_{512}\} \ . \tag{2.8}$$

The second major part of the algorithm is the partitioning routine
(see Fig. 2.1). Its task is to determine the minimum size of partition
P for the total time T such that only the minimum transit time $\tau_{AB}$ between
sensors A and B will be resolved and all other transit times greater than
$\tau_{AB}$ will be rejected. Since the data for A and B have already been parti-
tioned by P, the algorithm will only consider the first 512 data points in
A and B. The maximum transit time $\tau_{max}$ that can be resolved by the algo-
rithm is initially equal to $(512/4)\Delta t$, or $128\Delta t$ seconds. By the parti-
tioning of A and B, the algorithm has already rejected any transit time
greater than $128\Delta t$.

The next step is to cross-correlate the partitioned A and B data
using the following equation:

$$R_{AB}(\tau_j) = \frac{1}{(N-j)\Delta t} \sum_{n=1}^{N-j} a_n b_n + j \ , \tag{2.9}$$

where $\tau_j = j\Delta t$ with $j = 0, 128$; and $N = 512$, the initial partition size
of P. The reverse cross-correlation function $R_{BA}(\tau_j)$ is now searched
for a maximum value such that

$$R_{AB}(\tau_{AB}) = MAX[R_{AB}(\tau_j)], \ j = 1, \ \tau_{max}/\Delta t \ . \tag{2.10}$$

This determines a minimum transit time $\tau_{AB}$ for the initial partition size

P = 512 points. The value $\tau_{AB}$ is now compared to $\tau_{max}$, the maximum resolvable transit time for partition P, using the following expression:

$$\tau_{max} - \tau_{AB} \leq \epsilon_\tau, \quad \Delta t \leq \epsilon_\tau \leq 2\Delta t \quad . \tag{2.11}$$

If the above comparison is true, then the algorithm has found the minimum partition size P equal to 512 points. It has also determined the next minimum transit time $\tau_{AB}$ following $\tau_{AB}(0)$, the initial minimum transit time corresponding to V(0). The algorithm would not proceed to the averaging routine.

If the difference [Eq. (2.11)] between $\tau_{max}$ and $\tau_{AB}$ is greater than $\epsilon_\tau$ seconds, then there exists an even smaller size for the partition P of the data set, and the $\tau_{AB}$ calculated for P = 512 points is not the true minimum transit time for the data set. The algorithm now computes a new, smaller size for the partition P by setting it equal to $4\tau_{AB}/\Delta t$ data points. It also makes $\tau_{max} = \tau_{AB}$, the previously calculated minimum transit time. The algorithm again calculates $R_{AB}(\tau_j)$ [Eq. (2.10)], but with j = 0, $\tau_{AB}/\Delta t$, and N = $4\tau_{AB}/\Delta t$. A search is again made of $R_{AB}(\tau_j)$ according to Eq. (2.11) and a new minimum transit time $\tau_{AB}$ is found and compared to the new $\tau_{max}$ using Eq. (2.11). With each interaction of the partitioning routine, the larger transit times that were momentarily present during the total T seconds are rejected until the true minimum transit time for the T seconds of data is determined by the criterion in Eq. (2.11) and set equal to $\tau_{AB}$. At this point in the routine, the partitions of both the A and the B data set appear as

$$P(A) = \{a_1, a_2, a_3, \ldots, a_M\} \tag{2.12}$$

and

$$P(B) = \{b_1, b_2, b_3, \ldots, b_M\} .$$ (2.13)

where $M = 4\tau_{max}/\Delta t$.

Since the partitioning part of the algorithm has yielded only one estimate of the minimum delay time $\tau_{AB}$, the statistical precision is very poor and some form of averaging must be performed in order to increase the confidence in this estimate. Time averaging of cross-correlation functions calculated for a nonstationary process ordinarily introduces large amounts of error in the estimated transit time, but in this case the algorithm can only estimate the values of the transit time $\tau_{AB}(t)$ in fixed increments of $\Delta t$ seconds, the time between data samples. Thus, the number of time averages k that the algorithm can perform without introducing any more error in the transit time than $\Delta t$ is a function of the resolution $\Delta t$ and the rate of change of the transit time $\tau_{AB}(t)$ with respect to time. The averaging routine of the algorithm (see Fig. 2.1) takes advantage of the $\Delta t$ resolution of $\tau_{AB}(t)$ by using data shifting as a substitute for time averaging in the following way. Starting with the minimum size of the partition P resolved by the partitioning routine, the algorithm shifts this partition by one $\Delta t$. The shifted partitions of the A and B data sets now appear as

$$P(A) = \{a_1, a_2, a_3, \ldots, a_{M+1}\}$$ (2.14)

and

$$P(B) = \{b_1, b_2, b_3, \ldots, b_{M+1}\} .$$ (2.15)

The algorithm now calculates a cross-correlation function $R_{AB}(\tau_j)$ for the M data points using Eq. (2.9). The new $R_{AB}(\tau_j)$ is now searched for a maximum value using Eq. (2.10), which has a corresponding unique transit time $\tau_{AB}$. This $\tau_{AB}$ is compared with the $\tau_{max}$ that was calculated by the

I.1-17

partitioning routine using the following equation:

$$|\tau_{max} - \tau_{AB}| < \epsilon_\tau, \quad \Delta t < \epsilon_\tau \leq 2\Delta t \quad . \tag{2.16}$$

The comparison in Eq. (2.16) checks to see if, by shifting P by one $\Delta t$,
the new calculated $\tau_{AB}$ is still within the partition's ability to resolve
it. If the result of the comparison shows that the new $\tau_{AB}$ is outside the
partition's resolution, then a new partition will be necessary and the
algorithm stops averaging and proceeds to the next step, data shifting
(see Fig. 2.1). If the comparison given in Eq. (2.16) shows that the new
$\tau_{AB}$ is within $\pm\epsilon_\tau$ seconds of $\tau_{max}$, the algorithm adds the calculated
$R_{AB}(\tau_j)$ to a running sum and proceeds to shift P(A) and P(B) by one more
$\Delta t$. This procedure continues until at the K + 1 shift of P(A) and P(B),
the criterion of Eq. (2.16) is not met. At this point the algorithm
calculates an average cross-correlation function $\bar{R}_{AB}(\tau_j)$ for the K shifts
of the partition. This function is then searched using Eq. (2.10) for a
maximum value with its corresponding $\bar{\tau}_{AB}$, the average minimum transit
time for the time interval $0 \leq t \leq (M + K)\Delta t$, where M equals the size of
the minimum partition P and K equals the number of $\Delta t$ shifts made by the
partition. The algorithm calls $\bar{\tau}_{AB}$, the new mean estimate of the minimum
delay time $\bar{\tau}_{AB}(t_1)$, and places this estimate in time at the mean of the
time interval covered, $t_1 = \dfrac{M + K}{2} \Delta t$. The algorithm now calculates $V(t_1)$
using

$$V(t_1) = D/\bar{\tau}_{AB}(t_1) \quad , \tag{2.17}$$

where D is the distance between sensors A and B; $V(t_1)$ is also placed in
time at $t_1$ seconds.

Now that a mean velocity $V(t_1)$ has been estimated for the time
interval $0 < t < (M + K)\Delta t$, the algorithm is ready to make new velocity

I.1-18

estimates. To do this, each sensor's block of 1024 data points is shifted $(M + K)/2$ points, which corresponds to a time shift of $\frac{(M + K)}{2} \Delta t$ seconds. The data blocks for A and B sensors now appear as

$$A = (a_r, a_{r+1}, \ldots, a_s) \qquad (2.18)$$

and

$$B = (b_r, b_{r+1}, \ldots, b_s) , \qquad (2.19)$$

where $r = (M + K)/2$ and $S = 1024 - (M + K)/2$. Note that this shift of the data blocks retains the last half of the old data used to estimate $V(t_1)$. This is done so that no possible new cross-correlation between the old and the new data will be lost as a result of the shift. The algorithm now checks to see if enough data points (L) remain in the data blocks to continue processing. It does this by comparing the number of data points needed to resolve $V(t_1)$ with the number remaining after the shifts using the following expression:

$$L = s - r > 4\bar{\tau}_{AB}(t_1)/\Delta t . \qquad (2.20)$$

If the comparison in Eq. (2.20) shows that enough data remain in A and B data blocks, the algorithm returns to the partitioning routine and starts a new iteration to resolve $V(t_2)$. The algorithm will continue as above until the criterion in Eq. (2.20) is not met, at which time the algorithm will choose a new sampling rate based on the last velocity estimate $V(t_m)$ and proceed to sample the A and B sensors at the new sampling rate forming a new set of 1024 data points. The algorithm will then continue and repeat the same inner iterations outlined previously to resolve new velocity estimates.

I.1-19

## 2.3 Conclusions

An attempt has been made to develop a computer algorithm based on cross-correlation analysis techniques that will track a nonstationary fluid flow velocity and give minimally biased, maximally precise estimates of the velocity as a function of time. The algorithm is based on the idea that the total measurement time T can be so adjusted as to reject all but the minimum flow transit time between the two measuring devices. This procedure is somewhat analogous to the use of spectral filtering of unwanted signals in the frequency domain.

The algorithm is currently being tested using computer-generated velocity-transient data sets. Preliminary results show good agreement between the known velocities and the estimates by the algorithm.

## Reference

1.  J. S. Bendat and A. G. Piersol, *Random Data: Analysis and Procedures*, p. 30, Interscience, 1971.

# ORNL TWO-PHASE FLOW STUDIES

## FIGURES PRESENTED AT

## NRC TWO-PHASE INSTRUMENTATION REVIEW GROUP MEETING

## JANUARY 13-14, 1977

## SILVER SPRING, MARYLAND

PHOTO 0091 77
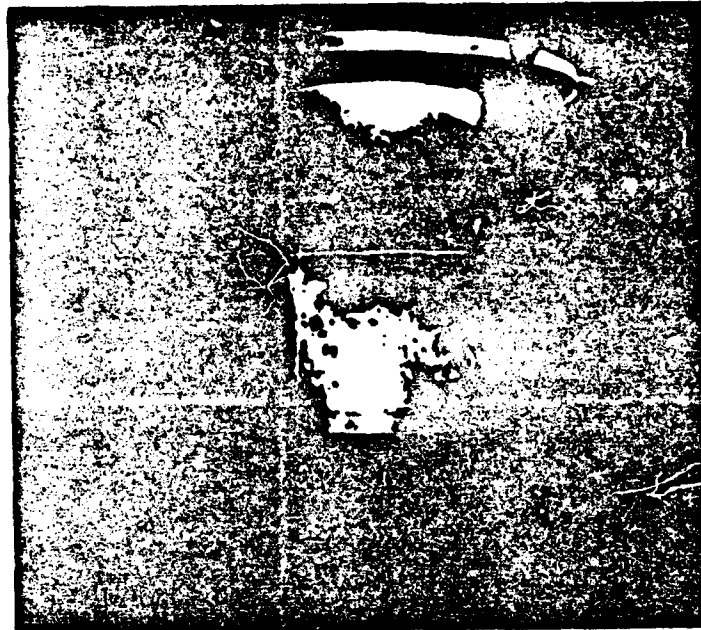


Air-water downflow in the Coring bubble regime
intersects a 6.4-mm-diam (1/4-in.) rod transverse
to flow in a 7.6-cm-ID pipe

I.1-21

PHOTO 0092-77

Air-water downflow in the Coring bubble regime intersects a 6.4-mm-diam (1/4-in.) rod transverse to flow in a 7.6-cm-ID pipe (5.6 m/sec superficial water velocity: 0.4 m/sec superficial air velocity)
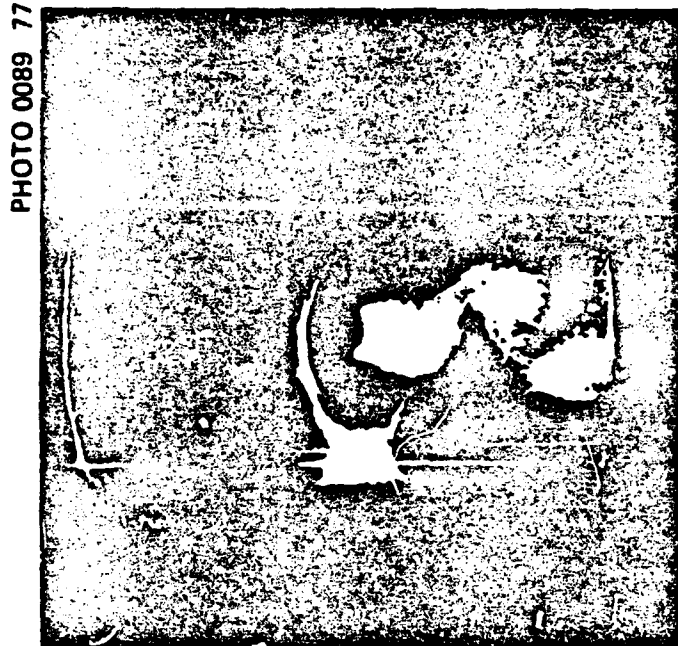


PHOTO 0089 77

Wake region of a 9.5-mm-diam (3/8-in.) tube transverse to flow (5.5 m/sec, 18 ft/sec) in a 7.6-cm-ID (3-in.) pipe (air aspirating through a hole in the downstream side of the tube)

I.1-22

PHOTO 2081 76

2 mV/div

500 msec/div

(a) NO DISPERSER

600 msec/div

(b) FLOW DISPERSER (4-20)

Fig. . Comparison of drag disk signals for air-water, two-phase flow through THTF instrumented spool piece with and without a flow disperser located upstream of the target (0.0011 m³/sec, 18 gpm water; 0.24 m³/sec, 512 scfm air; 1-in. target; 4-20 disperser; vertical downflow).

I.1-23
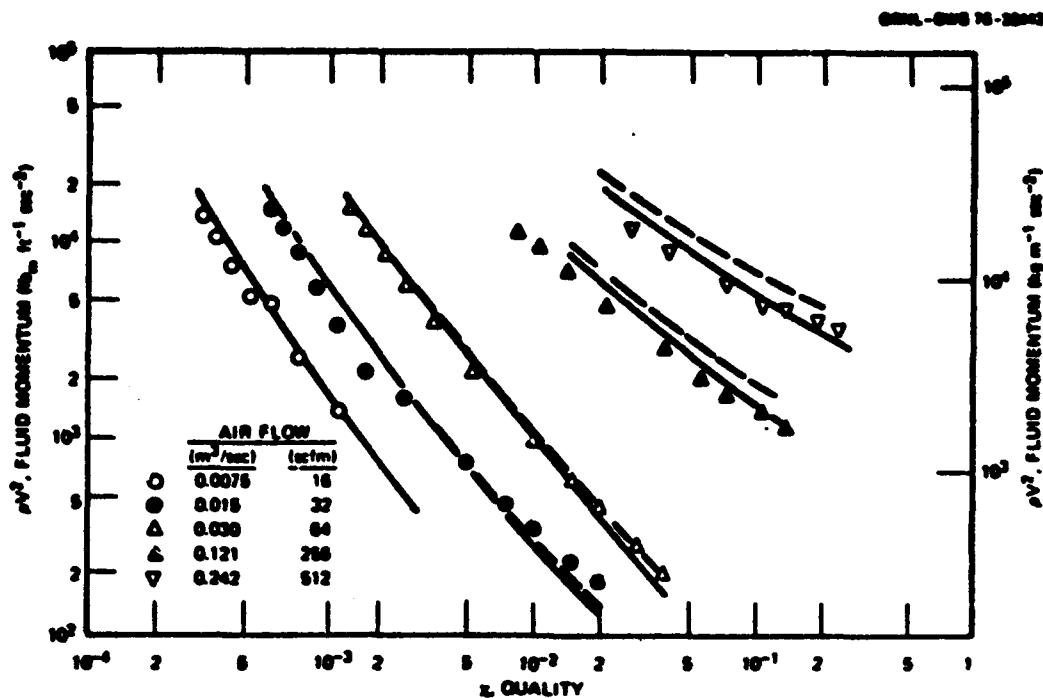
Two-phase fluid momentum measurements using a drag screen in the air-water loop. Curves through data were calculated from two-velocity models for separated flow using results from a turbine meter downstream of the drag screen (solid line, Aya; dashed line, Rouhani; 4-20 flow disperser upstream of drag screen).
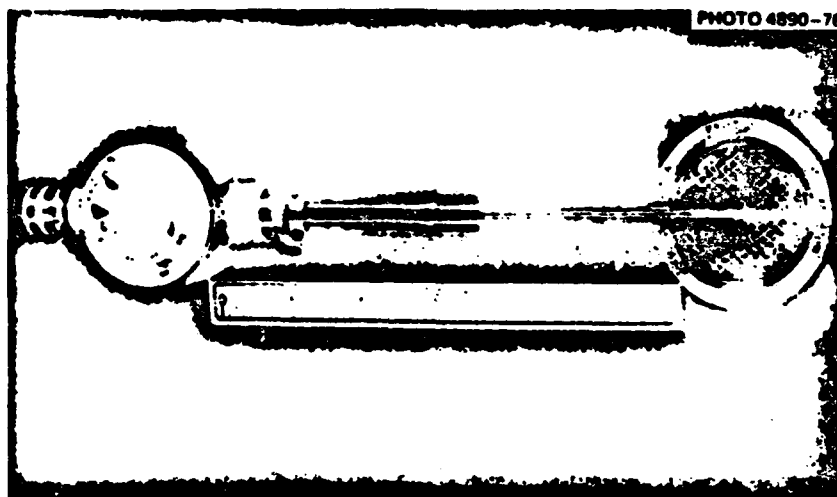


Drag screen tested in BDHT air-water facility shown in comparison to pipe cross section (5-mesh, 0.64-mm-diam wire screen).

I.1-24

ORNL-DWG 76-14390

ROTATING DISK

SOURCE

DETECTOR

20°

SOURCE

LEAD
SHIELD

DETECTOR

LEAD
SHIELD

SCALE

10 cm (3.94 in.)

Test assembly for transient response studies.

ORNL-DWG 76-14391

SIGNAL AMPLITUDE

TIME (50 msec/div)

Comparison of three detector systems with amplifier time
constant of 16 msec (source angular velocity = 15.7 radians/sec);
—— ionization chamber −2000-V bias; ——— plastic scintillator; ——— sodium
iodide scintillator.

ORNL-DWG 76-14370

SIGNAL AMPLITUDE

ANGULAR ROTATION (7.8°/div)
TIME (2 msec/div)

Comparison of signals from two detector systems with source
angular velocity of 56 radians/sec (amplifier time constant ≥0.5 msec);
—— ionization chamber −2000-V bias; ——— plastic scintillator.

I.1-25

$\longleftarrow$ 0.0540 m³/sec (856 gpm)

$\longleftarrow$ 0.0458 m³/sec (726 gpm)

0.0279 m³/sec (443 gpm)

BLOWDOWN

TIME (msec)

0   100   200   300

Fig. . Comparison of two flow calculations. Top curve is RELAP calculated flow. Middle curve is flow calculated from monitor output. Bottom curve is smoothed monitor output (FE-1A, THTF isothermal test 100).

# TURBINE METER DYNAMICS

### Rotor

$$\frac{dF_r(t)}{dt} = K\, F^2(t) - K\, F(t) F_r(t)$$

$$\tau_r = \left| \frac{1}{KF} \right|$$

### Electronics

$$\frac{dv(t)}{dt} = -\frac{v(t)}{RC} + \frac{i(t)}{C}$$

$$\tau_e = RC$$

I.1-26

Application of Cross-correlation Techniques to Non-stationary Flow
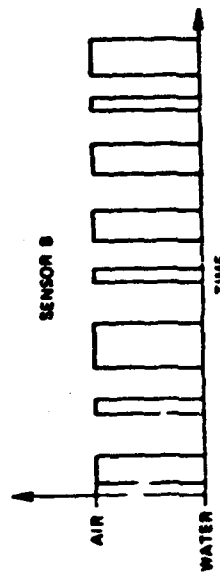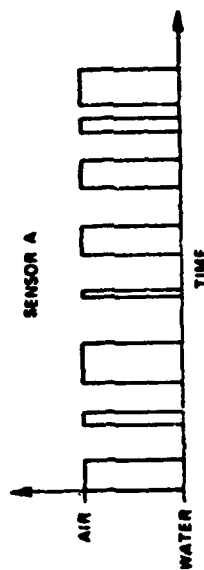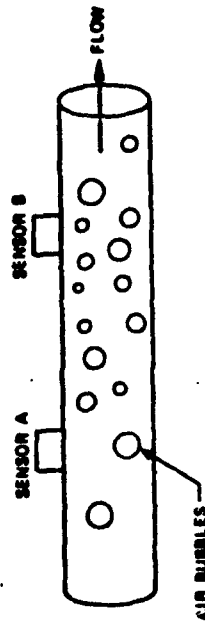
# ADAPTIVE CROSS-CORRELATION ALGORITHM

(1) INITIALIZING
(2) PARTITIONING
(3) AVERAGING
(4) DATA SHIFTING

$$R_{AB}(\tau) = \frac{1}{T} \int_0^T A(t)\, B(t+\tau)\, dt$$
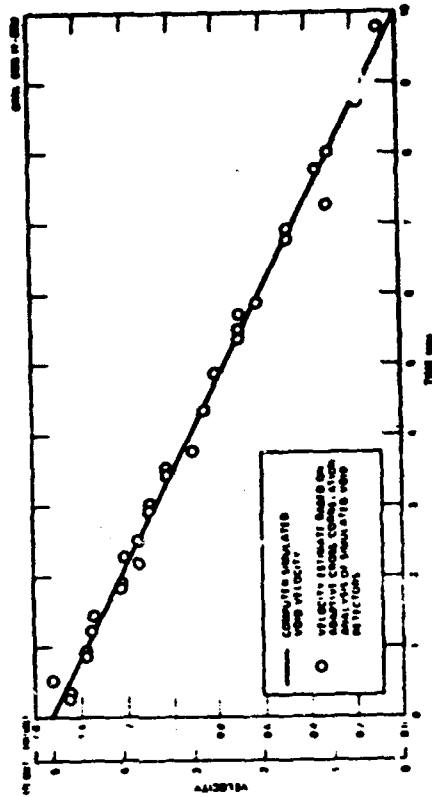


Fig. Test of adaptive cross-correlation algorithm using computer simulated void velocity transient (50% void detection efficiency).

SENSOR A
SENSOR B
FLOW
AIR BUBBLES
AIR
WATER
TIME
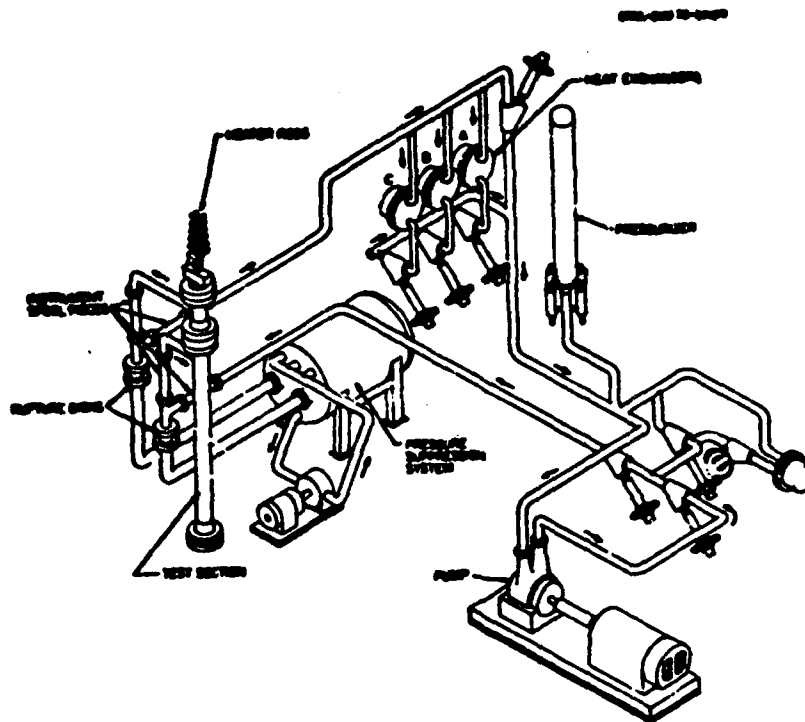
THERMAL HYDRAULIC TEST FACILITY
ORNL-PWR Blowdown Heat Transfer Separate Effects Program
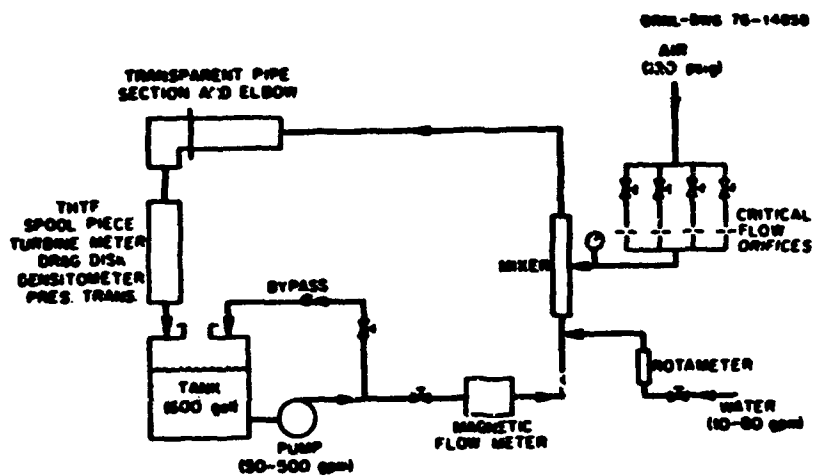


Fig. . Air-water Two-phase Flow Loop

HOMOGENEOUS ASSUMPTION

$$\dot{m}_t = \rho_a V_T$$

$$\dot{m}_t = \sqrt{\rho_a \overline{\rho V^2}}$$

$$\dot{m}_t = \overline{\rho V^2}/V_T$$

SEPARATED FLOW MODEL

$$\dot{m}_t = \alpha \rho_g V_g + (1 - \alpha) \rho_\ell V_\ell$$

$$X = \alpha \rho_g V_g / \dot{m}_t$$

### AYA MODEL

#### Turbine Meter

$$C_1 \alpha \rho_g (V_g - V_T)^2 = C_2 (1 - \alpha) \rho_\ell (V_T - V_\ell)^2$$

#### Drag Disk

$$\overline{\rho V^2} = C_3 \alpha \rho_g V_g^2 + C_4 (1 - \alpha) \rho_\ell V_\ell^2$$

#### Densitometer

$$\alpha = \frac{\rho_\ell - \rho_a}{\rho_\ell - \rho_g}$$

#### Phase Continuity

$$\dot{m}_g = \alpha \rho_g V_g$$

$$\dot{m}_\ell = (1 - \alpha) \rho_\ell V_\ell$$

I.1-29

# USNRC Sponsored Instrumentation Research
## at
## Rensselaer Polytechnic Institute (RPI)

R. T. Lahey, Jr.
Principal Investigator

The current sponsored instrumentation research at RPI can be conveniently divided into two categories.

(1) Instrumentation to be used in pressure suppression containment system experiments to determine the steam content in a steam/air flow.

(2) Two-phase flow instrumentation which can be used to determine the volumetric vapor (void) fraction.

This paper is a status report of the progress during the first two quarters of a twelve quarter program. First the facilities which have been constructed in which to develop the instrumentation will be described; then theory and/or instrumentation will be discussed. Exploratory "bench top" test results for various novel two-phase flow measurement devices will also be presented.

The first figure (Figure 1) is a schematic of the steam/air test loop. On the left-hand side of the figure, one can note that the compressed air is heated in a feedback controlled (for outlet temperature) air preheater. This preheating is done to avoid excessive condensation of the steam, which mixes with the air in a mixing tee at the bottom of the test section. The steam is produced in a pressure vessel and is piped into the mixing tee. The steam/air mixture then flows up the 3/4-inch square aluminum test section. Quartz windows are shown in the top of the test section. The infrared (IR) beams are passed through these windows to determine the steam content. Figure 2 shows the actual apparatus (with the insulation removed). The air is piped in on the right through a pressure regulator, orifice flow meter and the air preheater. The 3 kw steam generator is shown and the vertical insulated test sec-

**Preceding page blank**

I.2-1

tion is shown in place. Note the quartz windows near the top
of the test section and the platform on which to mount the
I.R. instrumentation.

The principal behind the operation of an I.R. device is
quite straight-forward. The intensity varies as

$$I_\lambda = I_{0\lambda} e^{-\kappa_\lambda x}$$

where,

$I_\lambda$ = Monochromatic intensity of the beam (photons/$cm^2$-sec)

$I_{0\lambda}$ = Monochromatic intensity if no absorbing medium
(i.e. steam) is present

$\kappa_\lambda$ = Monochromatic macroscopic cross section

$x$ = Beam length through the absorbing medium
(i.e. steam).

It is well known that steam absorbs some wave lengths ($\lambda$) much
more than others. The method used is to pass two wave lengths
($\lambda_1$ and $\lambda_2$) through the steam/air mixture. We chose $\lambda_2$ such that
it is strongly absorbed by steam and $\lambda_1$ such that it is not.
Figures 3a and 3a present the theory behind the technique.
The result is that we can directly determine the steam flow frac-
tion (y) using a two-beam I.R. device. The work during the next
two quarters will be directed toward constructing and calibrating
the I.R. device.

Let us now turn our attention to two-phase flow measurement
devices. As in the previous discussion, let us first consider
the facilities which have been constructed in which to develop
such devices. Figure 1 shows a photo of the RPI small air/water
loop. This loop is used for conceptual "bench-top" testing of
various instruments. Figure 5 is a schematic of the RPI medium
size air/water loop. It can be seen that in this loop
we only have air flow (i.e. no axial water flow). The air
is introduced into the bottom of the lower plenum through a
sparger. A dispersion plate is installed which distributes the
vapor and establishes the bubble size.

I.2-2

A Dresser coupling is installed so that various glass or plexi-glass test sections can be easily installed. Figure 6 shows this loop in operation.

Various two-phase flow regimes can be established in the one-inch I.D. test section. Figures 7a-7d show examples of: low quality bubbly flow, high quality bubbly flow, slug flow, and annular flow, respectively.

The medium size air/water loop will be the "work horse" in which the instrumentation is developed. In order to carry out this development work one needs to accurately know what the void fraction actually is so that the instrumentation under develop-ment can be properly calibrated and interpreted. The standard we have chosen is a dual beam X-ray device shown schematically in Figure 8. The basic theory behind this technique has been successfully used by others (Jones, Smith, Schrock, Staub, etc.) however, the techniques previously used to process the data were cumbersome. The theoretical basis for the experimental technique we plan to use is presented in Figures 9a-9b.

In theory, if we chose the D. C. level (I') of the reference beam correctly we can get rid of the undesirable 60 Hz ripple in both beams. It can be seen that the resulting expression for instantaneous chordal average void fraction, $a(t)$, is given by

$$a(t) = \frac{R(t) - R_L}{R_G - R_L}$$

where the R are log ratios of the test section and reference beams. This simple linear form suggests an easily calibrated circuit design.

Figure 10 is a schematic of the electronics systems. It can been seen that it follows the logic flow presented in Figures 9a-9b. It can also be seen that not only is the instantaneous chordal average void, $a(t)$, obtained, but, by passing this stochastic signal through a time-integrating digital volt meter (DVM) the time averaged chordal average void fraction, $\bar{a}$, is also obtained.

The merit of such a system is expected to be the ease with which it can be calibrated. With a test section full of water,

I.2-3

the $R_L$ potentiometer can be adjusted until $\bar{a} = 0$. Then with only air in the test section, the $R_G$ potentiometer can be adjusted to yield $\bar{a} = 1.0$. After that one can obtain a real-time reading of $\bar{a}$ on the DVM.

This calibration must be done at each transverse position, but it is expected that this electronic design should greatly speed-up data acquisition.

In addition to $\bar{a}$ we are also interested in looking at the statistical information in the void signal to see if we can develop a criterion for interpreting the signature of various flow regimes. In order to accomplish this the stochastic $a(t)$ signal is passed through a low pass filter having a 100 Hz break frequency. The purpose of this filter is to reject unwanted high frequency noise and to avoid aliasing errors when the signal is digitized.

It is planned that the probability density function (PDF) will be accumulated in a multichannel analyzer (MCA). The PDF will be taken, via paper tape output, to a PDP-15 computer for further analysis (e.g. determination of the moments). In addition to the PDF, the power spectral density function (PSD) will also be constructed. This will be accomplished by digitizing the signal with an (ADC) analog-to-digital convertor, and Fourier transforming the signal with a FFT algorithm on the PDP-15 data acquisition computer.

Now that we have discussed the facilities in which to develop multiphase instrumentation, and the X-ray standard against which the measurements will be calibrated, we are ready to discuss various two-phase instrumentation under development at RPI.

Figure 11 is a schematic of a visible red (V.R.) test apparatus. This device was pulsed at 53 KHz and passed through the transparent test section in the small air/water loop. The top view of the oscilloscope trace shown in Figure 12 shows the basic signal (on an expanded time scale) when only water is in the test section. The middle and bottom figures show how the basic signal was modulated by low quality bubbly flow and high quality bubbles flow respectively. It can be seen that the signal is

I.2-4

attenuated by bubbles and is very sensitive to voids.

Figure 13 is a schematic of an experiment to determine why bubbles cause I.R. beam attenuation (i.e. how much intensity loss is due to refraction and how much by reflection at the interface. Four I.R. transmitter - sensor units are shown. One test was run in which unit #1 was illuminating unit #2. In this test we were looking for I.R. beam attenuation and scattering (i.e. refraction and reflection) on the various units shown.

Figure 14 shows the actual unit in place. Near the top of the test section can also be seen a local probe which we will discuss shortly.

Figure 15 shows the oscilloscope trace of the various I.R. units. For low quality bubbly flow we had fine (~1/32 inch in diameter) air bubbles, and for higher quality bubbly flow, we had medium size (~3/16 inch in diameter) bubbles. Note in the two top figures in figure 15 that the presence of bubbles attenuate the I.R. beam, thus, since the exponential attenuation gets less (i.e. air has a much smaller macroscopic cross section than water), we are seeing the effect of scattering. Obviously the sensor in unit #4 has I.R. scattered in but this does not appear to be correlated with the scattering which occurs on bubbles in the main (1-2) beam.

In the lower left picture of figure 15, the 1-1 back scattering signal is shown. Surprisingly sensor #1 is normally illuminated and any scattering apparently causes a loss in illumination. The reason for this is not clear at the present time. The final picture on Figure 14 shows that there is very little scattering into sensor #3.

It is clear that we do not have isotropic scattering by the bubble. It is also clear that further, single bubble experiments are needed to quantify the scattering mechanisms. One likely test apparatus for further testing is shown in Figure 16.

Several local probes are under development. Figure 17 shows a new frequency modulated impedance (Z) probe. The probe itself is constructed from gold alloy wires inserted in a ceramic tube. Gold is used to avoid possible corrosion problems. The probe

forms an active element in the oscillator circuit. When the
probe is in water a lower frequency pulse is observed than when
it is in the vapor phase (in the case shown 625 Hz for water and
769 Hz for air, although these frequencies can be set as high as
you like). These pulses are picked up by a phase-locked-loop (PLL)
which sends out a signal of 5 volts for the air frequency and 0
volts for water. This technique is known as frequency-shift-keying
(FSK) and is known to be rather insensitive to minor pulse fre-
quency changes. This implies that the probe may not be sen-
sitive to water purity and temperature changes, a highly desirable
feature for a local Z probe. Finally, as shown in Figure 17, the
count statistics can be quite accurate since the lobes of the
square wave coming out of the PLL can be filled with high frequency
pulses using a pulse generator. The signal is then passed
through a single channel analyzer which determines the number of
counts in air ($N_{air}$).

The final probe to be reported on is shown in Figure 18.
The probe itself is the same as that used in the Z probe tests.
The difference is how the probe is excited. In this case the
probe is driven by a radio frequency (RF) generator. This genera-
tor is coupled to the probe through a tuned passive circuit. The
probe is a capacitive element in this circuit. In the case shown,
the circuit has been tuned to 17 MHz, although this is quite
arbitrary. If the RF generator is set at 17 MHz then we have no
indication of phase. Instead, if we set the RF generator
below 17 MHz (e.g. 16 MHz), we get pulses when we have bubbles
hitting the probe. In contrast, if we set the RF generator above
17 MHz (e.g. 18 MHz) the vapor phase causes a reduction in carrier
amplitude. Actually scope readings are shown in Figure 19.

The RF probe is also expected to be quite insensitive to
water purity and temperature and, due to the high frequency,
should have quite accurate count statistics.

STEAM GENERATOR

PRESSURE GUAGE

CONDENSATE COLLECTOR

3/4" I.D. COPPER TUBE

TEST SECTION

TOP FLANGE

WINDOW

COPPER TUBE

3/4" I.D. COPPER TUBE
(STEAM LINE)

WATER FILL LINE

UPPER WATER
LEVEL CONDUCTOR

LOWER WATER
LEVEL CONDUCTOR

INDICATOR
LAMP

CONTROL
BOX

HEATER GRID

FROM EXTERNAL
WATER SUPPLY

THERMOCOUPLE

AIR PREHEATER

1/4" COPPER TUBE

HEATER CONTROL

EXTERNAL POWER SUPPLY

ORIFICE

MANOMETER

FROM AIR COMPRESSOR
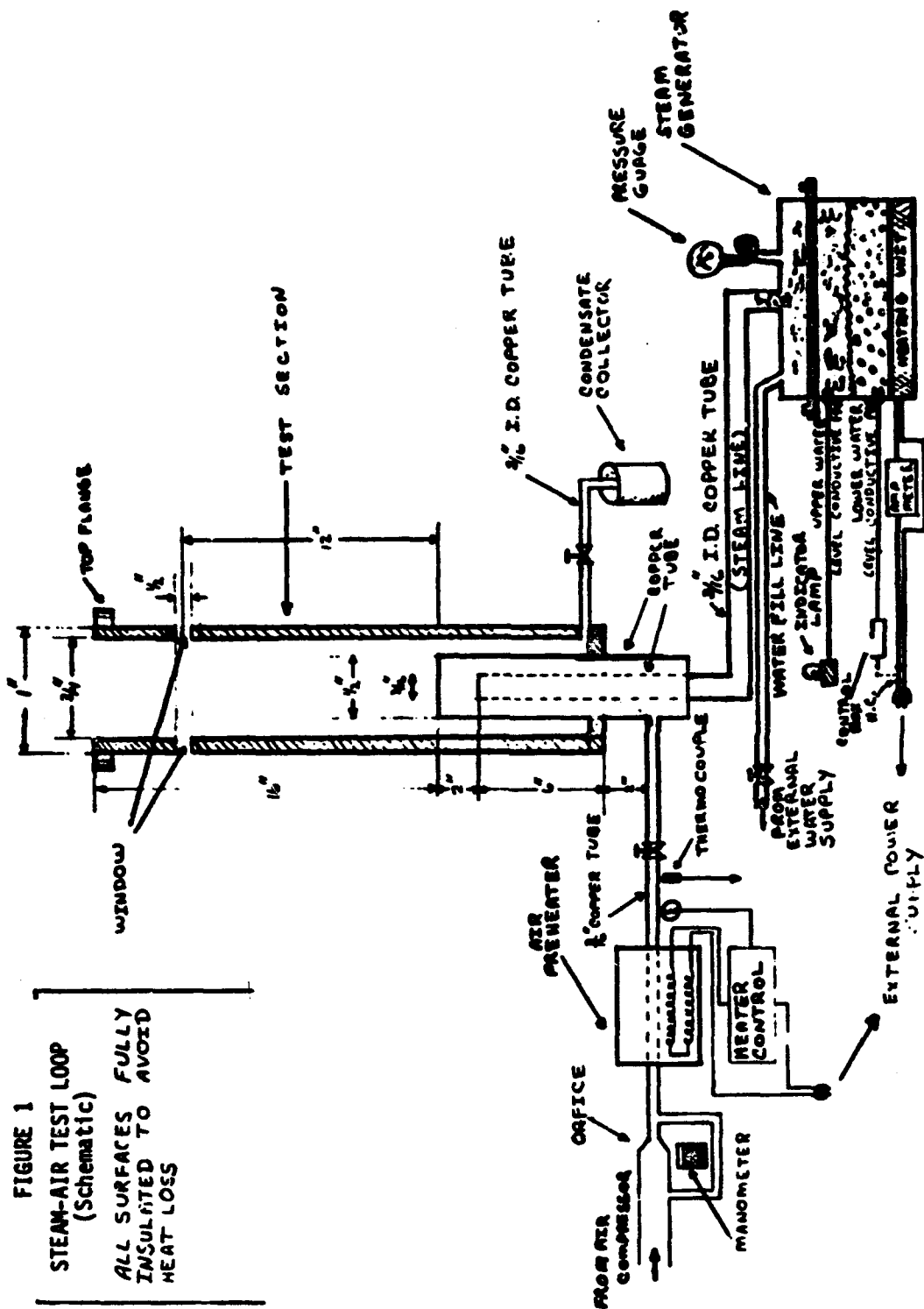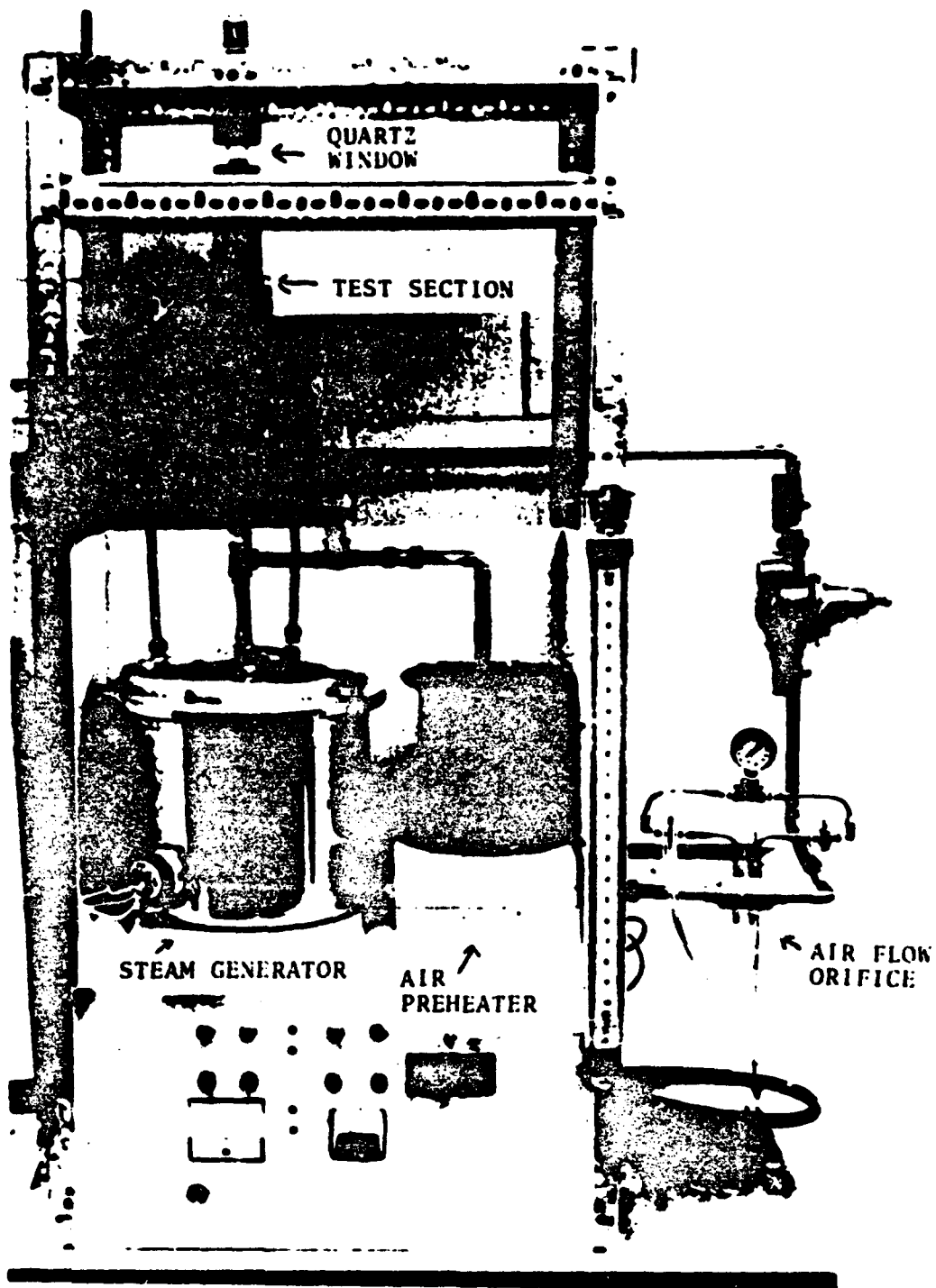
FIGURE 2
STEAM/AIR TEST LOOP

I.2-8

## DETERMINING STEAM/AIR RATIO BY I.R. TECHNIQUES

(For $\lambda_1$)　$I_1 = I_{o_1} e^{-\mu_1 x}$ $\qquad\qquad\qquad$ (1)

(For $\lambda_2$)　$I_2 = I_{o_2} e^{-\mu_2 x}$ $\qquad\qquad\qquad$ (2)

Taking log of Equations (1) and (2), and subtracting

$$\ln(I_1/I_2) = \ln(I_{o_1}/I_{o_2}) + (\mu_2 - \mu_1)L. \qquad\qquad (3)$$

where:

$$\mu_i = \frac{N_o \rho_i}{A_i} \sigma_i \qquad\qquad\qquad (4)$$

$$I_{o_{\lambda_1}} = I_{o_{\lambda_2}} \quad \text{(when no steam)} \qquad\qquad (5)$$

Equations (3) and (4), with the assumption $\sigma_1 = 0$ (i.e., $\mu_1 = 0$), yield:

$$\left(\frac{N_o}{A_2}\sigma_2\right) \rho_2 = \frac{1}{L} \ln(I_1/I_2)$$

or,

$$\rho_2 = \frac{A_2}{N_o \sigma_2 L} \ln(I_1/I_2) \qquad\qquad\qquad (6)$$

Thus,

$$\rho_{steam} = r \ln(I_1/I_2) \qquad\qquad\qquad (7)$$

Recalling Dalton's Law:

$$P = P_{air} + P_{steam} \qquad (8)$$

$$P_{steam} = \rho_{steam} R_{steam} T_{sat} \qquad (9)$$

Combining (8) and (9):

$$P_{air} = P - \rho_{steam} R_{steam} T_{sat} \qquad (10)$$

But,

$$P_{air} = \rho_{air} R_{air} T_{sat} \qquad (11)$$

Thus, combining (10) and (11):

$$\rho_{air} = \frac{1}{R_{air}} \left[ P/T_{sat} - \rho_{steam} R_{steam} \right] \qquad (12)$$

The steam/air fraction (y) is:

$$y \triangleq \frac{\rho_{steam} U_{steam}}{\left| \rho_{air} U_{air} + \rho_{steam} U_{steam} \right|} \qquad (13)$$

assuming $U_{steam} = U_{air}$,

$$y = \frac{\rho_{steam}}{\left| \rho_{air} + \rho_{steam} \right|}. \qquad (14)$$

Equations (7), (12) and (14) yield the required result.
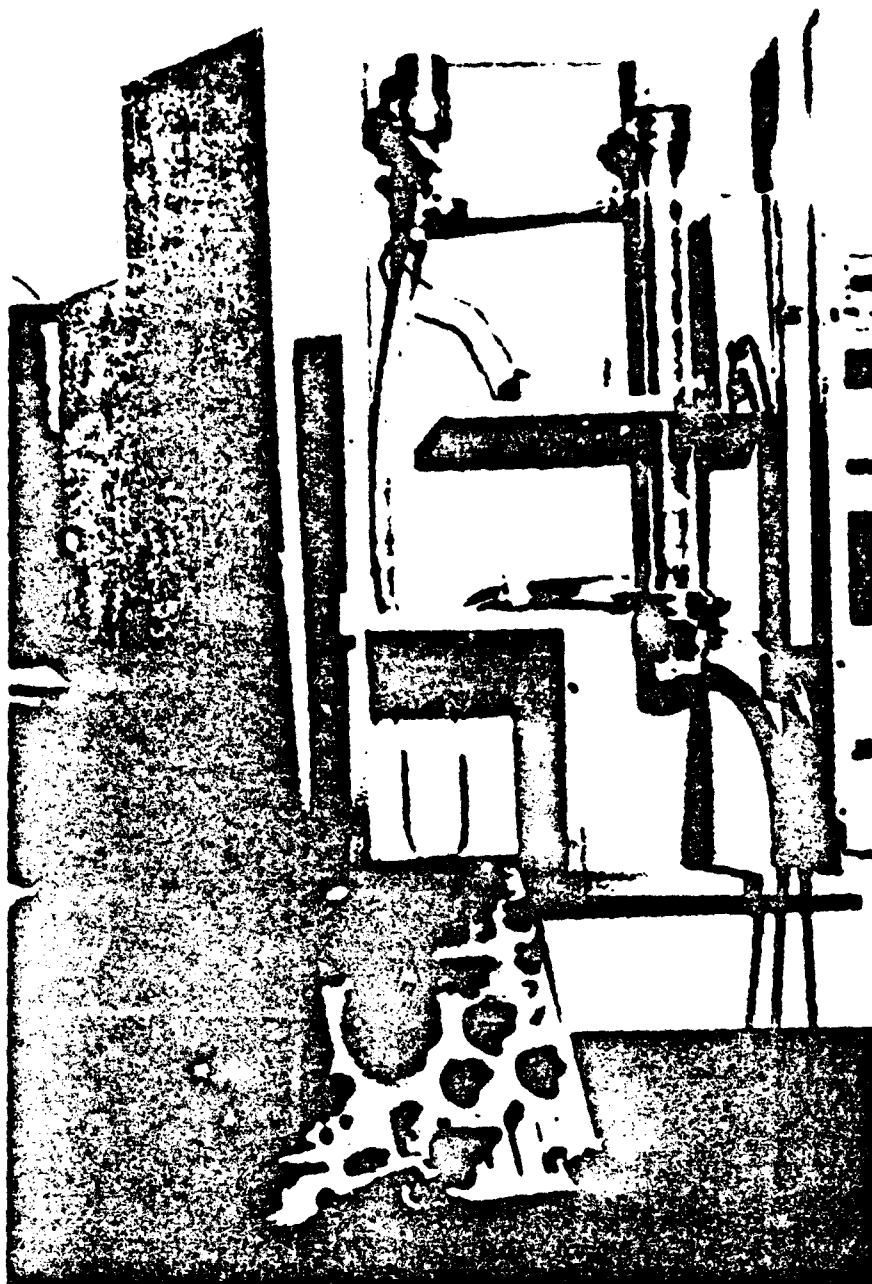
Figure 4

Small RPI Air/Water Loop

I.2-11

FIGURE 5
MEDIUM AIR-WATER
LOOP SIMULATOR

HINGED COVER

12"

10"

FILTERED
WATER
Supply

DRAIN

1 3/16" Oil Seal

1/4" Aluminum Plate,
Screwed Down

Approximate
Manometer
Hookup

6"

Test Section:
1" I.D., 1/8" Wall
Plexiglass or Glass
Tubing

REGULATED
DRY AIR
Supply

24"

DRESSER
Coupling

5"

Blocks &
Steel Band

1/2" Copper
Tubing

MACHINED TRANSISTION PIECE
1" Plexiglass

6"

PYRAMID

Dispersion Plate

4"

15"

GASKETED BOTTOM
Plate

1/2" Ball Valve

1/4" Brass Petcock

I.2-12

Figure 6
RPI MEDIUM SIZE AIR/WATER LOOP

I.2-13
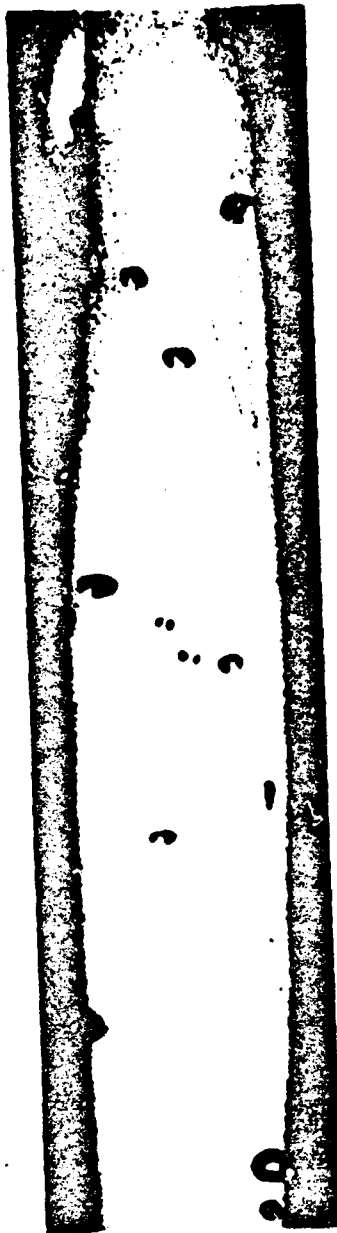
FIGURE 7a

LOW QUALITY BUBBLY FLOW

I.2-14

FIGURE 7b

HIGH QUALITY BUBBLY FLOW

I.2-15
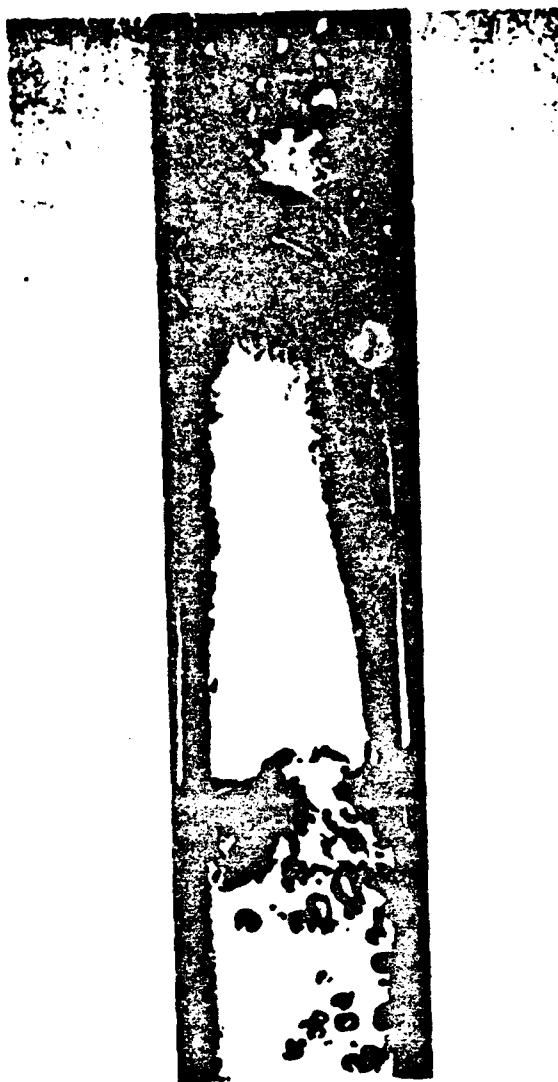
FIGURE 7c

SLUG FLOW

1.2-16

FIGURE 7d

ANNULAR FLOW

I.2-17
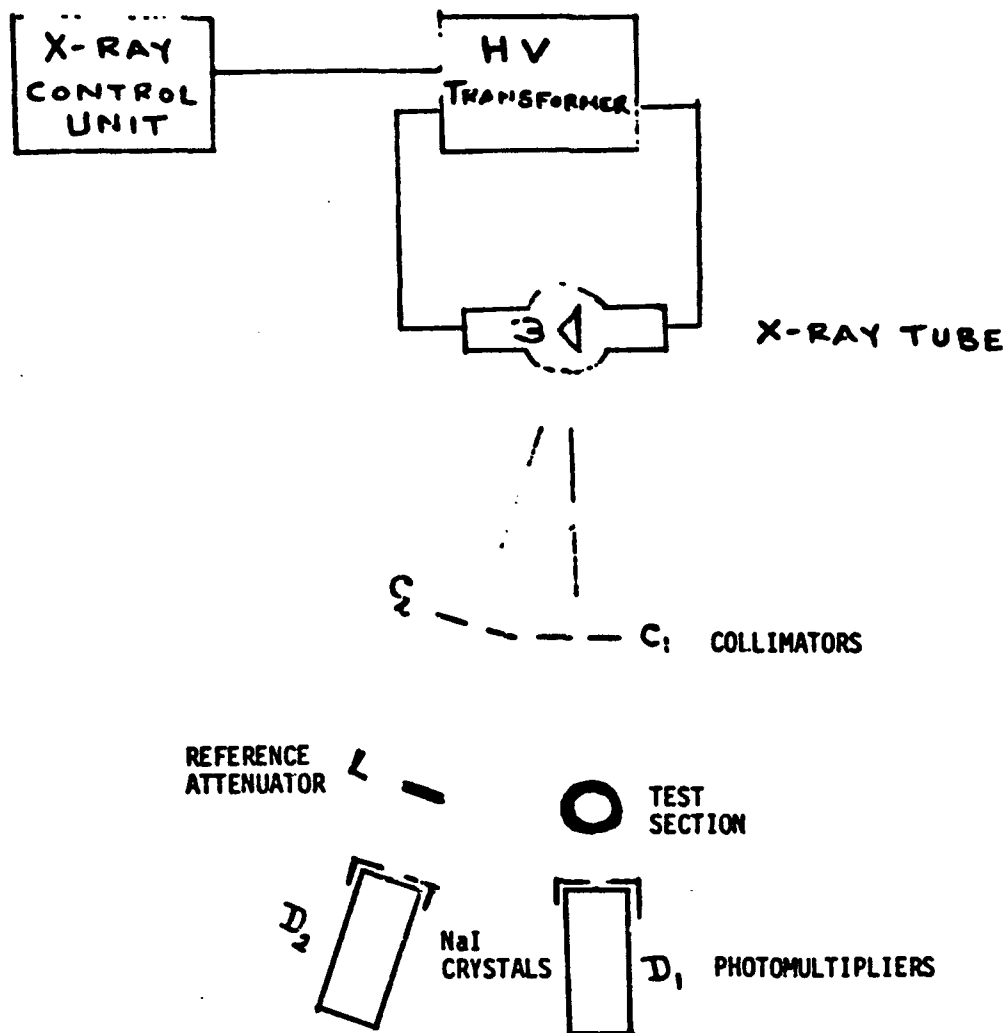
FIGURE 8

SCHEMATIC OF X-RAY EQUIPMENT

I.2-18

## FIGURE 9a

### DERIVATION OF
### VOID FRACTION EQUATION

**IN GENERAL:**

$$I(t) = I_o e^{-\mu x(t)}$$

**FOR THE TEST SECTION BEAM:**

(1) $A^*(t) = A(t) [ 1 + a \sin\omega t ]$

**For the Reference Beam (with D. C. Bias):**

$B^*(t) = B [ 1 + b \sin\omega t ] + D$

or,

(2) $B^*(t) = [ B + D ] [ 1 + \frac{Bb}{(B+D)} \sin\omega t ]$

taking the log of (1) and (2), and subtracting:

(3) $\ln \frac{A^*(t)}{B^*(t)} = \ln \frac{A(t)}{[B+D]} + \ln \frac{[ 1 + a \sin\omega t ]}{[ 1 + \frac{Bb}{(B+D)} \sin\omega t ]}$

If we set the D. C. bias at,

$D = B(b/a-1$

the last term in    disappears, hence (3) can be written:

$$\ln \left[ \frac{A^*(t)}{B^*(t)} \right] = \ln \frac{[ A_o e^{-\mu x(t)} ]}{[ B+D ]} = \ln [ \frac{A_o}{B+D} ] - \mu x(t)$$

I.2-19

Thus,

$$(4) \quad x(t) = \frac{1}{\mu} \left\{ \ell n \left[ \frac{A^*(t)}{B^*(t)} \right] - \ell n \left[ \frac{A_0}{B+D} \right] \right\}$$

The chordal average void fraction is given by:

$$(5) \quad \alpha(t) = 1 - \frac{x(t)}{C}$$

where $C$ is chord length through fluid.

● For an empty pipe, $\alpha=1$, and $x=0$,

thus (4) yields:

$$(6) \quad \ell n \left[ \frac{A_0}{B+D} \right] = \ell n \left[ \frac{A^*(t)}{B^*(t)} \right]_G \overset{\Delta}{=} R_G$$

● For a pipe full of water, $\alpha=0$

Equation (5) yields:

$$(7) \quad x=C$$

and Equations (4) and (6) yield:

$$(8) \quad \mu C = R_L - R_G$$

where,

$$(9) \quad R_L = \ell n \left[ \frac{A^*(t)}{B^*(t)} \right]_L$$

Combining Equations (4), (5), (6) and (8):

$$(10) \quad \boxed{ \alpha(t) = \frac{R(t) - R_L}{R_G - R_L} }$$

FIGURE 10

ELECTRONIC SYSTEM BLOCK

DIAGRAM (X-RAY SYSTEM)



I.2-21
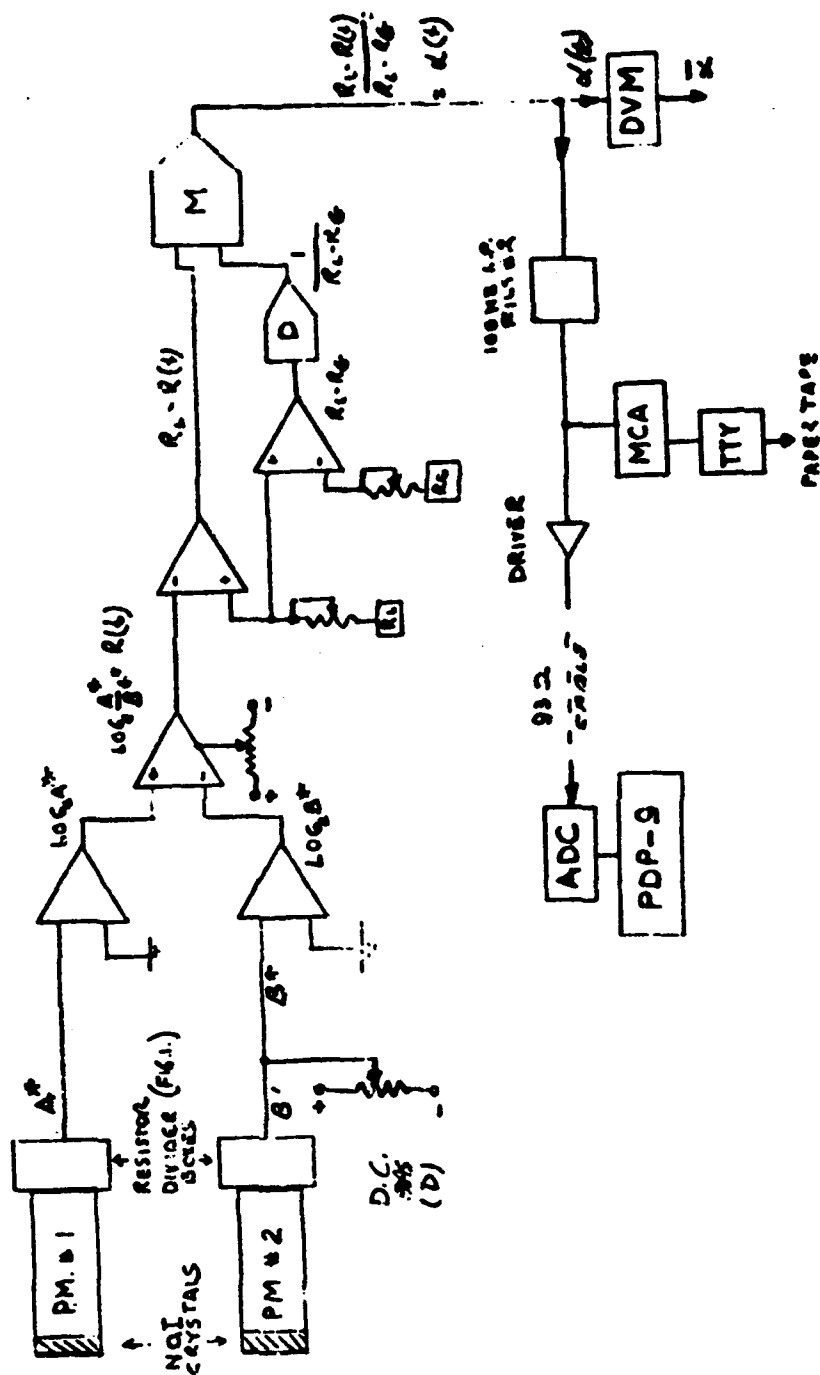
FIGURE 11

TRANSMITTER: PULSED VISIBLE RED
F = 53 KHZ

SOLID STATE
RECEIVER: SILICONE SURFACE BARRIER DET,

PREAMP, LINEAR AMP. + SCALER

DISCRIMINATOR
SCALER

N_LIQUID
(axis sig-D)

SCOPE

A

PR.

+67V

20 Meg.

38K/K

FLOW

LENS

RED
LED

Sв. WAVE
PULSE GEN
53 KHz

2M. ~~~~
0.V.

LIQUID
VARE

BUBBLY FLOW
(LOW QUALITY)

LIQUID
VARE.

BUBBLY FLOW
(HIGH QUALITY)

OSC. PICTURE OF
THE CARRIER 53.KHZ
EL.LIG.(NO FLOW)

2 V/CM.
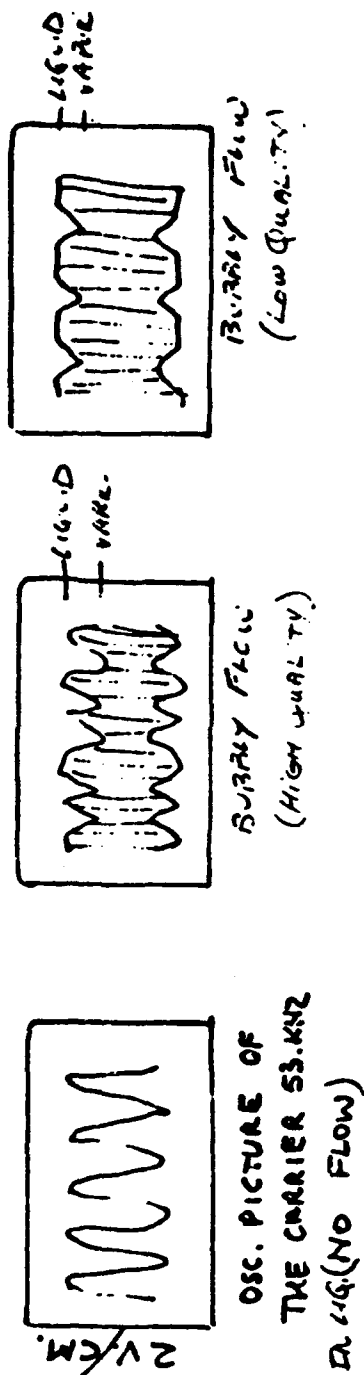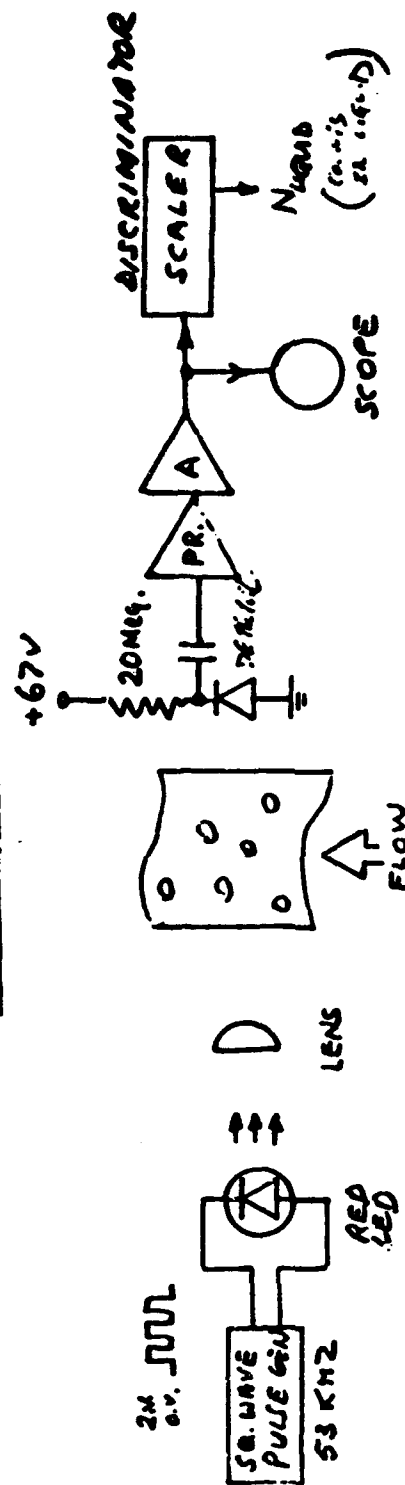
TRANSMITTER: PULSED VISIBLE RED    53 KHZ
DETECTOR: SILICONE SURFACE BARRIER DET.

LIQUID

VAPOR

BUBBLY FLOW
(LOW QUALITY)
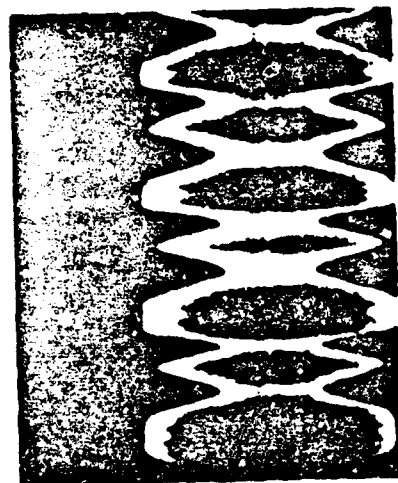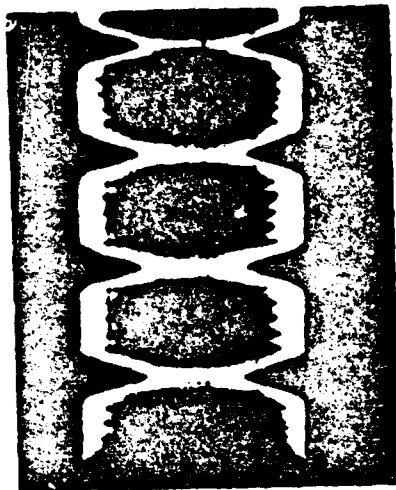
LIQUID

VAPOR

BUBBLY FLOW
(HIGH QUALITY)
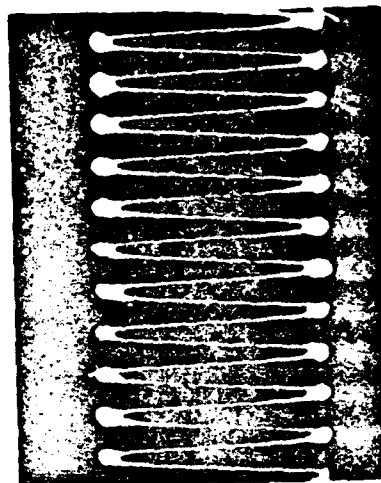
BASIC SIGNAL
(WATER ONLY)

FIGURE 12
VISIBLE RED PROBE

FIGURE 13

INFRARED ($\lambda = .94 \mu m$) TRANSMITTER & SENSOR UNIT

T = TRANSMITTER
S = SENSOR

GLASS LENS

LEXAN PIPE

I.2-24
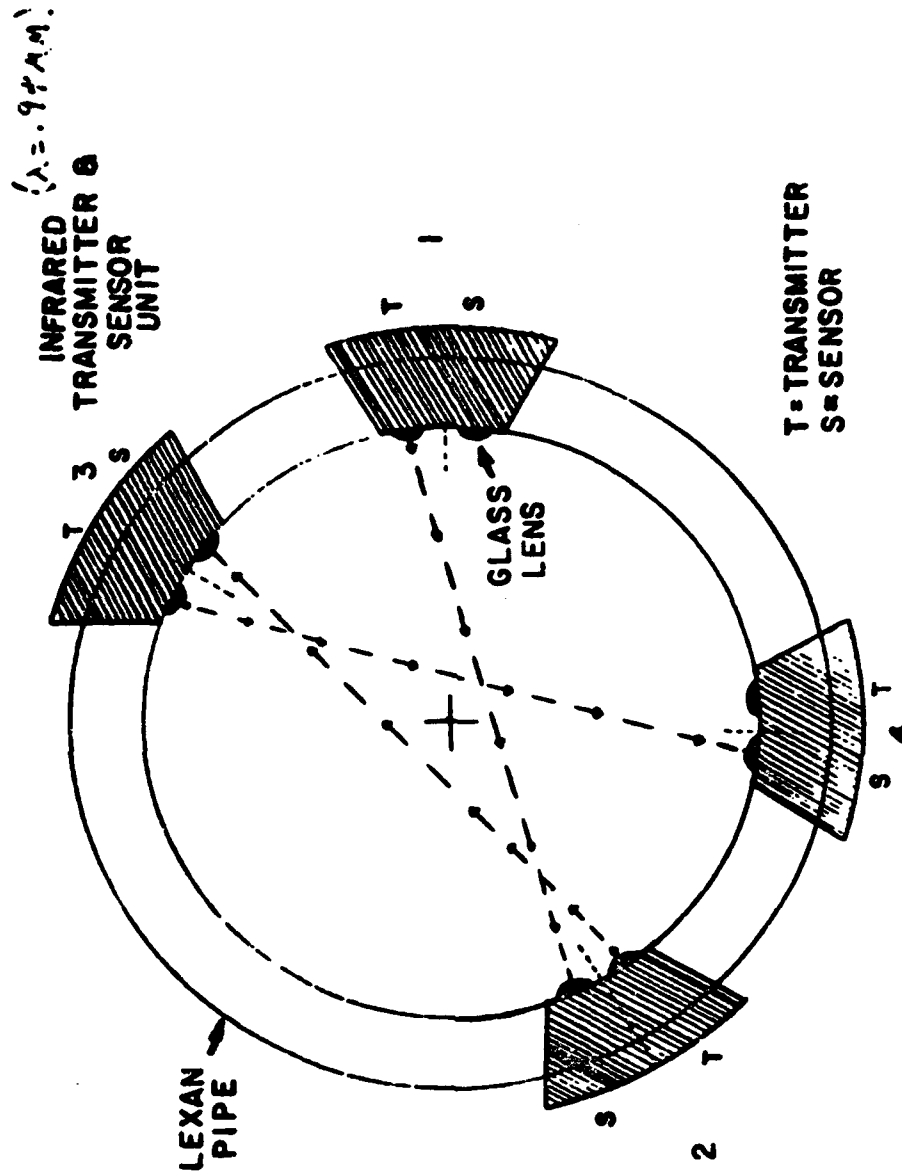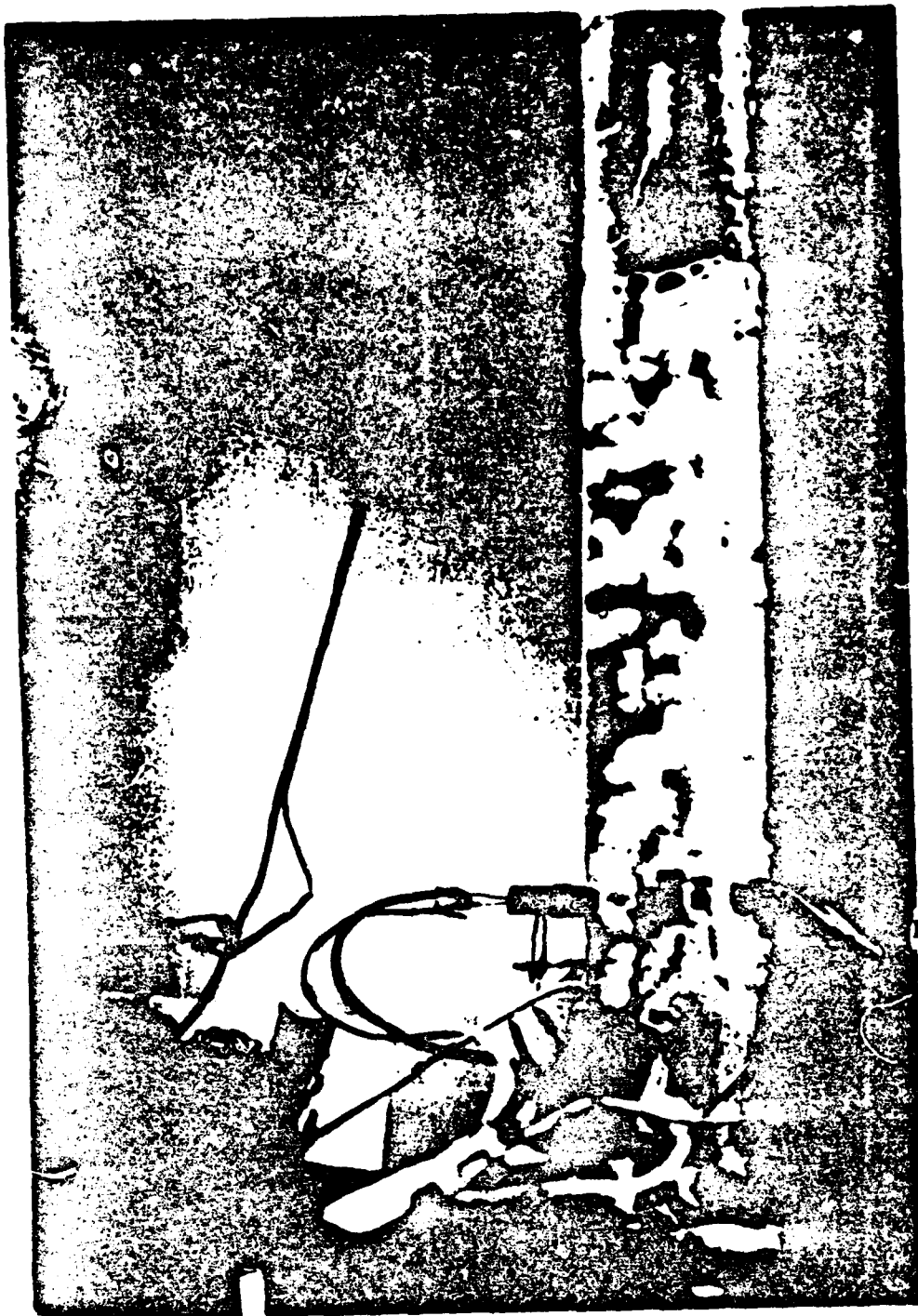
R.F./Z
PROBE

I.R. PROBES

FIGURE 14

<u>RPI</u>  SMALL AIR/WATER LOOP
SENSORS

1.2-25

BUBBLES

MEDIUM 3/16" DIA.

MEDIUM 3/16" DIA.

FINE 1/32" DIA.

MEDIUM 3/16" DIA.

I-2

I-4

I-2

I-3

I-2

I-4

I-2

I-1
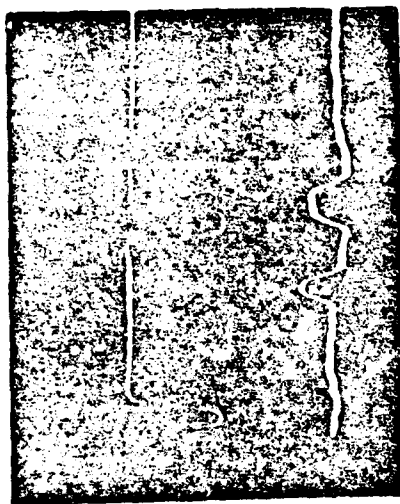
LIQUID

VAPOR

SCATTER IN

SCATTER IN

SCATTER OUT

FIGURE 15

1.2-26

LINEAR DIODE DETECTOR

SIG. OUT

10 MIL FIBEROPTICS

LEXAN PIPE

LASER DIODE

FIGURE 16

I.2-27
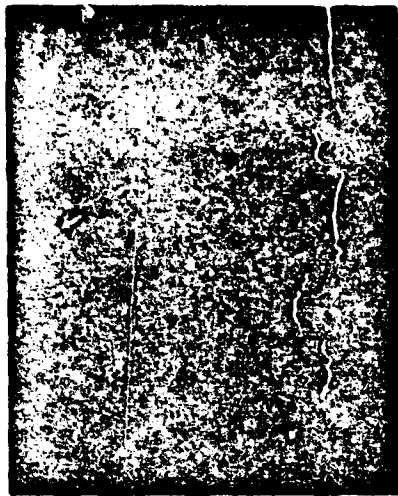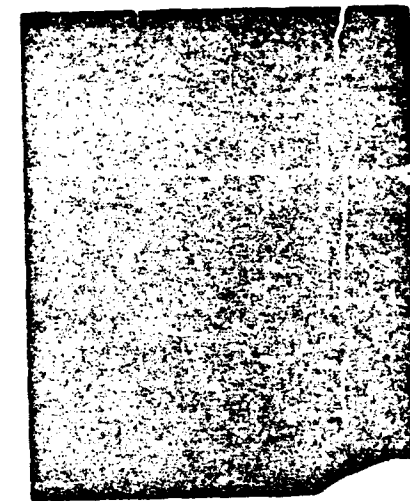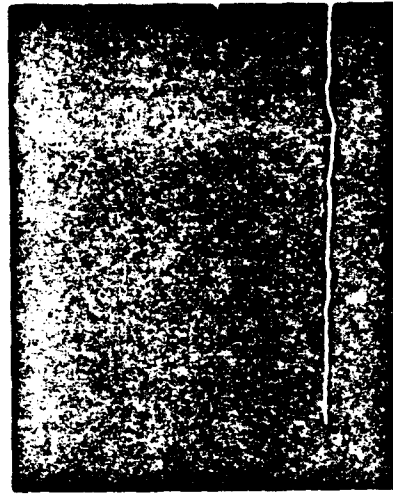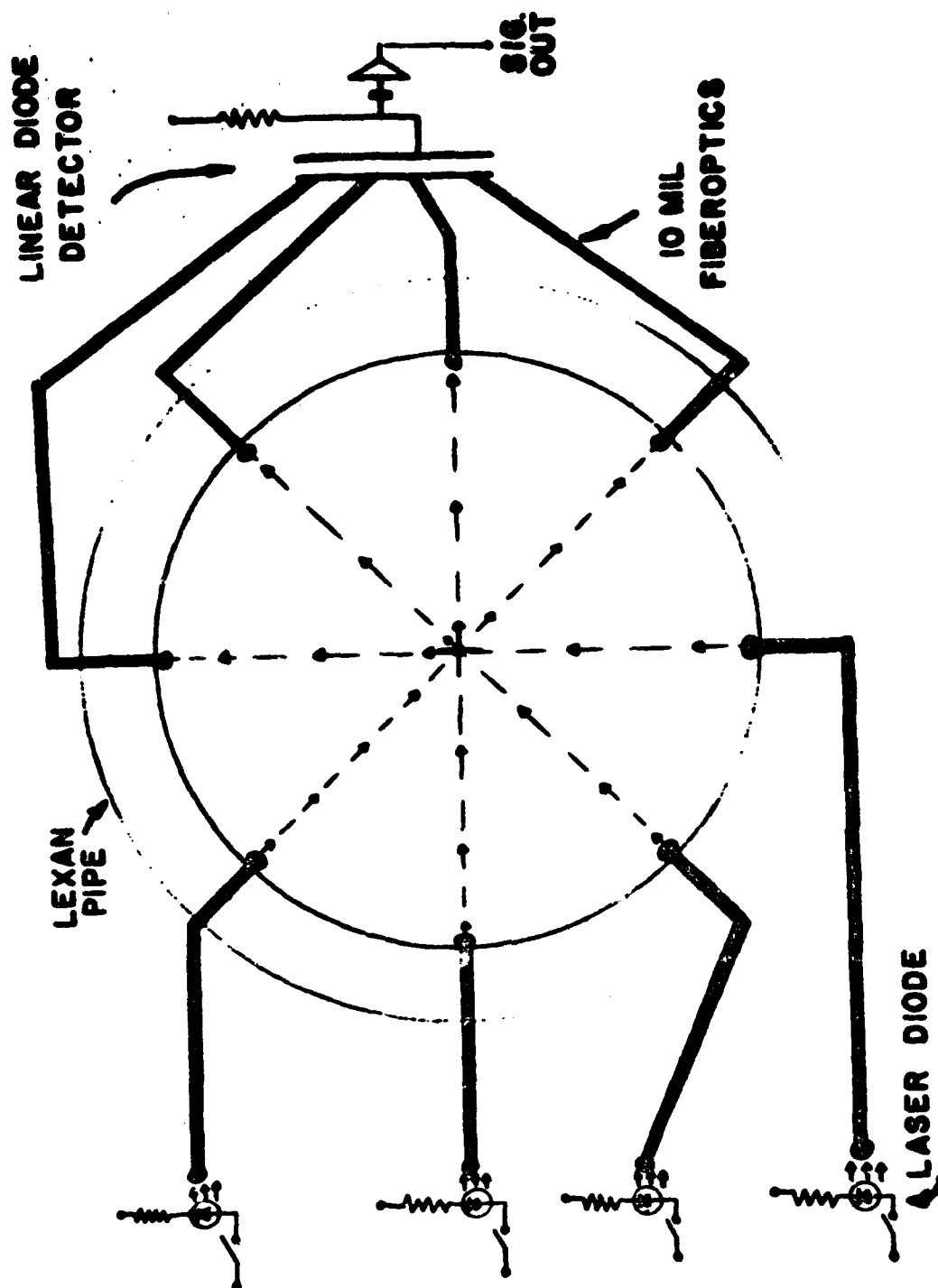
FIGURE 17

F.M. "Z" PROBE
F.S.K. (FREQUENCY SHIFT KEYING)

I.2-28
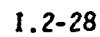
FIGURE 18
R. F. PROBE
CENTER FREQUENCY (17 MHZ)



17 MHZ

R.F. GEN

GOLD PROBE

SCOPE

VAPOR
WATER
GEN. 16 MHZ
WATER
VAPOR

CARRIER

WATER
AIR
GEN. 18 MHZ
AIR
WATER

CARRIER

I.2-29
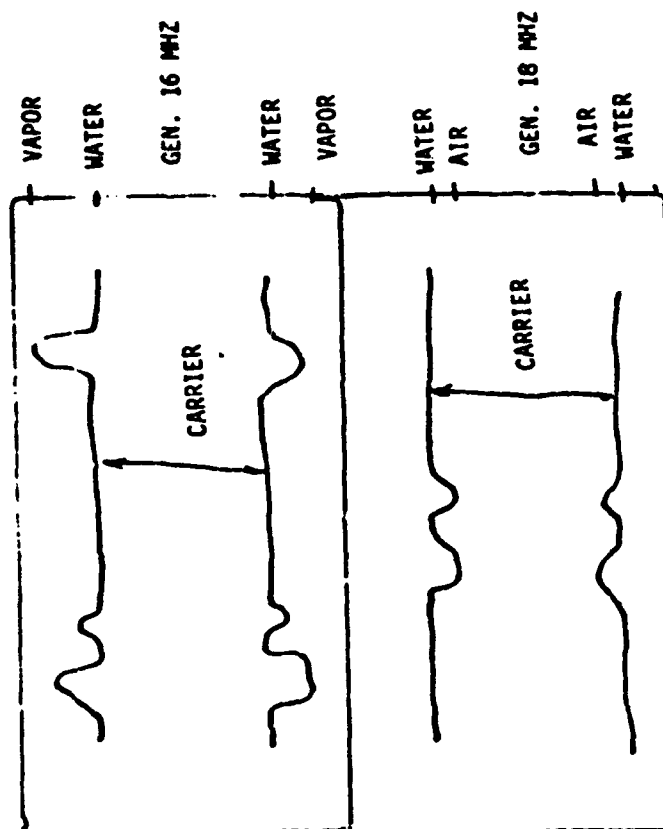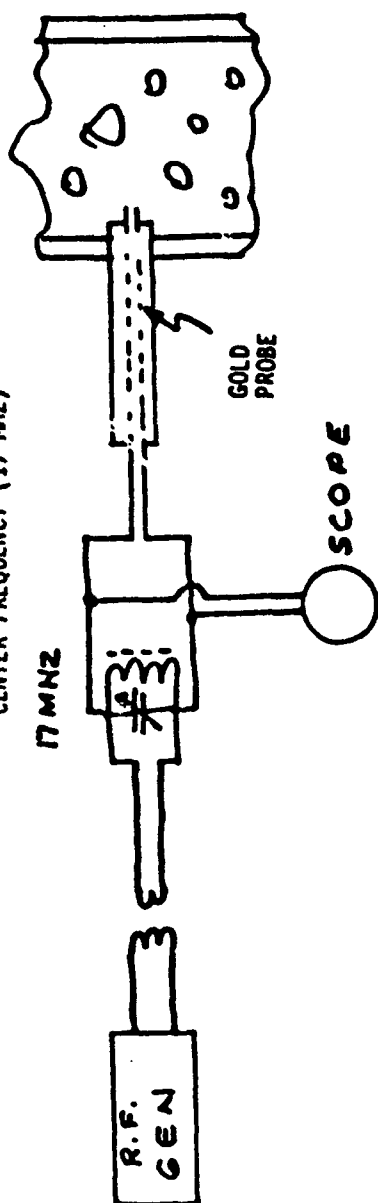
FIGURE 19

# R.F. PROBE
# CENTER FREQUENCY 17.00 MHZ



**16 MHZ**

**18 MHZ**

I.2-30
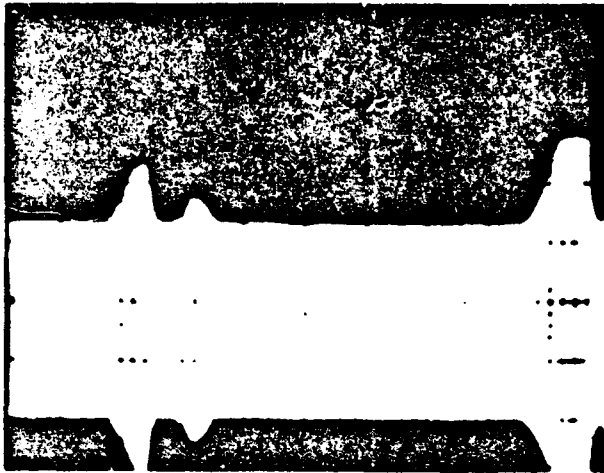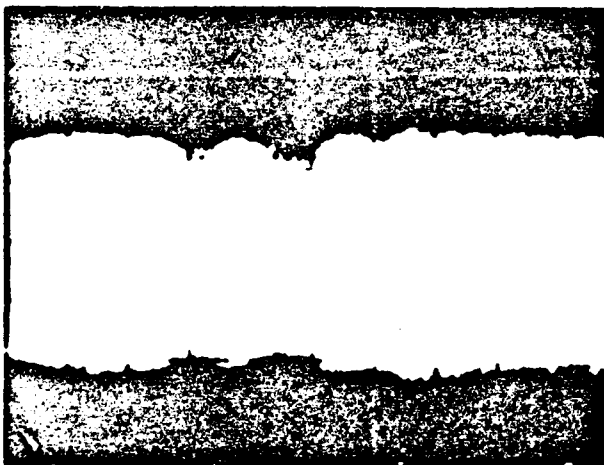
BNL Light Water Reactor Thermohydraulic Development Program:
Instrumentation Tasks

Presented by

Owen C. Jones, Jr.
Reactor Safety Programs
Department of Applied Science
Brookhaven National Laboratory
Upton, New York  11973

## ABSTRACT

A program was begun on July 1, 1977, the first part of which had as its main objective the development of analytical expressions for the non-equilibrium rates of vapor generation under various circumstances of interest in accident analysis. In support of this development effort, an experimental program is being undertaken to measure the actual vaporization rates in flashing flows.  Instrumentation is being constructed and developed in support of this effort to obtain both global and local measurements necessary to provide the desired information.   This instrumentation includes a global densitometer using radiation attenuation techniques and miniature optical probes for obtaining local information regarding vapor residence time fractions and interfacial passage velocities.  This presentation summarizes the work to date and the current status of this portion of the overall program.

## OVERVIEW OF PROGRAM

The overall program consists of two parts as shown in Figure 1: Development of Constitutive Relations; Development of Instrumentation Techniques. Task 1.1 involves the development of calculational procedures applicable to advanced confirmatory codes which will allow accurate predictions of the non-equilibrium rates of vapor generation to be made under such conditions as post-dryout heat transfer, sub-cooled boiling, downcomer condensation, and decompressive flashing. Experiments are being planned and constructed to provide a broad base of direct measurements of vapor generation in flashing flows.  This effort is identified in Tasks 1.2 and 1.3.  In support of this experimental program, certain two-phase instrumentation methods are being developed.  Development of these techniques

constitutes Part 2 of the overall program and it includes both local and global instrumentation. The global instrumentation of direct application to the current experiments includes the global densitometer which is based on gamma-attenuation techniques, and involves no major extension of previously existing technology. The local instrumentation required for measurement of local void time fractions and interfacial passage velocities, involves extension of existing methodology into conditions beyond those of current application. These conditions include both the application to higher temperature flows and higher speed flows than have been encountered in previous investigations.

In addition to the instrumentation development work of direct support to the current experiments, longer term goals of analytical and experimental evaluation of global instrument techniques applicable to LOFT/semi-scale type instruments are included in this program. Work in this vein, however, is not expected to begin until after fiscal 1977.

## IDEOLOGY

The experimental measurements are designed to provide information for direct determination of the volumetric rate of vapor generation, $\Gamma_v$, in flashing flows in ducts. In order to do this use is made of the continunity equation for the vapor phase given by

$$\frac{\partial <\alpha \rho_v>}{\partial t} + \frac{\partial <\alpha \rho_v V_v>}{\partial z} = \Gamma \tag{1a}$$

or alternately, the continuity equation for the liquid phase given by

$$\frac{\partial <(1 - \alpha)\rho_\ell>}{\partial t} + \frac{\partial}{\partial z} <(1 - \alpha)\rho_\ell v> = \Gamma_l = -\Gamma_v \tag{1b}$$

Under steay-state conditions, it is seen that the determination of the actual volumetric rate of vapor production involves both the measurement of the local phase volume fraction as well as the local phase velocity, which is then integrated over the cross-sectional area to obtain cross-sectional averaged values. These values must then be obtained at different axial locations so that effective determination of the axial gradient of the phase mass flux can be determined. In actual practice, especially at low reduced pressures, interfacial velocities will most nearly follow the liquid velocity as a result of the interfacial mass balances. That is, the vapor produced must move away from an interface with a

I.3-2

Velocity proportionately higher than the liquid velocity coming into the interface due to the density ratio of the two phases. It is easily seen that if $G_{\ell v}$ is the evaporative mass flux, the liquid and vapor velocities in terms of the interfacial velocity are given by

$$v_\ell = v_s + \frac{G_{\ell v}}{\rho_\ell} \tag{2a}$$

and

$$v_v = v_s + \frac{G_{\ell v}}{\rho_v} \tag{2b}$$

It is thus seen that the liquid velocity varies little from the interfacial velocity while the vapor velocity varies greatly from the interfacial velocity because of the much lower density. For practical purposes of measurement, Equation (1a) may be written in the steady state as

$$\Gamma_v = G \frac{dx}{dz} \sim G \frac{(x_2 - x_1)}{(z_2 - z_1)} \tag{3}$$

for the case of a constant area duct. The errors involved in determination of $\Gamma_v$ are thus associated with errors in determination of the mass velocity, quality, and axial positions at which the quality is determined. We must in effect measure the axial quality gradient. The relative standard deviation in the vapor generation rate is thus given by

$$\frac{\sigma_{\Gamma_v}}{\Gamma_v} = \left\{ \left(\frac{\sigma_G}{G}\right)^2 + \frac{\sigma_{x_1}^2 + \sigma_{x_2}^2}{(x_2 - x_1)^2} + \frac{\sigma_{z_1}^2 + \sigma_{z_2}^2}{(z_2 - z_1)^2} \right\}^{1/2} \tag{4}$$

where if both the mass velocity and the actual positions are accurately known, the largest source of error occurs in the measurement of the quality itself. In terms of the volume fractions and velocities, the quality may be given as

$$x = \cfrac{1}{1 + \cfrac{1 - \alpha}{\alpha} \cfrac{\rho_\ell}{\rho_v} \cfrac{v_\ell}{v_v}} \qquad (5)$$

such that, neglecting property errors, the relative standard deviation in the quality is given by

$$\frac{\sigma_x}{x} = \left\{ \left(\frac{1-x}{1-\alpha}\right)^2 \left(\frac{\sigma_\alpha}{\alpha}\right)^2 + (1-x)^2 \left(\frac{v_r}{v_g}\right)^2 \left[\left(\frac{\sigma_{v_r}}{v_r}\right)^2 + \left(\frac{\sigma_{v_\ell}}{v_\ell}\right)^2\right] \right\}^{1/2} \qquad (6)$$

The results of Equation (6) are plotted in Figure 2. It is seen that in the range of atmospheric pressure to 450 psi that even for quite large values of relative velocity, $v_r$, the error in quality determination can be maintained at a relatively low level providing the relative standard deviations in the measured void fraction and liquid velocities are kept low.

## METHODOLOGY

The methods to be used in measuring the non-equilibrium vapor generation rates in flashing flows are based directly on the previously described ideology. That is, we intend to provide a method for establishing a steady circulation of water at a well controlled level of temperature and flow, and utilize a test apparatus inserted in this circulation loop which allow determination of the flashing conditions under the following requirements:

a) Minimum power requirements;

b) local information may be obtained;

c) global reference data may be obtained;

d) minimum effects due to upstream instrumentation disturbances.

In addition to the loop and the test section, suitable sensing devices must be provided to yield the appropriate information regarding phase volume fraction and velocities, and suitable methods must be developed for handling and analysis of the signals derived from the instrumentation. Each of these items shall be discussed in turn below.

## Test Facility

A schematic diagram of the test facility to be used in these experiments is shown in Figure 3. This test facility is patterned after the MOBY DICK loop currently '- use at CENG. The facility is being designed and constructed for maintainii .ie appropriate circulatory conditions with static temperature and pressure ratings of 150 psi at $350^\circ$ F.

Status of the test facility to date is as follows

a) The major test facility modules are on hand including pumping modules, heat exchangers, water purification system, water filtration system. steam drum, control panels, and miscellaneous valves and fittings;

b) The thermodynamic design is approximately 80 to 90% complete;

c) the component interconnection design is approximately 50% complete.


## Signal Analysis System

The signal analysis system is shown schematically in Figure 4. This system is a mini-computer based system which will acquire slow speed and intermediate speed information directly, and will acquire high speed information through play-back of previously recorded analog tape data at a reduced speed. In the design of this system, emphasis has been placed on capability for future expansion, rapid turn-around and quick visual display of acquired information, and interactive flexability with users. The system will operate in a real time, multi--user, multi-program environment, which will allow for simultaneous development of different capabilities by more than one user. It is intended that the calculational and operational capabilities of the HP-5451B Fourier analyzer will be emulated.

The status of this system is as follows:

a) Honeywell 9600, 4MHZ tape recorder ha: been received, checked out, and is operational;

b) The digital sys.em control and display modules have been received, intergrated, and are operational;

c) Driver design and development is in progress;

d) The multi-user, real time operating system is operational;

e) The specifications for potential vendors of the multiplexed analog digital conversion system are under study.


I.3-5

## Test Section

Schematic diagrams of the test section are shown in Figures 5 and 6. It is seen that this test section involves a converging-diverging region through which a probe rake having a number of local probes can traverse the test section in both radial and axial directions. While relatively simple in concept, the test section is quite complex in execution and major development efforts are associated with the probe rake itself, the pressurized linear flow seal, and the positioning slide mechanism, as well as methods for mechanical support yielding minimum obstruction to the gamma-densitometer.

## Global Densitometer

A bidirectional, scanning, gamma-densitometer is being designed to provide reference information for the local void fraction measurements which are known to be inaccurate by as much as 10 to 15%. The local measurements will be corrected by comparison with the global measurements. The designs specifications for the gamma densitometer are as follows:

a)  multi-beam capability with radial coverage for pipe sizes up to 2 inches

b)  transient accuracy shall be within 5% for any 1.0 m sec time slice

c)  output shall be linear with fluid density within + 2%

d)  The maximum steady-state error shall be 2%

e)  axial scanning capability will be 24 inches

f)  transverse scanning capability will be over 6 inches

g)  a calibration mode shall be included in the device

h)  the maximum source--detector distance shall be 4 inches

Design studies of the system have been completed to date. For the test section geometries shown in Figures 5 and 6, the energies have been optimized to the 30-35 Kev range. Since no suitable nuclear sources exist in this exact range, an iodine or thulium source shall probably be used. The detection system shall be based on cadmium-telluride detectors used in the pulsed mode with pulse-to-volt conversion and logarithmic linearization of the signal.

## Local Probes

The local detection of phase volume fraction and velocity shall be measured using dual optical probes in a set up similar to that shown in Figure 7. Because it is expected that under intermediate and high speed, two-phase flow conditions the phase structure will be quite amorphous, a high interfacial passage frequency

is likely. If, for instance, a pair of liquid vapor interfaces seperated by a distance of 0.5 mm passes by the sensor at a velocity ⁻1 m/s, the pulse-width is 10 ums. By examination of the Fourier represer. .n of a square wave having dominant frequencies of 100 khz, it is seen that unoistorted recording of the 20th harmonic is necessary to obtain accurate zero and unity crossing times within approximately 3%. Transient measurement and recording capabilities flat to 2.0 Mhz are thus seen to be required, indicating measurement bandwidths of 4.0 Mhz. As a result, attention must be paid to the fine details of interaction of the probes with the flow structure itself. The schematic design shown in Figure 7 attempts to minimize these interactions.

The optical sensor design currently being pursued is based on the joining of two rectangular optical wave guides having been previously beveled at the end to an angle of 45° with respect to the axis of the wave guide. The resultant 90° angle at the tip of the probe will thus have the capability of reflecting light back through a second, seperate wave guide from the source wave guide, and having a very narrow zone of fluid interaction with a high degree of rejection of light sources external to the sensor tip itself. The ideal signals are shown in the lower half of Figure 7. The phase volume fraction is obtained by a simple time average of the ideal signal, while the interfacial passage velocity is obtained by determining the time lag for the interface to pass between the two sensors seperated by a known distance. In practice, since the leading probe may also act as a nucleation source of suffficient intensity to mask the inuividual transient time information, it may prove necessary to utilize cross correlation between the two signals to determine this velocity on the average. This would, of course, imply the assumption of independence between passage time and interfacial velocity, or, in other words, independence between interfacial velocity and void structure. For high speed flows, this should not be a bad approximation. At this time vendors have been contacted who indicate they can supply the material. Necessary procedures to effect the shaping and joining of the individual fiber should not pose difficulties. It is expected that quotations for the specific design shall be obtained by the end of March.

With regard to the local instrumentation, there are several areas that require development to one extent or another. These are shown in Table 1 along with possible solutions being persued in each area. As far as the mechanical design is concerned, alternate designs are also being examined as shown ir Figure 8. The emph:sis in these alternate designs is mainly on producing a single fiber detector so as to minimize the internal volume requirements for the probe rake, and reduce interaction with the flow structure to a minimum. The problem, of course, in sensors of such small size, is in obtaining a suitable bifurcation method that will allow seperation of source and detector to an acceptable degree. There is no doubt that, should all previous methods fail, the U-bend sensor developed by Delhaye can be used.

With respect to the other development areas, the work effort is in various stages of progress. Methods of accounting for electronic signal distortion have been examined, and signal reconstruction techniques based on Fourier inversion processes have been tried and found to be acceptable. The methodology, shown schematically in Figure 9, simply involves the reamplification and back phase shifting of each frequency component in the Fourier spectrum of a particular signal according to the previously determined transfer function of the measurement system.

This is equilivalent to division of the signal by the complex transfer function in the frequency domain. Difficulties involved in this methodology arrise due to aliasing, frequency broadening due to the sampling frequency not being an intergral multiple of a characteristic frequency, errors due to truncation of the times series, and decreasing signal to noise ratio as the frequency component increases.

In addition to simple electronic signal distortion on the signal measurement channel, problems associated with time incoherrancies when examining correlations between two parallel channels have posed some difficulties in the past. When the auto correlation of a particular signal is examined, it is seen to have a maximum value equal to the mean square of the signal at zero time delay. If an identical signal is recorded on two parallel channels, then the cross correlation between two channels will have a maximum equal to the mean square value of the signal, (assuming identical amplification in each channel), but having this maximum occuring at a value for time delay equilivalent to the recording incoherrancy between the two channels. It is expected, then, that this recording incoherrancy can be determined within the required accuracy by a simple cross correlation of identical signals recorded on two or more channels.

With regard to the latter two development areas, hydrodynamic signal distortion, and the relation between interface and phase velocity, it is anticipated that these problems can be attacked by the use of independent global references. That is, hydrodynamic disortions lead to inaccuracies in both the phase volume fractions, and the measurement of the actual velocities. As previously indicated, the gamma-densitometer is expected to be used as an independent global reference for the local void fraction measurements. In addition to the void fraction reference, there are other references which have accuracies at least as good as that expected to obtained from the gamma densitometer. These include the actual mass flow in the test section, and the total energy flow through the test section. Since the mass velocity and energy flow are both integral values of the localized phase values, it is seen that there are two additional independent references that can be used for calibration and correction procedures should the need be determined.

SUMMARY

This presentation has summarized in general the overall purpose of the current BNL Light Water Reactor Thermohydraulic Development Program, and emphasied those particular aspects of this program involving instrumentation development. It has been shown that the development procedures are not so much ones of new methods or new techniques, but more of extension of existing methods and techniques to conditions beyond those previously investigated.

With respect to the program as a whole, the major test facility modules have been received and the design of the test apparatus is in progress. Development of the methodology to be used for obtaining the desired measurement of non-equilibrium vapor generation rates in flashing flows has determined the direction that this work has taken in both the hardware and the analytical aspects of the program. The high velocities and amorphous phase structures expected to be encountered have indicated to us that considerable attention to the details of the sensor design

I.3-8

and signal handling and analysis methodology had to be utilized. Determination of the system requirements and specifications for our long lead development items has occupied a major portion of the experimental development effort. During the next six months it is expected that the actual hardware will be obtained and the local probes required will be tested.

| DEVELOPMENT AREAS | SOLUTIONS |
|---|---|
| ● Mechanical Design | Alternate Designs |
| ● Electronic Signal Distortion | Signal Reconstruction |
| ● Recording Incoherencies | Cross Temporal Elimination |
| ● Hydrodynamic Signal Distortion | Independent Global Reference |
| ● Relate Interface to Phase Velocities | Independent Global Reference |

Table 1: Development Area for Local Probe Design

PART I:  DEVELOPMENT OF CONSTITUTIVE RELATIONS

    Task I. 1  Analytical Modeling - Non-Equilibrium Vapor Generation

        ● Effects of Heat Flux - Post CHF

        ● Effects of Pressure Change - Flashing

    Task I.2  Design and Construction of Experimental Equipment

        ● Test Facility

        ● Test Section

        ● Global Densitometer

    Task I.3  Experimental Evaluation

      Volumetric Vapor Generation in Flashing Steam-Water Flows

        ● Steady State

        ● Transient


PART II: DEVELOPMENT OF INSTRUMENTATION TECHNIQUES

    Task II.1  Analytical Modeling

        ● Local Instruments

        ● Global Instruments

    Task II.2  Design and Construction of Experimental Equipment

        ● Local Void Fraction

        ● Local Phase Velocity

        ● Global, LOFT/Semiscale-Type Instruments

    Task II.3  Experimental Evaluation

        ● Local Instruments (Part of Task I.3)

        ● Global Instruments - Provide Calibration Techniques
          (Combined with Task II.1)

          ● Steady State

          ● Transient


Figure 1:  Program and Task Overview


I.3-10

Figure 4: Schematic of Signal Analysis System



Figure 5: Schematic of the Test Section in Axial Cross-Section

I.3-12
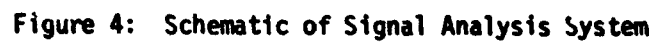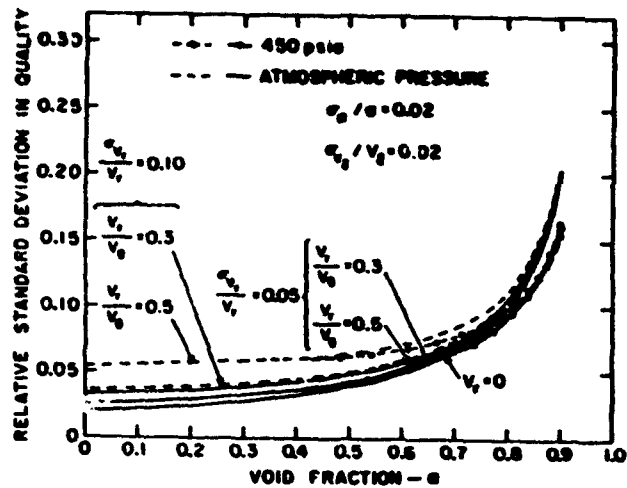
Figure 2: Relative Error in Quality Determination Due to Errors in Determining Parameters
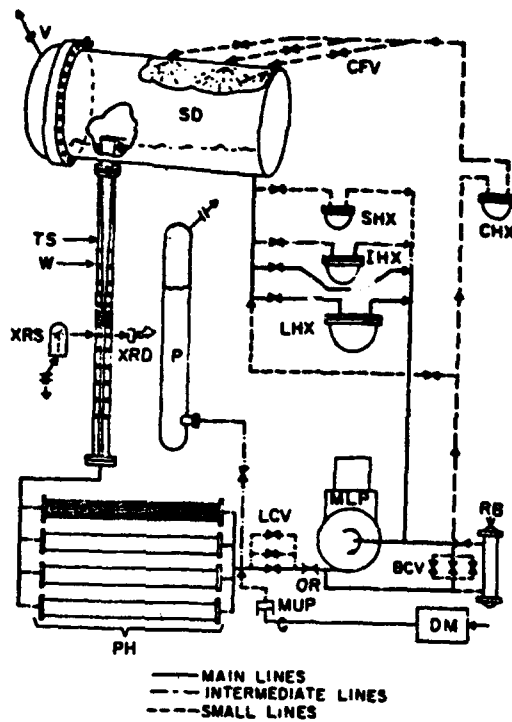


Figure 3: Schematic Diagram of the Test Facility

I.3-11

Figure 6:  Schematic of the Test

Section in Radial Cross-Section

Figure 7:  Schematic of Dual

Optical Probe System

DUAL OPTICAL PROBE CONCEPT
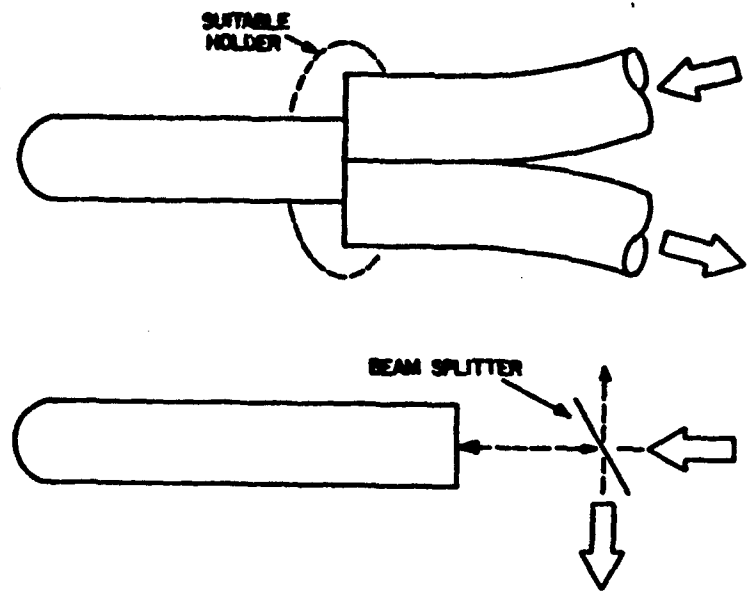
**Figure 8:  Alternate Local Optical Probe Design**
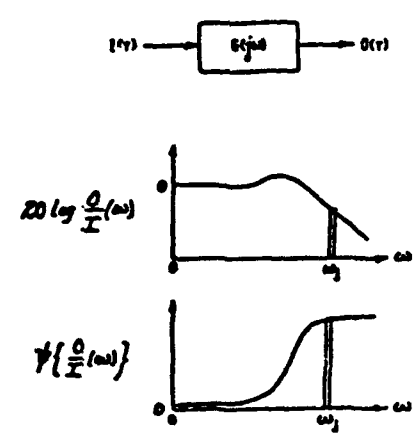


**Figure 9:   Fourier Inversion Schematic**

I.3-14

# LASER-DOPPLER ANEMOMETRY TECHNIQUE
## APPLIED TO TWO-PHASE DISPERSED FLOWS

by

S. L. Lee and J. Srinivasan

Department of Mechanical Engineering
State University of New York at Stony Brook
Stony Brook, N.Y. 11794

## ABSTRACT

The ultimate aim of this experimental investigation is to study droplet hydrodynamics under conditions simulating steam water droplet flow predicted to occur during the reflood portion of LOCA. This research will support the development of advanced systems code for which constitutive laws must be developed ultimately for predicting heat transfer during core reflooding in the vicinity of the rising water level where droplets are formed by violent boiling and broken up by the Leidenfrost phenomenon. The technique involved the utilization of SUNY-SB developed Laser-Doppler anemometer and experimental hardware for flow measurements. In order to do this, an entirely new methodology and the accompanying special electronic instrumentation would have to be developed. To test and verify this new scheme, a solid particle-water flow system has been used. Some preliminary results are presented.

I.4-1

## INTRODUCTION

Although the use of laser-Doppler anemometry in single phase
flows has been established for some time, its application in two-phase
dispersed flow still presents considerable problems in obtaining
statistics on such flow properties as particle size number density
and velocity distributions. One of the problems in particle measure-
ment is the ambiguity in the Doppler signal due to the presence in
the measuring volume of more than one scattering particle at the same
time. If the dispersed phase is reasonably dilute in a usually extremely
small optical measuring volume, such an ambiguity can be readily removed.

A far more serious problem is the ambiguity originating from the
inherent nonuniformity of illumination in the optical measuring volume.
In order to extract information on sizing, in addition to information
on velocity of particles from Doppler signals, it is desirable to devise
a scheme by which a central core region of the optical measuring volume,
where the illumination is more uniform, can be isolated out to serve as
a new probing volume in the flow.

### Laser-Doppler Anemometry

Laser anemometry is a technique which utilizes scattered light
from particulates in a fluid to measure the velocity of that fluid.
In theory the laser anemometer is linear, needs no calibration, and
measures velocity independent of fluid properties. A relatively small
measuring volume and inherently fast response give its ability to
follow rapidly changing velocities in the fluid. Only light needs tc

I.4-2

enter the fluid to the measuring point. Generally two basic modes of operation, e.g. dual beam and reference beam are used.

Dual beam is the crossing of two laser beams of equal intensity at a point in the fluid to be measured. Where these beams cross, they interface with each other to form 'fringes'. A particle moving through the crossing point in the plane of the two beams then goes through a region of very low light intensity (light cancelling) to a region of high intensity and back again. A photodetector is used to pick up the scattered light from the particle. The frequency of the signal, so obtained, is proportional to the velocity with which the particle is moving across fringes.

Reference beam operation is generally described in terms of Doppler shift of the scattered light and it requires only one light beam at the measuring point. The scattered light from a particle is mixed with a reference beam, to detect the shift in frequency. The photo-detector responds to the difference in frequency, which is proportional to the velocity of the particle.

In both operations, the shape of the measuring volume is approximately ellipsoidal and is as shown in figure 1. The laser beams generally have a Gaussian intensity distribution. This causes the amplitude variation shown, with maximum amplitude occurring in the center of the measuring volume. The three measurable characteristic parameters of a Doppler signal are as shown in figure 2.

I.4-3

## Ambiguities

The fringe spacings and other inherent nature of dual beam operations limit the application of this system only to very small particle sizes.

The amplitude of Doppler signal is mainly a function of particle size, number of particles in measuring volume and particle length in the measuring volume. Most measurements in two-phase suspensions are restricted to some rather over-simplified cases[1-6]. Considerable effort has been devoted to this difficult task of precise sizing and velocity measurement of individual particles by concentrating on particles of large enough size for the technique of geometrical optics to be rendered useful[7] and by making use of an additional property of the signal[8,9], for example. One additional serious problem in signal ambiguity originates from the inherent non-uniformity of illumination in the optical measuring volume[8]. Some effort has been attempted to by-pass this difficulty, for instance, by incorporating a second optical system designed for particle sizing which is focussed around the same probing point[10]. It still remains desirable to devise a scheme by which a central core region of the measuring volume where the illumination is more uniform, can be isolated out to serve as a new probing volume in the flow.

## Theory of the proposed scheme

We selected the reference beam mode of operation as this can be extended for larger size particles. We decided to operate in a

dilute dispersed flow system and hence, the signal amplitude will now be mainly a function of particle size, d, and particle path length in the measuring volume. This restriction of dilute flow to get one particle in the measuring volume is not serious as our measuring volume is so small, the maximum allowable number densities possible are quite large (particles can have a number density of up to about $10^5$/cc).

If we focus our attention then to only central core of the measuring volume, a very difficult feat so far not obtained by others, the signal amplitude will depend only on the size of the particle, d. This can be achieved by electronically isolating a central core of measuring volume, Figure 3.

The path length of a scattering particle through this measuring volume, $\ell_v$ as shown in Figure 3, can be determined from the product of the time of duration of the signal, $\tau$, and the velocity of the particle, $v_j$, which is determined by the Doppler frequency of the signal itself, $\ell_v = \tau v$. By then ignoring all signals whose corresponding particle's path length is smaller than a chosen lower limiting value $\ell_v$, we can essentially eliminate the dependency of signal amplitude on particle position in the measuring volume. The maximum path length, $\ell_m$ (the one going through the geometrical center of the measuring volume) is obtained empirically, by determining the path lengths of many particles through calibration. The lower limiting value of the path length for the central core, $\ell_v$, is determined by the choice of a window size for the amplitude discrimination.

After signal amplitude discrimination, a discrimination against the path length, $\ell_v$, with the limiting path length, $\ell_v$ of the central core of the measuring volume as the lower bound, only signals within the selected amplitude window from particles passing through the central core will be allowed to go through. Then an additional discrimination on velocity will produce the required statistics on the particle size and velocity distributions in the flow of a suspension.

By setting a lower limit on the time duration $\tau$, say $\bar{\tau}$, using a time discrimination scheme, and a related lower limit on the velocity $v_j, \ell_v/\bar{\tau}$, using a velocity discrimination, we will retain signals within the velocity range $\ell_v/\bar{\tau} < v_j < \ell_v/\bar{\tau}$ which can only be produced by particles going through the central core region of the measuring volume, $\ell_v < \ell_v < \ell_m$, as shown by the sketch of Figure 4.

However, this is not to say that these signals represent the signals produced by all the particles of the specified size $d_i$ (corresponding to signals of amplitude $A_i$) which pass through the central core region, because the signals from those particles which have a velocity above the upper limit of the local admissable velocity range, $\dfrac{\ell_v}{\bar{\tau}}$, that pass through the central core region, will not be registered. In order to obtain the correct number count appropriate for the determination of the velocity probability density distributions and particle size number densities from the measured number count so obtained, a correction factor $K$, the ratio of actual number count to correct number count, has to be determined. This correction factor

I.4-6

is strictly a function of geometry only and can be determined from calibration with a flow of known number density $(N_i)_o$ and a uniform particle size $d_i$ with the same velocity $(v_j)_o$.

Let $N_{i,j}$ = no. of particles of size $d_i$ per unit volume, per unit velocity range and unit size range with the center velocity $v_j$.

Then

$$\dot{n}_{i,j} = N_{i,j} \, v_j \qquad (1)$$

and

$$N_i = \sum_j N_{i,j} = \sum_j \frac{\dot{n}_{i,j}}{v_j} \qquad (2)$$

where

$N_i$ = number density of particles of size $d_i$.

But for the over-simplified calibration run, the value of $(\dot{n}_{i,j})_o$ simply stands for the number count of particles of size $d_i$ having velocity $(v_j)_o$ per unit cross-sectional area of flow. By comparing this to the total number count for the whole central core region, obtained by a scheme of gradually raising the lower limit on the duration time discrimination, $\bar{\tau}$, the value of $\tilde{s}_o$, the cross-sectional area, can be obtained, since $\tilde{s}_o$ is simply the ratio of this total number count to the number count per unit cross-sectional area of the central core, $(\dot{n}_{i,j})_o$. For a measuring volume approximately elliptical in shape, the plot of the number count n against $(\bar{\tau})^2$ should be made up of two approximately straight segments as shown in Figure 5.

I.4-7

It is of interest to note that since the number count n and the path length $\ell_v$, for this over-simplified case, are proportional respectively to $B_0$ and $\bar{\tau}$, the correction factor K, needed for converting the actual number count to corrected number count, can be readily obtained

$$K = \frac{1}{3} \frac{(2\bar{\tau}_m - \bar{\tau}_m \bar{\tau}_v - \bar{\tau}_v^2)}{(\bar{\tau}_m - \bar{\tau}_v^2)} \qquad (3)$$

## Instrumentation and Experimental Apparatus

Instead of measuring the amplitude $(A_i)$, time duration $(\tau)$ and velocity $(v_j)$ of each signal, the output of the LDA is filtered as shown in Figure 6. After an amplitude discrimination set on signal amplitude $A_i$ and a time discrimination set on the lower limit on the signal path duration time $\bar{\tau}$, only the signals having an amplitude within the pre-selected narrow amplitude window in the neighborhood of $A_i$ and a duration time $\tau \geq \bar{\tau}$ car reach the tracker. The tracker then converts the Doppler frequency of the signals into voltage signals proportional to the particle velocities. The output of the tracker is passed to a velocity discriminator ci. uit which allows through only those signals with a voltage (corresponding to the particle velocities) above a certain value (equal to $\frac{\ell_v}{\bar{\tau}}$). This results in signals for which the product $v_j \cdot \tau = \ell_v$ is a value greater than $\ell_v$, and hence only for those particles passing through the central core region. The number count of such signals is executed on an electronic counter to give the measured number count of particles of a particular size and a particular

velocity as previously described. By changing the time discriminator lower limit $\bar{\tau}$ and the corresponding velocity discriminator lower limit $\dfrac{\ell_v}{\bar{\tau}}$, number counts at different velocities can be obtained for particles of the same size range. Then, by systematically changing the setting of the amplitude discriminator and repeating the aforementioned time and velocity discrimination schemes, statistics for the complete particle size range can be readily accomplished. Furthermore, by analyzing signals from particles of small enough size, the velocity probability distribution for the fluid phase can also be obtained, using these small particles as tracers. An instrumentation block diagram is shown in Figure 7.

The operational arrangement of our reference-mode Laser-Doppler Anemometer is shown in the sketch of Figure 8. The oncoming laser beam from a 15mw He-Ne CW laser is split into two beams: the scatter beam which forms an angle of 7.5° with the transverse axis in a horizontal plane, and the reference beam. The measuring, scattering volume is approximately ellipsoidal, 250µ in diameter and 800µ in length. The receiving lenses are symmetrical with the sending lenses, and the scattering angle is fixed at nominally 15 degrees. The received scattered beam from a moving scattering body passing through the scattering volume is brought to mix with an unshifted reference beam to generate a heterodyne on the photomultiplier tube surface to produce the Doppler frequency shift signal.

The flow apparatus consists mainly of a precision close-loop water channel which has an effective length of 6.10m and inside

I.4-9

dimensions of 45.7cm wide and 30.5cm deep with walls made of
optical grade plate glass. The entire optical system is mounted on
top of a heavy traversing base, matching and aligned with the water
channel, which is capable of positioning the optical measuring volume
inside the water channel accurate to 25μ in all three directions.
The water channel receives its water supply from a Micronite filter
with a maximum pore size of 3μ. Precision neutrally buoyant hollow
glass spheres of sizes in a distributed range of up to 35μ are added
to the channel water loop to serve as the suspended phase. The Doppler
signals from the optical anemometry system are first recorded on
magnetic tape which is afterwards played back at a slower speed for
data procession in the instrumentation system.

## Calibration

According to the calibration scheme as shown in Figure 5,
particles of one single precise size are needed, a feat not easily
attainable because of the difficulty of obtaining such particles. A
substitute way has been found in experimenting with very dilute sus-
pension of particles of distributed sizes.

The optical measuring volume was placed in that portion of
the water channel where a laminar uniform free stream flow, $(v_j)_o$ =
6.43 cm/sec, was established as shown in Figure 9. In a preliminary
trial run, the amplitude discrimination window was deliberately made
very narrow to scan over the whole amplitude range to obtain a rough
picture of the signal amplitude distribution pattern. Due to the

I.4-10

dilution of particles and the very narrow amplitude window size used, the signal amplitude displayed near discrete size distribution at a very few isolated amplitudes. One of them, $A_j = 770 \sim 810$ mv was finally adopted and its suitability for this task is demonstrated in the well behaved calibration curve of signal number count, n, vs. square of lower limit on duration time, $\bar{\tau}^2$, as shown in Figure 10. The duration time $\bar{\tau}$, based on tape speed of 15 inches/sec., is twice as large as $\bar{\tau}$, based on the recording speed of 30 inches/sec., and the operational amplitude window size $\Delta A_j = 0.05 A_j$. The total tape length is 605 ft. The two important quantities characterizing the central core of the measuring volume for this case are found to be:

$$\ell_v = 228\mu$$

$$\ell_m = 267\mu.$$

And the correction factor needed for converting the actual number count to corrected number count, according to Eqn. (3), has the value:

$$K = 0.536.$$

The next step is to establish a calibration between the signal amplitude and particle size from the signal number count and particle number density from independent measurement of the water sample. The accumulative actual signal number count, [n], for signals of amplitude from $A_i$ to $A_{max}$, the maximum amplitude, for the various signal amplitudes is plotted in Figure 11. The curve gives the limiting value:

$$[n] = 1, \text{ at } A_{max} = 1.08v.$$

I.4-11

Water sample taken immediately downstream of the measuring volume with an isokinetic probe was analyzed with a Coulter (Model B) counter. The resulting accumulative particle number density count, [N], for particles of size from $d_i$ to $d_{max}$, the maximum size, for the various particle sizes is plotted in Figure 12. The curve gives the limiting value:

$$[N] = 1, \text{ at } d_{max} = 33.4\mu$$

By definition, we have for the uniform flow,

$$n_i = K N_i (v_j)_o \hat{B}_o T_o = k N_i$$

where

$n_i$ = actual signal number count of sig... of amplitude $A_i$

$K$ = correction factor for signal num...

$N_i$ = number density of particles of siz...

$(v_j)_o$ = uniform mixture velocity

$\hat{B}_o$ = base cross-sectional area of central c... of measuring volume,

$T_o$ = tape recording time

$k$ = $K(v_j)_o \hat{B}_o T_o$, a constant

Therefore, we have the relationship

$$[n] = k[N]$$

between the two accumulative quantities. Furthermore, if we let

$$A^* = A_i/A_{max} \text{ and } d^* = d_i/d_{max}$$

we can show that by probability theory

$$\ell n[N]\Big|_{\text{at } d^*} = \ell n[n]\Big|_{\text{at } A^*}$$

I.4-12

which establishes a unique correlation relationship between d* and A* as shown by computional scheme of Figure 13. The resultant calibration curve between the normalized particle size d* and signal amplitude is shown in Figure 14. Results from direct amplitude measurement using particles of five precise size ranges are also plotted for comparison. The dimensional calibration curve between particle size and signal amplitude is plotted in Figure 15. Using this calibration, the resultant particle size and number density distribution in this laminar uniform free stream flow is plotted in Figure 16.

Further, for the previous calibration run for the determination of $\ell_v$, $\ell_m$ and K as shown in Figure 10, we have

$$(n)_o = (N_i)_o (v_j)_o \, \delta_o \, T_o$$

where $(n)_o = 18$, the stabilized number count

$(N_i)_o = 20/cm^3$, the number density of particles of sizes between 10.5μ and 12.5μ, corresponding to amplitudes of 770 mv and 810 mv respectively, through the calibration curve, Figure 15, at $13/cm^3 - μ$ from the number density distribution curve, Figure 16.

$(v_j)_o = 6.43$ cm/sec, the uniform free stream velocity

$T_o = 484$ sec., the tape recording time,

and therefore, the base cross-sectional area of central core of measuring volume is then:

$$\delta_o = 4.44 \times 10^4 μ^2.$$

I.4-13

## Measurement in Turbulent Shear Flow

A measuring point was selected on the edge of the wake behind a transverse rectangular body, as shown in Figure 9, where significant particulate accumulations and sizable velocity fluctuations are expected. The particle number counting rate per unit cross-sectional area per unit velocity range and unit size range was obtained from a length of tape of 325 ft. recorded at 30 inches/sec. for two representative particle size ranges (4.60-4.95$\mu$ and 5.65-6.10$\mu$). The velocity distributions for these particle ranges are shown in Figure 17.

## Conclusion

A new experimental scheme has been developed for the measurement of the local number densities and velocity probability densities of a dilute two-phase suspension which has a distribution of particle size and a predominate direction of flow orientation by the use of laser Doppler anemometry. An accompanying indirect calibration method needed for this scheme has also been developed based on the probability correlation between Doppler burst counts and the independently obtained mixture sample sizing number counts.

Results of measurements using this scheme have been presented for a laminar free stream flow and a turbulent shear flow of a dilute two-phase suspension of neutrally buoyant, spherical glass particles of distributed sizes in water. Reproducibility of these results has been confirmed.

I.4-14

## Acknowledgement

## REFERENCES

1. Lee, S. L. and Einav, S., "Migration in a Laminar Suspension Boundary Layer Measured by the Use of a Two-Dimensional Laser-Doppler Anemometer," Progress in Heat and Mass Transfer, Vol. 6, pp. 385-403, Pergamon Press, 1972.

2. Einav, S. and Lee, S. L., "Particles Migration in Laminar Boundary Layer Flow", International Journal of Multiphase Flow, Vol. 1, pp. 73-88, 1973.

3. Ben-Yosef, N., Ginio, O., Mahlab, D. and Weitz, A., "Bubble Size Distribution Measurement by Doppler Velocimeter", Journal of Applied Physics, Vol. 46, No. 2, pp. 738-740, February, 1975.

4. Mason, J. S. and Birchenaugh, A., "The Application of Laser Measurement Techniques to the Pneumatic Transport of Fine Alumina Particles", Conference and Exhibition on the Engineering Uses of Coherent Optics, Univ. of Strathclyde, Scotland, April 8-11, 1975.

5. Golovin, V. A., et al., "Study of the Model of a Two-Phase Flow Using an Optical Quantum Generator (Laser). UDC 541.12.012.(1971).

6. Matthes, W., et al., "Measurement of the Velocity of Gas Bubbles in Water by a Correlation Method," Rev. of Sci. Inst., Vol. 41, June 1970.

7. Durst, F. and Zaré, M., "Laser Doppler Measurements in Two-Phase Flows", The Accuracy of Flow Measurements by Laser Doppler Methods, Proceedings of the LDA-Symposium, Copenhagen 1975, pp. 403-429.

8. Farmer, W. M., "Dynamic Particle Size and Number Analysis Using a Laser Doppler Velocity Meter", Applied Optics 11; 2603 (1972).

9.  Durst, F. and Eliasson, B., "Properties of Laser Doppler Signals and Their Exploitation for Particle Size Measurements", <u>The Accuracy of Flow Measurements by Laser Doppler Methods</u>, Proceedings of the LDA-Symposium, Copenhagen 1975, pp. 457-477.

10. Durst, F. and Umhauer, H., "Local Measurements of Particle Velocities, Size Distribution and Concentration with a Combined Laser-Doppler Particle Sizing System", <u>The Accuracy of Flow Measurements by Laser Doppler Methods</u>, Proceedings of the LDA-Symposium, Copenhagen 1975, pp. 430-456.
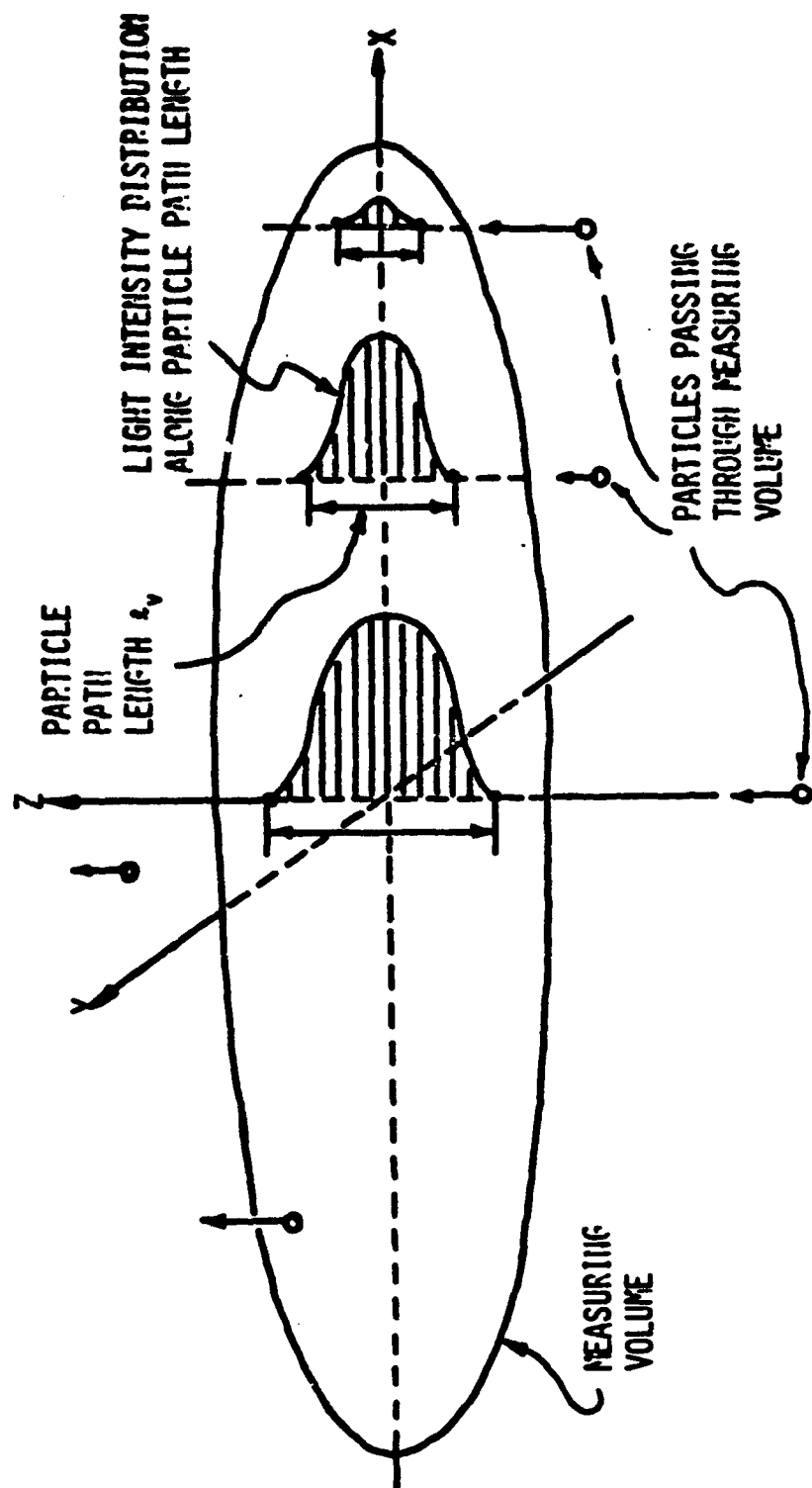
FIG. 1. SKETCH OF OPTICAL MEASURING VOLUME

1.4-18
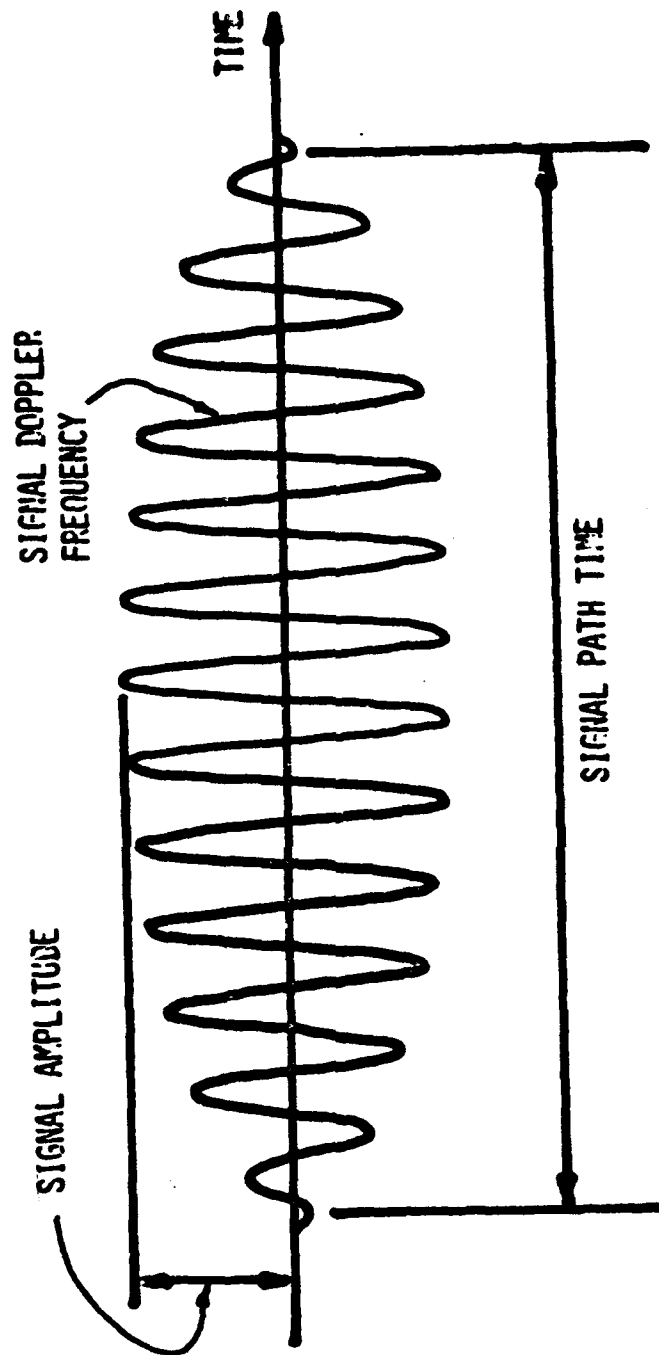
FIG. 2. SKETCH OF PARTICLE DOPPLER SIGNAL

I.4-19
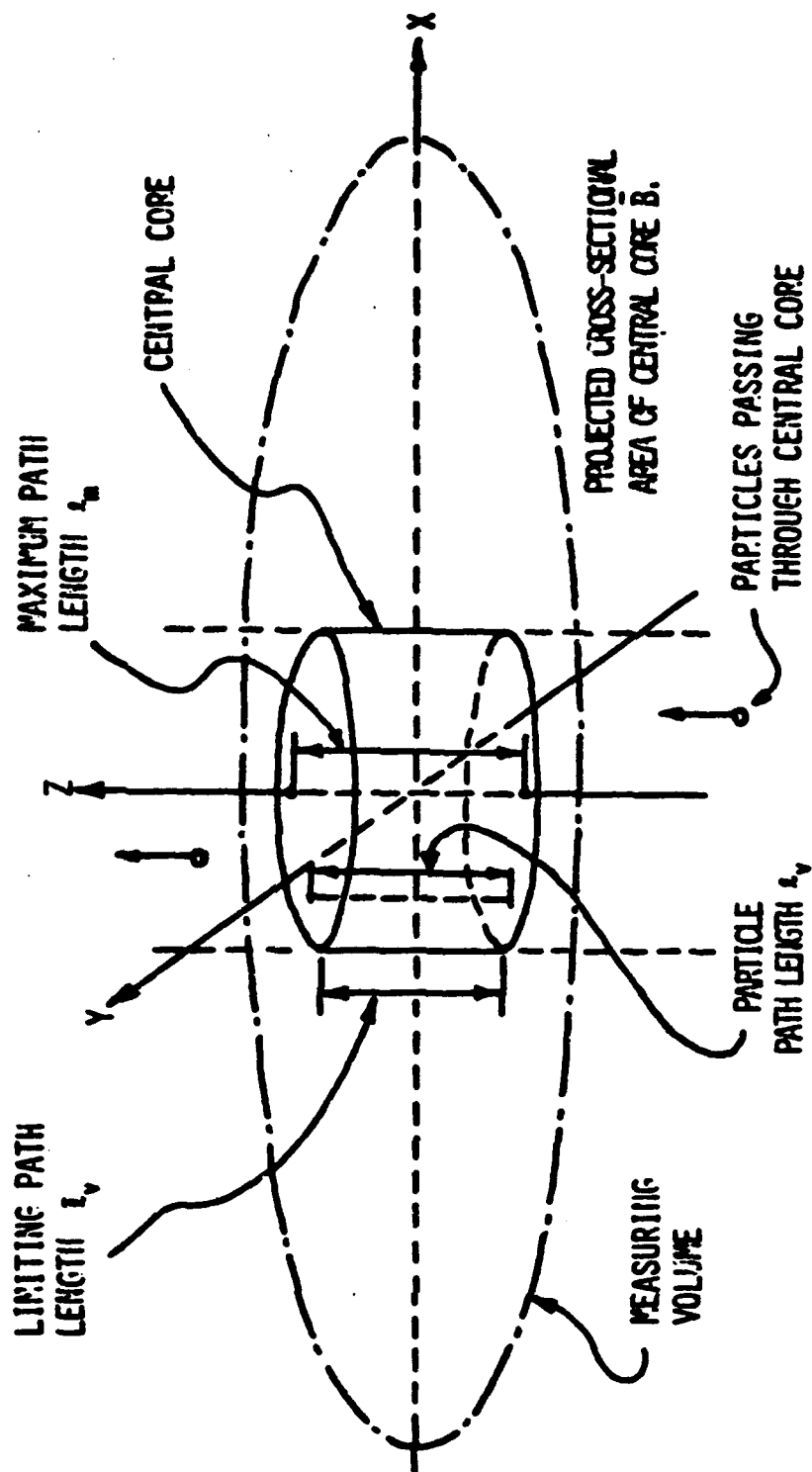
FIG. 3. SKETCH OF ELECTRONICALLY ISOLATED CENTRAL CORE OF MEASURING VOLUME

I.4-20
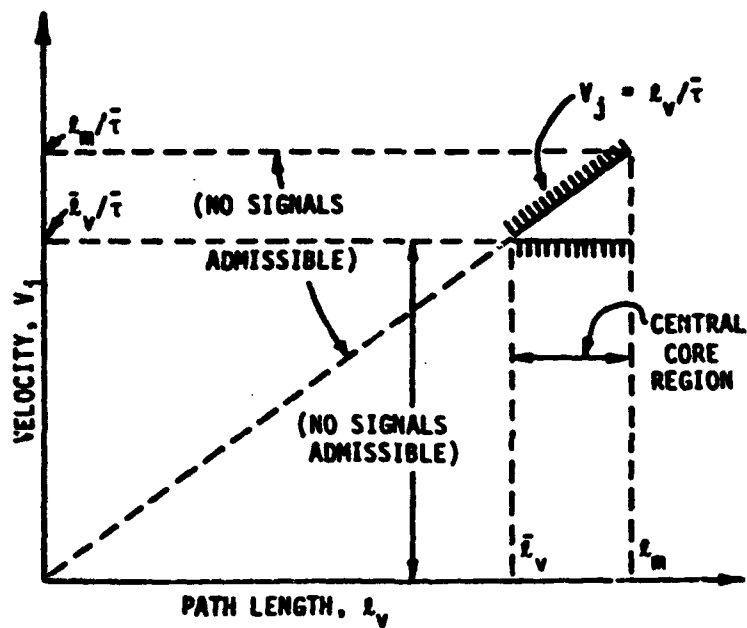
FIGURE 4. SKETCH OF CRITERION OF SIGNAL
ADMISSIBILITY DUE TO DURATION
TIME DISCRIMINATION

I.4-21
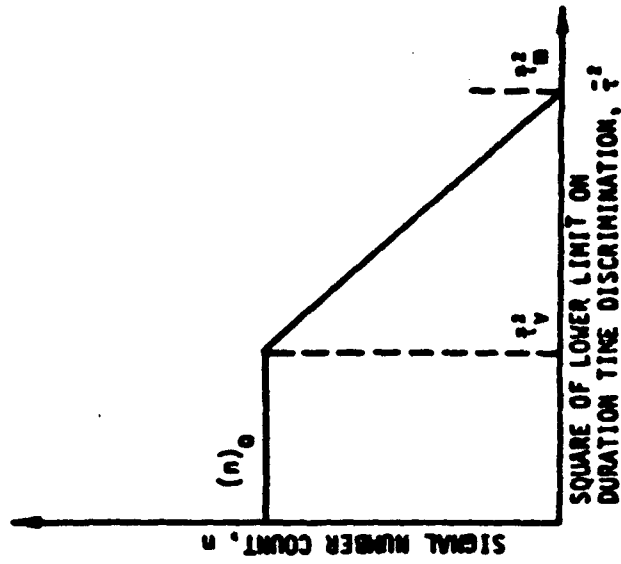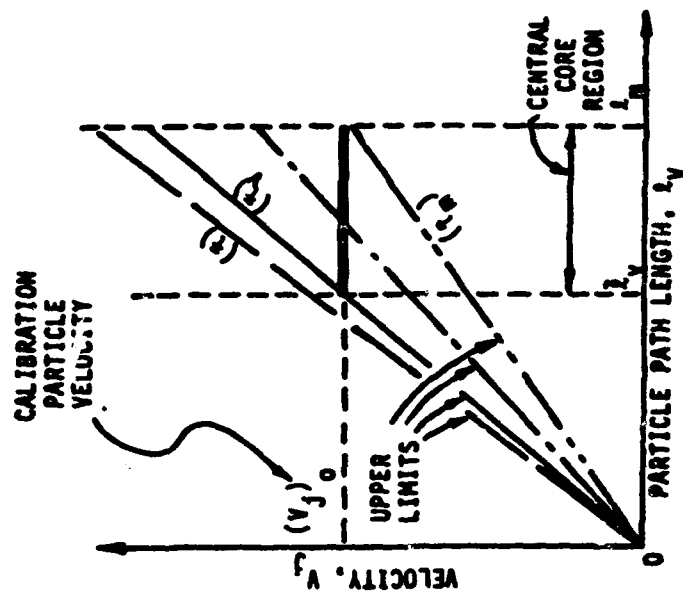
FIGURE 5. SKETCH OF CALIBRATION SCHEME

I.4-22
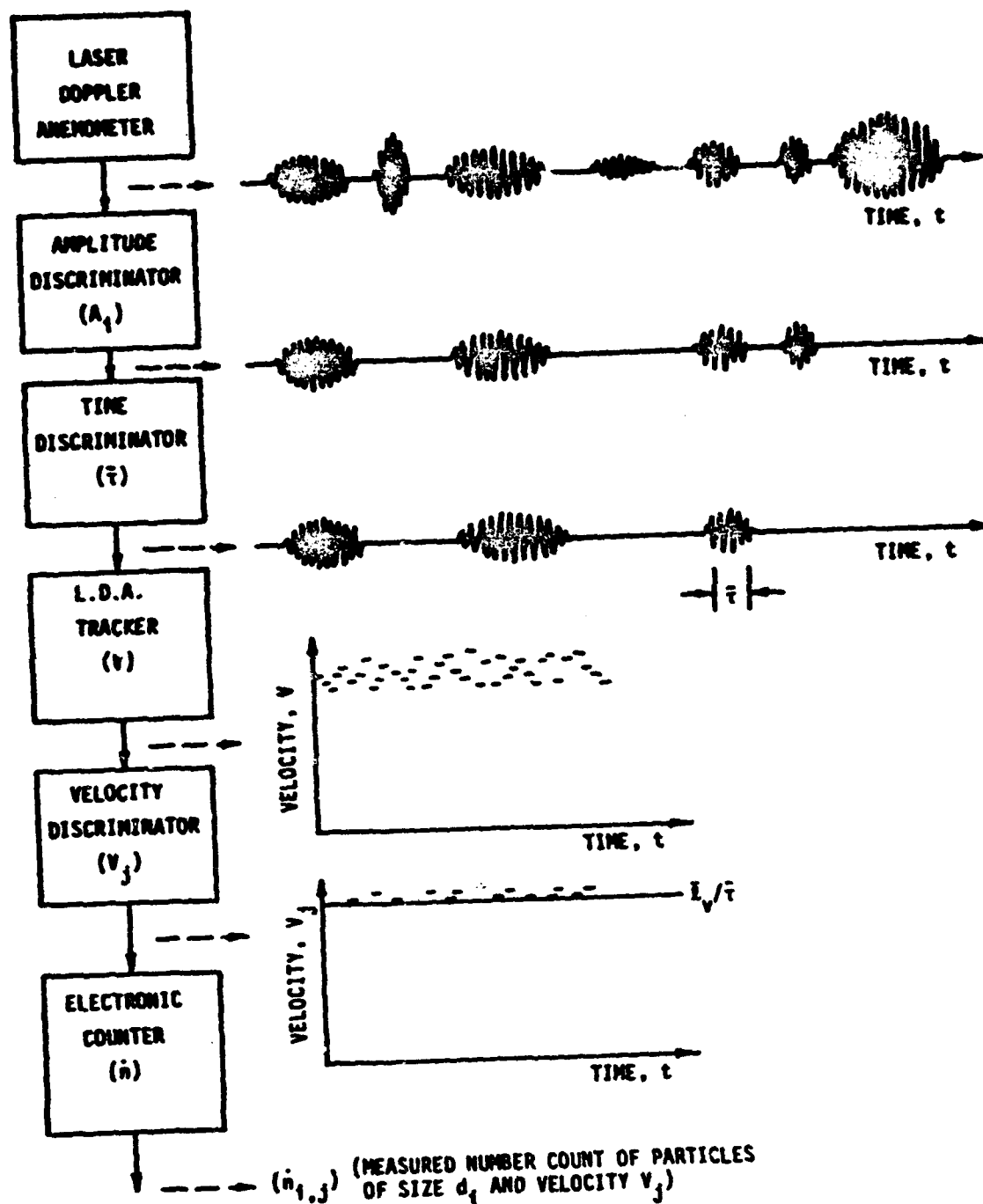
FIGURE 6. OPERATIONAL BLOCK DIAGRAM FOR SIGNAL DISCRIMINATION SCHEME

I.4-23
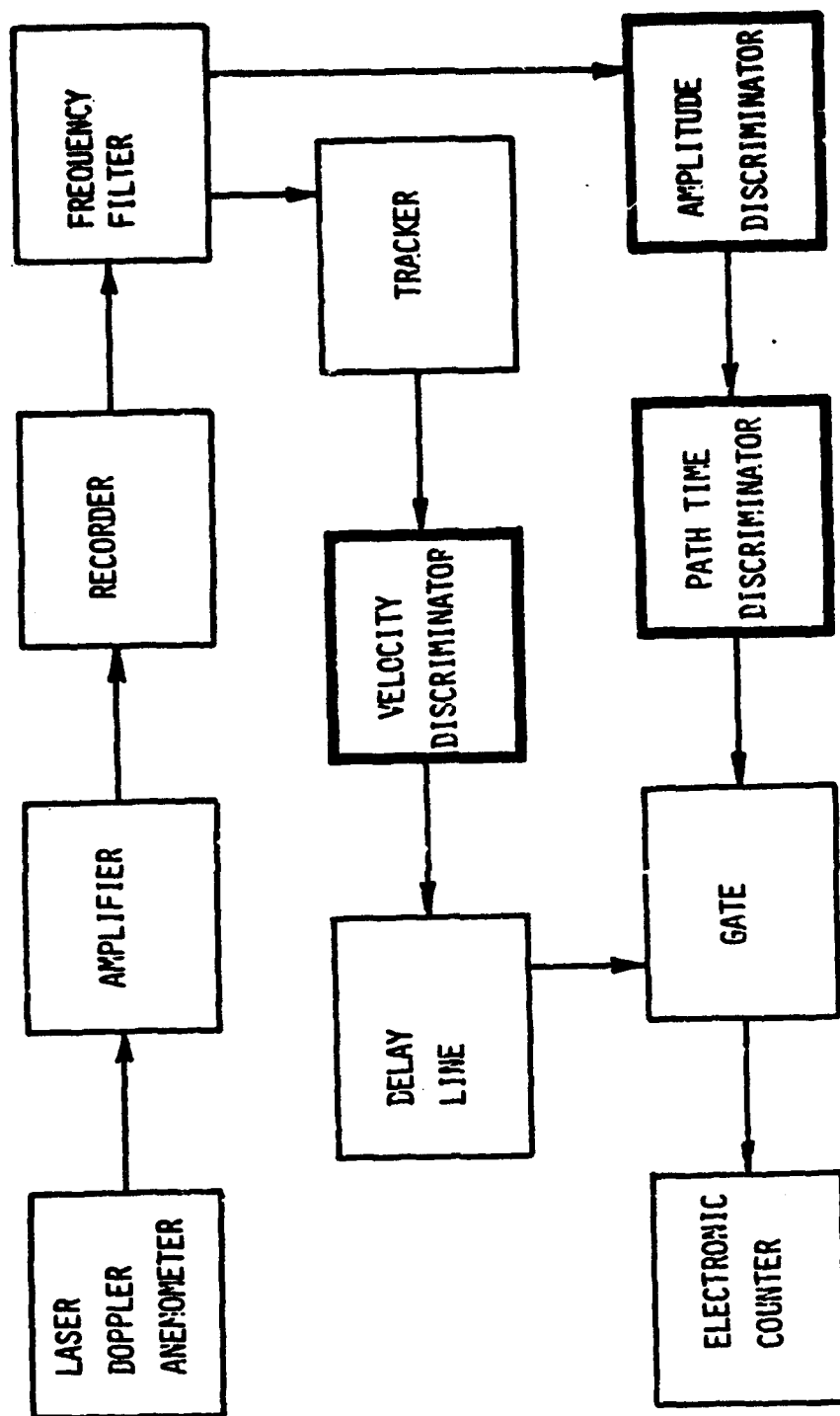
FIG. 7. INSTRUMENTATION BLOCK DIAGRAM

I.4-24
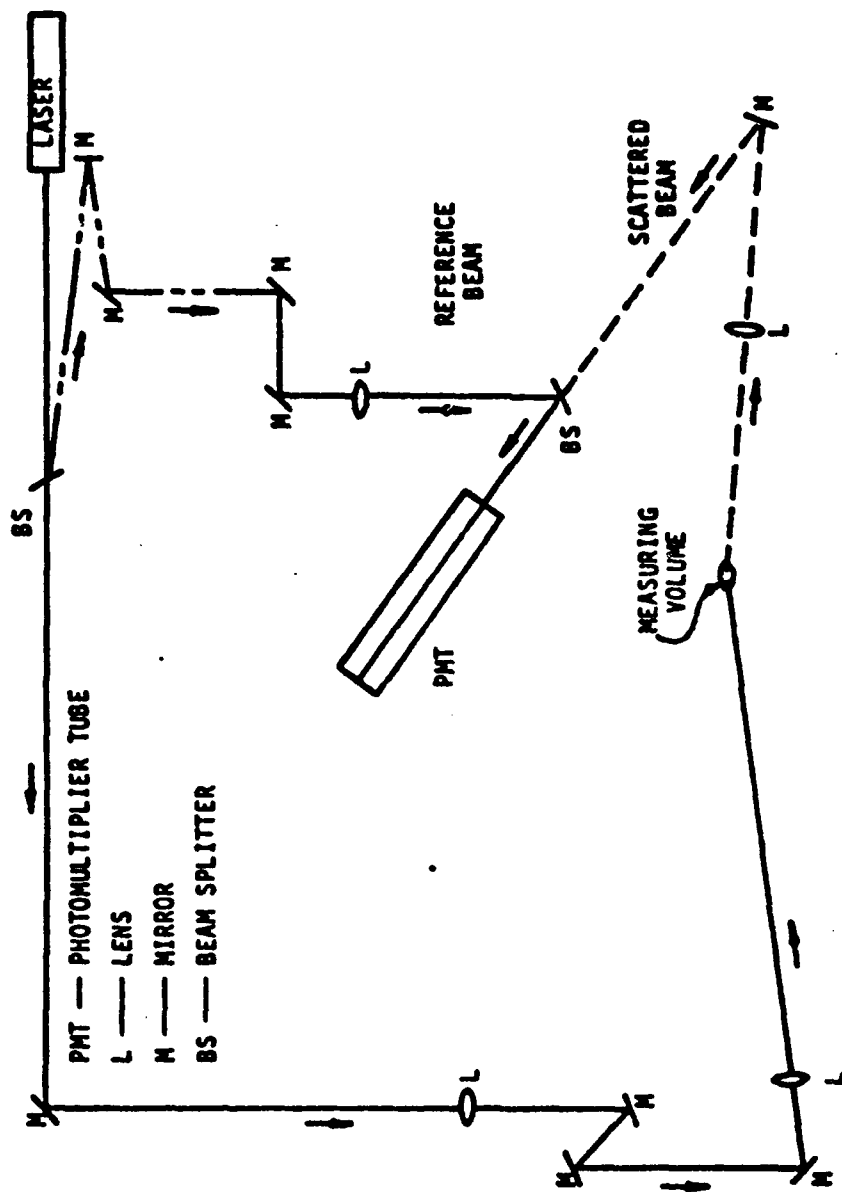
FIGURE 8. OPTICAL ARRANGEMENT

PMT — PHOTOMULTIPLIER TUBE
L ——— LENS
M ——— MIRROR
BS —— BEAM SPLITTER

I.4-25

MEASURING POINT IN TURBULENT SHEAR FLOW

MEASURING POINT IN LAMINAR UNIFORM FREE STREAM FLOW
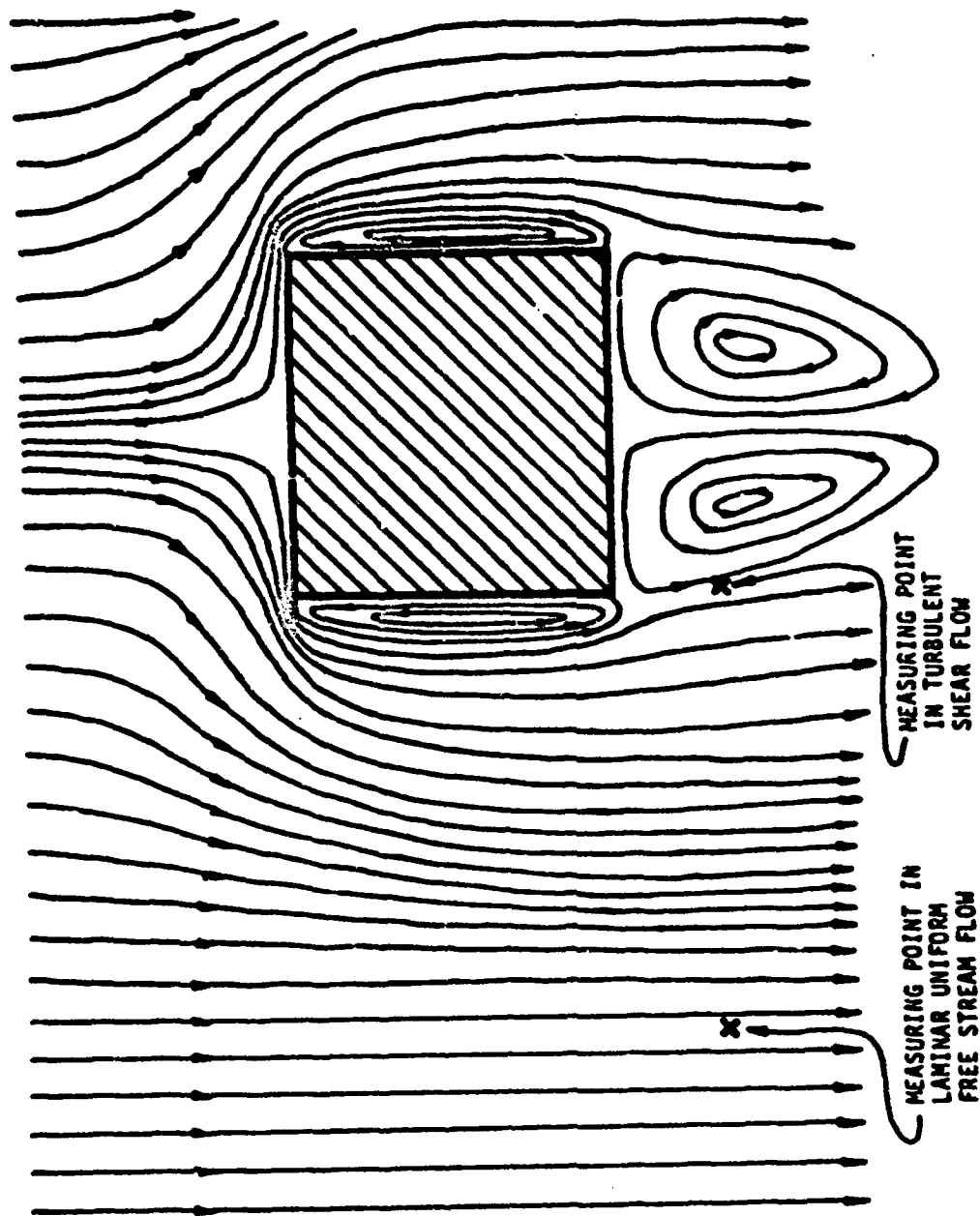
FIGURE 9. FLOW OF A TWO-PHASE SUSPENSION AROUND A TRANSVERSE RECTANGULAR BODY

FIGURE 10.

CALIBRATION SCHEME FOR
DETERMINATION OF LIMITING
AND MAXIMUM PARTICLE PATH
LENGTHS IN CENTRAL CORE OF
MEASURING VOLUME

RELATING TO
MAXIMUM PATH
LENGTH

RELATING TO
LIMITING PATH
LENGTH

SQUARE OF LOWER LIMIT ON DURATION TIME (AT TAPE SPEED)
DISCRIMINATION, $\tau^2$, ms$^2$

SIGNAL NUMBER COUNT, n

FIG. 11. SIGNAL AMPLITUDE AND NUMBER COUNT DISTRIBUTION

A=1.08 VOLT FOR [n]=]

ACCUMULATIVE NUMBER COUNT, [n]

AMPLITUDE OF DOPPLER SIGNAL, A, VOLT

I.4-28

FIG.12. PARTICLE SIZE AND NUMBER DENSITY DISTRIBUTION OBTAINED FROM COULTER SIZING OF MIXTURE SAMPLE

d=33.4μ
FOR[n]=1

I.4-29

FIG. 13. CORRELATION SCHEME USED TO OBTAIN RELATIONSHIP BETWEEN PARTICLE SIZE AND SIGNAL AMPLITUDE

LN(n) VS. A*

LN(n) VS. d*

LOG OF ACCUMULATIVE PARTICLE NUMBER DENSITY, LN(n), NO./CM$^3$
LOG OF ACCUMULATIVE SIGNAL NUMBER COUNT LN(a)

NORMALIZED PARTICLE SIZE, d*, AND SIGNAL AMPLITUDE, A*

I.4-30
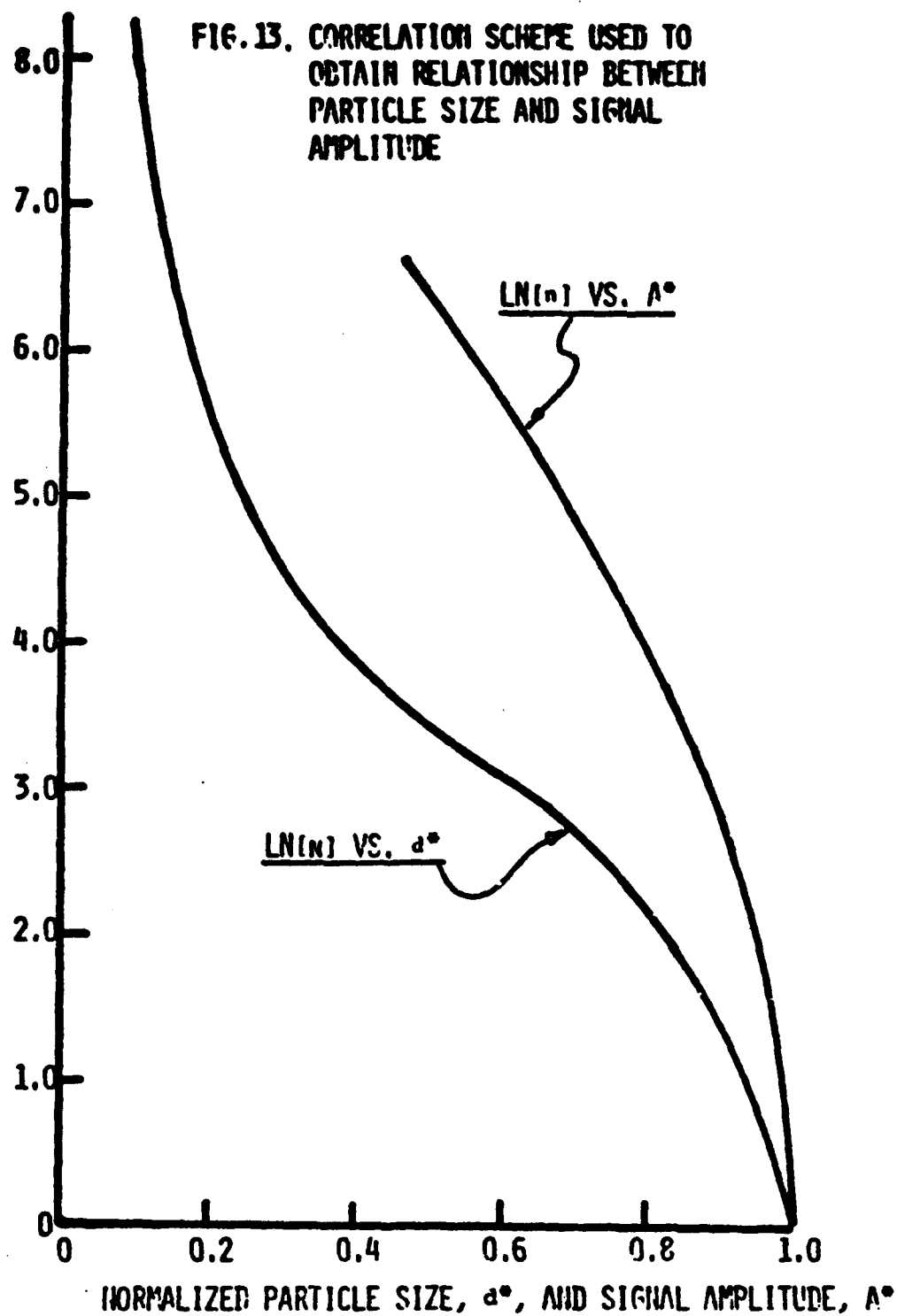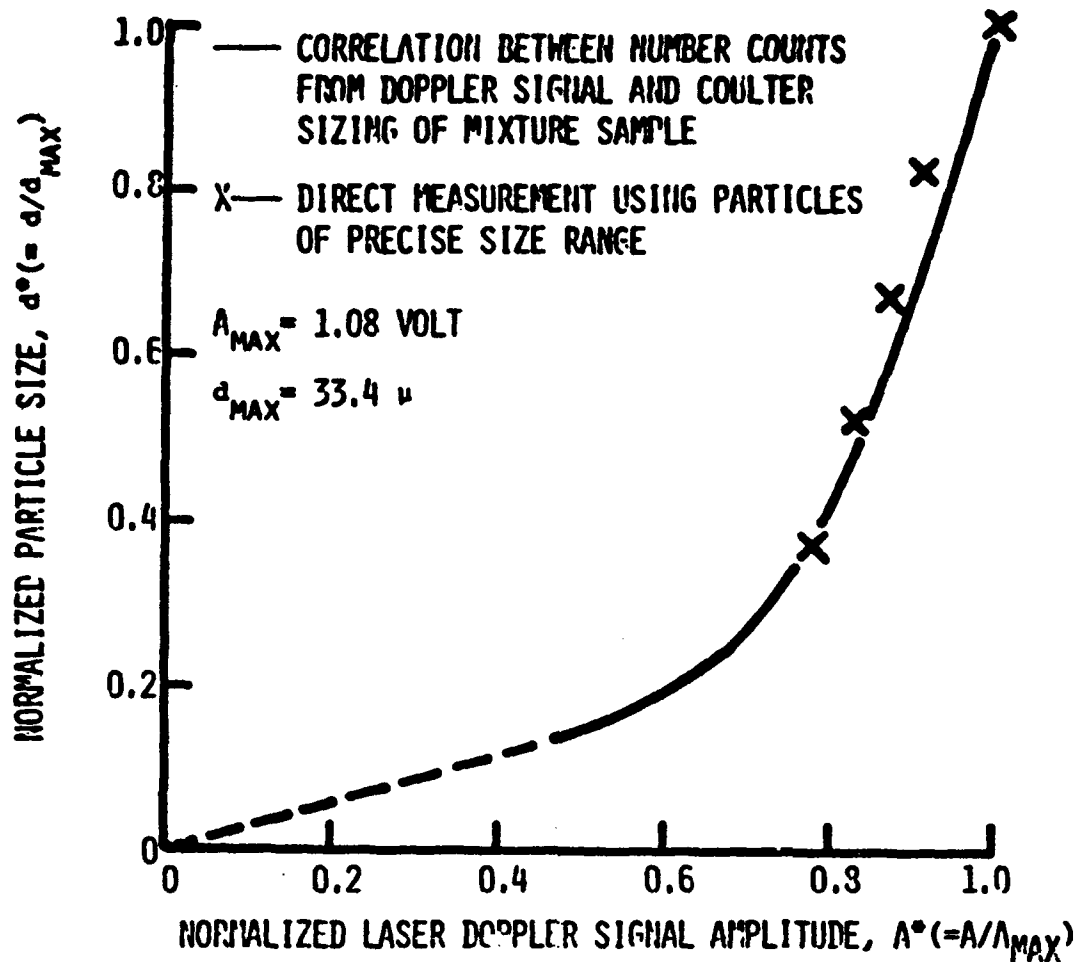
FIG. 14. COMPARISON OF SIGNAL AMPLITUDE CALIBRATION RESULTS FROM NUMBER COUNT CORRELATION AND DIRECT MEASUREMENT USING PARTICLES OF PRECISE SIZE RANGE

I.4-31

FIG. 15. CALIBRATION CURVE OBTAINED
FROM CORRELATION BETWEEN
NUMBER COUNTS FROM DOPPLER
SIGNAL AND COULTER SIZING
OF MIXTURE SAMPLE

PARTICLE SIZE, d, μ

AMPLITUDE OF DOPPLER SIGNAL, A, VOLT

I.4-32

FIG. 16. PARTICLE SIZE AND NUMBER DENSITY DISTRIBUTION IN LAMINAR FREE STREAM FLOW

PARTICLE SIZE, d, μ

PARTICLE NUMBER DENSITY PER UNIT SIZE RANGE, $N_i$, NO./CM$^3$-μ

I.4-33

TURBULENT SHEAR FLOW OF A SUSPENSION

PARTICLE SIZE RANGE
d = 4.60-4.95μ

d = 5.65-6.10μ

VELOCITY, V, CM/SEC.

PARTICLE NUMBER COUNTING RATE PER UNIT
CROSS-SECTIONAL AREA PER UNIT VELOCITY
RANGE, $\dot{n}_{i,j}$, NO./SEC-CM²-(CM/SEC)

8x10³

6x10³

4x10³

2x10³

0

0    2    4    6    8    10    12

FIG. 17.   VELOCITY DISTRIBUTION FOR PARTICLES OF SELECTED SIZE RANGES

I.4-34

# PERFORMANCE OF DRAG-DISC TURBINE AND GAMMA

## DENSITOMETER IN LOFT

By

R. D. Wesley
EG&G Idaho, Inc.

IDAHO NATIONAL ENGINEERING LABORATORY

Presented at NRC Two-Phase Flow Instrumentation Meeting at
Silver Spring, Maryland, January 13, 1977

I.5-1

# TABLE OF CONTENTS

## FIGURES

## TABLES

# 1. INTRODUCTION

The Loss-of-Fluid Testing (LOFT) experiment has been designed to do safety testing for the Water Reactor Safety Agency. The objectives of the experimental program are[1].

(1) To provide data required to evaluate the adequacy and improve the analytical methods currently used to predict the loss-of-coolant accident (LOCA) response to large pressurized water reactors (LPWRs). The performance of engineered safety features (ESF) with particular emphasis on the emergency core cooling system (ECCS) and the quantitative margins of safety inherent in the performance of the ESF are of primary interest.

(2) To identify and investigate any unexpected event(s) or threshold(s) in the response of either the plant or the ESF and develop analytical techniques that adequately describe and account for such unexpected behavior.

LOFT is presently in the prenuclear checkout phase and has made three nonnuclear blowdowns to date. The flow instrumentation is of major interest in measuring the blowdown results since the flow measurement parameters are of prime importance in the code predictions.

One of the major purposes of the nonnuclear test series is to determine that the equipment/systems function properly. This includes the experimental instrumentation of which the flow instrumentation is a part and is the topic of this paper.

## 2. LOFT DESCRIPTION

LOFT is a 55 (MWt) pressurized water reactor facility intended to simulate the major behavioral aspects of generic 1000 (MWe) LPWRs in a carefully conducted Loss-of-coolant experiment (LOCE). The nuclear core is approximately 5-1/2 ft long and 2 ft in diameter and contains 1300 fuel pins and four control assemblies of typical LPWR design. The primary coolant system is designed with a similar primary system volume-to-core power ratio as exists in typical LPWRs.

The unbroken LPWR reactor coolant loops are simulated by the single, unbroken circulating loop in the LOFT primary coolant system (PCS), operating loop, Figure 1, and the postulated broken LPWR loop is simulated by the LOFT blowdown loop, Figure 2. Quick-opening valves (with opening times adjustable from approximately 10 to 50 msec) simulate the initiation of primary coolant piping ruptures. Primary coolant blowdown effluent is collected in a blowdown suppression tank which can model the significant portions of the various LPWR containment back-pressure transients. An emergency core cooling system (ECCS) is provided to model the loss-of-coolant ESFs in LPWRs. The principal components of the reactor plant are located on the mobile test assembly (MTA).

Heat is transferred from the PCS to the secondary side of a vertical U-tube steam generator. Steam generated at approximately 750 psig is fed to an air-cooled condenser and is condensed at approximately 300 psia.

Fluid pressure, temperature, velocity, and density are monitored at key points at the reactor systems by extensive instrumentation. Core thermocouples are provided to monitor fuel pin clad temperatures and support tube temperatures at in-core locations. Fixed nuclear detectors and the traversing in-core nuclear detector system measure core nuclear response and neutron flux shapes.
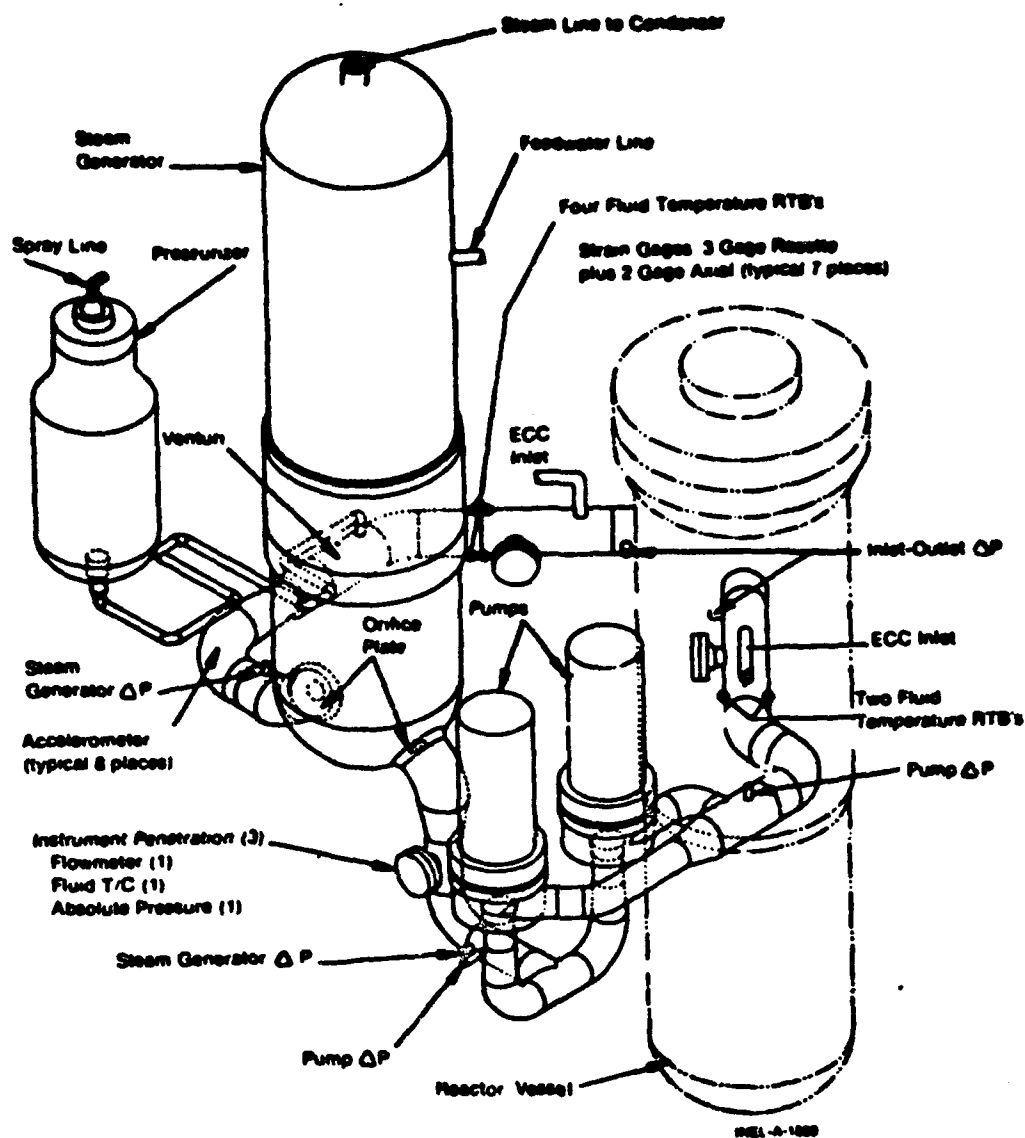
**Fig. 1 Operating loop with instrument locations.**

Of primary interest to us for this discussion are the flow locations. There are three instrument penetrations in the PCS (See Figure 1) and two penetrations in the blowdown loop (See Figure 2). At each of these locations, there is a drag-disc turbine transducer (DTT), a fluid thermocouple, an absolute pressure transducer and a gamma densitometer. There are also five DTT(s) located inside the reactor vessel for nuclear testing to provide flow information.

Fig. 2 Blowdown loop with instrument location.

Strain Gages. 2 Three Gage Rosettes plus 2 Gages Axial (typical 5 pieces)

Absolute Pressure (typical 2 pieces)

Fluid T/C (typical 2 pieces)

Quick Opening Valve (2)

Fluid T/C (typical 2 pieces)

To Suppression Vessel

Isolation Valve (2)

Absolute Pressure

8-in Sch 160 Pipe

Break Plane ΔP
Absolute Pressure

Reflood Assist Bypass

Contraction ΔP Simulated Vessel Nozzle (typical 2 pieces)

ΔP Expansion into Steam Generator Simulator

Accelerometer

Steam Generator Simulator

ΔP Steam Generator Simulator Orifice Plates

ΔP Contraction from Steam Generator Simulator

Absolute Pressure

Break Plane ΔP

ΔP Pump Simulator

Pump Simulator

5-in XX Pipe

Instrument Penetration (typical 2 pieces)
Flowmeter (1) Fluid T/C (1) Absolute Pressure (1)
Densitometer (1)

Reactor Vessel

I.5-8

# 3. DTT DESCRIPTION

The drag-disc turbine transducer (DTT) essentially is a drag meter, a turbine flowmeter, and a thermocouple combined in a single body and mounted in series as shown in Figures 3 and 4.

The drag disc is mechanically linked to a variable reluctance transducer. The associated electronic system generates an output voltage proportional to the displacement of the drag disc, which is proportional to the force on the drag disc. The polarity of the output voltage indicates the direction of the fluid flow.

The turbine consists of the turbine and an eddy current transducer which senses the passing of each turbine blade. The electronic system then generates an alternating voltage with frequency equal to the frequency of the passing of each turbine blade, and also an analog signal proportional to this frequency. Friction in the turbine bearings determines the minimum fluid velocity that can be measured; this is about 1.5 ft/sec for water.

Data from these measurements will be used to calculate the thermo-dynamic properties, mass flux, and mass flow rate of the fluid in which the DTT is installed. Three transducer models are available. One model is used in various vessel or plenum installations; the other two are used in piping installations. The transducer is constructed so that, in the event of a transducer mechanical failure, pieces of the unit will be contained so as to not affect the nuclear system.
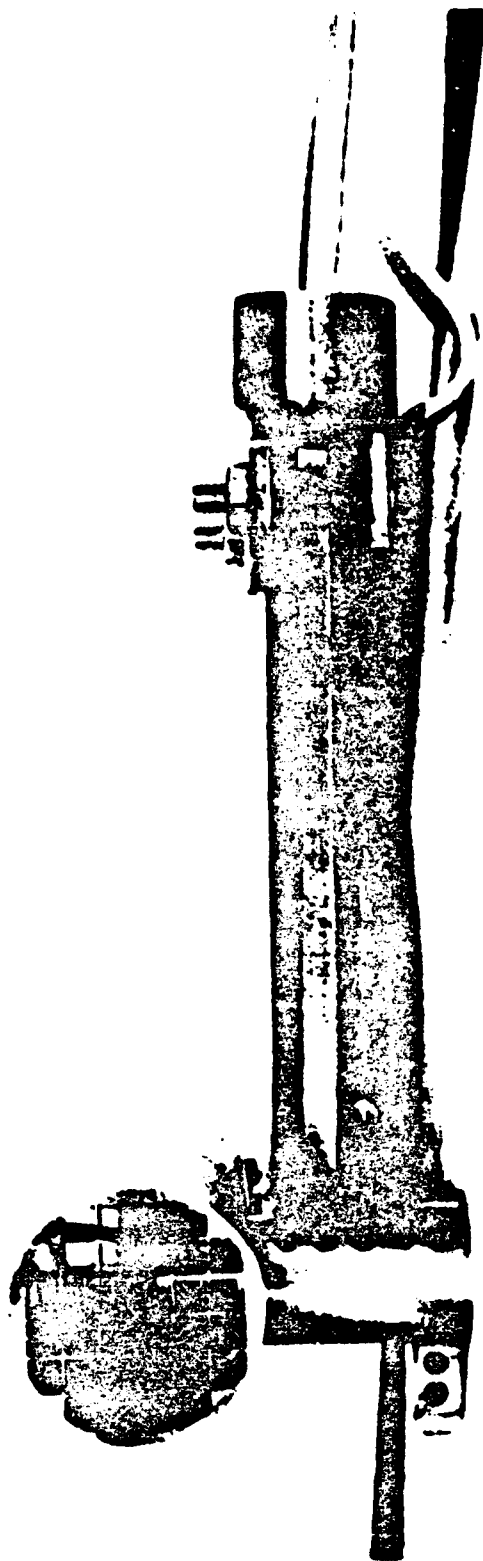
Fig. 3 Drag-Disc -- turbine transducer (DTT).

I.5-10
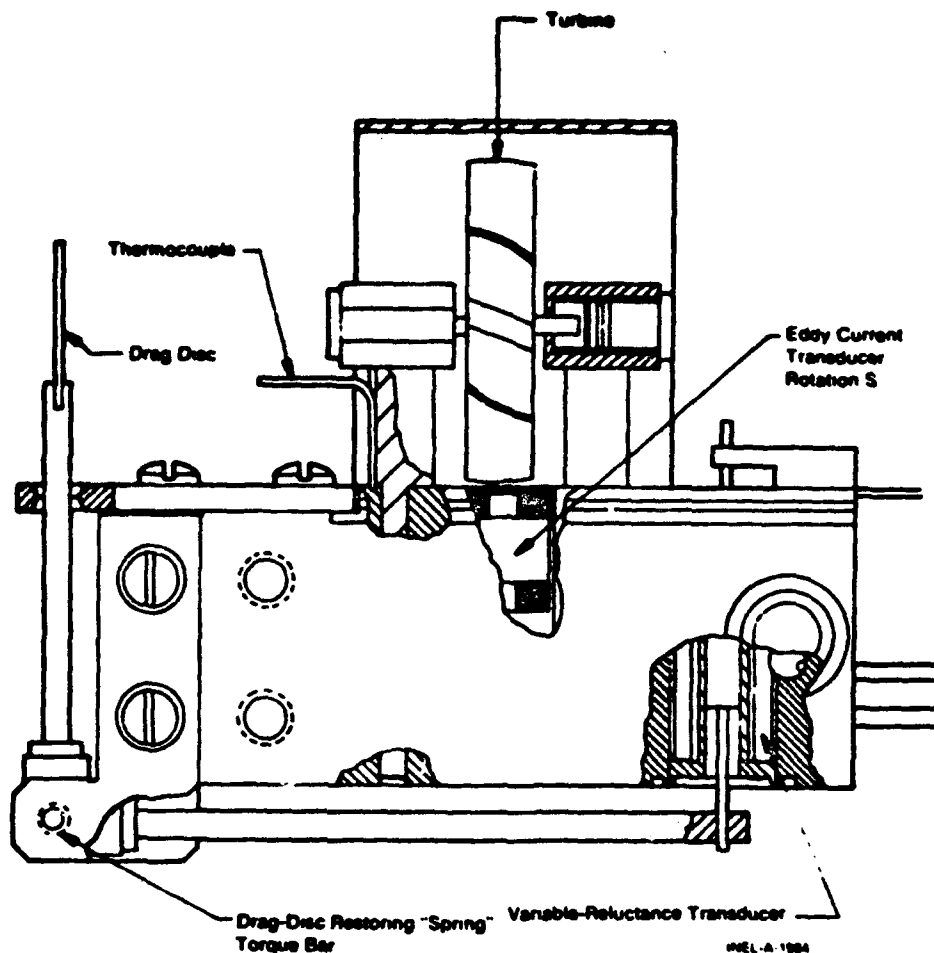
Fig. 4 Drag-Disc turbine transducer (transducer only).

## 4. DTT UNCERTAINTY

The uncertainty of the DTT has been established from testing in
both single- and two-phase flow.  Tests have been conducted at Idaho
National Engineering Laboratory (INEL) and Wyle Laboratories in all
water large size piping, and at Westinghouse Canada Limited (WCL) in all
water and two-phase flow.  One of the largest contributors of the total
uncertainty measurement is the two-phase flow calibration.  A summary of
the DTT uncertainty analysis is shown in Table I.  A comparison of the
density obtained from the drag disc and the turbine with the gamma
densitometer is shown in Table II.

## TABLE I

### SUMMARY OF
### DTT UNCERTAINTY ANALYSIS

| Parameter | Uncertainty ($2\sigma$, + S) | | | |
| --- | --- | --- | --- | --- |
| | Turbine | | Drag Disc | |
| | Single-Phase | Two-Phase | Single-Phase | Two-Phase |
| Calibration | 2 RG | 9 RG | 10 RG | 10.1 RG |
| Linearity and Repeatability | 1.4 RG | 1.4 RG | 6.1 RG | 16 RG |
| Pressure | N.A. | N.A. | 1.0 RG | 1.0 RG |
| State of Knowledge of Measurement Principle | 0 RG (est.) | 1.0 RG (est.) | 2.0 RG (est.) | 2.0 RG (est.) |
| Electronics | 0.1 RG | 0.1 RG | 1.0 RG | 1.0 RG |
| Miscellaneous (Temperature, Mounting, etc.) | 1.5 RG | 1.5 RG | 1.5 RG | 1.5 RG |
| Measurement Channel (RSS) | 2.9 RG | 9.3 RG | 12 RG | 19 RG |

## TABLE II

### COMPARISON OF DENSITY FROM DTT
### WITH DENSITOMETER
### (TEST L1-1)

| Time (sec) | Densitometer lbm/ft$^3$ (kg/m$^3$) | DTT lbm/ft$^3$ (kg/m$^3$) |
|---|---|---|
| 2 | 44.2 (708) | 47.6 (762) |
| 4 | 41.0 (657) | 43.9 (703) |
| 6 | 48.4 (775) | 42.4 (679) |
| 8 | 35.8 (573) | 40.9 (655) |
| 10 | 33.2 (532) | 40.2 (644) |
| 12 | 32.0 (513) | 37.3 (597) |
| 14 | 26.0 (416) | 35.1 (562) |
| 16 | 22.1 (354) | 30.1 (482) |
| 18 | 18.0 (288) | 27.0 (432) |
| 20 | 16.8 (269) | 25.3 (405) |
| 22 | 12.0 (192) | 26.0 (416) |
| 24 | 9.5 (152) | 25.4 (407) |
| 26 | 7.0 (112) | 23.7 (380) |
| 28 | 4.8 (77) | 19.6 (314) |
| 30 | 4.0 (64) | 15.3 (245) |
| 32 | 3.0 (48) | 8.1 (130) |
| 34 | 2.2 (35) | 2.6 (42) |
| 36 | 1.2 (19) | 1.2 (19) |
| 38 | 1.0 (16) | 1.0 (16) |
| 40 | 0.8 (13) | 1.2 (19) |

## 5. GAMMA DENSITOMETER DESCRIPTION

The gamma densitometer used in nonnuclear testing to make the LOFT density measurement is as shown in Figure 5.
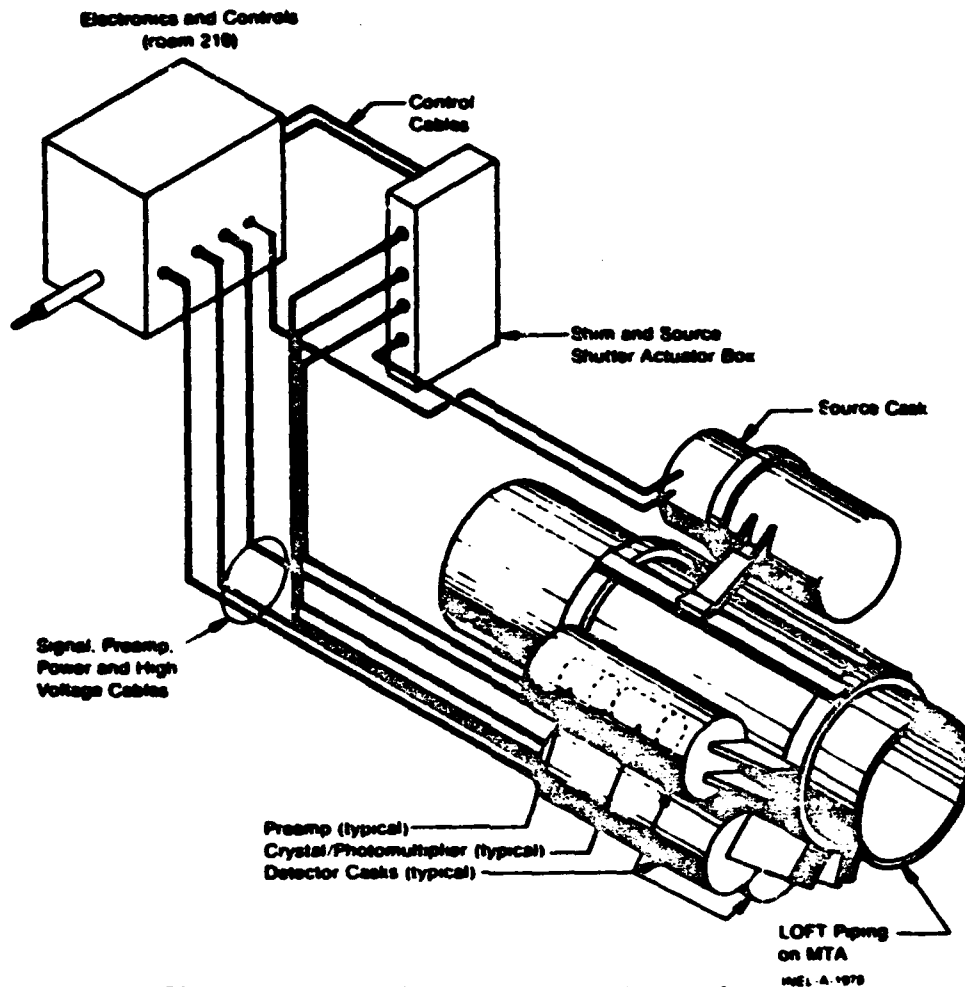


Fig. 5 Gamma densitometer system isometric.

The Model FM-14 gamma densitometer system contains all the necessary electrical and mechanical elements for monitoring the density of a fluid in a pipe.

The basic elements of the system are (1) Cs-137 gamma source housed in a shield cask, (2) three each, integral scintillation detectors, (3)

I.5-14

three each, shielded casks for the detectors, (4) three each, high
voltage power supplies, (5) three each, preamplifiers, (6) three each,
amplifier/control units and, (7) an actuator control panel.

The Cs-137 source consists of 30 Curies of cesium chloride, Cs-137
Cl. The source material is pelletized and a shim is used to prevent
movement of the pellet in the source housing.

The gamma source lead casks limit radiation to less than 50 mr/hr
at contact with the source in the stored position and meets the U.S.
Department of Transportation (DOT) regulations as an approved shipping
container. The cask is designed to be rigidly mounted on a pipe fixture.
The unit is 8 in. in diameter and 18 in. long exclusive of the mounting
device. An air operated source positioner with a fail-safe (stored)
mechanism provides remote control of the source. An electrically oper-
ated solenoid driven latch assembly is also provided to lock the source
in the exposed position.

Each scintillation detector consists of a 2 x 2 in. NaI (thallium
activated) crystal and a photomultiplier tube mounted as an integral
unit.

The scintillation detectors are installed in shielded detector
casks, see Figure 5. The cask is 16 in. long by 6 in. in diameter and
contains a cooling coil for water cooling. The unit is constructed of
lead-filled stainless steel and tungsten to provide shielding and
collimation. Two remotely controlled calibration shims, which are
attached to each of the detector casks are provided to simulate a known
change in density. The SHIM LO simulates a change of approximately 10
lbs/ft$^3$ while SHIM HI simulates a change of approximately 45 lbs/ft$^3$
in the 14 in. schedule 160 pipe for Beam "B" (diametrical beam). For
Beam "A" and "C", the SHIM LO and SHIM HI values are 11.5, 52.3, and
16.2, 73.3 lb/ft$^3$, respectively, beam locations are shown in Figure 6.
A NEMA box is supplied to house the air actuator valves that control the
air to the gamma source positioner and calibration shim air cylinders.
Also provided in the unit is an air regulator, filter, and relief valve
to prevent buildup of pressure inside the box.
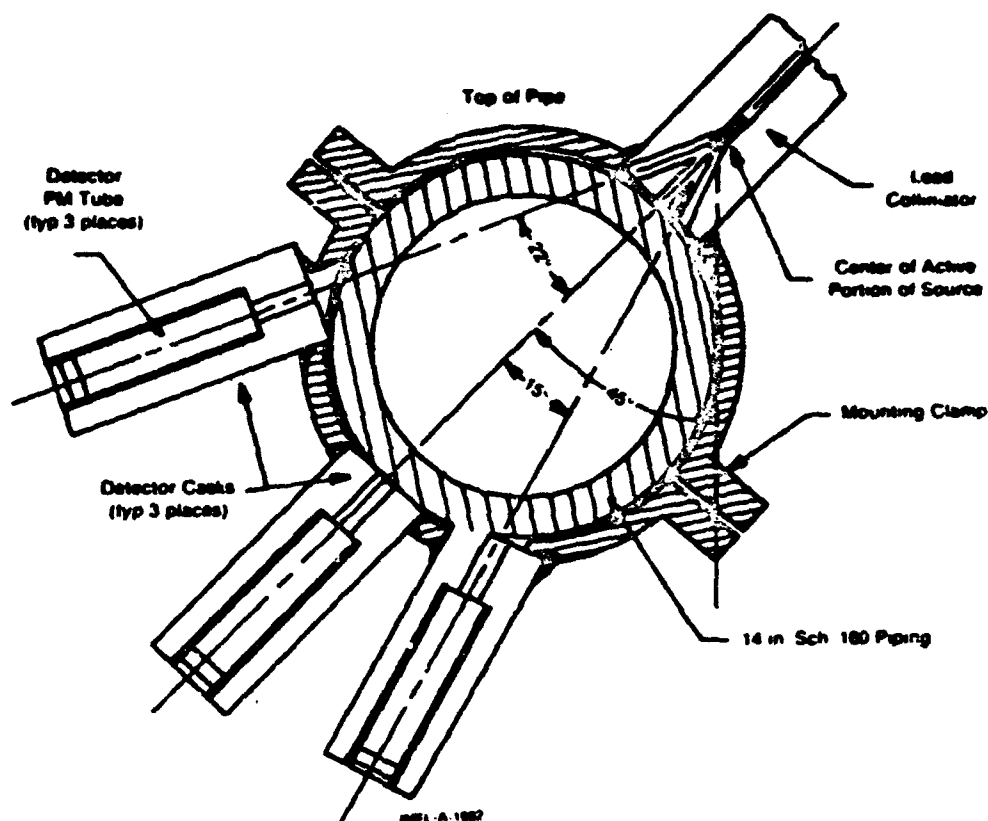
Fig. 6 Three beam gamma densitometer.

The high voltage power supply is a calibrated, high voltage power supply designed for use with photomultiplier systems requiring a high stability, low noise, well regulated power source. It mounts in a standard NIM Bin as in AEC (ERDA) Specification TID-20893 (Revision 3), "Standard Nuclear Instrument Modules," and occupies two module widths. It is supplied with an integral three-wire power cord and NEMA plug and does not use the NIM Bin Power Source for operation.

The high voltage power supply incorporates over voltage and arc protection circuits which prevent damage to the supply and its load if

I.5-16

the supply fails or voltage transients are caused by sustained arcing at
the load and its associated wiring.

The preamplifier supplied with the system provides current to
voltage conversion at the detector assembly. This converter is a very
stable, low-noise unit that provides an accurate and linear conversion
as well as gain to boost and drive the signal through the cable to the
amplifier.

The amplifier has two stages ($A_1$ and $A_2$) of amplification to
provide flexible output ranges. These amplifiers assure stable and
low-noise operation.

A potentiometer ZERO ADJUST provides an adjustable reference vol-
tage to the differential amplifier, $A_1$, which results in a zero shift
(bias) of the recorder output so that the user can better match the
signal level to the dynamic range of his recorder or indicator. A
three-pole double throw toggle switch provides + and − polarities for
the ZERO ADJUST voltage while a single-pole double throw switch grounds
the $A_1$ amplifier positive input (reference voltage is switched out). A
front panel meter monitors the output of amplifier $A_1$ and provides the
operator with a visual indication of system operation.

The filter selector switches the output of amplifier $A_2$ directly to
the recorder output or to a 10 Hz plug-in, six-pole Bessel filter  The
OUTPUT ADJUST potentiometer controls the full-scale output of the re-
corder. Internal adjustments are provided for the panel meter full-scale
indication and to zero all amplifiers.


6. GAMMA DENSITOMETER UNCERTAINTY


The gamma densitometer system was thoroughly tested with simulated
flow regimes of various materials. These included annular, bubbly, and
stratified. Calculations were made from the known densities of the

I.5-17

materials and then inserted in a section of LOFT piping and measured
with the gamma densitometer system, one such configuration for annular
flow is shown in Figure 7. The system was also tested with various
depths of water (stratified flow regime) which was accurately measured,
and the density calculated for each beam. This was compared with the
actual measure density. A summary of the uncertainty of each beam is
shown in Table III.

## TABLE III

### SUMMARY OF GAMMA DENSITOMETER UNCERTAINTIES

|  | Beam (Percent of Full Scale) | | |
|---|---|---|---|
|  | A | B | C |
| Statistical Error | 0.55 | 0.36 | 0.88 |
| Nonmonoenergetic | 0.5 | 0.5 | 0.5 |
| Stability | 0.1 | 0.1 | 0.1 |
| Calibration | 0.6 | 0.6 | 0.6 |
| Linearity | 0.2 | 0.2 | 0.2 |
| Noise | 0.4 | 0.4 | 0.4 |
| DAVDS (DDAPS) | 0.13 | 0.13 | 0.13 |
| RSS | 1.1 | 1.0 | 1.3 |
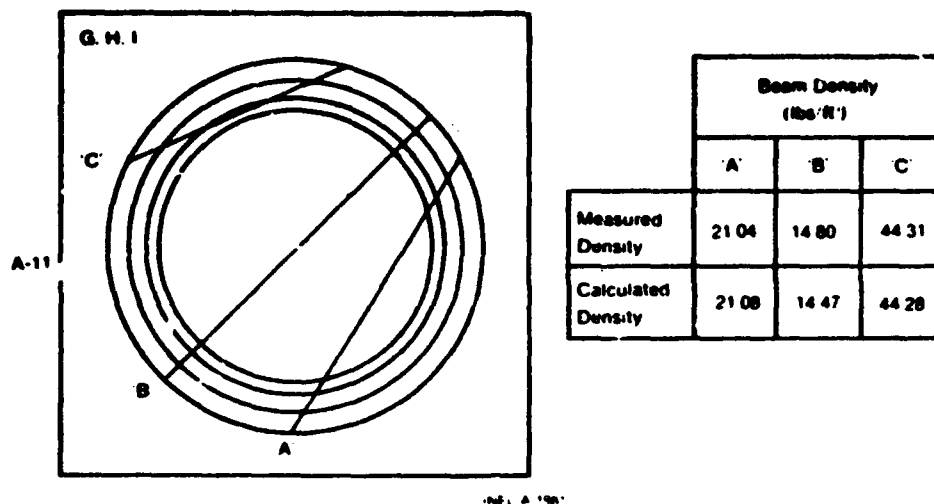
Fig. 7 Three beam densitometer static test data for annular flow configuration.


Although uncertainty is of major importance we can also determine flow regime by utilizing the three beams in a simple truth diagram, Figure 8.
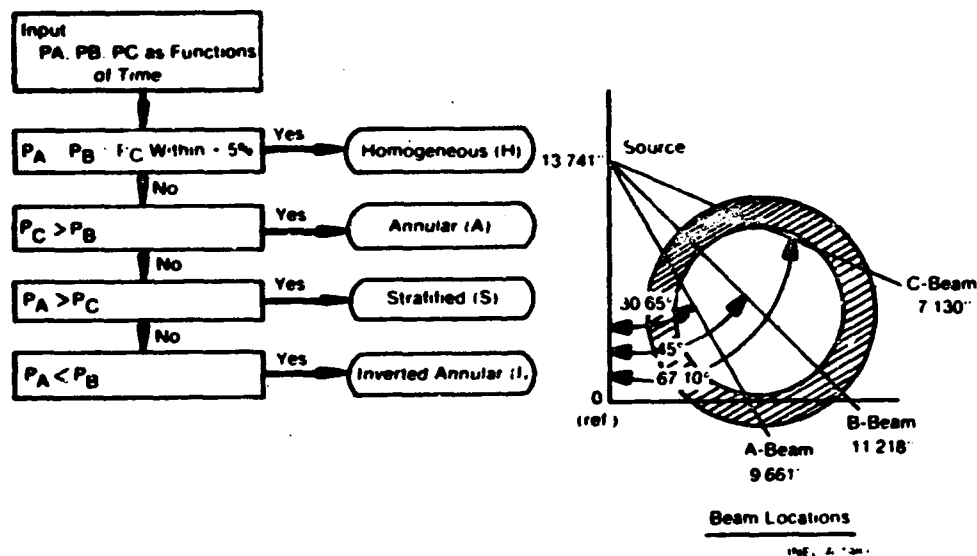


Fig. 8 Gamma densitometer flow regime logic.

# 7. DATA

The DTTs and gamma densitometers have proven to be good transducers for the measurement of the flow parameters in the first three nonnuclear tests.

Typical of the data from the gamma densitometer is that shown in Figures 9 and 10. This shows the three beams displayed on the same graph of broken loop reactor inlet location, Test L1-1 as in Figure 9. It can readily be seen that the flow is stratified during the saturated blowdown from the respective readings of each of the three beams and applying the readings to the truth table shown in Figure 8. Later during ECC injection, more stratification is in evidence. At the intact loop locations slug flow is very prevalent as shown in Figure 10.

With this information on flow regime, it is much easier to interpret the DTT data. Since the DTT is a point measurement located in the center of the pipe, it is important to know the flow regime in the pipe. Typical data from Test L1-3A as recorded from the DTT are shown in Figures 11 and 12 which depict respectively the momentum flux and the velocity. Complete data sets are available[2,3,4]. Since the DTT is a point measuring system, this is the primary factor in the measured differences in density from the drag disc turbine versus density from the gamma densitometer previously shown in Table II.
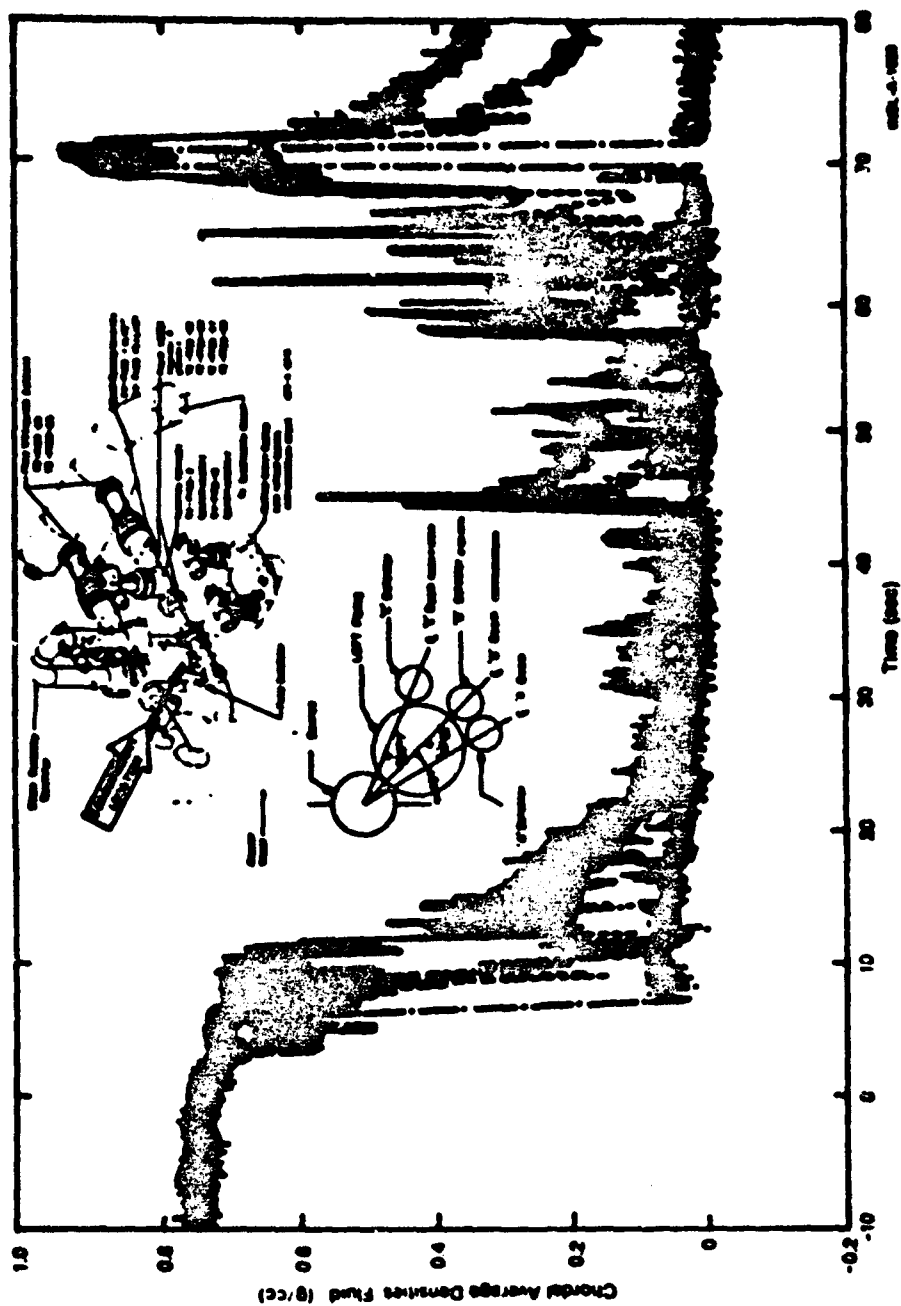
Fig. 9 LOFT experiment L1-1 chordal average densities from 3-Beam densitometer at broken loop reactor inlet cold leg.

I.5-21
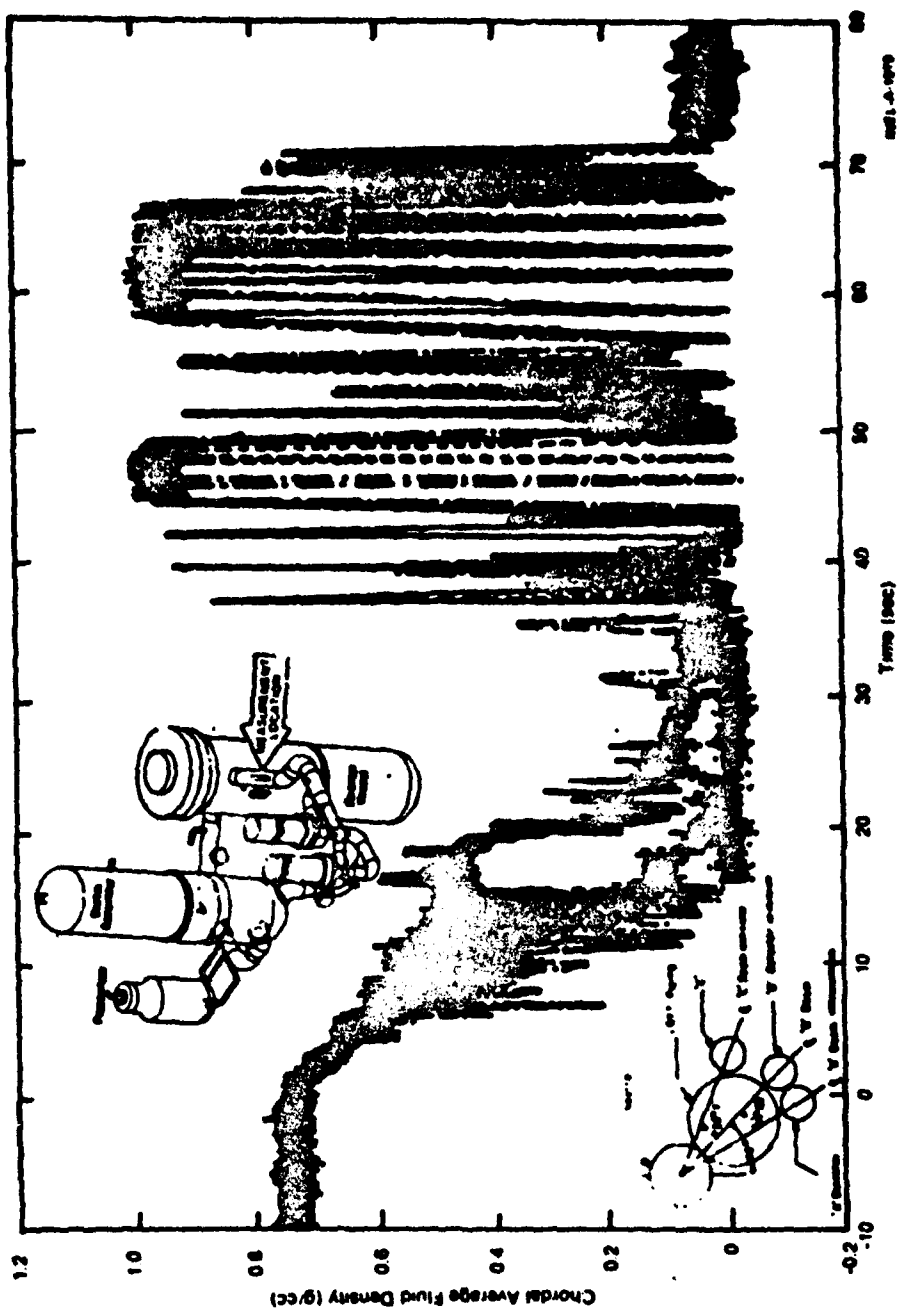
Fig. 10 LOFT experiment L1-1: chordal average densities from 3-Beam densitometer at intact loop reactor inlet cold leg.
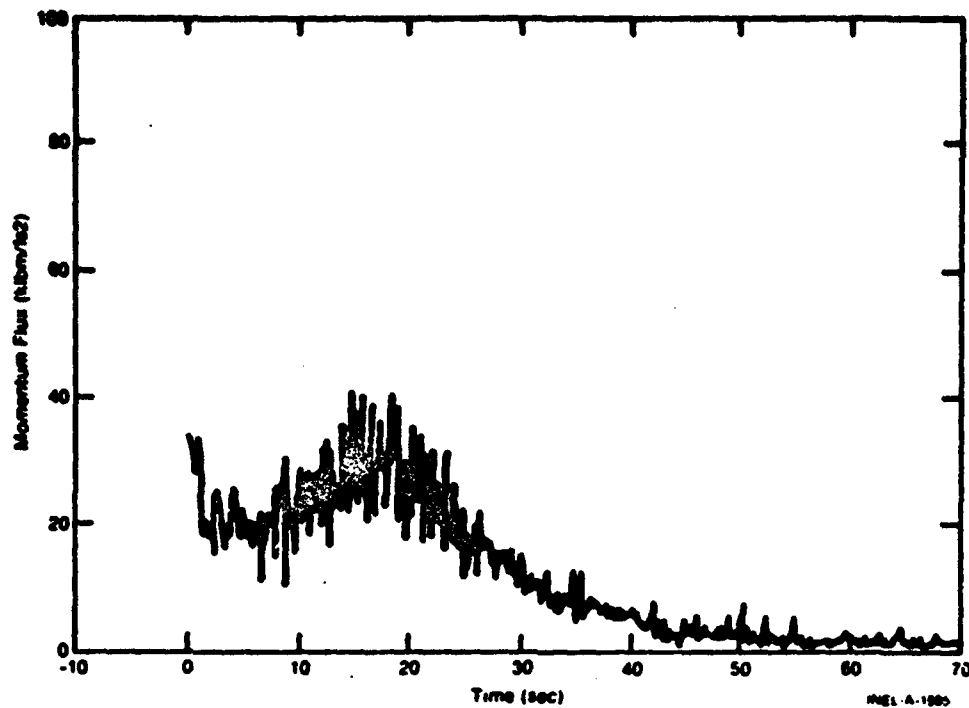
Fig. 11 Loss-of-coolant experiment L1-3A momentum flux -- broken loop cold leg.
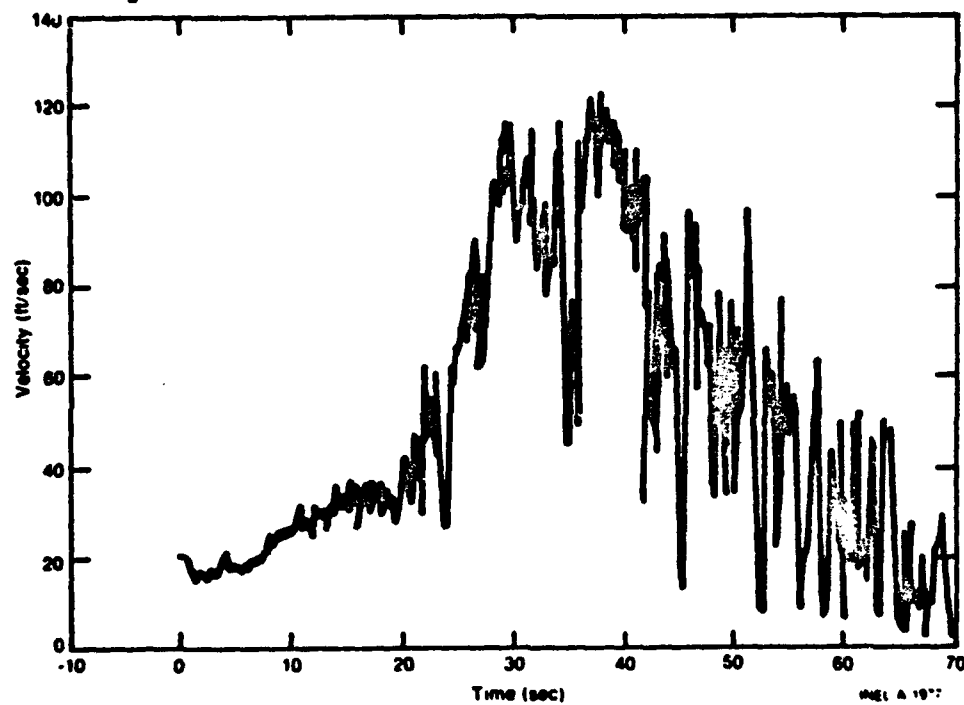


Fig. 12 Loss-of-coolant experiment L1-3A velocity -- broken loop cold leg.

I.5-23

# 8. SUMMARY

We have been successful in making density, velocity, and momentum flux measurements on LOFT. This is partly due to the large amount of performance and calibration testing of the transducers. Much additional separate effects testing was also done to characterize the flow transducers. Our present transducer performance is well documented and uncertainties have been derived for both single- and two-phase flow. The present combination of the drag disc turbine and the multibeam gamma densitometer have provided very good correlations of the data. Reliability of the transducers has been good although we feel it can be improved and are actively pursuing an improvement program. This is especially true in the case of the gamma densitometer which must be changed for nuclear operations.

# 9. REFERENCES

1.  H. C. Robinson, LOFT Systems and Test Description (Loss-of-Coolant Experiments Using a Core Simulator), TREE-NUREG-1019 (November 1976).

2.  J. R. Chappell, Experiment Data Report for LOFT Nonnuclear Test L1-1, TREE-NUREG-1025 (January 1977).

3.  H. C. Robinson, Experiment Data Report for LOFT Nonnuclear Test L1-2, TREE-NUREG-1026 (January 1977).

4.  G. M. Millar, Experiment Data Report for LOFT Nonnuclear Test L1-3A, TREE-NUREG-1027 (December 1976).

# STATE OF THE ART - TWO-PHASE FLOW

## CALIBRATION TECHNIQUES

by

Marland L. Stanley

EG&G IDAHO, INC.

IDAHO NATIONAL ENGINEERING LABORATORY

Presented at NRC Two-Phase Flow Instrumentation Meeting at
Silver Spring, Maryland, January 13, 1977

I.5-25

## CONTENTS

## TABLES

**Preceding page blank**

# 1. INTRODUCTION

The nuclear community faces a particularly difficult problem relating to the calibration of instrumentation in a two-phase flow steam/water environment. The rationale of the approach to water reactor safety questions in the United States demands that accurate measurements of mass flows in a decompressing two-phase flow be made. An accurate measurement dictates an accurate calibration. This paper addresses three questions relating to the state of the art in two-phase calibration:

(1) What do we mean by calibration?

(2) What is done now?

(3) What should be done?

It may not be possible to answer all three of these questions, particularly the last one. Perhaps the stage can be set for thinking and discussion to follow this afternoon.

# 2. WHAT IS CALIBRATION

According to the dictionary, calibration means to check, adjust, or systematically standardize the graduations of a quantitative measuring instrument. There are some key words to this definition. They are: standardize and quantitative.

To calibrate anything it implies a standard of comparison exists, and further, that a known set of conditions can be recreated at will. Before we can have a two-phase flow calibration, a standard must exist. The title of this paper infers this, but it has been submitted that perhaps this is ludicrous. Let us examine the other key word, quantitative.

Preceding page blank

I.5-29

Again, the dictionary tells us, pertaining to or susceptible to measurement. We have assembled here for the purpose of discussing many creative and imaginative attempts to test the susceptability to measurement of some rather elusive parameters. A two-phase flow calibration must embody some, perhaps all, of these measurement techniques.

## 3. WHAT IS DONE NOW

Techniques employed currently involving a steady state two-phase flow calibration involve measurement of flow rate of each component in single-phase mixing, taking a heat balance, and calculating the quality assuming equal phase velocities. What is known about these kinds of systems?

The mass flow in steady state is known, the pressure and the temperature are also known, provided we arrange for a saturated condition to exist. What is not known is phase velocity and distribution, flow regimes, and temperature. Where there are mixed streams of different temperatures, this is of particular interest in view of the ECC problem.

Dr. Estrada indicates that a flow instrument which is to be tested may actually consist of several measuring devices from which individual phase mass flows and regime can be inferred. This would seem to indicate that any two-phase flows standard would not be a single reference instrument but rather a group of instruments from which a two-phase standard would be inferred. This thinking is more or less universal in the instrumentation community charged with the two-phase flow measurement problem. The types of measurements that are made are numerous. A number of good reports have summarized single-phase and two-phase flow measurement capabilities. Among them are two EPRI reports. (EPRI NP-195 by Brockett and Johnson and EPRI RP-446 by Hewett.)

Tables I through VI present a broad brush listing of the few two-phase flow loops known and briefly discuss the kinds of measurements

I.5-30

## TABLE I

### TWO-PHASE FLOW TEST LOOP, KARLSRUHE

---

**Steady State Two-Phase Flow**

Steam/Water or Air/Water
Pressures to 2250 psi
Temperatures to 350°C
Mass flows to 5 kg/sec
Horizontal Test Section

**Measurements (Single-Phase)**

Inlet Steam Flow (Orifice)
Inlet Water Flow (Orifice)
Pressure
Temperature

**Measurements (Two-Phase)**

Drag Body
True Mass Flow Meter
Radionuclide Tracer
Nuclear Magnetic Resonance
Drag Body, Turbine, $\gamma$ Densitometer Combination
Flow Pattern
    High Speed Photography
    Multibeam $\gamma$ Densitometer
    Impedance Probe

---

being made in these laboratories. This information is by no means intended to be all inclusive. Corrections or additions are welcome.

The two-phase flow loop facility located in Karlsruhe, Germany, is a steady state flow loop. Pressure capabilities to 2250 psi, temperatures to 350°C, and mass flows to 5 kg/sec utilize a horizontal test section. The unique feature of this loop is that it is capable of also operating in air/water. Measurements made are single-phase inlet steam flow, inlet water flow, pressure, and temperature. Measurements made on the two-phase test section are drag body type measurements, the true mass flowmeter which they have developed, the radio-nuclei tracer for phase velocity measurement, nuclear magnetic resonance techniques, and a

## TABLE II

### TWO-PHASE FLOW TEST LOOP -- CISE, ITALY

---

**Steady State Two-Phase Flow (Some Transient Capability)**

Steam/Water
Pressure to 3689 psi
Temperature to 300°C
Mass Flows > 25 kg/sec
Verticle Test Section

**Measurement (Single-Phase)**

Inlet Steam Flow
Inlet Water Flow
Pressure
Temperature

**Measurements (Two-Phase)**

Quick Closing Valves
Impedance Probes
Pressure
Flow Pattern
    No special technique is at present available.
    Measurement of local and instantaneous flow
    rates in two-phase conditions.

---

combination drag body turbine gamma densitometer. For flow pattern recognition, they use high speed photography and multibeam gamma densitometers, plus some work has been done with an impedance probe.

The two-phase flow test facility in Italy has some transient capabilities. The maximum pressure is 3689 psi, temperatures to 300°C, and mass flows in excess of 25 kg/sec with a vertical test section. Measurements of the input to the two-phase test section include inlet steam flow and inlet water flow pressure and temperature. Unique measurements within their two-phase test section are made with quick closing valves. Impedance probes pressure measurements are also made. At the present time. no special technique exists for flow pattern identification.

1.5-32

## TABLE III

### TWO-PHASE FLOW TEST LOOP, WCL, CANADA

---

**Steady State Two-Phase Flow**

> Steam/Water
> Pressure to 900 psia
> Temperature to 350°C
> Mass Flow 22 kg/sec
> Horizontal or Vertical Test Section

**Measurements (Single-Phase)**

> Inlet Steam Flow
> Inlet Water Flow
> Pressure
> Temperature

**Measurements (Two-Phase)**

> Quick Closing Valves
> Multibeam $\gamma$ Densitometer
> Turbine
> Pitot Tubes
> Flow Pattern
> > Not Known

---

At the WCL Loop in Canada, measurements are made at the inlet steam flow, the inlet water flow, pressure, and temperature. In the two-phase test section, quick closing valves, multibeam gamma densitometers, turbines, and pitot tubes are utilized. Types of flow pattern instrumentation are not known.

The French have numerous facilities. A summary of their total capability of the various facilities is given in Table IV. Two-phase flow measurements include microthermocouples, optical probes, hot wire and hot film anemometers, a unique liquid bearing turbine meter, neutron beam attenuation, quick closing valves, and multibeam gamma densitometers.

During a recent visit to Japan, several large test facilities were visited. These test facilities gave the impression that instrument development is very limited.

## TABLE IV

### TWO-PHASE FLOW TESTING, FRANCE

**Many Loops Available**

      Frenesie. Graziella (Freon 12)
      Patricia, Omega, Ersec, Moby Dick, Canon (Water)
      Dedif (Water/Argon)

**Measurements (Two-Phase)**

      Microthermocouple
      Optical Probes
      Hot Wire or Hot Film Anemometry
      Electrical Probes
      Turbine Flowmeters (Fluid Bearings)
      Venturi -- Orifice Meters
      Neutron Beam Attenuation
      Multibeam Gamma Densitometers
      Quick Closing Valves

The two-phase flow test loop in Idaho is an air/water loop. Again, inlet air flow, inlet water flow, temperature, and pressure measurements are made. Measurements made in the two-phase test section of the loop are turbine meter, drag body, both discs and screens, multibeam gamma densitometers, high speed photographs, and differential pressure.

Also located at INEL is a transient two-phase flow loop, featuring a quick opening valve, and a partial blowdown capability for rapid testing turnaround time. Measurements made in the transient two-phase loop are multibeam gamma densitometers, single-beam gamma densitometers, quick closing valves, turbines, drag body, pressure, and temperature.

The calibration of all mass flow instrumentation for Semiscale occurs in ambient water. All the instruments, turbine meters, and drag discs are calibrated in place. A USNBS traceable turbine meter serves as a standard. The air/water loop previously mentioned is utilized to

## TABLE V

### TWO-PHASE FLOW TEST LOOP, INEL, IDAHO

---

**Steady State Two-Phase Flow**

    Air/Water
    Pressure 60°F
    Temperature 130 psi
    Mass Flow 22 kg/sec

**Measurements (Single-Phase)**

    Inlet Air Flow
    Inlet Water Flow
    Temperature
    Pressure

**Measurements (Two-Phase)**

    Turbine
    Drag Body
        Disc
        Screens
    Multibeam $\gamma$ Densitometers
    High Speed Photographs
    Differential Pressure

---

study the relative accuracy of water calibrations when applied to two-phase steam/water environments such as occurs during the Semiscale blowdowns.

Steam/water two-phase flow testing of the Semiscale spool pieces in the Karlsruhe two-phase flow water/steam loop is being planned. Presently, much the same approach is taken for the calibration of LOFT drag-disc turbine. Calibration is made against the standard flowmeter in ambient water.

The Semiscale calibration in ambient water has proven to give reasonable results. There is, however, some criticism of the Semiscale experiment in that the piping sizes are not typical - that the size almost guarantees a homogeneous two-phase flow. Perhaps we have "lucked out" on Semiscale because of this. If one does a mass balance using

## TABLE VI

### TRANSIENT TWO-PHASE FLOW, INEL, IDAHO

---

Transient Two-Phase Flow

    Quick Opening Valve
    Partial Blowdown Capability

Measurements (Transient Two-Phase)

    Multibeam $\gamma$ Densitometer
    Single Beam $\gamma$ Densitometer
    Quick Closing Valves
    Turbine
    Drag Body
    Pressure
    Temperature

---

Semiscale data, the results are found within reason. Two-phase mass flow measurements appear to have been made.

This is good for such a complicated integrate type experiment. We are now obtaining mass flow data from LOFT. The flow is definitely not homogeneous. We know from our multibeam densitometers that it is stratified. We currently have no method of measuring phase velocities, slip velocities, or density distribution.

## 4. WHAT SHOULD BE DONE

These measurements are difficult even under ideal laboratory conditions. How can such measurements be performed in a LOFT? Those instruments which can be ruggedized to take the environment must be selected and then it must be figured out how to interpret what they say. Continued bench type laboratory testing will be required if personnel are to get a handle on the subtleties of the two-phase flow measurement problems. Such testing requires that certain of these unique methods be adopted and agree, to utilize them so that data may be compared from one laboratory to another.

It must be learned how to establish repeatable conditions - not only from one day to the next within a given laboratory, but from laboratory to laboratory. A universally acceptable standard or set of standards must be established. This implies the ability to obtain repeatable conditions. To do this, phase velocity, flow regime, and density distribution must be known.

Current technology seems to indicate that the best bets for phase velocity measurements are tracer techniques or local probes. The most attractive of these are the tracer techniques because they do not disturb the environment.

For flow regime, multibeam gamma densitometers are suggested since nearly all laboratories have some experience with them, but local probes could be used. Again the densitometers do not perturb the environ, instead they measure.

Furthermore, these same devices could provide the density distribution. It can be said that flow regime and density distribution imply the same thing and these two can be combined.

To summarize, calibration has been defined, although the specific question of what we mean by a two-phase calibration may not have been answered. A look has been taken at what techniques are available to us and it has been concluded that a standard is needed. Right now, one does not exist. The problems are large and complicated. Universal two-phase flow standards must be adopted.

# PROGRESS REPORT ON INEL

## "FULL FLOW DRAG SCREEN"

by

A. E. Arave

J. B. Colson

J. R. Fincke

EG&G IDAHO, INC.

IDAHO NATIONAL ENGINEERING LABORATORY

**Preceding page blank**

## SUMMARY

The objective in developing a full flow drag screen is to obtain a
total momentum flux measurement which when combined with a suitable
independent velocity or density measurement will yield a total mass
flux. The major design considerations are predicated by the fact that an
accurate momentum flux measurement must be made over a wide range of
flow conditions. The device should exhibit a constant calibration
regardless of Reynolds number, void fraction, slip ratio, or flow
regime. The dynamics of drag devices are well understood in single-
phase flows. This is not true for two-phase flows. The present develop-
ment program is directed toward gaining an understanding of the dynamics
of drag devices which sample the total area of a pipe in two-phase flow
and developing a method for deducing mass flow rate using such a device.

Various geometric arrangements are to be investigated. Testing to
date has shown excellent results using a round wire mesh screen in the
Semiscale air/water loop. Future air/water testing will include per-
forated plates and wire meshes with both rectangular and diamond shaped
cross sections.

Analytical models of the hydrodynamics of the drag screen as well
as the associated density or velocity measuring device are being used to
select the optimum configuration. Alternate force sensing methods are
also being considered. These include single and multiple transducer
arrangements. Multistage springs and pressure drop across the body are
to be evaluated for extending the dynamic range of the drag body.

Preceding page blank

I.5-41

# CONTENTS

## FIGURES

## TABLE

Preceding page blank

# 1. INTRODUCTION

A full flow drag screen is being developed to obtain total momentum flux measurements in Semiscale, Loss-of-Fluid Test (LOFT), and Bettis Flask. Measurement requirements appear in Table I. The device itself consists of a screen or perforated plate which samples the entire cross-section of a given flow conduit and a mechanical arrangement to measure the force on the screen. A pressure drop measurement across the screen is made at the same time.

The prototype Semiscale unit utilizes a three point mount and three independent force sensors, Figure 1. This device has been used to evaluate the performance of a round wire screen, and is currently being used to test rigid perforated plates supplied by the LOFT development program.

The first prototype unit built by LOFT will use a single force sensing device, Figure 2. The entire sensor assembly will be contained within the pressure boundary. An eddy current displacement sensor will be used to obtain a measurement of spring element displacement.

# 2. OBJECTIVE

The objective is to obtain a better mass flow measurement by suitable combination of two-phase momentum flux measurement with an independent density or velocity measurement. For homogeneous flow without slip an average density measurement $\rho$ from a gamma densitometer may be simply combined with $\rho V^2$ to yield a mass flow rate $\rho V$. For flows with slip where the momentum flux of each phase is of the same order of magnitude the combination is not so straightforward. This problem will be addressed both experimentally and analytically in the present development program. Suitable independent velocity measurement could be made

**Proceeding page blank**

## TABLE I

### DRAG SCREEN MEASUREMENT REQUIREMENTS

| | LOFT | Semiscale | Bettis Flask |
|---|---|---|---|
| Momentum Flux (lbm/ft-sec$^2$) | 200-188,000 | 10-1,000<br>2,000-200,000 | 10-1,000<br>2,000-200,000 |
| Density lbm/ft$^3$ | 47-0.15 | 47-0.15 | 47-0.15 |
| Re No./ft (Single-Phase) | $1.0 \times 10^5 - 1.0 \times 10^7$ | $2.0 \times 10^4 - 1.0 \times 10^7$ | $2.0 \times 10^4 - 10. \times 10^7$ |
| Location | Near Break Plane<br>8-in. Diameter | Pipe and Incore<br>3-in., 1-1/2-in. Diameter | Pipe<br>3-in. Diameter |

I.5-46

Sliding Plate
(3 places)

0.060 Diameter
on 0.300 Centers

Lever Arm Force Sensors
3 Pieces

View A-A - Alternate Designs

INEL-A-1805
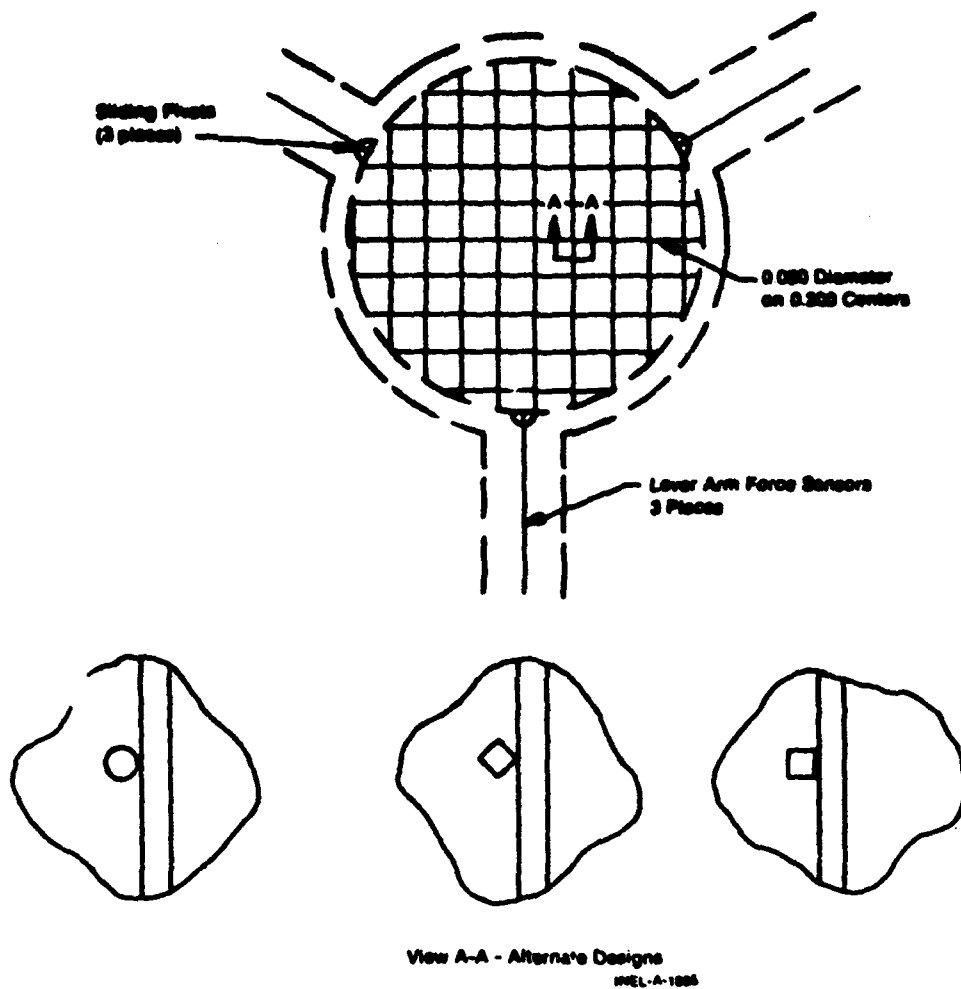
Fig. 1 Three transducer drag screen mounting configurations.

I.5-47
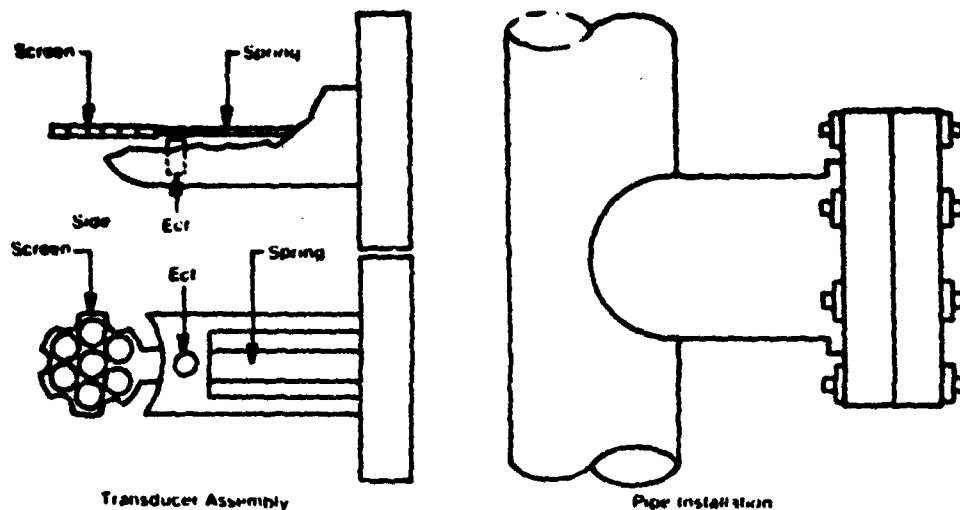
Fig. 2 Proposed LOFT drag screen design configuration.

by a turbine or pitot tube. Present data indicate that more detailed velocity field measurements may be needed to properly interpret drag screen data and deduce a mass flow measurement.

### 3. PRESENT AIR/WATER TESTING

To date the only data which have been analyzed in detail are round wire screen data in the Semiscale air/water loop. The combination of momentum flux values with average density from a two-beam densitometer is seen. Figure 3 yields an adequate mass flow measurement for the range tested. Other types of screen elements to be tested are perforated plates with and without beveled edges.

### 4. FUTURE AIR/WATER TESTING

First generation LOFT prototypes will be fabricated in 3-in. schedule 160 pipe. Phase I development testing will be performed in the

I.5-48
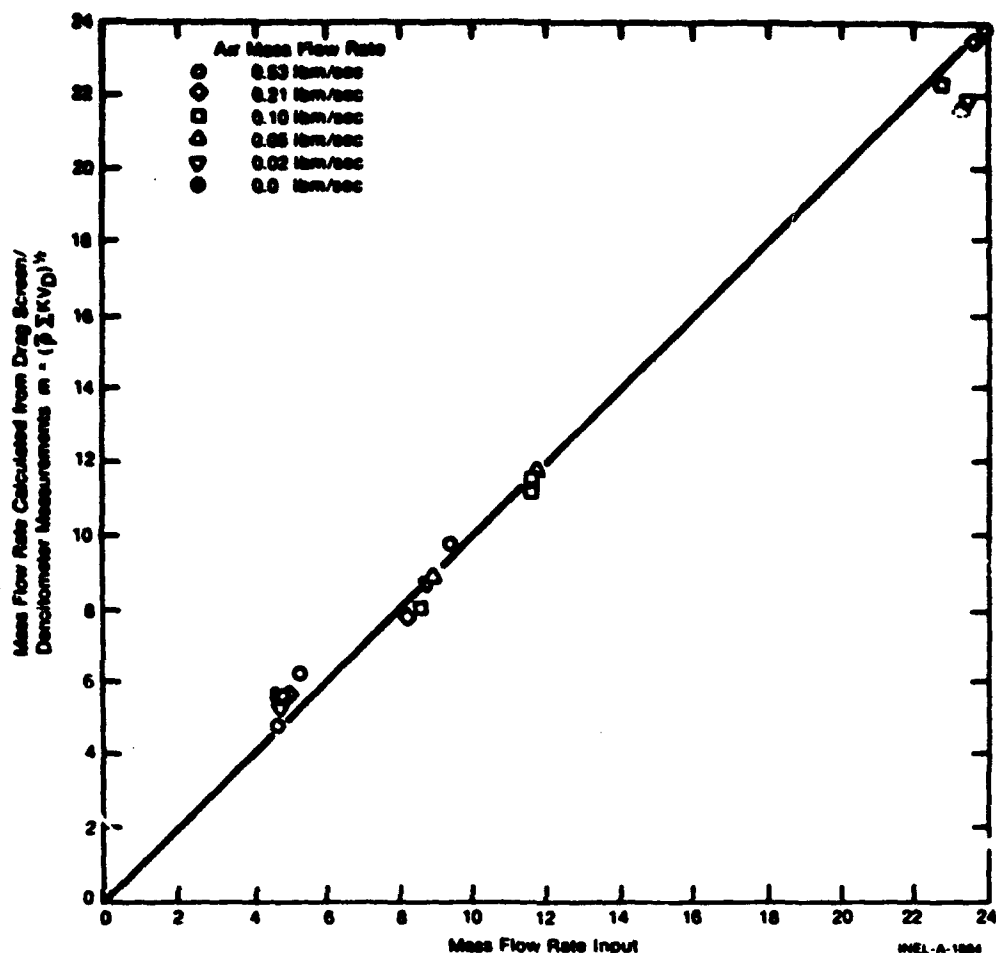
Fig. 3 Semiscale drag screen air/water data (0.02-in. diameter round mesh on 0.2-in. centers).

Semiscale air/water loop.  The objective of these tests is to check mechanical function and to develop screen elements which provide a constant drag coefficient over a wide range of flow conditions, Figures 4, 5, and 6.  Parameters which should be considered for screen design are insensitivity of drag coefficient to Reynolds number, flow regime, slip ratio, and void fraction.  The flow restriction should be minimized as much as possible and still make an accurate total momentum flux measurement.
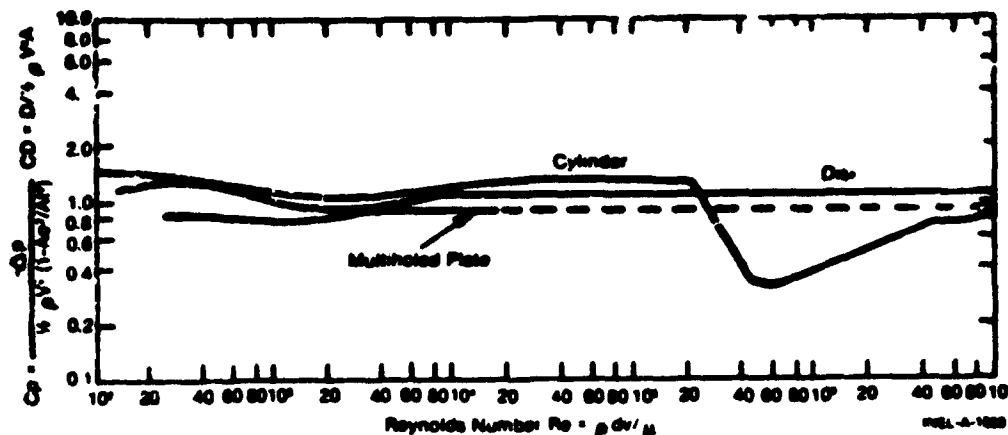
**Fig. 4** Reynolds number dependence in single-phase flow (drag coefficient for a circular cylinder and thin disc and pressure drop coefficient for a multiholed plate).

## 5. FUTURE STEAM/WATER TESTING

Phase II development testing will be transient flows of steam/water performed in the Bettis Flask Blowdown Facility. The objective of these tests is to verify performance in a transient steam/water flow.

## 6. CONCLUSIONS

Preliminary data have shown that a full flow drag screen can make an accurate measurement of total momentum flux over a wide range of flow conditions. For certain ranges these data can be combined with average density from a gamma densitometer to yield an accurate mass flow rate. More development testing is required to be confident that a good mass flow measurement can be obtained over the wide range of conditions present in a LOFT blowdown.

I.5-50
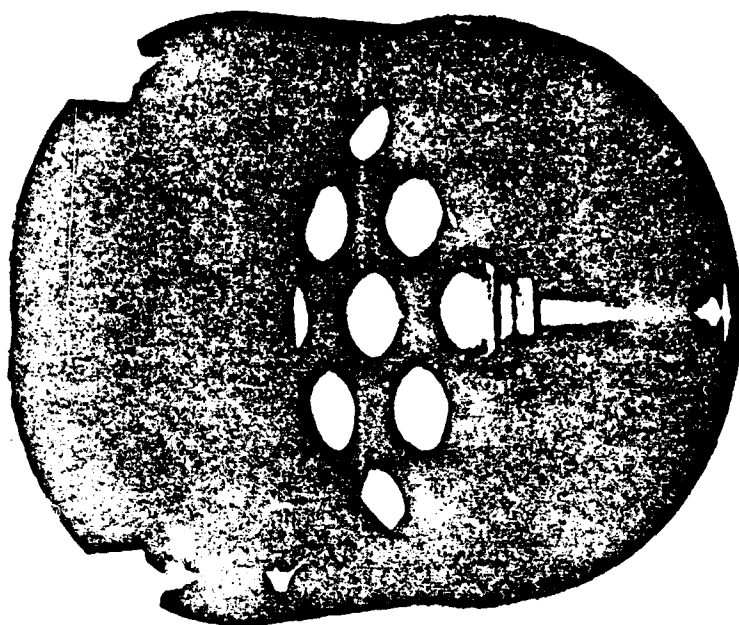
Fig. 5 Air/water test section insert.

I.5-51

3-in Diameter Drag Screens Single Bearing Tests
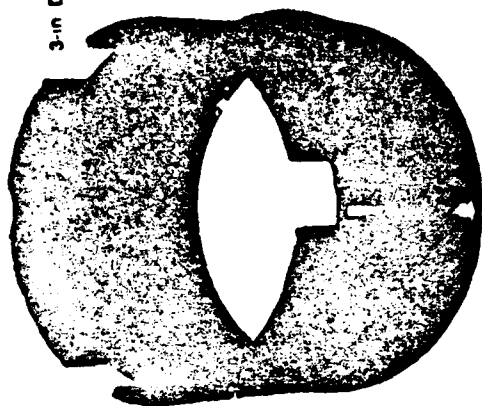
Hole Area
Total Area · 0.77 in
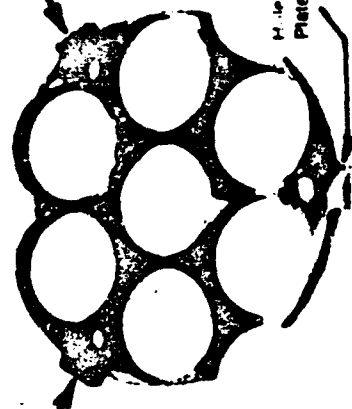
Hole Diameter · 0.84 in.
Plate Thickness · 0.18 in.

Mounting
Point
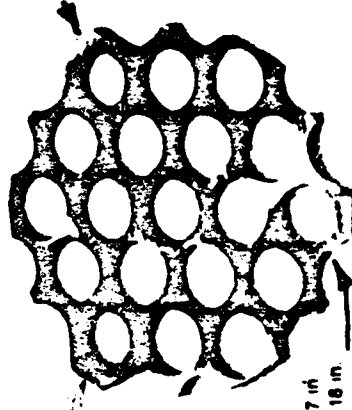
Hole Area
Total Area · 0.6? in

Hole Diameter · 0.47 in.
Plate Thickness · 0.18 in.

Fig. 6 3-in. diameter drag screens.

# APPENDIX A

## DRAG SCREEN DESIGN PARAMETER CONSIDERATIONS

I.5-53

# APPENDIX A

## DRAG SCREEN DESIGN PARAMETER CONSIDERATIONS

Some blunt bodies are known to exhibit constant drag coefficients for Reynolds numbers above a certain minimum value. For example, thin circular or square plates for Reynolds numbers are based on height or diameter above about 3000[1]. For a given Reynolds number held constant, and the length to height ratio of a rectangular section varied, the drag coefficient becomes a constant for a length to height ratio of approximately 1/3[1]. Thus, for a drag body in an infinite flow field (a small body in a large pipe) to behave like a thin plate or disc, its thickness should be less than 1/3 its height.

For multiple bodies such as screens or multiholed plates this criterion is probably unnecessarily restrictive for the height to length ratio. The phenomenon which causes the drag coefficient for a thin disc or plate to become constant for a large enough Reynolds number is the behavior of the flow field around the body. The flow is unable to negotiate the sharp corner and separates from the body. For Reynolds numbers above $3 \times 10^3$, the flow field changes very little and the drag coefficient is essentially constant. If the body is made thicker, the possibility of the separated flow reattaching itself to the body must be considered. If this occurs, the drag coefficient will change, possibly reduced by as much as a factor of $2^{[1]}$.

It is well known that a pressure rise is required for reattachment of a separated shear layer to a body[2,3,4]. This pressure rise is achieved through the transport of momentum or mixing (either laminar or turbulent) which accelerates the fluid in the recirculation zone and results in a net slowing or diffusing of the fluid in the external flow[5]. This slowing of the external flow creates a pressure rise. The acceleration of the slower moving fluid in the recirculation zone

**Preceding page blank**

increases its kinetic energy which eventually enables it to overcome the adverse pressure gradient and leads to reattachment as shown in Figure A-1.
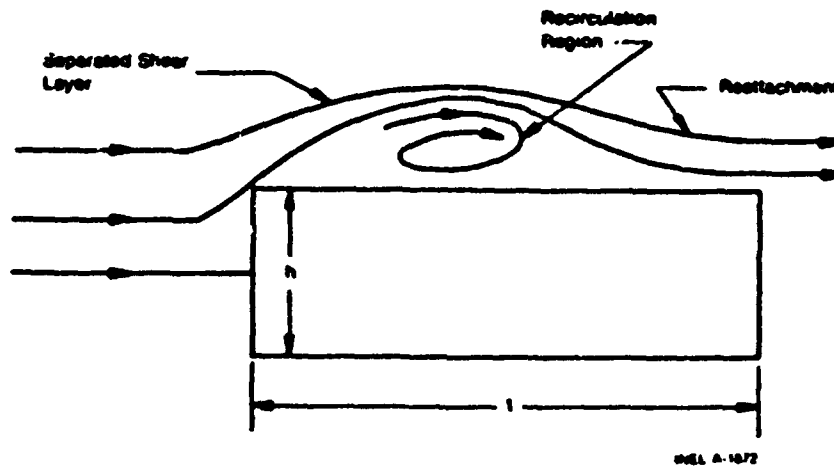


Fig. A-1 Sketch of the recirculation zone.

As the Reynolds number increases, a turbulent shear layer attains a limiting form and thus becomes independent of Reynolds number. This effect is easily seen in case of constant drag coefficient for a thin disc or plate for Reynolds numbers above 3000. The same effect is apparent for many other types of turbulent flows, such as the discharge coefficient of single hole orifice plates[6] for large Reynolds numbers. For a separated shear layer on a semiinfinite blunt flat plate[2] the length to height ratio required for reattachment is on the order of 5. In the Reynolds number range studied in Reference 2, $Re = 2 - 7 \times 10^5$, the shear layer is turbulent and the length required for reattachment is constant.

Consider a screen with square mesh or multiholed orifice plate with square corners. If the flow blockage is significant, greater than about 10%, there will be a pressure drop across the device due to the acceleration of the fluid caused by a reduction in area available to the flow.

Since a negative pressure gradient is imposed on the separated shear layer by the accelerating external flow the pressure rise

associated with reattachment is never attained regardless of the
Reynolds number. The drag coefficients of the configurations described
above should thus be constant for any Reynolds number above about $10^3$.
For very thick devices, the flow channel could conceivably accelerate
the flow, then act as a diffuser and recover pressure. A review of
subsonic conical diffuser data[5] shows this to be very unlikely unless
the plate is on the order of several screen or orifice plate hole diameters
thick. Screen elements made from blunt bodies should not suffer from
Reynolds number effects.

## REFERENCES

1. S. F. Hoerner, Fluid-Dynamic Drag, published by author, 1958.

2. T. Ota and M. Itasaka, A Separated and Reattached Flow on a Blunt
   Flat Plate, ASME 75-FE-18.

3. A. Roshko and J. C. Lau, "Some Observations on Transition and
   Reattachment of a Free Shear Layer in Incompressible Flow," Proceedings
   of the 1965 Heat Transfer and Fluid Mechanics Institute, Standard
   University Press, pp 156-157.

4. T. Ota, An Axisymmetric Separated and Reattached Flow on a Longi-
   tudinal Blunt Circular Cylinder, ASME 75-APM-A.

5. W. W. Bower, "Analytical Procedure for Calculation of Attached and
   Separated Subsonic Diffuser Flows," J. Aircraft, Vol. 13, No. 1,
   (January 1976).

6. Fluid Meters, Their Theory and Application, ASME, 1959.

PROGRESS REPORT ON LOFT

"RAKE DESIGNS"


by

R. G. Bearden




EG&G IDAHO, INC.

IDAHO NATIONAL ENGINEERING LABORATORY




Presented at NRC Two-Phase Flow Instrumentation Meeting at
Silver Spring, Maryland, January 13, 1977


**Preceding page blank**

# SUMMARY

Evaluation of data from Loss-of-Fluid Test (LOFT) nonnuclear tests has shown a need for profile measurements at several locations in the LOFT piping. A prototype rake consisting of three Drag-Disc Turbine Transducers (DTT) has been designed and fabricated for installation at one location (FE-BL-1) in the blowdown loop. After successful operation during a LOFT nonnuclear test (L1-4) scheduled for May, 1977, additional rakes will be installed in the primary and blowdown loops. A research program to develop a pitot tube rake for measurement of steady state and transient two-phase flows is in progress at McMaster University, Hamilton, Ontario. A rake of thermocouples and pitot tubes will be developed for installation near the emergency core coolant (ECC) injection points.

# CONTENTS

## FIGURES

## TABLE

# 1. INTRODUCTION

Evaluation of data from Loss-of-Fluid Test (LOFT) nonnuclear tests
has shown a need for profile measurements at several locations in the
LOFT piping. Instrument arrays (rakes) have been designed and fabri-
cated to both improve the accuracy and provide redundancy for measure-
ments. This presentation will summarize the status of the LOFT rake
implementation program.

## 2. MASS BALANCES USING LOFT INSTRUMENTS

Figure 1 shows a view of a Drag-Disc Turbine Transducer (DTT)
manufactured for installation in the 14-in. O.D. schedule 160 LOFT
piping. Note that the instrument is positioned such that a single free-
field measurement is made at the center of the pipe. A three-beam gamma
densitometer to measure average chordal density is strapped around the
pipe near the DTT location. Figures 2 and 3 show DTT instrument
locations on the LOFT primary and blowdown loops. Three DTT locations
are identified in the primary loop and two are located in the blowdown
loop. Figure 4 shows mass calculations made using data taken during the
LOFT L1-2 nonnuclear test with the combinations of instruments as
identified. The solid horizontal line represents the total mass of
fluid in the system. The dashed horizontal line represents the mass
actually measured by the various instruments. The mass of fluid
initially in the piping downstream of the DTT locations has been sub-
tracted. Note that a mass balance resulting from integration of drag-
disc turbine measurements (curve tagged with small squares) gives a
result which is almost twice the correct value. During a LOFT loss-of-
coolant experiment (LOCE) test, stratified flow occurs and a single free
field measurement is inadequate. Rakes of three DTTs will be installed
at each of the piping locations where single units are now installed to
improve accuracy and increase redundancy. The curves also show a mass

**Preceding page blank**

I.5-63
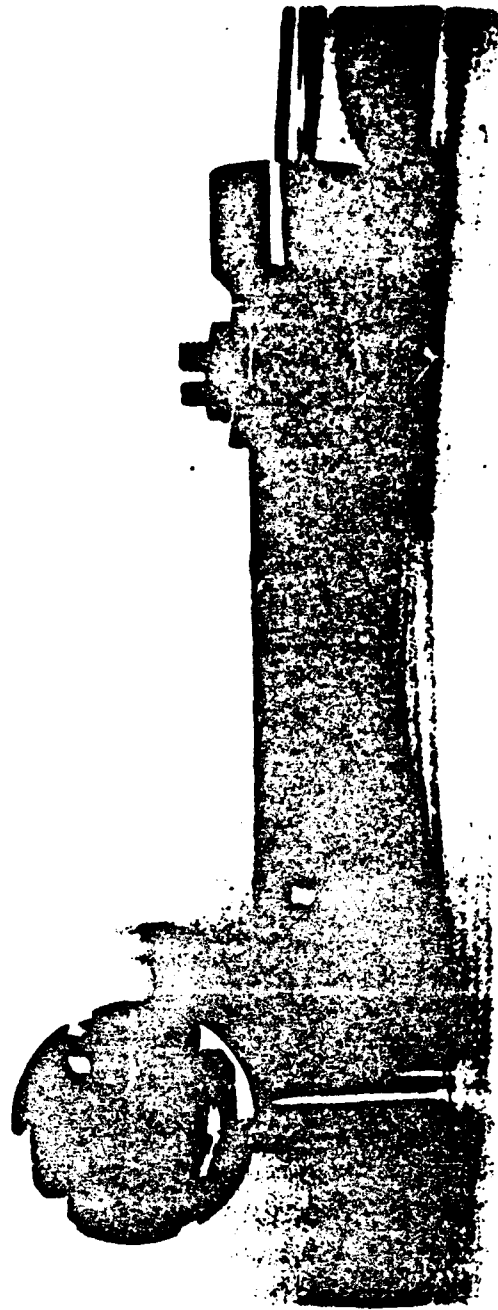
Fig. 1 LOFT DTT piping probe.
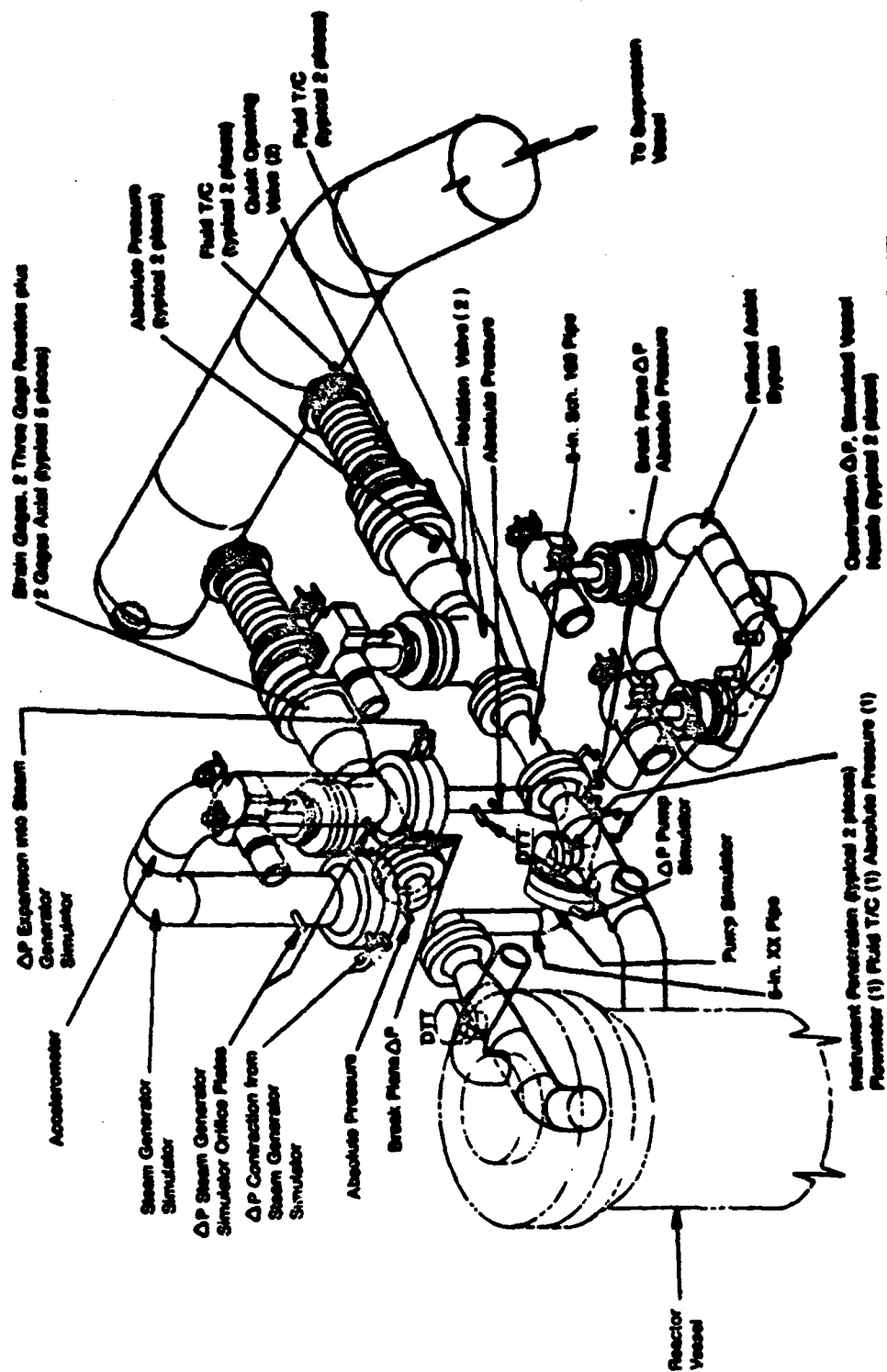
I.5-64
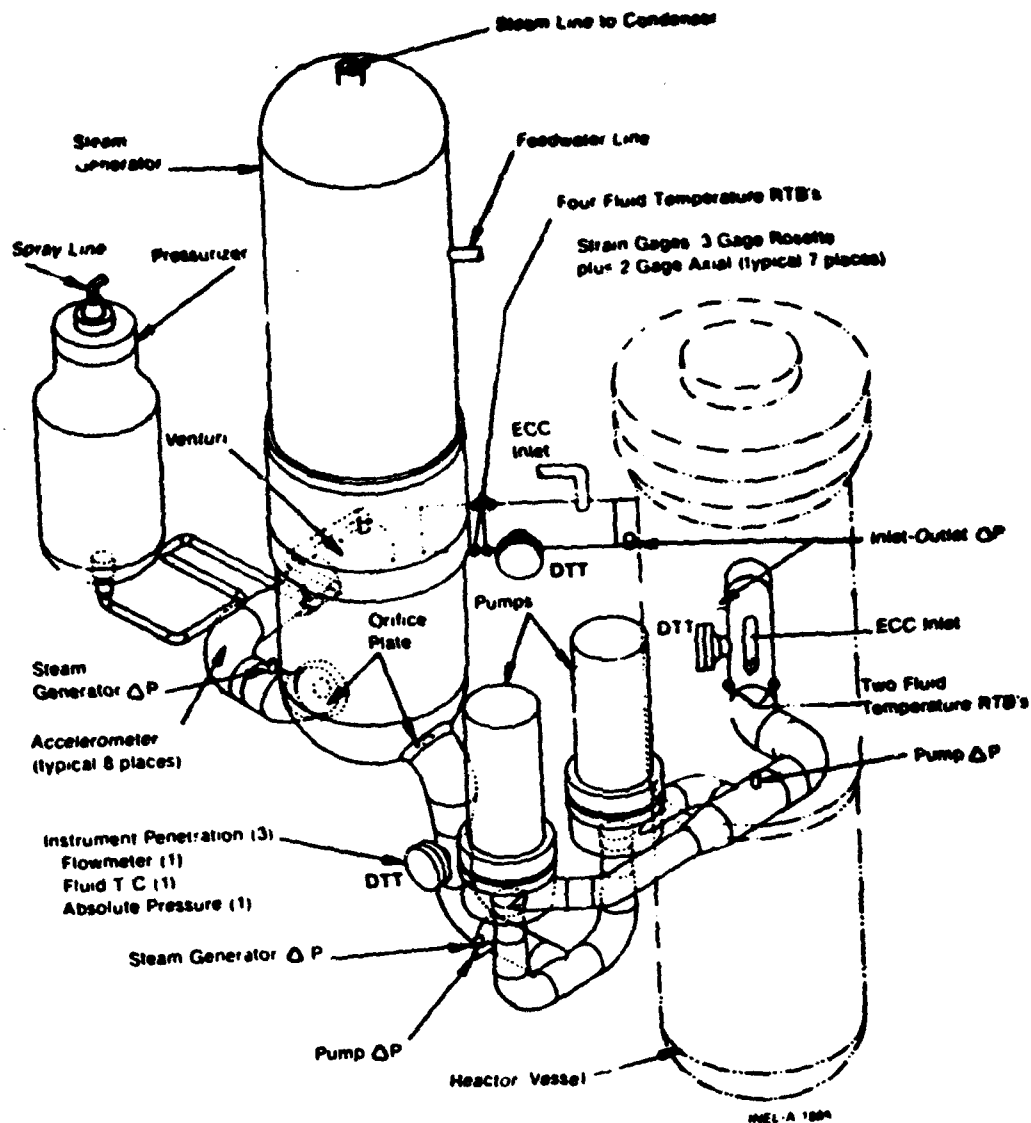
Fig. 2 LOFT operating loop with instrument locations.

I.5-65

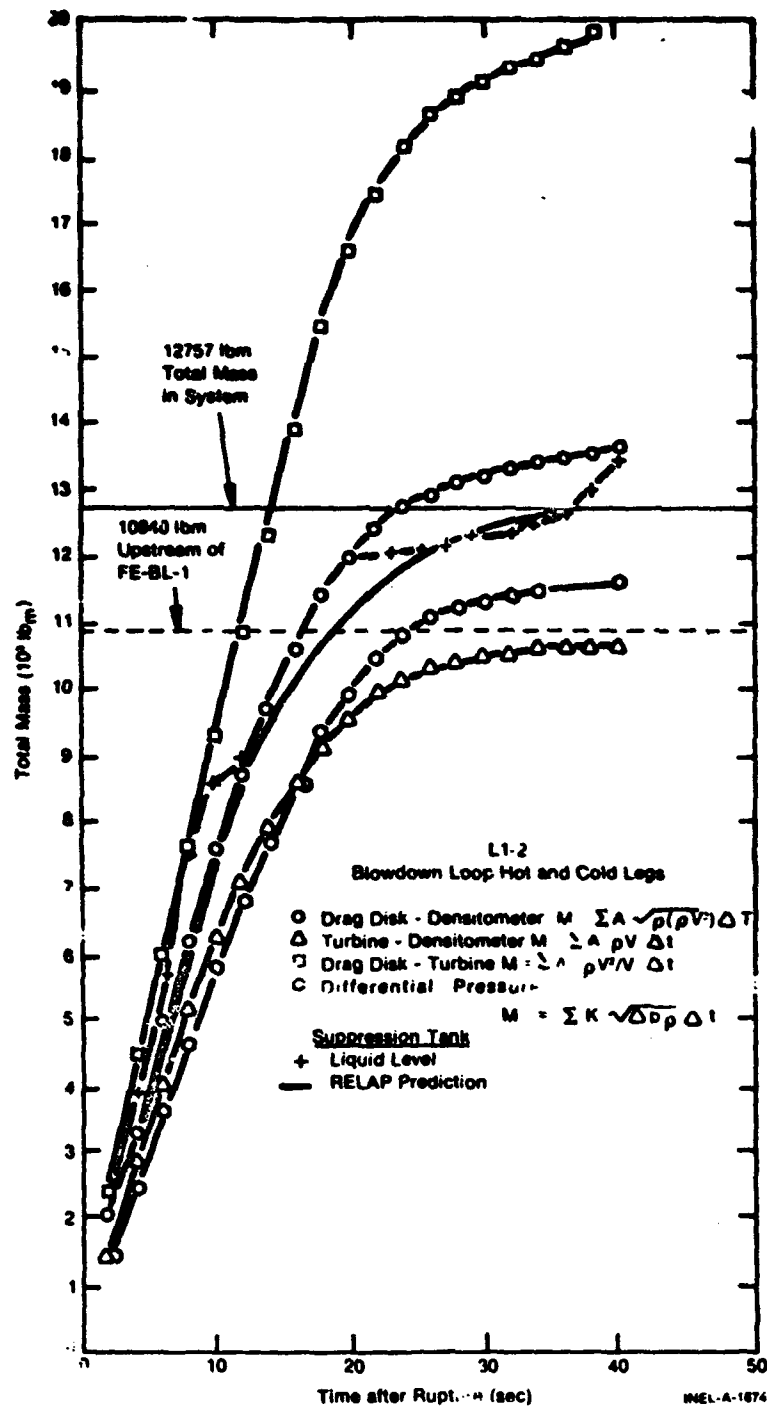Fig. 3 LOFT blowdown loop with instrument locations.

12757 lbm
Total Mass
in System

10840 lbm
Upstream of
FE-BL-1

Total Mass ($10^3$ lb$_m$)

L1-2
Blowdown Loop Hot and Cold Legs

O Drag Disk - Densitometer $M = \Sigma A \sqrt{\rho(\rho V^2)} \Delta T$
△ Turbine - Densitometer $M = \Sigma A \rho V \Delta t$
▢ Drag Disk - Turbine $M = \Sigma A \rho V^2/V \Delta t$
C Differential Pressure

$$M = \Sigma K \sqrt{\Delta p \rho} \Delta t$$

Suppression Tank
+ Liquid Level
— RELAP Prediction

Time after Rupture (sec)

INEL-A-1874

Fig. 4 Mass calculation method comparison.

I.5-67

balance using calculated mass flow based on density measured via the gamma densitometer and a differential pressure (measured at a piping location entitled "contraction $\Delta p$" on Figure 3). The calculated mass balance using $\Delta p$ is in good agreement with the actual initial value. Pitot tube arrays will be designed, fabricated, and installed in the LOFT piping to facilitate calculation of flow profiles.

## 3. RAKE REQUIREMENTS

The LOFT facility is a scaled design of a Westinghouse type pressurized water reactor (PWR). Each of the rake designs will require penetrations of the primary coolant pressure boundaries. The same codes and standards required for PWR reactors will be followed during the design, fabrication qualification, and installation of the rakes on the LOFT system.

### 3.1 DTT Rakes

A formal requirements document was prepared and approved after design reviews. Table I summarizes the environmental conditions and required ranges. The maximum momentum flux value for design purposes was 188,000 lbm/ft-sec$^2$ as determined from RELAP computer models and previous nonnuclear tests.

### 3.2 ECC Rakes

One of the goals of the LOFT LOCE testing program is to define emergency core cooling (ECC) mixing phenomena. Temperature measurement arrays on either side of the ECC injection points would give indications of ECC oscillations about the injection port and the rate at which the water temperature increases. A similar array on the broken loop will indicate the condition of ECC bypass. Installation on both hot and cold leg sides is required for potential use of hot leg ECC injection.

I.5-68

## TABLE I

### DTT RAKE REQUIREMENTS

1. Design to Meet RDT Standards for LOFT Conditions:
       Temperature 300-650°F (150-345°C)
       Pressure 2250 psig (155 BAR)
    Maximum Velocity 100 ft/sec (30.5 m/sec)

   Radiation
       Neutrons
               Normal Operations $1 \times 10^8$ nv
               Total Exposure $7 \times 10^{14}$ nvt

       Gammas
               Normal Operation 1000 R/hr
               Total Exposure $7 \times 10^9$ R

| Ranges: | | $(lb/ft\text{-}sec^2)$ | $(Kg/m\text{-}sec^2)$ |
|---------|------|------------------|------------------|
| #1 | Top | 2,000-50,000 | 2,976-74,400 |
|    | Middle | 2,000-50,000 | 2,976-74,400 |
|    | Bottom | 2,000-50,000 | 2,976-74,400 |
| #2 | Top | 200-3,500 | 298-5,209 |
|    | Middle | 800-14,000 | 1,191-20,835 |
|    | Bottom | 200-3,5( | 1,191-5,209 |

   In addition to the temperature measurement, it is possible to include
other measurements on the probe to further improve flow measurement
accuracy. INEL is currently sponsoring a university investigation of
the usefulness of pitot tubes fo two-phase flow measurements. Pitot
tubes will also provide a good measurement of the initial flow profile
in the pipes. The initial ECC rake design will thus incorporate pitot
tubes and thermocouples.

   Summarizing the ECC rake design requirements include the following:

   Range:

       Pitot Tubes - 20 - 200,000 $lb/ft\text{-}sec^2$ (30-207,600 $Kg/m\text{-}sec^2$)
       T/CS - 100 - 1300°F (38-722°C)
                           Response 100 msec

Installation: PC-1 (A & B), PC-2 (A,B) BL-1, BL-2

Location of Probes:
    PC-1 (A&B), PC-2 (A&B)
        10 Pitot Tubes, 5 T/CS Each
    BL-1, BL-2
        5 Pitot Tubes, 5 T/CS Each

Maximum Forces During Blowdown:
    180,000 lbs/ft-sec$^2$ (279,800 Kg/m-sec$^2$)

A total of six ECC rakes will be fabricated and qualified with two each installed at locations PC-1 and PC-2 on the primary coolant loop and one each installed at locations BC-1 and BC-2 on the broken loop. McMaster University, Hamilton, Ontario (Dr. S. Banerjee, principal investigator), has received a FY 77 subcontract to investigate the performance of pitot tubes in two-phase flow. The results of this research will be incorporated into the ECC rake design.

## 4. PITOT TUBE RESEARCH AT MCMASTER UNIVERSITY

Dr. S. Banerjee was in attendance at the Nuclear Regulatory Commission (NRC) conference. He mentioned that the program would include evaluation of pitot tubes in both steady state and transient two-phase phenomena. The steady state data have been taken using an array of five pitot tube probes in three different pipe diameters - 1-1/2, 2- and 3-in. O.D. The data from the tests are still being evaluated. Dr. Banerjee did show Figure 5 and pointed uc that the calibrations made with all water (void fraction zero) seemed to also hold for the higher void fraction test data. The transient steam/water tests will be run this spring and summer. A summary report will be available by the end of FY 77.

I.5-70
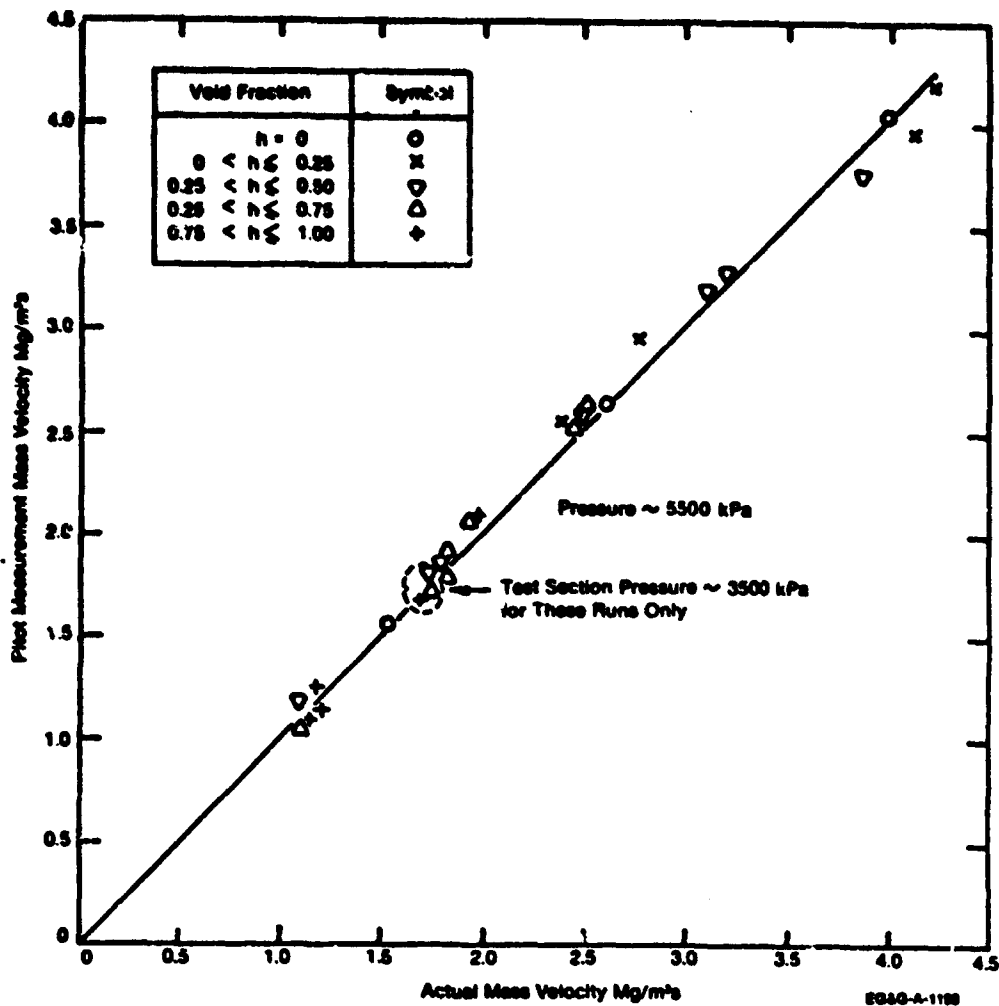
Fig. 5 Pitot t... measured mass velocity.

## 5. CONCLUSIONS

### 5.1 DTT Rake

The design and supporting analyses for qualification are nearly complete for the three DTT rakes. A model of the rake design is pictured in Figure 6. Two copies of the rake design are in fabrication. One DTT

I.5-71
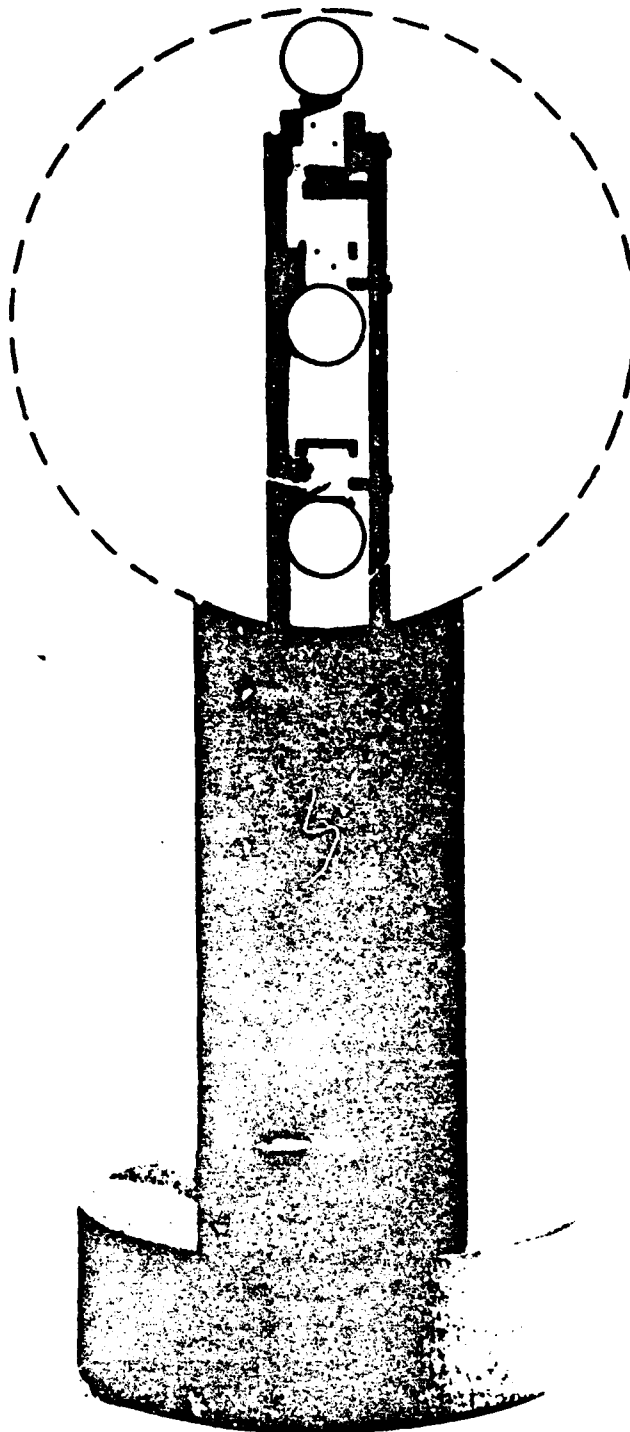
Fig. 6 Model of 3-DTT rake assembly.

I.5-72

rake will be installed at location BL-1 for the next LOFT nonnuclear test, test L1-4 scheduled for May 1977. The second unit will be used for additional tests. After evaluation of the L1-4 test data, the rake design will be modified as required and the remaining DTT rakes fabricated and installed at locations BL-2, PC-1, PC-2, and PC-3.

## 5.2 ECC Rake

The requirements for the ECC rake are still being developed. Several conceptual designs have been considered. One of the conceptual designs is shown in Figure 7. Fabrication of the ECC rakes will be completed in time for installation prior to the L1-5 LOFT nonnuclear test.
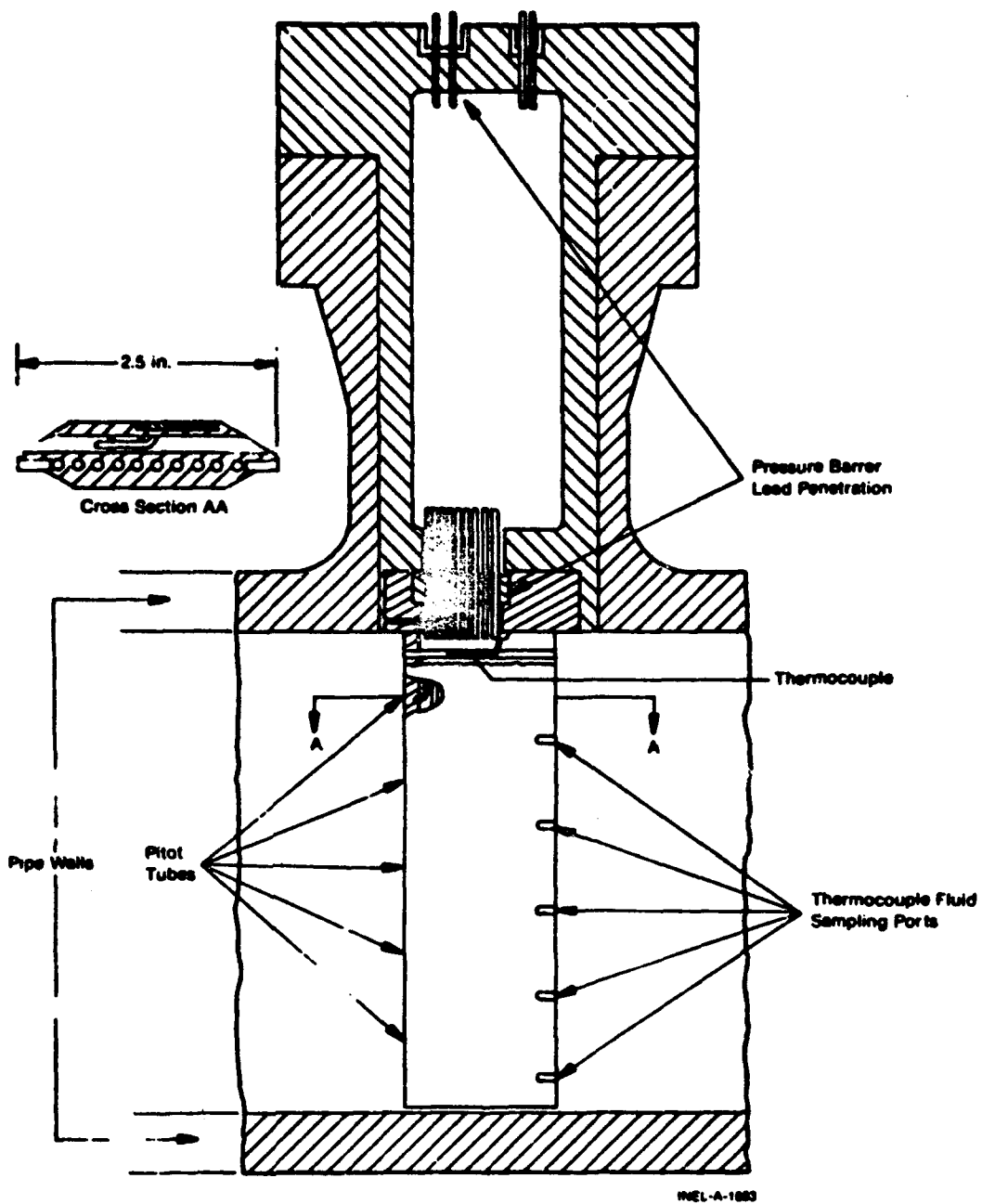
Fig. 7 Pitot tube/thermocouple rake installation.

PROGRESS REPORT ON LOFT

"UPGRADE DRAG-DISC TURBINE SEPARATE EFFECTS TESTS"

by

R. G. Bearden

EG&G IDAHO, INC.

IDAHO NATIONAL ENGINEERING LABORATORY

Presented at NRC Two-Phase Flow Instrumentation Meeting at
Silver Spring, Maryland, January 13, 1977

I.5-75

## SUMMARY

The present Drag-Disc Turbine Transducers (DTT) installed in the Loss-of-Fluid Test (LOFT) facility were analyzed and redesign goals were established during FY 76. A prototype DTT was developed and single-phase and separate effects testing was completed. An alternate eddy current sensor for the DTT drag body was developed and tested during FY 76. The results of the separate effects testing program will be incorporated in the design and development of a second prototype which will be tested under single- and two-phase conditions during FY 77.

# CONTENTS

## FIGURES

## TABLES

# 1. INTRODUCTION

The design and performance of the Drag-Disc Turbine Transducer
(DTT) currently installed at various locations in the Loss-of-Fluid-Test
(LOFT) facility were analyzed and redesign goals were established during
FY 76. The redesign goals included: (1) retain as many of the presently
used components (sensors, turbine blade, etc.) as feasible; (2) make
separable/replaceable turbine and drag-disc transducers; (3) extend
ranges; (4) streamline where possible; (5) improve turbine bearing
lifetime; (6) reduce friction in the drag-disc sensor linkage;
(7) define performance analytically and performance of adequate calibra-
tions. A two year program was initiated to improve the DTT. The design
and test program stressed component improvements - particularly modularity
of units, improvement of turbine bearings, and development of an alter-
nate drag body sensor. The results of the separate effects testing
program will be summarized. The FY 77 goals for development and testing
of a second prototype DTT will be presented.

# 2. FIRST PROTOTYPE DTT

The DTT currently qualified for installation is shown in Figure 1.
The single body instrument incorporates a six bladed turbine mounted on
a 17-4 PH steel shaft contained by gold alloy sleeve bearings in each of
two support posts. The rotation of the turbine blades is sensed via an
eddy current sensor located in the body below the blades. The other end
of the DTT instrument has a circular disc drag body attached to lever
arms and a pivot to position a variable reluctance transformer core
as the fluid momentum flux on the disc acts against a torsion bar
restoring spring. The prototype I design is shown in Figure 2. The
sensors from the present LOFT DTT, which had previously been qualified
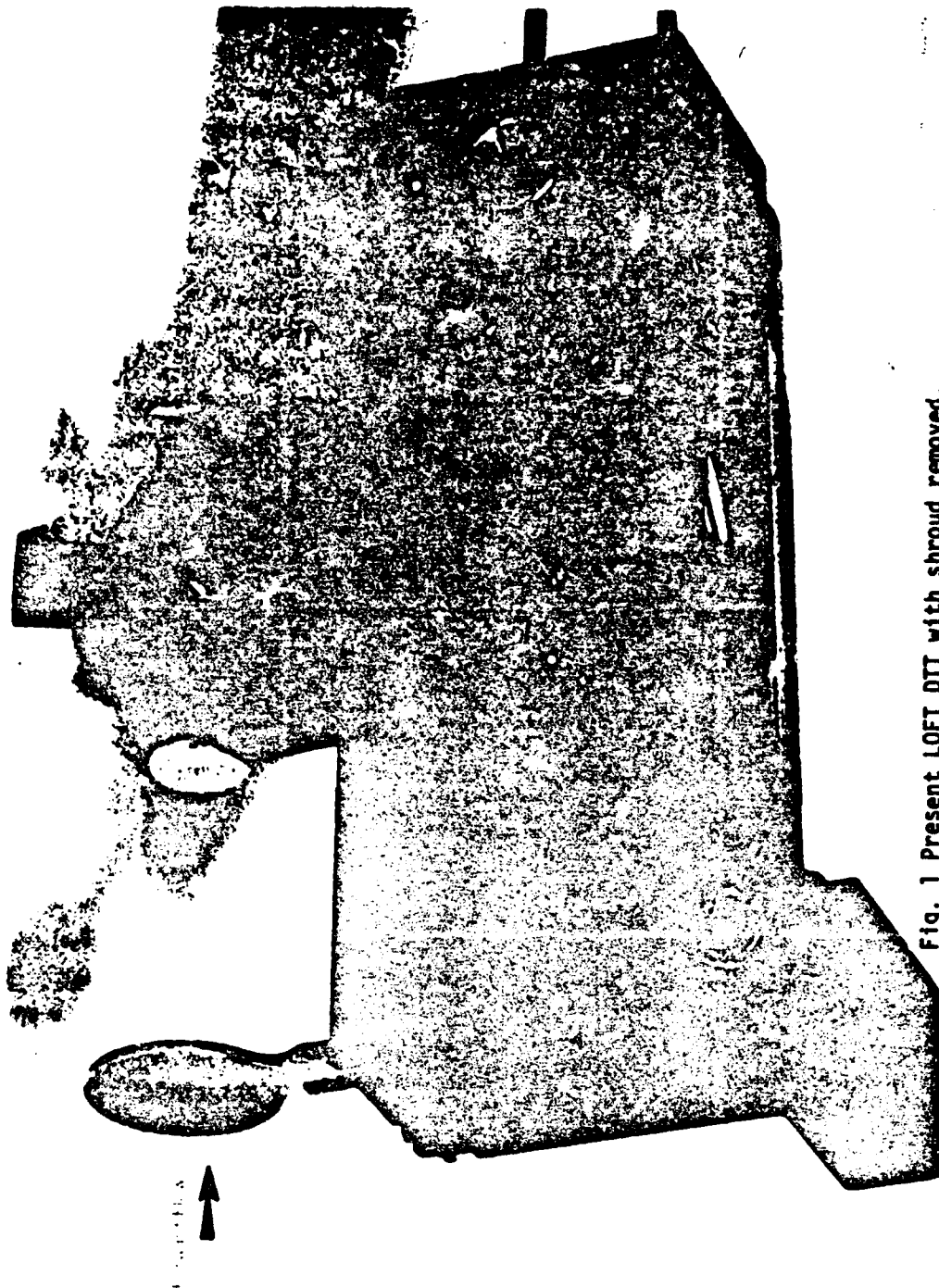for LOFT service, were used in the prototype.

I.5-79

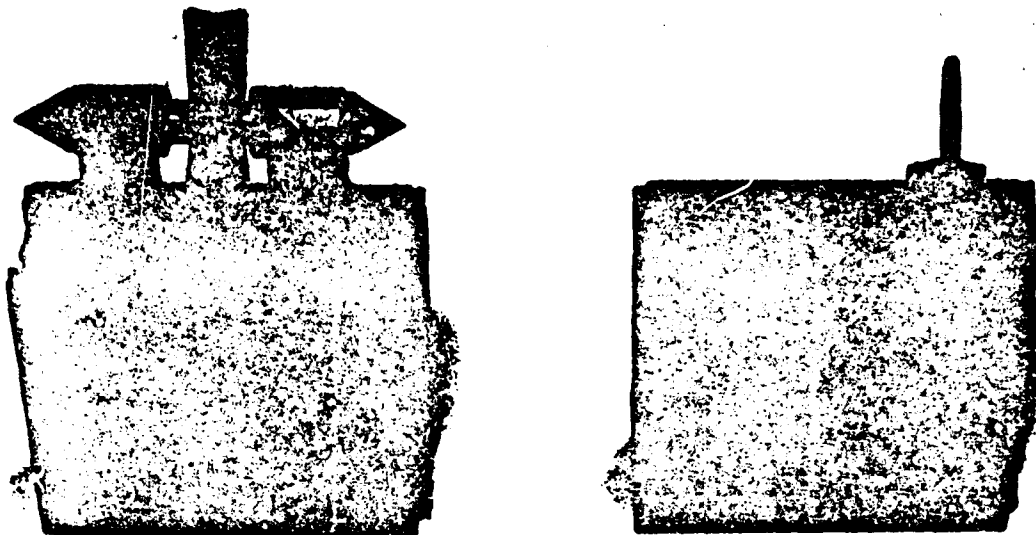Fig. 1 Present LOFT DTT with shroud removed.

Fig. 2 Modular prototype DTT.

## 2.1 Modular Design

As seen in Figure 3, the turbine and drag body are constructed as identical sized separate units with interlocking key-ways in order that single or multiple units can be joined together as required. Results of fabrication and testing of three copies each of the turbine and drag body units showed that the manufacturing costs could be reduced. Stress analyses showed that the shroud and other modular parts would withstand the maximum conditions encountered during LOFT LOCE.

## 2.2 Performance Tests

In the single phase tests of the prototype, the LOFT environmental conditions of 2250 psig and 650°F were simulated by the use of a large autoclave chamber. Autoclave tests on each of the three copies of the prototype DTT indicated that the combined effects due to changes in temperature and pressure from ambient to LOFT conditions caused less than 1% (of full scale) error. Test results showed that the turbine unit had a useful range of 5 to 40 ft/sec. The drag-disc pivot spring

I.5-81
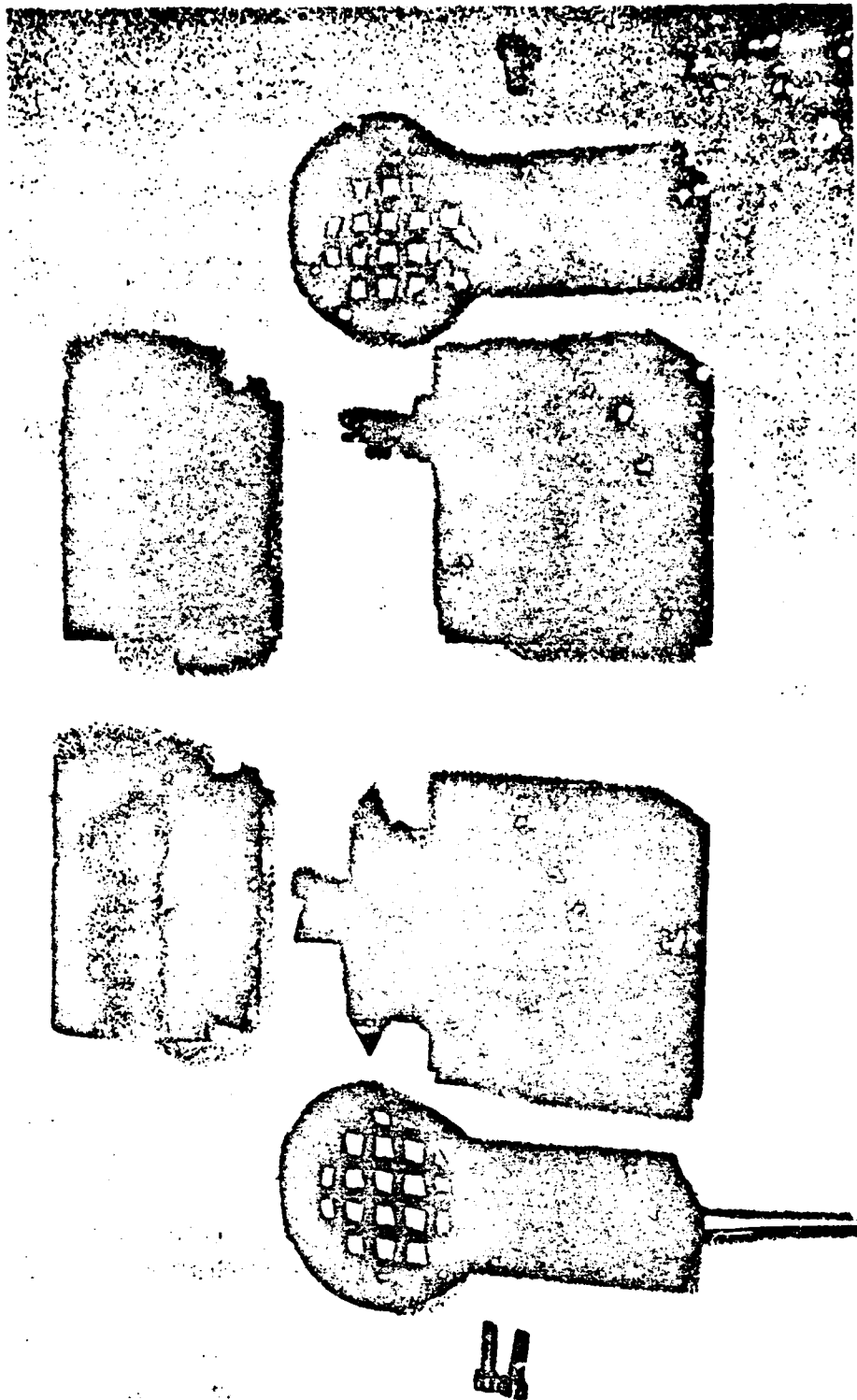
Fig. 3 Disassembled prototype DTT.

I.5-82

failed after $10^5$ cycles of full scale deflection. The spring will be redesigned to meet a failure life of $10^6$ cycles.

# 3. TURBINE BEARING IMPROVEMENT PROGRAM

The service life goal for turbine flowmeters installed in the LOFT system is 10,000 hours of operation at LOFT conditions. The improvement program includes life testing on bearing materials, testing of alternate turbine bearing designs, and development of compound bearing concepts.

## 3.1 Bearing Life Tests

Table I shows the test conditions of the test loop in which various combinations of bearing materials have been tested. A summary of the results to date is shown in Table II.

### TABLE I

### BEARING LIFE TEST CONDITIONS

| | |
|---|---|
| Flow Velocity: | 13 ft/sec (4 m/sec) |
| Temperature: | 600-620°F (Approximately 320°C) |
| Operating Pressure: | 2200 psi (153 BAR) |
| Demineralized Water with Low Chlorides and Oxygen Content | |

## 3.2 Single Post/Bearing

A single post turbine has been developed as shown in Figure 4, for evaluation of the design, bearing materials combinations, and the effects of forced fluid lubrication. The combinations of materials to be tested include sleeve bearings of (1) H/H gold alloy, (2) P-658-RCH graphite and (3) 440C stainless steel each combined with a one piece 440C stainless steel shaft and collar. The same combinations will

I.5-83

## TABLE II

### TURBINE BEARINGS LIFE TEST RESULTS

Over 100 Combinations of Sleeve Bearings,
Shafts and Thrust Washers were Tested

Best Candidates of Each Part:

| Sleeve Bearing | Shaft | Thrust Washer |
|---|---|---|
| H/H Gold Alloy<br>(5500 Hours) | 17-4 PH<br>(2000 Hours +) | Stellite 19<br>(2000 Hours) |
| 440C Stainless<br>(2500 Hours +) | 440C<br>(2500 Hours +) | 17-4 PH<br>(2000 Hours +) |
| P-658-RCH Graphite<br>(3500 Hours) | Stellite 19<br>(2000 Hours) | 440C<br>(1000 Hours) |

be tested in a single post/bearing with water lubrication.  A 440C
sleeve and shaft impregnated with diamond powder will be tested.

### 3.3 Compound Bearing

Dr. Jack Cole, University of Arkansas, has a research contract for
FY 77 to develop/test a compound bearing concept.  Figure 5 shows a
compound bearing which is currently under development and testing by
the Mechanical Engineering Department of the University of Arkansas
under a FY 77 subcontract (Dr. Jack Cole, principal investigator).
The bearing concept consists of a jewelled bearing which acts against a
spring loaded thrust bearing until forces on the turbine assembly
exceed the spring constant, then the jewelled bearing seats against a
friction shoulder.  Sleeve bearings act as rugged long-life bearing
surfaces as long as the high thrust conditions exist.  A patent
application has been filed on the concept.
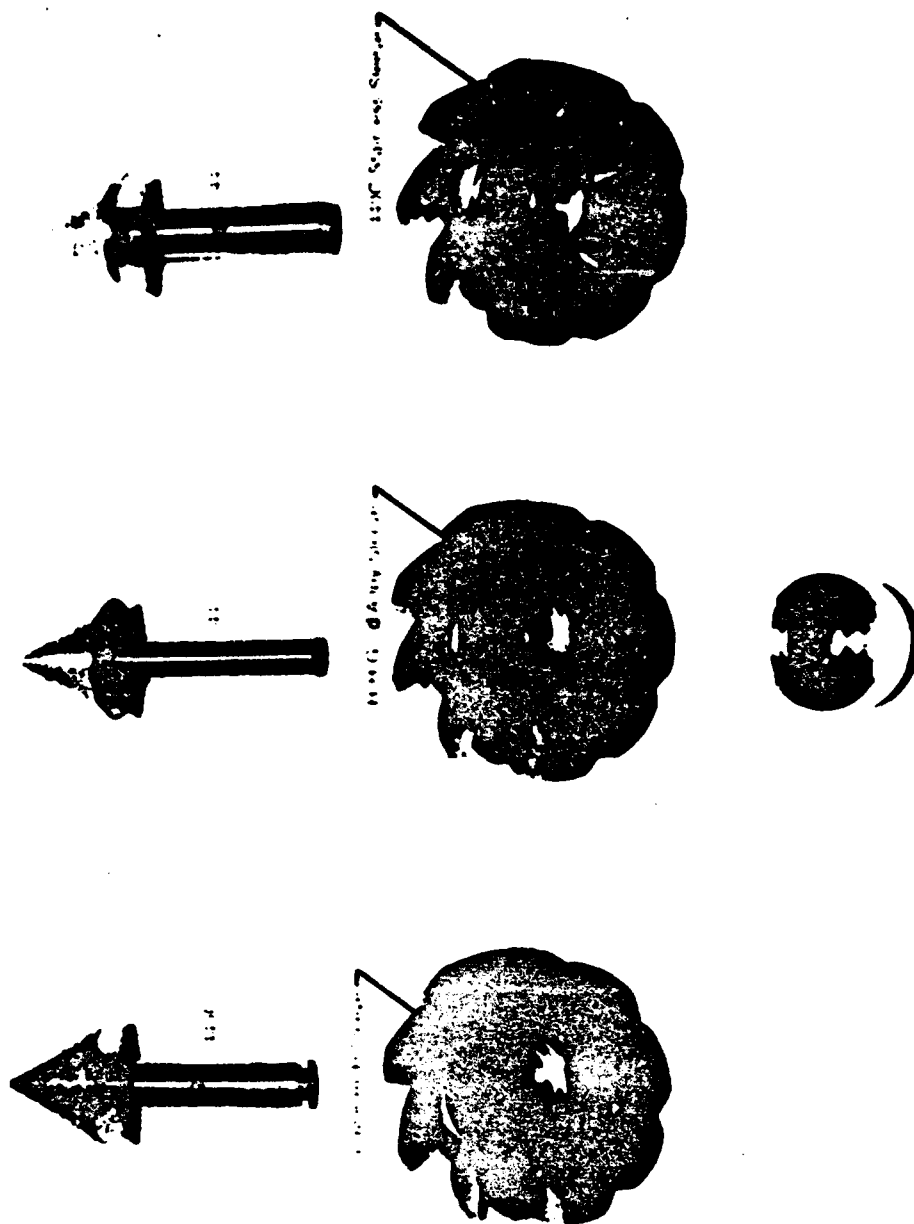
Fig. 4 Single bearing tests.
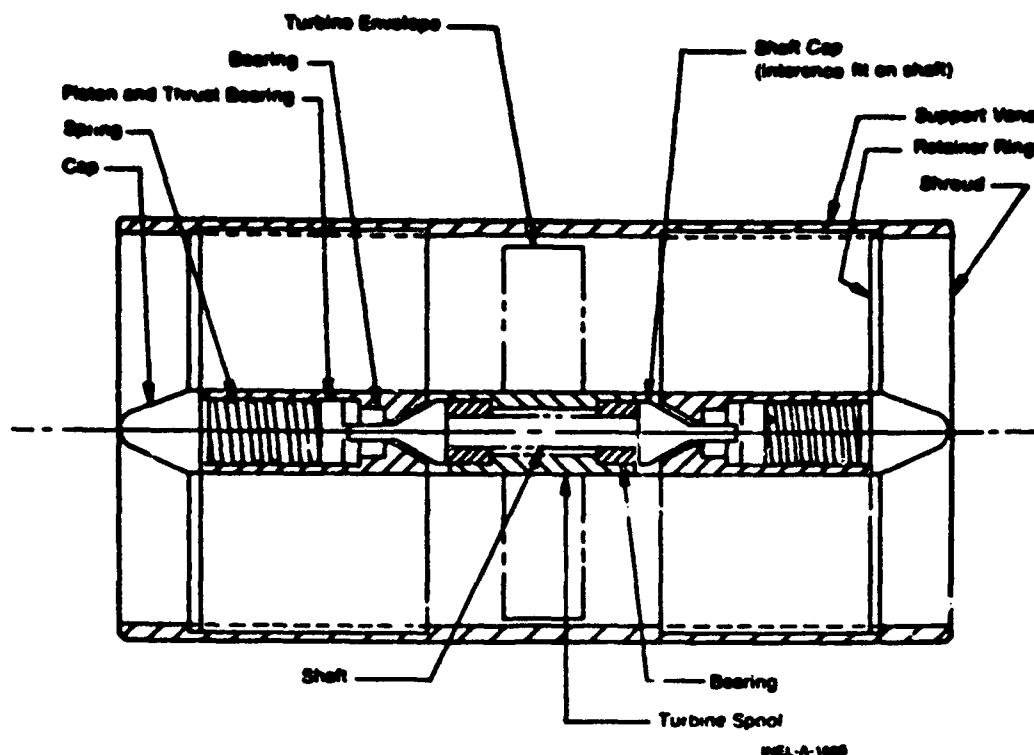
**Fig. 5 Compound bearing turbine flowmeter concept for reducing friction at low flows.**

## 4. IMPROVED DRAG BODY SENSOR

### 4.1 Design

The present LOFT DTT unit has a Variable Reluctance Transformer (VRT) and core as a sensor. The lever arms, pivot bearings, and VRT clearances give rise to fabrication, calibration, and service life problems. An alternate sensor has been designed, fabricated, and tested which utilizes eddy current sensor coils to measure displacement of the drag-disc arm without any contact or connection required. The assembled eddy current sensor is shown in Figure 6. One end of the sensor contains a sensing coil to sense a reference target and the other end has an identical coil to measure deflection. The coils are wound with identical geometries and electrical properties. When connected into an ac bridge circuit, the identical coils are very insensitive to large changes in temperature.

I.5-86
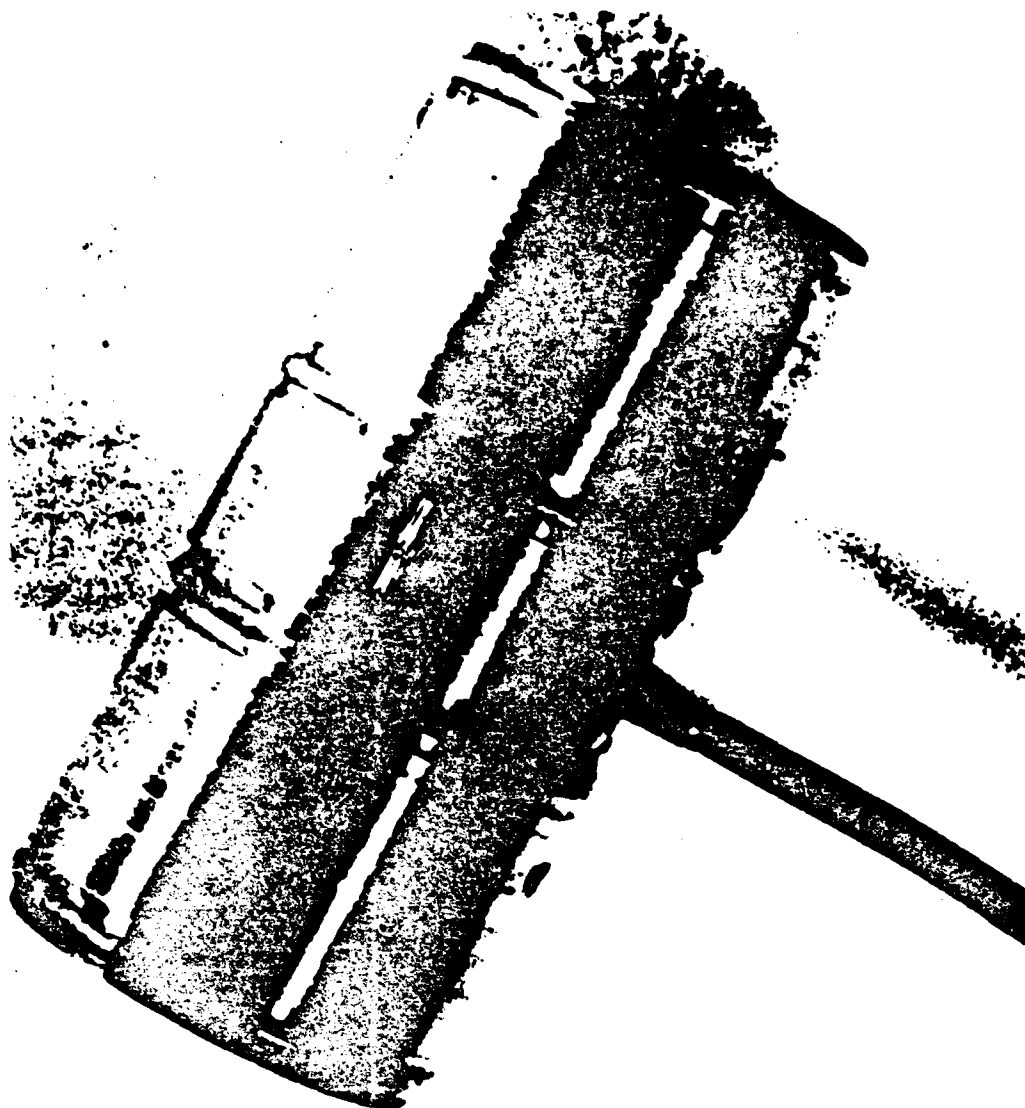
Fig. 6 Assembled eddy current transducer.

## 4.2 Test Results

Figure 7 shows a plot of test results. The sensor has a useful
displacement measurement range of 0.0 to 0.150 in. The expected range over
which the sensor will be used in a drag-disc is 0.080 in. as indicated
by the vertical marks intersecting the curves. Test results have shown
that the effects of sudden temperature changes from 689 to 73°F cause
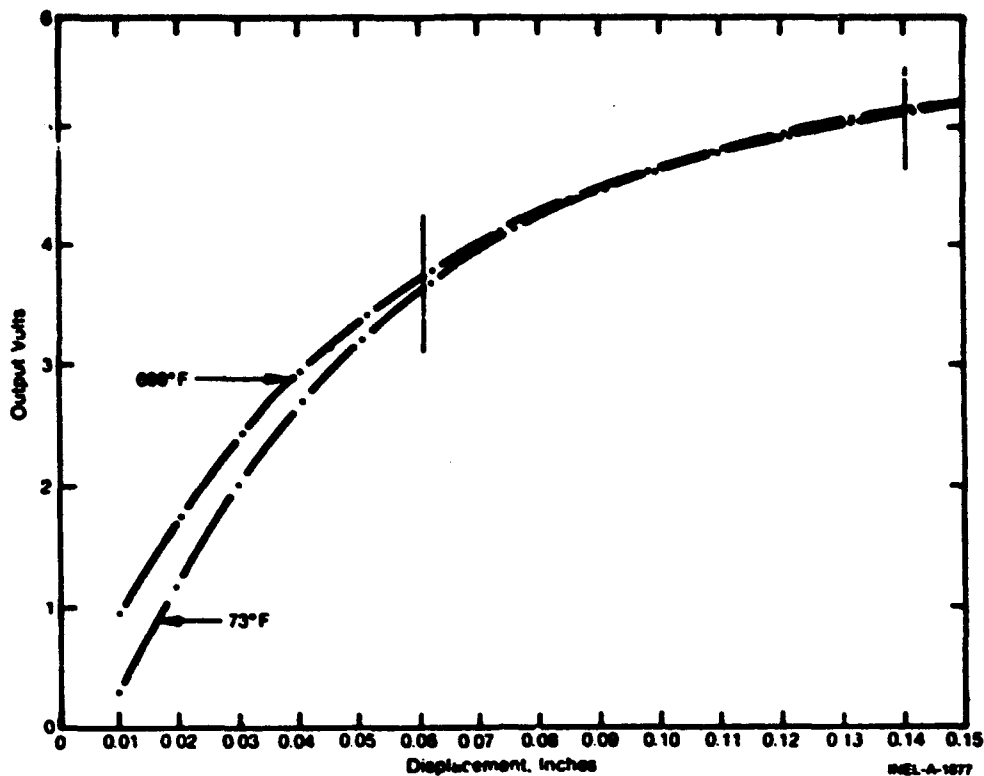
Fig. 7 The eddy current transducer's dc output versus target displacement.

less than 5% (of full-scale) error. The tests in an autoclave indicated that effects of pressure changes from ambient to 2250 psig caused less than 2% (of full-scale e ror).

## 5. CONCLUSIONS AND FY 77 GOALS

### 5.1 FY 77 Goals

The FY 77 goals include (1) reduction in size; (2) new turbine bearings; (3) new drag-disc sensor; (4) removable sensors, and (5) two-phase calibrations. A final design review to evaluate the prototype I will be held in March, 1977. A second prototype will be designed to the FY 77 goals, fabricated and testing/calibrations begun during the remainder of FY 77 will be completed.

I.5-88

## 5.2 Analytical Models

RPI (Dr. R. Lahey Jr., principal investigator) has accepted a subcontract to develop and evaluate analytical performance models for the LOFT turbine and DTT units. Table III summarizes the objectives of the program for FY 77.

### TABLE III

### RPI (DR. R. LAHEY) OBJECTIVES OF PROGRAM

1. Develop a detailed analytical model for the transient response of a turbine meter in single-phase and two-phase flow. This model would include such things as rotor inertia, bearing friction, etc.

2. Synthesize a method of interpreting local readings in terms of global parameters of interest.

3. Investigate the effect of virtual mass on the response of a drag-disc in transient two-phase flow.

4. Suggest experiments to investigate the interaction that occurs between instruments in series (e.g. How does the turbine affect the drag-disc?). Based on the results of these experiments, to provide analytical models and/or correlations, to account for these interaction mechanisms.

5. Model and/or instrument changes will be proposed based on the results of the analytical and experimental work done in items 1-4 above.

## 5.3 Conclusions

Evaluation of data taken during three nonnuclear tests of the LOFT facility, indicated that the presently installed DTTs have provided valuable and essential information; however, problems in manufacture, accuracy, and reliability were noted. Test results from single effects testing and from the design, development, and testing of a prototype I demonstrated that most of the problems could be minimized or eliminated. Defined design directions for a second prototype are to be developed during FY 77.

PROGRESS REPORT ON LOFT

ADVANCED DENSITOMETER

by

A. G. Stephens

EG&G IDAHO, INC.

IDAHO NATIONAL ENGINEERING LABORATORY

Presented at NRC Two-Phase Flow Instrumentation Meeting at
Silver Spring, Maryland, January 13, 1977

Preceding page blank

# SUMMARY

Measurement requirements and initial constraints have been defined for the nuclear fueled Loss-of-Fluid Test (LOFT) densitometer. The principal problem is to make the photon transmission measurement in the presence of an expected heavy background radiation field due to nitrogen-16 and other activated fluid and corrosion products in the water. Also, further information on the mass distribution over the flow field is desired. Different instrumental techniques are being considered to solve these problems.

We are conducting hardware tests at the Advanced Test Reactor (ATR) to determine the feasibility of solving the background radiation problem by straightforward shielding and digital background subtraction (energy discrimination) techniques. Error analyses of the chordal average density measurement show the advantages to be gained by selection of detector position and source energy.

The configuration presently being pursued consists of the NaI type detector, single source, and digital background subtraction. Subsequent modifications may include use of Germanium detectors, multiple sources, and perhaps on-line analog background subtraction.

# CONTENTS

## FIGURES

## TABLES

# 1. INTRODUCTION

Densitometers used during the nonnuclear LOFT testing need to be modified in order to perform their intended function when subjected to the high background radiation field expected during nuclear-fueled LOFT work. The development work involves, first, determination of the design requirements for the electronic and mechanical equipment and second, determination of data reduction techniques to account for flow regime and small L/D flow disturbance effects. The work accomplished to date is in support of the first objective.

## 2. MEASUREMENT REQUIREMENTS AND TECHNIQUES BEING EVALUATED

Measurement requirements, revised to reflect data gathered from the first few nonnuclear LOFT tests, have been established for the advanced densitometer. These requirements, along with the principal measurement constraint, (background radiation) are given in Table I.

### TABLE I

### LOFT DENSITOMETER MEASUREMENT REQUIREMENTS

|  | Required | Goal |
|---|---|---|
| Range, $lb/ft^3$ | 0.7 - 62.4 | 0.06 - 62.4 |
| Accuracy, $lb/ft^3$ | $\pm 0.6$ | $\pm 0.3$ |
| Maximum Sampling Time, sec | 0.1 | 0.016 |
| Number of Beams | at Least 2 | 9 |
| Background Radiation Source Strength | $140 \, \frac{\mu Ci}{cm^3} - N\text{-}16$ | Plus $20 \, \frac{\mu Ci}{cm^3}$ Mixed Activation, Fission and Corrosion Products |

Preceding page blank

The primary method of addressing the background radiation problem
is to separately measure and subtract it from the combined signal plus
background measurement. Photon energy analysis type instrumentation is
used to accomplish this background subtraction. The standard method
involves off-line digital background subtraction, an instrument block
diagram for which is shown in Figure 1. With this equipment, the
information obtained and recorded is only the portion of the total
photon energy spectrum of interest to the densitometer measurement.
This portion of the spectrum consists of the full energy (photo) peak
plus twenty to forty channels on either side of the peak used to
establish the coefficients of an equation for the background. This
equation is used to determine background values under the peak which are
subtracted in order to obtain the net peak area (above background). This
net peak area is the number which is properly related to the chordal
average density. Once the off-line digital technique has been instituted,
and its accuracy and capabilities established, it may be possible to
simplify the equipment and data processing procedures by going to an
on-line analog background subtraction technique. The block diagram for
this is shown in Figure 2. Essentially, the background under the peak is
determined by averaging the background on either side. This can be done
with analog techniques during the conduct of the test, so that only the
(approximate) peak area is actually recorded. Figure 3 shows both the
existing single source/triple beam type densitometer and a proposed
improvement to that, the triple source/nine beam densitometer. Each
source emits photons of different energies and radiates to all three
detectors. Thus, each detector sees all three sources and three spectral
peaks occur for each detector channel. These energy peaks are associated
with the corresponding fluid chordal path, so that a total of nine
simultaneous measurements are made. (Such a setup would be more con-
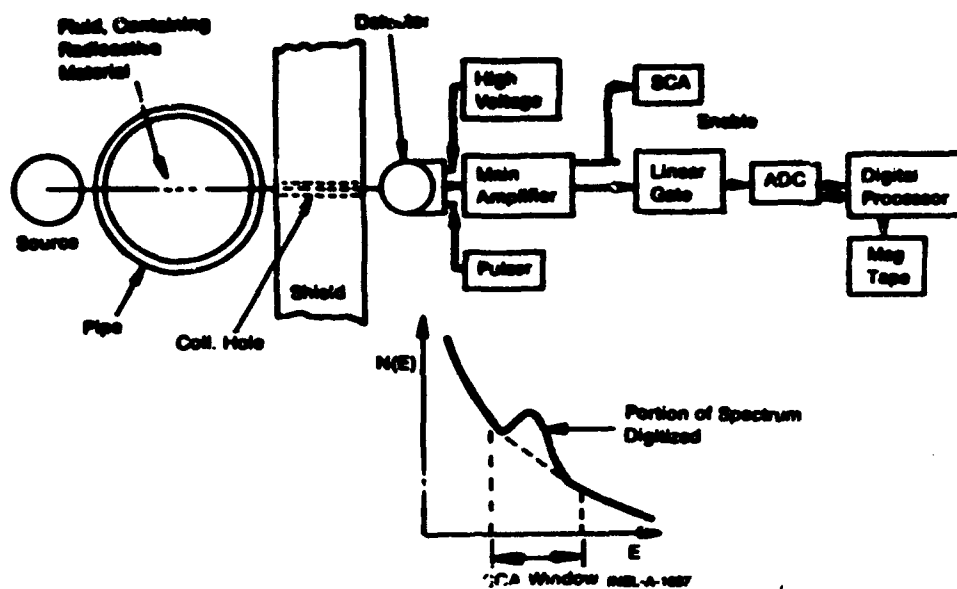sistent with the off-line digital background subtraction technique.)

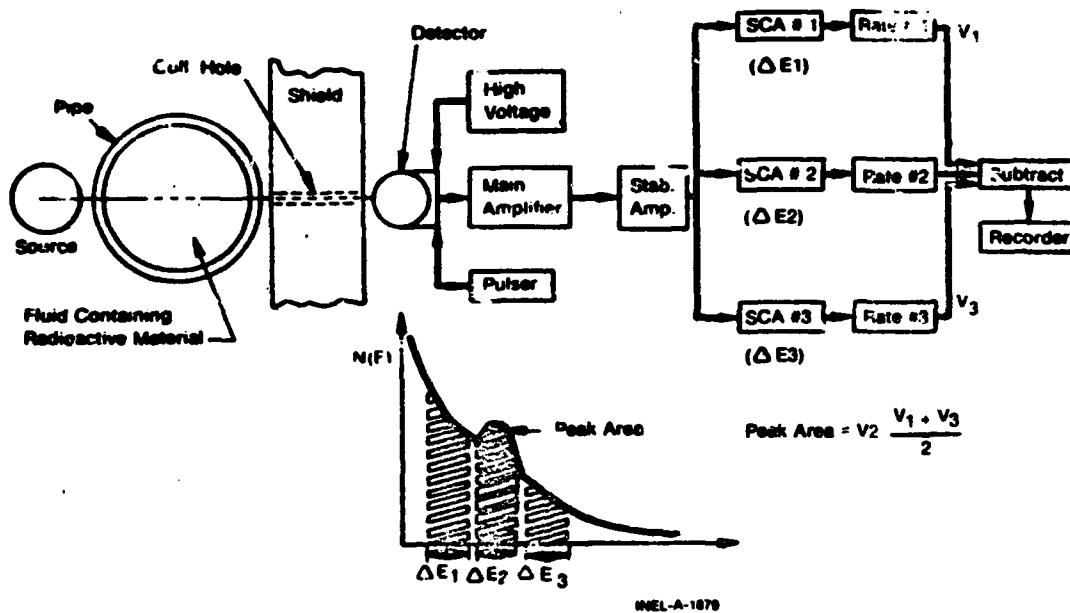Fig. 1 Off-line digital background subtraction.



$$\text{Peak Area} = V_2 \frac{V_1 + V_3}{2}$$

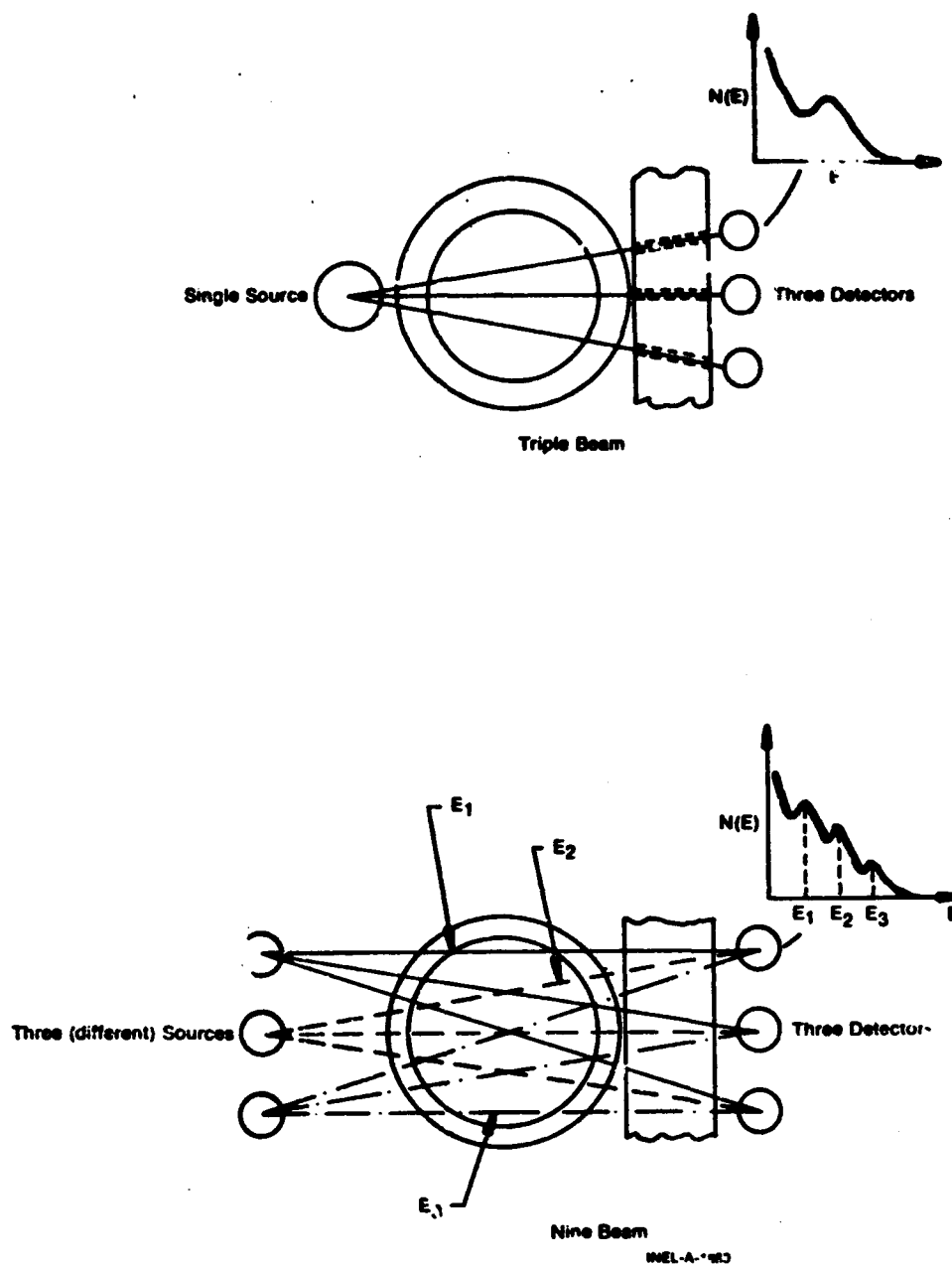Fig. 2 On-line analog background subtraction.

I.5-97

Fig. 3 Instrumental techniques being considered.

# 3. EXPERIMENTAL MEASUREMENTS

To experimentally establish the feasibility of the simple, direct background subtraction technique, tests have been conducted at the Advanced Test Reactor. Figure 4 shows the overall test arrangement of the source/detector setup at one of the reactor's primary coolant outlet lines. Figure 5 shows photographs of the actual installation. Figure 6 is a photon energy spectrum obtained from this test. The main peak is due to the densitometer Cs-137 source. The Nitrogen-16 background radiation leaking through the shield, as well as radiation from other activated fluid and corrosion products causes the observed background. Since the N-16 concentration is larger than expected in LOFT, the volume of water is larger and the pipe wall is thinner, the radiation source strength is considered to be substantially larger than will be experienced in LOFT. Thus, this result serves to establish the feasibility (at least for steady conditions) of the use of background subtraction in a high background radiation field.
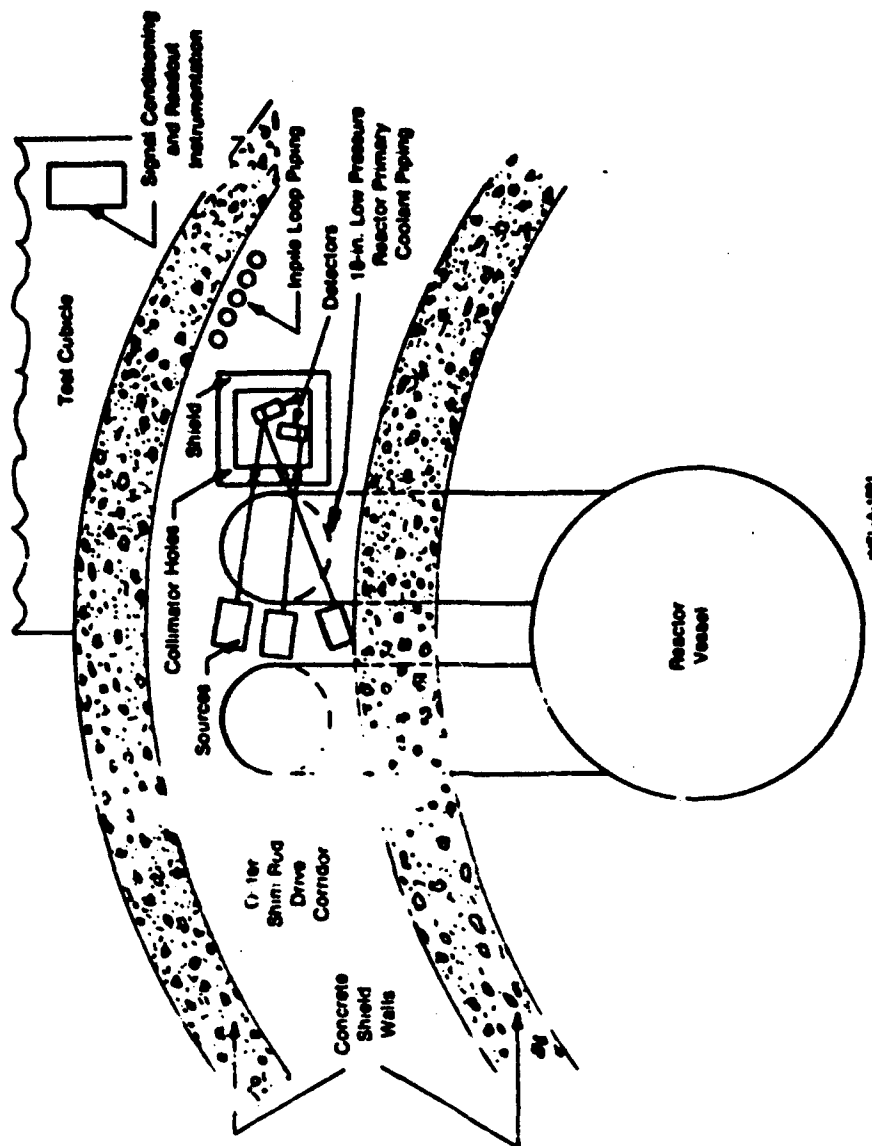
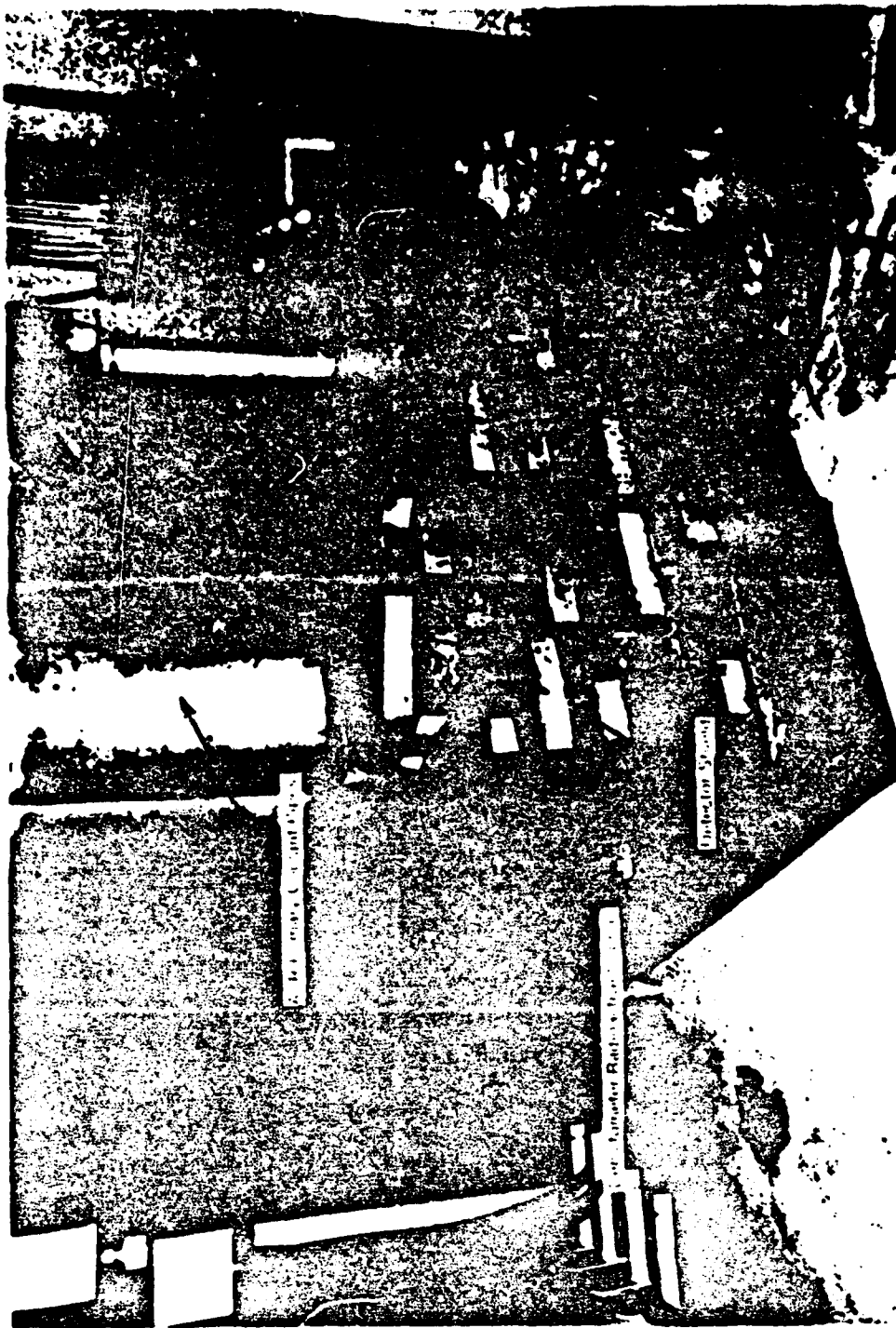Fig. 4 Experimental setup for ATR background radiation hardware test.

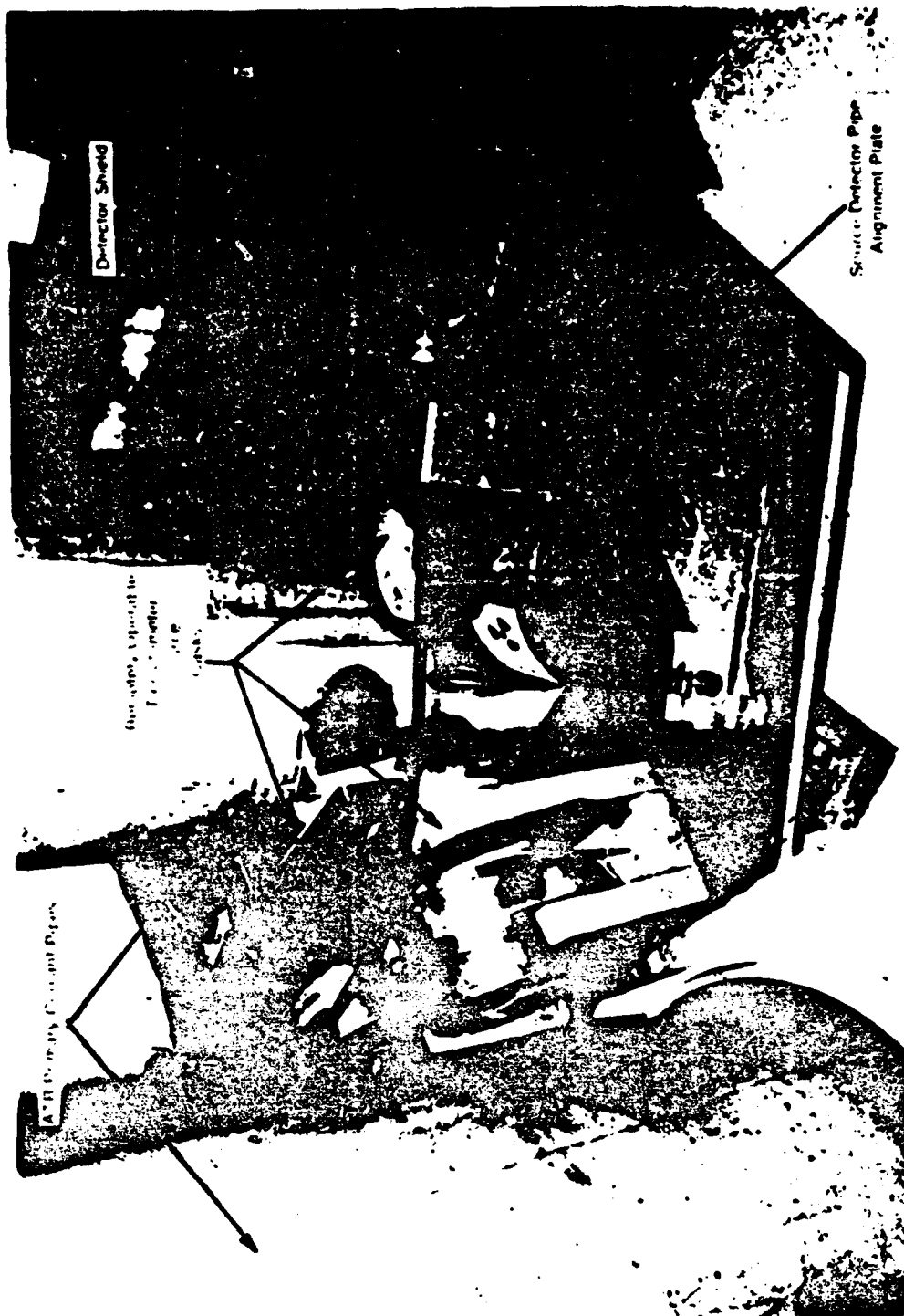Fig. 5a ATR background radiation test (general view in reactor's shim rod drive corridor).

I.5-101

**Detector Shield**

**Source-Detector Pipe Alignment Plate**

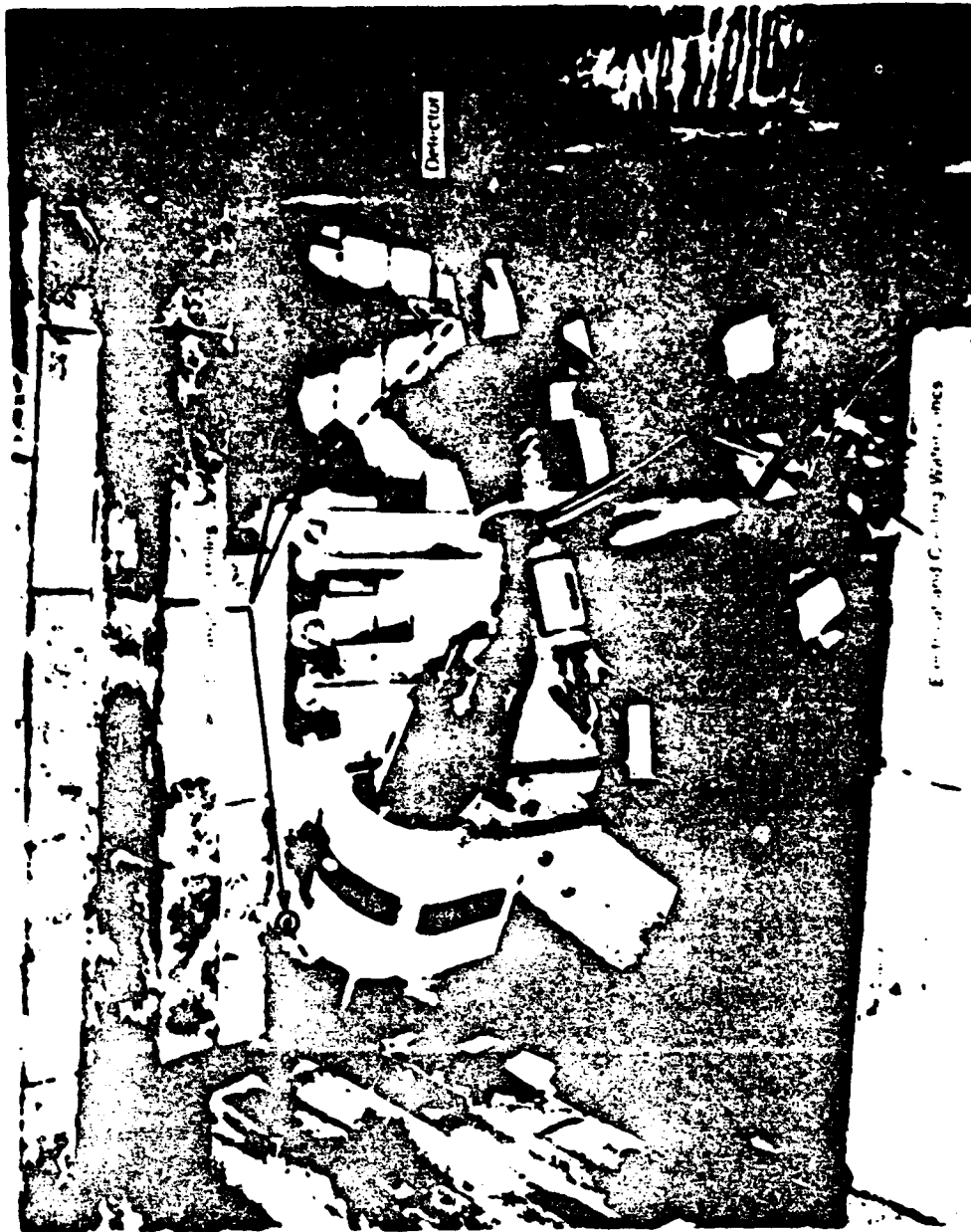Fig. 5b ATR background radiation test (view of sources, pipe, detector shield).

I.5-102

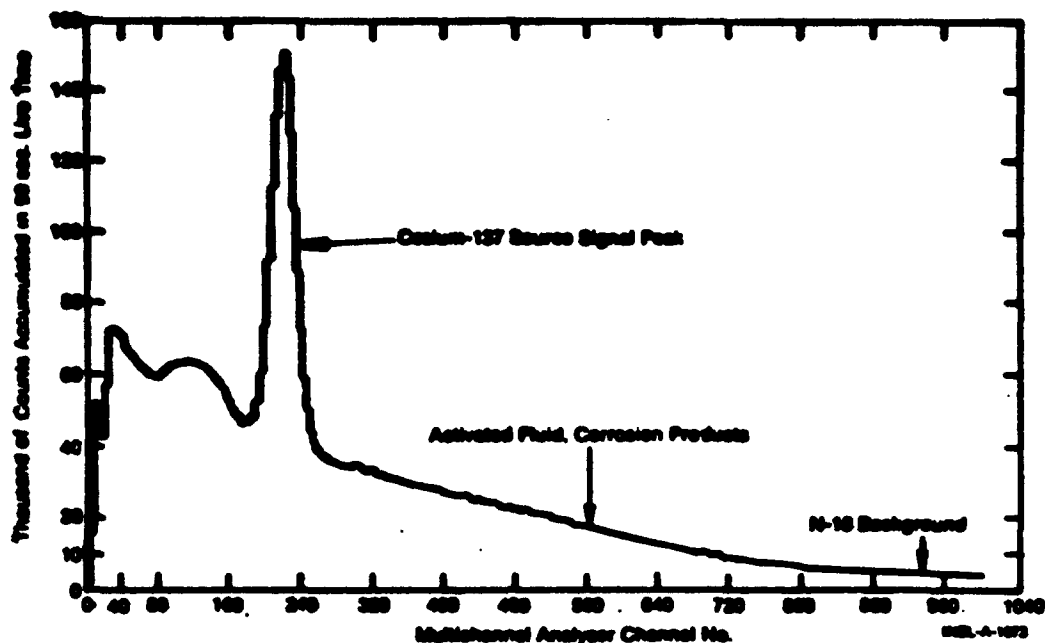Fig. 5c ATR background radiation test (view inside shield).

I.5-103

Fig. 6 Photon energy spectrum from advanced test reactor and Cs-137 source.

## 4. THEORETICAL WORK

An error analysis of the chordal average density measurement was undertaken. Some of the initial results are shown in Figures 7 and 8. In both figures, a statistical error factor is plotted which, when divided by 13.67 $\rho_c$, gives the percentage error in the chordal average density, for the LOFT setup (large pipe). As shown in Figure 7, the minimum error occurs for a diametral beam path ($\theta = 0°$) and increases rapidly beyond about 16°. In Figure 8, the error factor is plotted against photon energy for two angles and four densities. The minima are more mild here because the large fluid path drives the optimum photon energy to high values where the mass attenuation coefficients are both small and change little with energy.
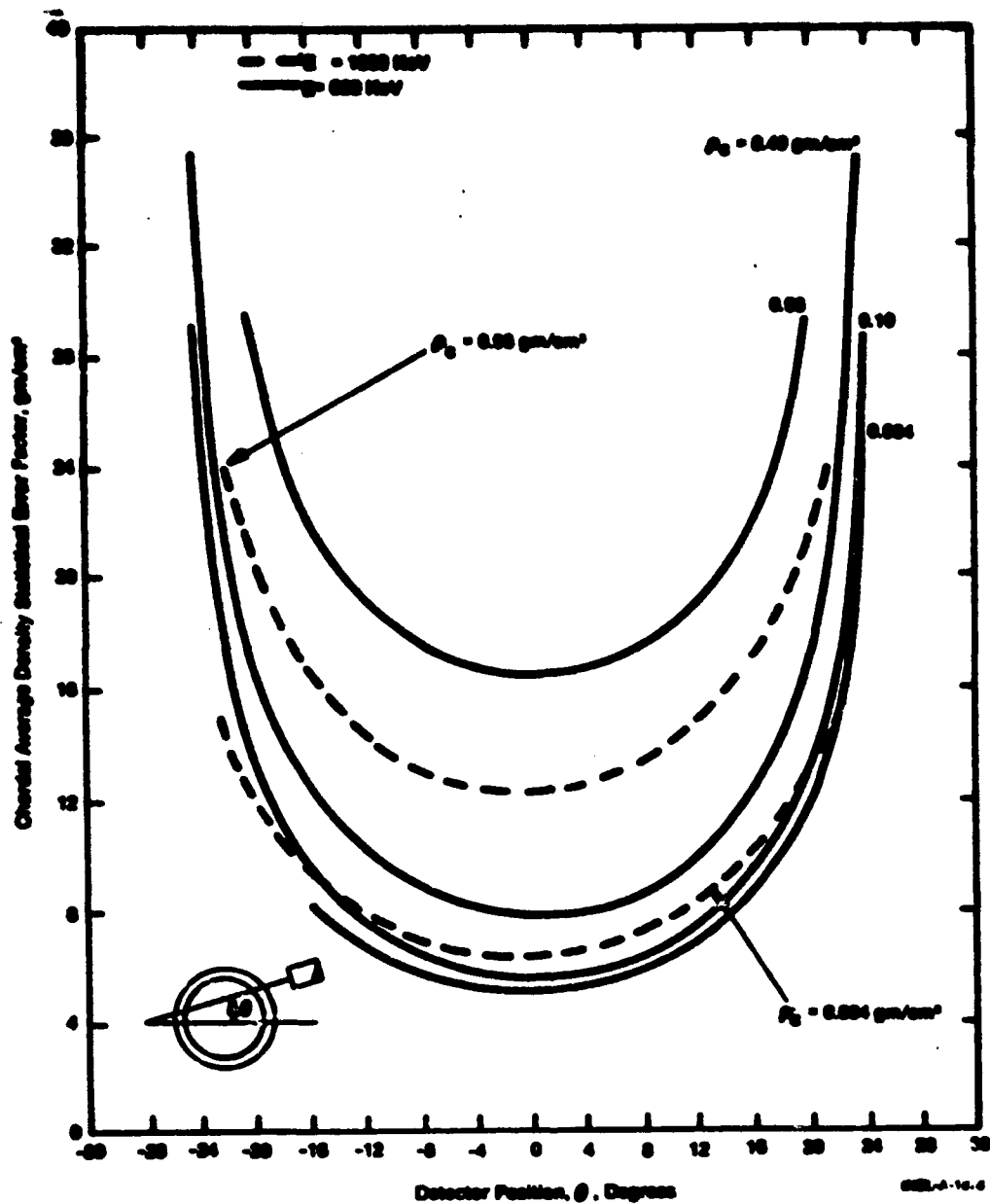
I.5-104

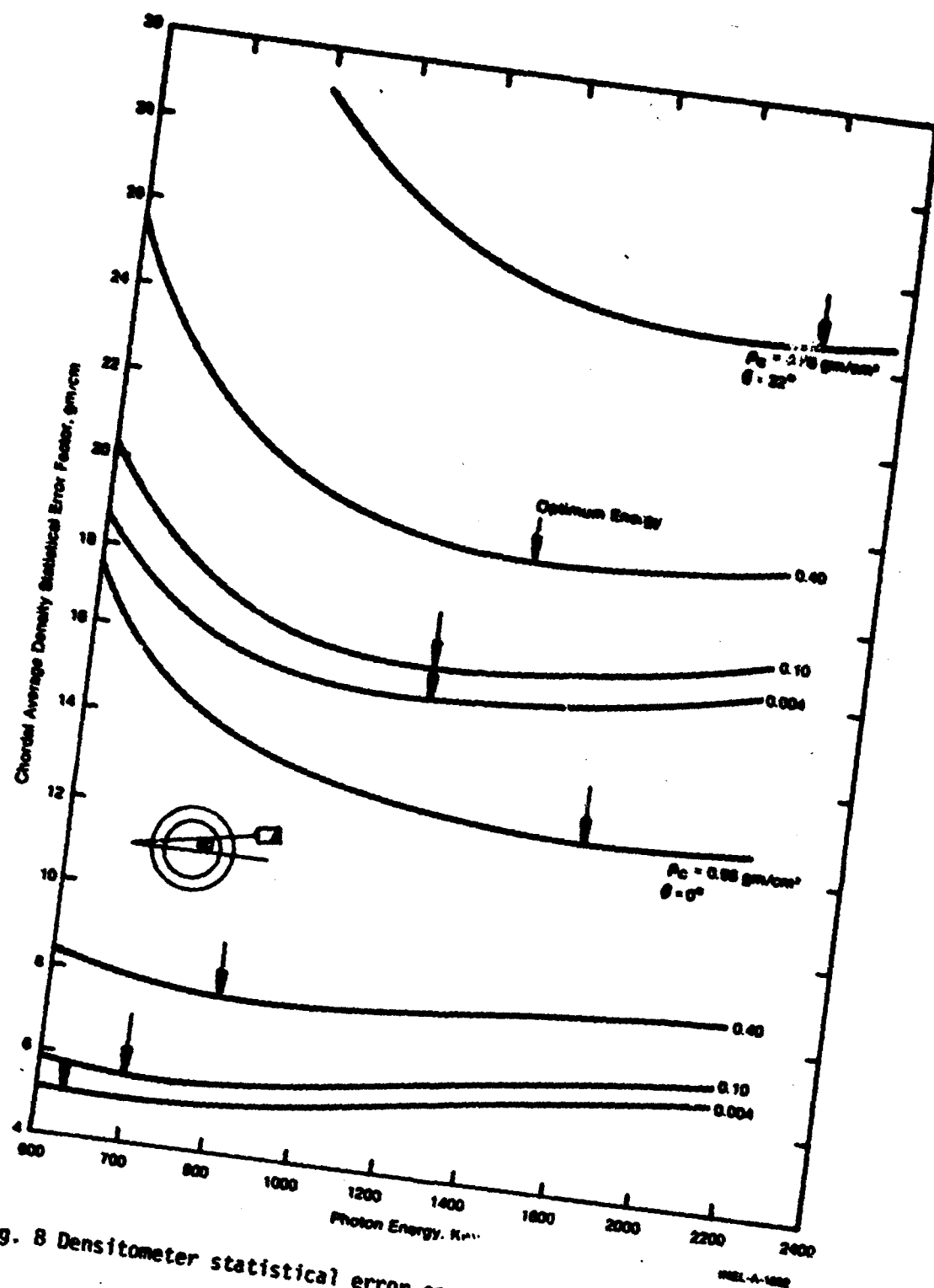Fig. 7 Densitometer statistical error detector position dependence – large pipe.

Fig. 8 Densitometer statistical error energy dependence – large pipe.

I.5-106

# 5. CONCLUSIONS TO DATE AND FUTURE WORK

Summarizing a few of the conclusions to date, the detector shield needed to make the measurement feasible will be at least 8 in. thick. A high energy gamma source (1.5 - 2.0 MeV) will give a lower error and a better signal/noise ratio (smaller background) than the existing Cs-137 source. The present design configuration being pursued includes use of a NaI type detector in the pulse counting mode, a single source and off-line digital background subtraction. Table II details the development work areas and the near and long term directions.

## TABLE II

### FUTURE WORK

|  | Near Term | Long Term |
|---|---|---|
| Detector Development | Improve NaI | Investigate Germanium Application |
| Signal Conditioning | Develop Transient Digital Processor | Investigate Online Analog Background Subtraction |
| Densitometer Source | Develop High Energy Source(s) Supply | Consider Embedded Source |
| Software Development | Calculate Flow Cross Sectional Average Density | Develop Local Density Calculation |
| Background Radiation Determination | Lawrence Livermore Laboratory Study & Evaluation | Loft Shielding Study |

PROGRESS REPORT ON LOFT

"TRANSIT TIME FLOWMETER"


by

G. D. Lassahn




EG&G IDAHO, INC.

IDAHO NATIONAL ENGINEERING LABORATORY




Presented at NRC Two-Phase Flow Instrumentation Meeting at
Silver Spring, Maryland, January 13, 1977



**Preceding page blank**

I.5-109

## SUMMARY

Experiments and preliminary theoretical results indicate that transit time flowmeters using thermocouples as sensors are not useful in Loss-of-Fluid Test (LOFT) blowdown experiments. Work is in progress to determine whether transit time flowmeters using other types of sensors might be useful in LOFT.

## CONTENTS

## FIGURES

# 1. INTRODUCTION

Transit time flowmeters are being considered as an alternative to turbine flowmeters for velocity measurement in LOFT blowdown experiments.

A transit time flowmeter (TTF), in this discussion, consists of two basic parts: a pair of sensors and a data analysis system. The sensors are located one downstream from the other. They sense naturally occurring random fluctuations in some fluid property, such as temperature or density, for which the fluctuations move with the fluid rather than propagating through the fluid. The data analysis system is some device, traditionally a correlator, that determines the relative time delay between the signals from the two sensors. A correlator, for example, generates a curve of correlation magnitude versus delay time. This curve hopefully has one dominant peak which indicates some sort of average or dominant delay time between the two signals. This delay time is interpreted as the (average or dominant) transit time of the fluid between the two sensors. The velocity is trivially obtained by dividing the spacing between the two sensors by the transit time. It is convenient to use a device that generates a curve of transit time versus real time, or perhaps velocity versus real time. Such a curve will always have at least a little noise, because the peak in the correlation curves moves a little in real time even for perfectly steady fluid flow. This point will be further discussed later.

There are several potential advantages of transit time flowmeters over turbine flowmeters:

1. TTFs may disturb the fluid flow much less than turbine flowmeters, depending on the type of sensor used.

2. The hardware inside the pipe is usually much simpler and more reliable than a turbine, depending on the type of sensor used.

Preceding page blank

I.5-113

3. In principle, no calibration is required with a TTF. Even if calibration is necessary, the calibration problems are much less severe than with turbines.

4. In principle, a TTF can indicate the distribution of flow velocities present in the measurement region. In two-phase flow with slip for example, a good TTF could give separate indications of the gas velocity, the liquid velocity, and the interface velocity. (In fact, this ideal is far removed from the present state of the art.)

Transit time flowmeters offer a potential for either very localized or global velocity measurements, including the potential for determining both the average velocity and velocity probability density function for an entire pipe with a single TTF.

## 2. PAST WORK

We have tested an experimental TTF using thermocouples as sensors[1]. The pipe section with the TTF sensors is sketched in Figure 1, and the details of the thermocouples mounting are shown in Figure 2. These thermocouples had response times (0-63%) of about 16 msec, for a roll-off frequency of 10 Hz. It is not known how to make significantly faster thermocouples that will survive the required 3000 hours in 350°C water.

In an effort to learn about the effects of sensor spacing in a TTF, five thermocouples were mounted in the pipe with spacings between pairs of adjacent thermocouples ranging from 0.4 to 29.7 cm. Data from all five thermocouples were recorded simultaneously on analog magnetic tape, and pairs of signals were analyzed later.

The most important conclusion of this experimental work comes from steady flow, all-liquid data. Figure 3 shows four graphs of inverse velocity (transit time ÷ sensor spacing) versus real time, for four
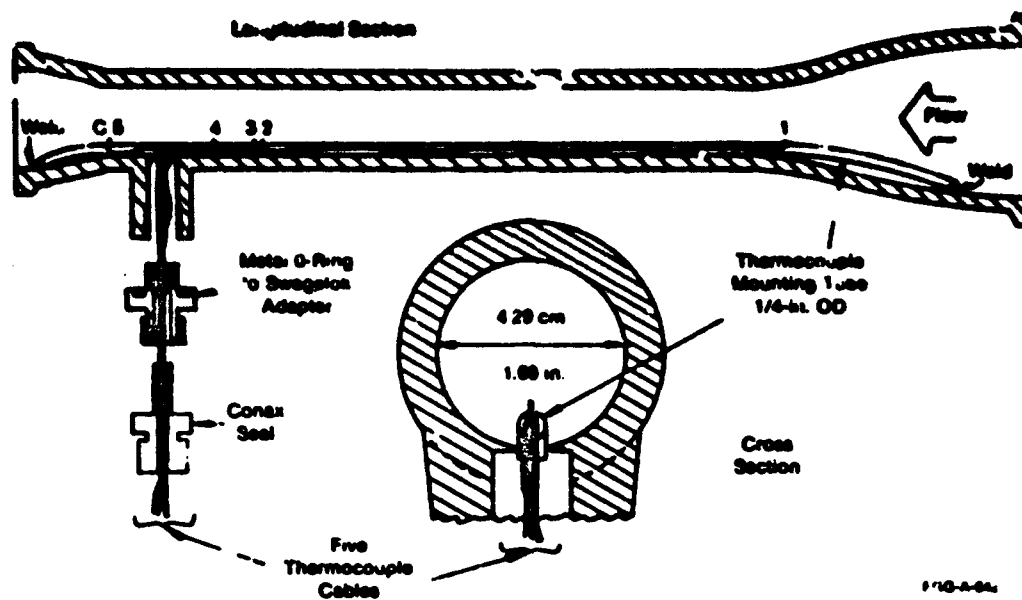
I.5-114

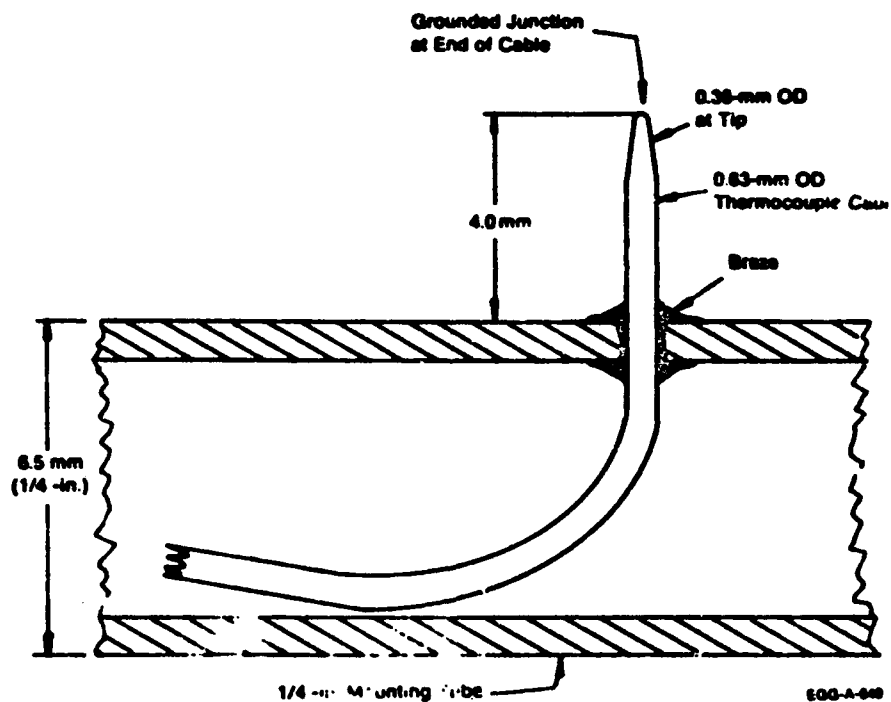Fig. 1 Longitudinal section and transverse section of pipe with transducer.



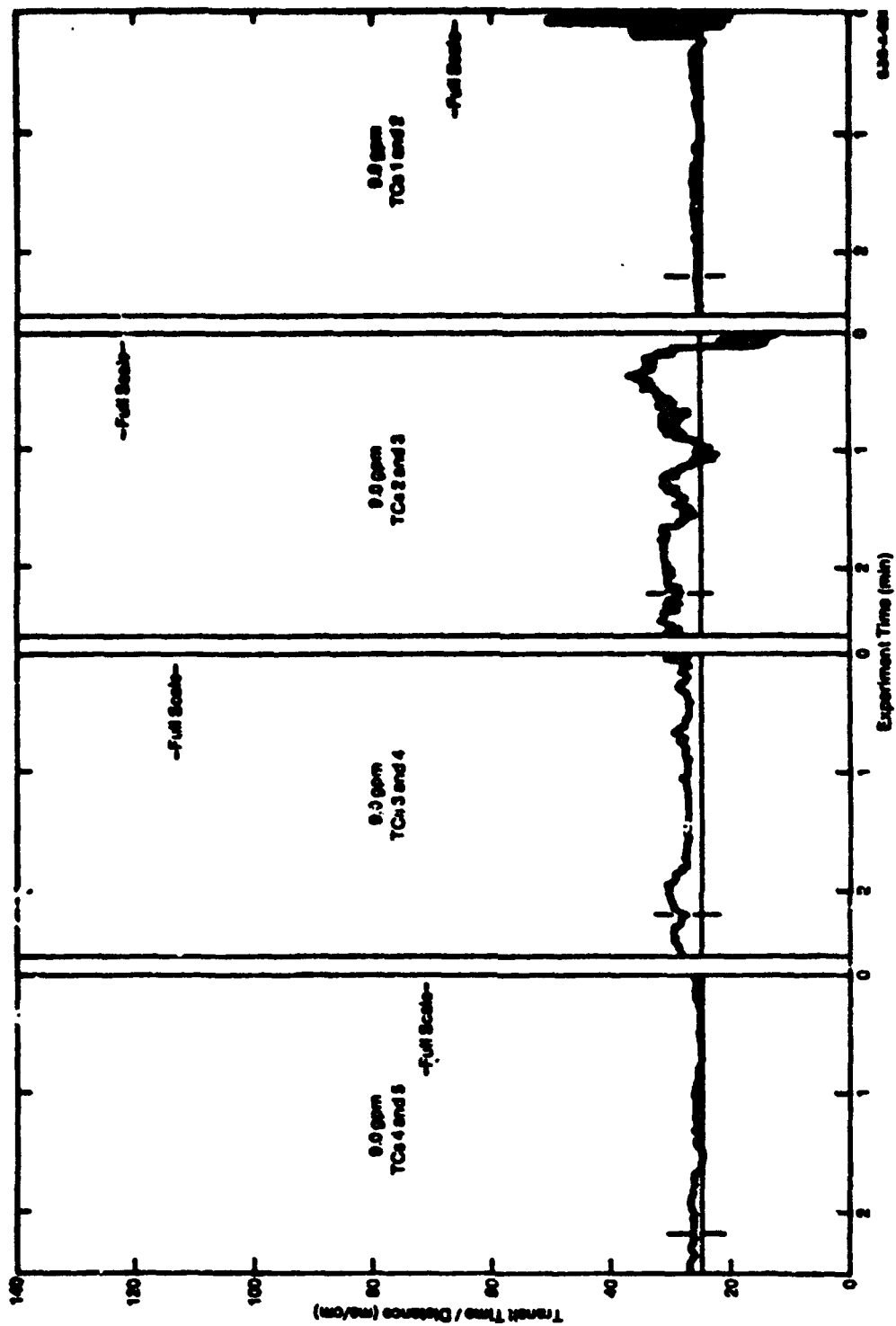Fig. 2 Thermocouple and mounting details.

I.5-115

Fig. 3 Transit time curves obtained with 20-sec averaging time.

different sensor spacings. The noise in the first few seconds of some of
the graphs is an artifact of the system, and should be ignored. These
four graphs should all be the same, if the TTF worked ideally. If a
flat velocity profile is assumed, the four graphs should all lie on the
straight lines that are drawn in at 25 msec/cm, to agree with turbine
flowmeter measurements. These four graphs indicate a good potential for
making steady state velocity measurements with this TTF. However, when
we try to use this system in transient flow, we cannot use a 20-sec
averaging time in the data analysis, as we did for the curves of
Figure 3. The averaging time for blowdown data must be only a fraction
of a second, because the velocity is not even approximately constant for
time intervals greater than 1 sec. Figure 4 shows the results of the
same data and analysis procedures represented in Figure 3, except that
the averaging time was reduced from 20 to only 1 sec for the Figure 4
curves. Obviously, the curves of Figure 4 are much more noisy, with
some noise peaks approaching the full range of the analysis system
(indicated by the "FULLSCALE" notation in the figure). For steady flow
data, these curves can be smoothed to get a reasonable indication of the
fluid velocity. But for transient flow, the curves cannot be smoothed,
and it is unknown whether the peaks in the curve represent random
statistical noise or real velocity fluctuations.

An approximate theoretical treatment predicts that the noise
(standard deviation of the curve about the mean) in a transit time curve
obtained from a cross-correlation analysis is about 20% of reading for
the best data obtained in these tests. This is in reasonable agreement
with the observed noise level.

The noise in the curves of Figures 3 and 4 is inherent in any
transit time flowmeter that uses random fluctuations of the fluid
properties. The effect of the noise may be less severe in some types of
data analysis systems, but it will always be present in at least a
qualitatively similar form. The noise magnitude decreases as the
averaging time increases and as the bandwidth of the correlated signals
increases, but for a given TTF system in a transient flow application,
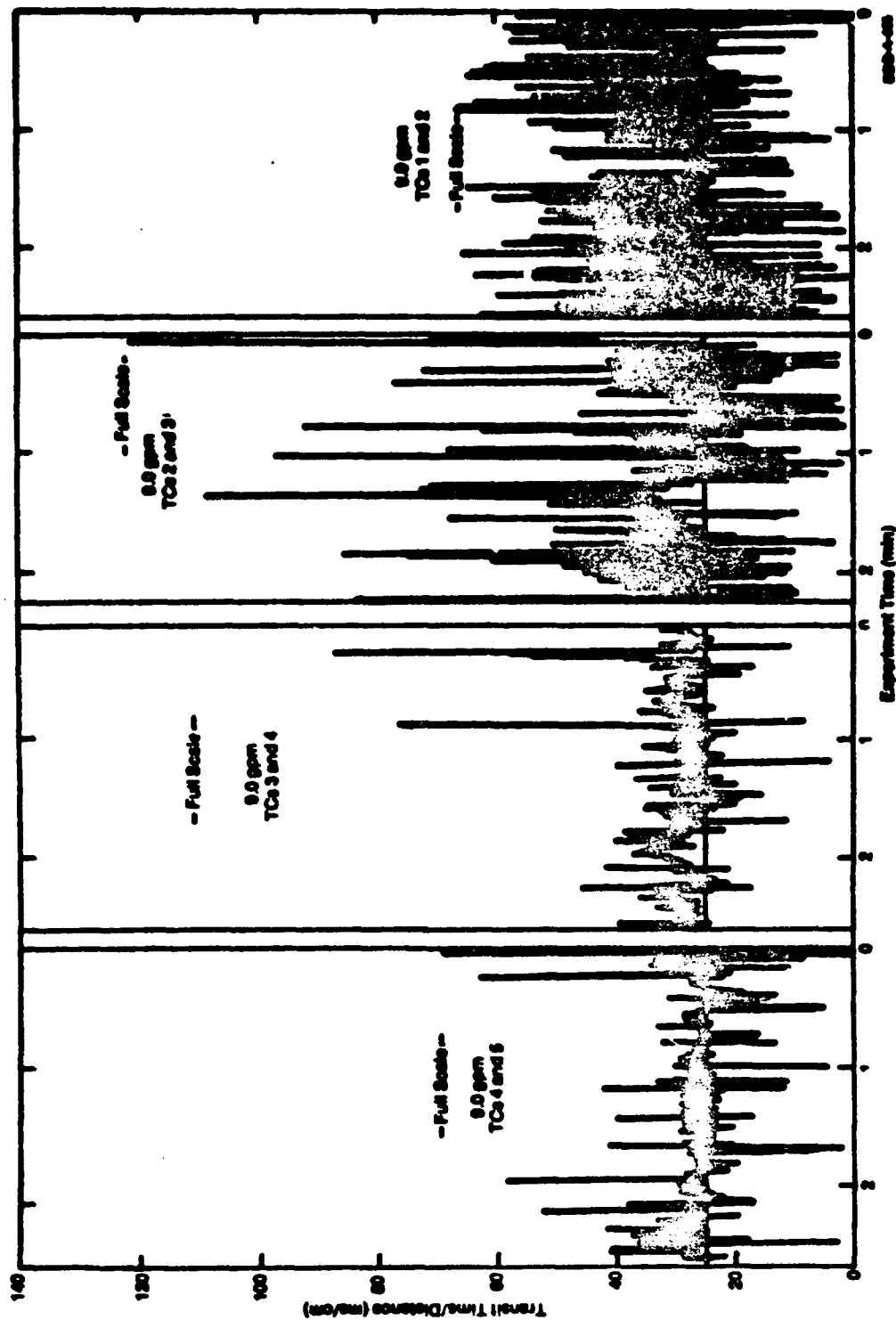the parameters cannot be increased at will.

Fig. 4 Transit time curves obtained with 1-sec averaging time.

I.5-118

It can be concluded that this TTF system is not useful in LOFT blowdown experiments unless errors of at least 20% of reading are acceptable. The present state of knowledge dictates a pessimistic attitude about possible improvements resulting from different data analysis systems. However, TTFs using thermocouples as sensors should be very useful in applications in which longer averaging times are acceptable, and in less severe environments in which faster response thermocouples can be used.

## 3. CONTINUING WORK

The negative results obtained with the thermocouple type TTF do not imply that no transit time flowmeter system can work in LOFT blowdowns. At this time optimism is high about the potential of any TTF system in which the correlated power bandwidth is 100 Hz or greater. Of course, such a TTF needs sensors with a response bandwidth of at least 100 Hz. We are therefore preparing experiments in which four alternative sensors -- drag screens, gamma densitometers, ultrasonic void sensors, and electrical conductivity void sensors -- will be evaluated in steam/water blowdown tests in the Bettis Flask facility at INEL. These sensors will all be designed with bandwidths in excess of 100 Hz. The most important information to be gained from these tests will be the bandwidths of the signals obtained from the fluid under blowdown conditions. We also hope to gain some information about the coherence time or the coherence length of the signal in the fluid. That is, we hope to learn how long the signals last in the fluid, or how far the fluid travels before the signals become uncorrelated or incoherent.

This experimental information is necessary but not sufficient to predict the performance of a TTF in transient flow. We also must understand quantitatively the errors in TTF readings and how they depend on such parameters as the power spectral density (cross- and auto-) and the record length or averaging time. We are, therefore, doing a theoretical study concurrently with the experimental work. This study

I.5-119

will consider several possible types of data analysis techniques, including the traditional cross-correlation, the more informative (potentially) impulse response function, and an optimally weighted average of the contributions of separate frequency components.

Figure 5 shows some early results from this theoretical study. This is a graph of $\omega_2 \sigma_\tau$ versus $\omega_2 T$ for several values of $\rho$, where

$\omega_2$    is the angular frequency cutoff of the correlated power

$\sigma_\tau$    is the standard deviation of the position of the peak in the cross-correlation curve, or the error in the transit time reading

T    is the record length or averaging time

$\rho$    is the correlation coefficient or the normalized correlation magnitude at the peak of the correlation curve.
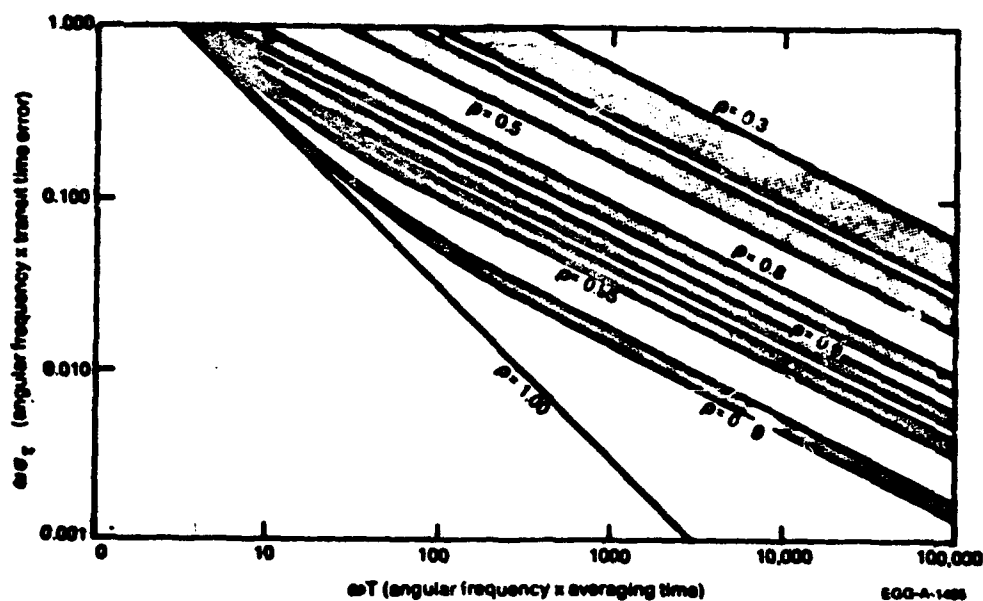


Fig. 5 Graph for predicting noise magnitude in transit time curves.

I.5-120

In this calculation, the cross power spectral density was assumed to be flat for $0<\omega<\omega_2$, and zero for $\omega_2<\omega$. The auto power spectral densities were assumed flat for $0<\omega<\omega_1$, and zero for $\omega_1<\omega$, with $\omega_2\leq\omega_1$.

In the best case of the previously discussed Semiscale data, we had $\rho = 0.5$ and $\omega_2 = 2\pi$ 10 Hz = 62.8 sec$^{-1}$. If we choose T = 1 sec, we find that $\sigma_\tau$ is between 11 and 17 ms, which is greater than 20% of reading. For T = 20 sec, $\sigma_\tau$ is between 2.5 and 3.8 ms. These values are in reasonable agreement with experimentally observed values. The exact value of $\sigma_\tau$ in the specified ranges (i.e., the exact position in the shaded band on the graph) depends on the value of $\omega_1$. Smaller $\omega_1$ values give points along the lower edge of the shaded band.

## 4. CONCLUSIONS

It is felt that transit time flowmeters using thermocouples as sensors cannot be used in LOFT blowdown experiments. However, TTFs using other types of sensors may be useful. Experimental and theoretical work to evaluate the potentials of TTFs using other sensors is presently being done.

## 5. REFERENCE

1. G. Lassahn, Feasibility Study of Thermocouple Correlation Type Transit Time Flowmeter in Transient Steam-Water Flow, TREE-NUREG-1011 (February 1977).

INVESTIGATION FOR VERTICAL, TWO-PHASE STEAM-WATER FLOW

OF THREE TURBINE MODELS

by

S. Silverman
L. D. Goodrich

EG&G IDAHO, INC.

IDAHO NATIONAL ENGINEERING LABORATORY

Presented at NRC Two-Phase Flow Instrumentation Meeting at
Silver Spring, Maryland, January 13, 1977

I.5-123

# CONTENTS

## FIGURES

## TABLES

I.5-126

# 1. INTRODUCTION[a]

One of the basic quantities of interest during a loss-of-coolant experiment (LOCE) is the primary system mass flow rate. Presently, there are no transducers commercially available which continuously measure this parameter. Therefore, a transducer was designed at EG&G Idaho, Inc. which combines a drag-disc and turbine into a single unit. The basis for the design was that the drag-disc would measure momentum flux ($\rho V^2$), the turbine would measure velocity and the mass flow rate could then be calculated from the two quantities by assuming a flow profile.

For two-phase flow, the outputs are approximately proportional to the desired parameter, but rather large errors can be expected under those assumptions. Preliminary evaluation of the experimental two- and single-phase calibration data has resulted in uncertainty estimates of $\pm 8\%$ of range for the turbine and $\pm 20\%$ of ra...ye for the drag-disc. In an effort to reduce the errors, further investigations were made to determine what the drag-disc and turbine really measure. In the present paper, three turbine models for vertical, two-phase, steam/water flow are investigated; the Aya Model, the Rouhani Model, and a volumetric flow model[2,3,4]. Theoretical predictions are compared with experimental data for vertical, two-phase steam/water flow. For the purposes of the mass flow calculation, velocity profiles were assumed to be flat for the free-field condition. It is appreciated that this may not be true for all cases investigated, but for an initial inspection, flat profiles were assumed.

It should be noted that because of the physical arrangement of the drag-disc and turbine and because of unique blade geometry, the results should be applied with caution to other turbines. See Figure 1a for transducer geometry.

---

[a] This paper is condensed from Reference 1.
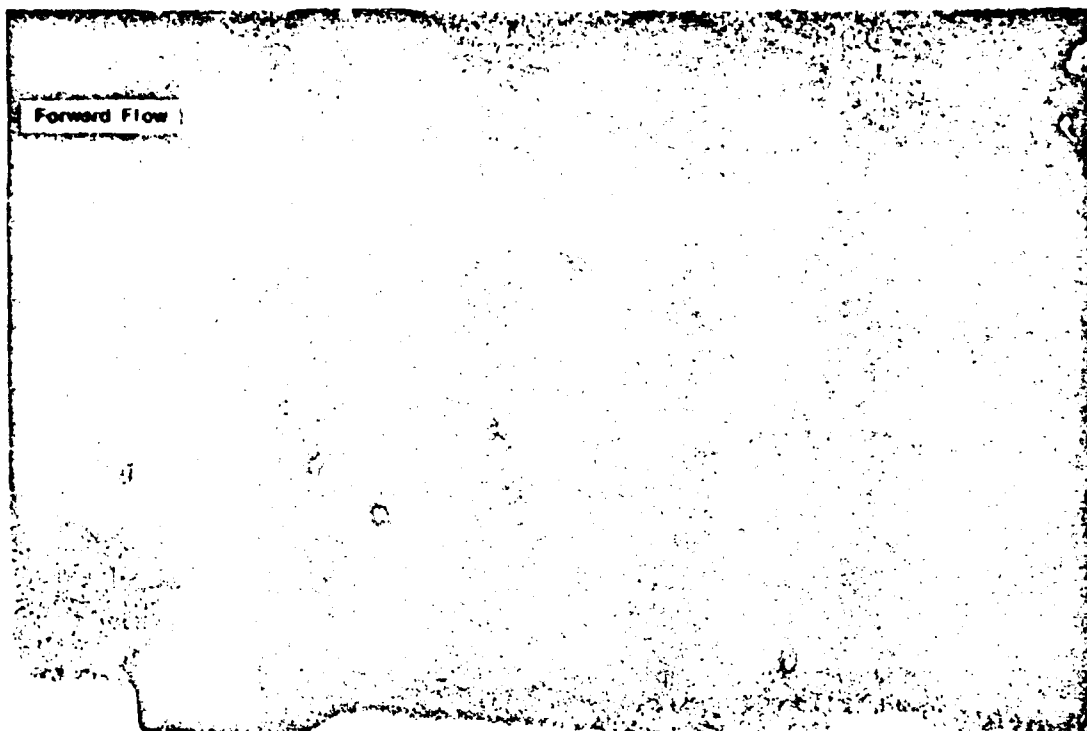
Fig. 1a LOFT drag-disc turbine transducer geometry (shroud removed).

The experimental data employed in the investigation were obtained at Westinghouse Canada Limited (WCL) in two series of tests[5]. In one series, all flow went through the turbine; this is denoted as the "full flow" series. In the other series, a 4.05-in. ID pipe was employed; this is denoted as the "free-field" series since flow could bypass as well as pass through the 1.18-in. diameter turbine. The ranges of the test variables are summarized in Table I.

# TABLE 1

## RANGES OF THE TEST VARIABLES

| | Quality X | Nominal Pressure psi | Nominal Temp. °F | Void Fraction Calculated from αg (γ) a | Given ρf/ρg Slip Calculated[a] from Ref. 8 S | ρf lbm/ft³ from Ref. 7 for Nominal Temp. | ρg lbm/ft³ from Ref. 7 for Nominal Temp. | Nominal Velocity fps | Number of Data Points |
|---|---|---|---|---|---|---|---|---|---|
| Full Flow | 0-0.52 | 300 & 900 | 420 & 530 | 0 - 0.94 | 1.0 - 2.3 | 47 - 56 | 0.37 - 2.0 | 2.3 - ,30 | 22 |
| Free Field | 0-0.62 | 300 & 900 | 420 & 530 | 0 - 0.96 | 1.6 - 2.3 | 47 - 56 | 0.62 - 2.1 | 2.6 - 19 | 41 |

[a] For LOFT Test L1-1 through L1-3A, the maximum slip is estimated as about 6.0.

I.5-129

## 2. DESCRIPTION OF AYA'S MODEL

A model of the behavior of a turbine meter was proposed by Aya[2].
It is assumed the flow is dispersed with the steam moving faster than
the water. The forces acting on the blade are visualized as a steam
force acting on the upstream portion of the blade and a resisting water
force acting on the downstream portion. The turbine is assumed to be
turning at a speed that corresponds to a fluid velocity $V_t$ which lies
between the steam and water velocities. It is assumed that the steam is
trying to drive the turbine into the water and the water on the other
side of the blade resists this driving force. The derivation presented
in Reference 2 is followed below.

The blade is shown in Figure 1b. The tangential velocity at a
point is $r\omega$, where r is the radial distance from the ax`, to be the
point and $\omega$ is the angular frequency of the blade.

The gas velocity is usually greater than or equal to the liquid
velocity in two-phase flow. For steady state flow, the forces acting
across the blade and normal to the turbine axis of rotation must be in
equilibrium. Assuming that the forces acting normal to the blade are
drag forces and that viscous forces can be neglected, the equilibrium
equation is as follows (see Figure 2).

$$(1/2) \, \rho_g \, C_{tg} \, A_g \, (V_g - V_t)^2 \sin^2\phi \qquad\qquad (1)$$

$$= (1/2) \, \rho_f \, C_{tf} \, A_f \, (V_t - V_f)^2 \sin^2\phi.$$

where

$V_t$ can be obtained either from blade geometry or an all water
calibration.
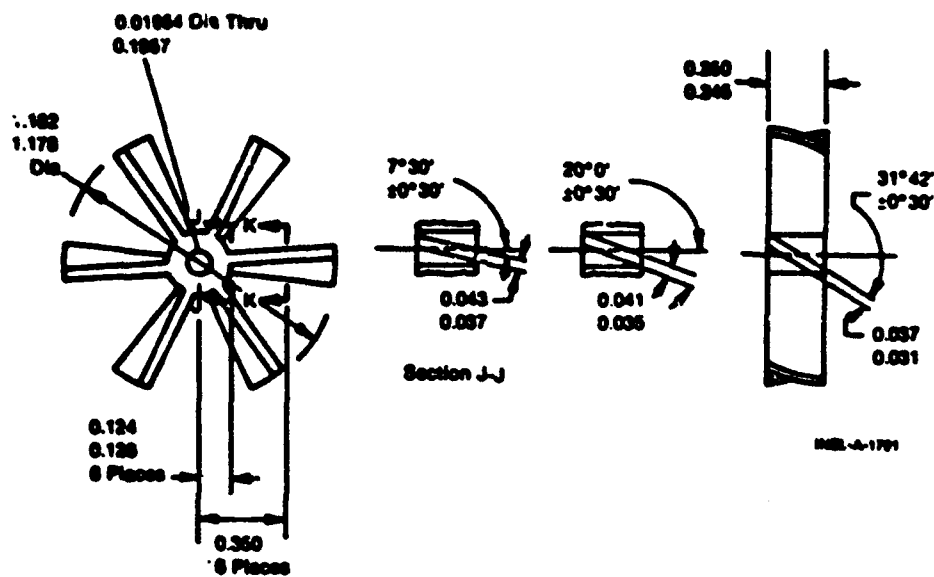
Fig. 1b Turbine blade geometry (plenum meter).
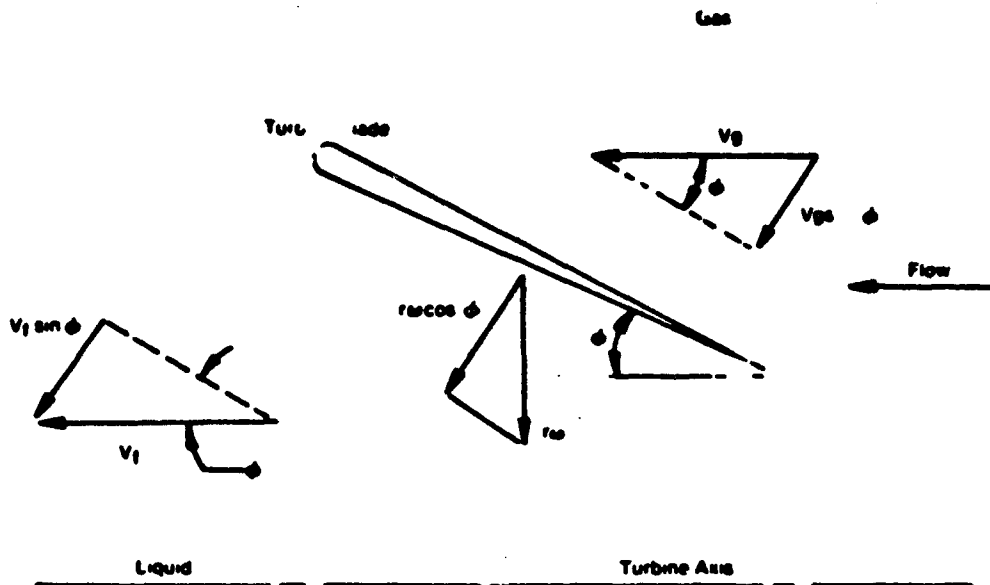
Fig. 2 Velocity vectors for the Aya model.

Equation (1) simplifies to

$$\alpha \rho_g \, (V_g - V_t)^2 \, C_g = (1 - \alpha)\rho_f C_f \, (V_t - V_f)^2$$

For the foregoing equations the following are defined:

$A_g$ = flow area occupied by the steam

$A$ = total flow area

$\alpha$ = $\dfrac{A_g}{A}$ (void fraction)

$\rho_g$ = mass density of steam at test temperature

$V_g$ = velocity of steam

$C_g$ = drag coefficient for turbine blade in steam flow

I.5-132

$\rho_f$ = mass density of liquid at test temperature

$V_f$ = velocity of liquid

$C_f$ = drag coefficient for turbine blade in liquid flow

$S = \dfrac{V_g}{V_f}$ (slip).

Dividing both sides of the equation by $V_f$ and rearranging yields

$$\frac{\left(\dfrac{V_g}{V_f} - \dfrac{V_t}{V_f}\right)^2}{\left(\dfrac{V_t}{V_f} - 1\right)^2} = \frac{\rho_f}{\rho_g} \frac{1-\alpha}{\alpha} \frac{C_{ft}}{C_{tg}} .$$

This is one equation with six parameters so that further relations are required. Once five of these parameters are determined, Equation (1) can be solved for $V_f$, the fluid velocity.

The drag coefficients depend on Reynolds number and the cavitation number and not the type of fluid. Assuming the ratio of drag coefficients is one, introducing the slip ratio $S = V_g/V_f$, and solving the quadratic equation yields

$$V_f = \frac{V_t \left[\dfrac{\rho_f}{\rho_g} (1-\alpha) - \alpha\right]}{\left[(1-\alpha)\dfrac{\rho_f}{\rho_g} - \alpha S\right] + \left\{\left[\alpha S - (1-\alpha)\dfrac{\rho_f}{\rho_g}\right]^2 - \left[(1-\alpha)\dfrac{\rho_f}{\rho_g} - \alpha\right]\left[(1-\alpha)\dfrac{\rho_f}{\rho_g} - \alpha S^2\right]\right\}^{1/2}} . \quad (2)$$

Knowing the fluid velocity, the gas velocity can be calculated from the slip ratio. The mass flow rate can then be computed as

$$\dot{M}_t = \dot{M}_f + \dot{M}_g \qquad (3)$$

$$= \rho_g V_g A_g + \rho_f V_f A_f$$

$$\dot{M}_t = \left[ \alpha \rho_g V_g + (1\alpha) \rho_f V_f \right] A \qquad (4)$$

where A is the total flow area. It has been assumed that the velocity profile is flat over the area.

## 3. ROUHANI'S MODEL

Rouhani[3] developed a model based upon physical reasoning that the higher velocity steam is driving the turbine into the slower velocity liquid. By application of the linear momentum equation with no body forces, the following governing equation was obtained[a].

$$V_g = V_t \, S \left( \frac{1}{1 + (S-1)x} \right) \qquad (5)$$

where x is defined as the flow quality

$$x = \frac{\dot{M}_g}{\dot{M}_t} \qquad (6)$$

and

$\dot{M}_g$ = mass flow rate of gas

$\dot{M}_t$ = total mass flow rate

By employing the relation[6]

$$S = \frac{x}{(1-x)} \frac{(1-\alpha)}{\alpha} \frac{\rho_f}{\rho_f} \qquad (7)$$

[a] The equation presented in Reference 3 can be recast into the equation presented.

The governing equation can be rewritten as

$$V_f = V_t \frac{\alpha S + (1-\alpha)\frac{\rho_f}{\rho_g}}{\alpha S^2 + (1-\alpha)\frac{\rho_f}{\rho_g}} \quad . \tag{8}$$

## 4. VOLUMETRIC FLOW MODEL

This model assumes that the turbine measures volumetric flow rate regardless of whether the flow is single- or two-phase. Thus, the volumetric flow rate is given as

$$Q = A_g V_g + A_f V_f = \alpha \bar{A} V_g + (1-\alpha) \bar{A} V_f \tag{9}$$

where $\bar{A}$ is the flow area through the turbine. Introducing slip yields

$$Q = \bar{A}[1 + \alpha(S-1)] V_f \quad . \tag{10}$$

and solving for $V_f$

$$V_f = \frac{Q}{\bar{A}[1+\alpha(S-1)]} \quad . \tag{11}$$

## 5. ALL WATER CALIBRATION DATA

Prior to the two-phase tests, all water calibration tests were conducted. The results of the tests are

$$V_{av} = \begin{cases} -0.116 + 34.47\ E_0 & \text{Full Flow} \\[2mm] 0.344 + 39.19\ E_0 & \text{Free Field} \end{cases} \tag{12}$$

I.5-135

where $V_{av}$ is the average flow velocity in the pipe and $E_o$ is the turbine output volts.

For all water flow, the three models simplify to ($\alpha$=0, S=1).

$$V_f = \begin{cases} V_t = V_{av} & \text{Aya's and Rouhani's model} \quad (13) \\ \dfrac{Q}{A} = V_{av} & \text{Volumetric flow model} \end{cases}$$

## 6. MODEL COMPARISON WITH EXPERIMENT

Calculations for the three models were made as follows:

$\rho_f, \rho_g$ = obtained from ASME steam tables[7] for the test temperature

S = obtained from Reference 8, Figure 3, as a function of $\rho_f/\rho_g$

x = flow quality known from the tests

$\alpha$ = obtained from Equation (7) once S and x are known

$V_t$ = from all water calibration, Equation (13).

The ranges of the test variables may be seen in Table I.

## 7. RESULTS

If no modeling were conducted then the basic calibration data for the turbine would be as shown in Figure 3. The WCL velocity was calculated from the relationship
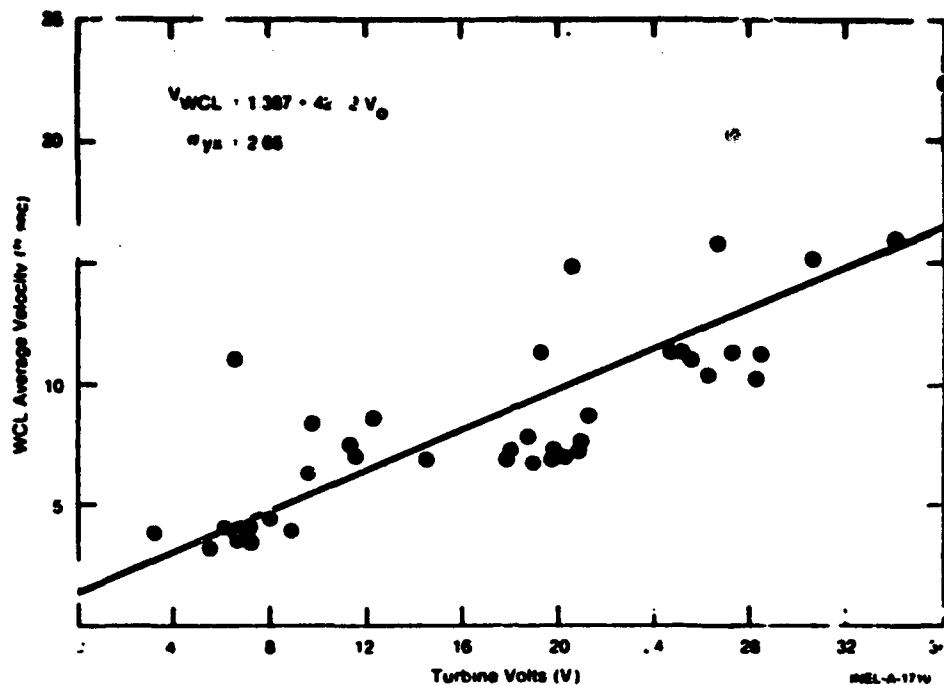
Fig. 3 Turbine calibration with no modeling.

$$V_{WCL} = \frac{\dot{M}_f + \dot{M}_g}{\rho_{WCL} A}$$

where $\rho_{WCL}$ is the average fluid density and was obtained from measured test parameters and A is the net flow area at the instrument.

The effect of modeling on the calibration may be seen in Figures 4 and 5. In Figure 4 is shown the liquid velocity versus turbine volts for Rouhani's model. Steam velocity versus turbine volts is shown for slips of 1.6 in Figure 5a and 2.3 in Figure 5b. Similar results are obtained for the other two models.

The best test for the model is a comparison of predicted versus measured mass flow rate. This is done for the free field tests in Figures 6, 7, and 8 for the Rouhani, volumetric flow and Aya models.
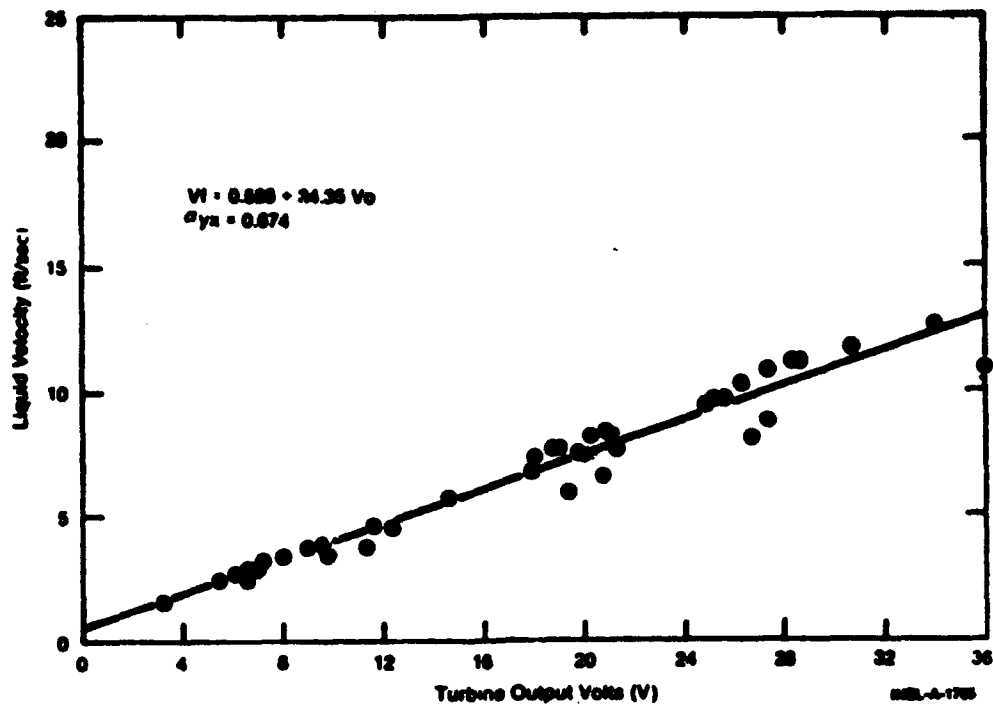
Fig. 4 Liquid velocity calibration from the Rouhani model.



Fig. 5a Steam velocity calibration from the Rouhani model (slip = 1.6).

I.5-138

Fig. 5b Steam velocity calibration from the Rouhani model (slip = 2.2).
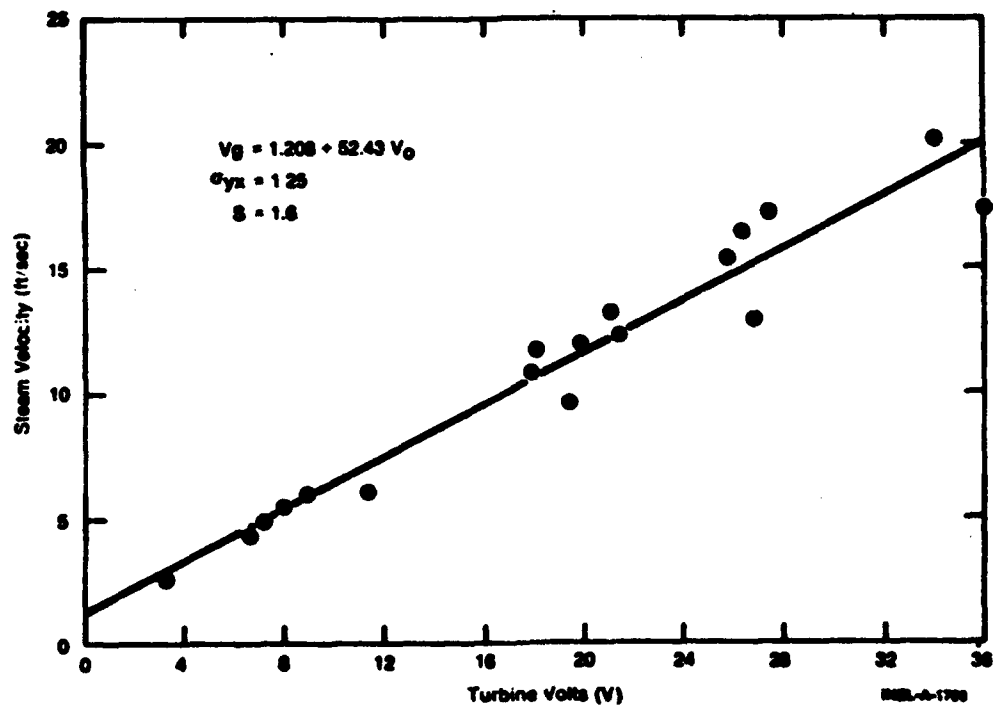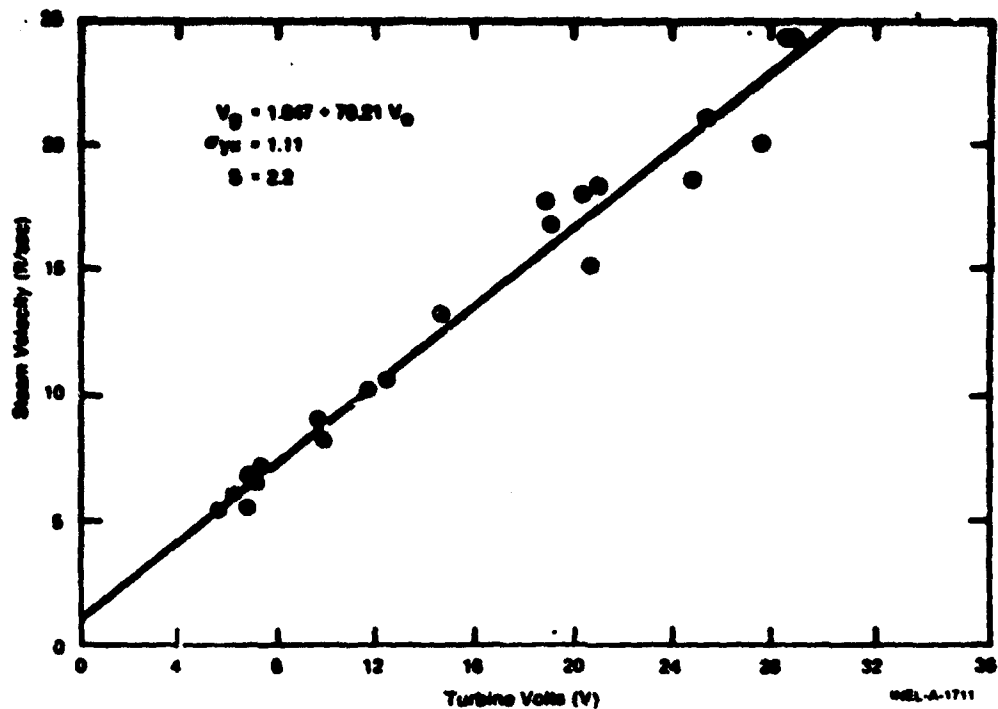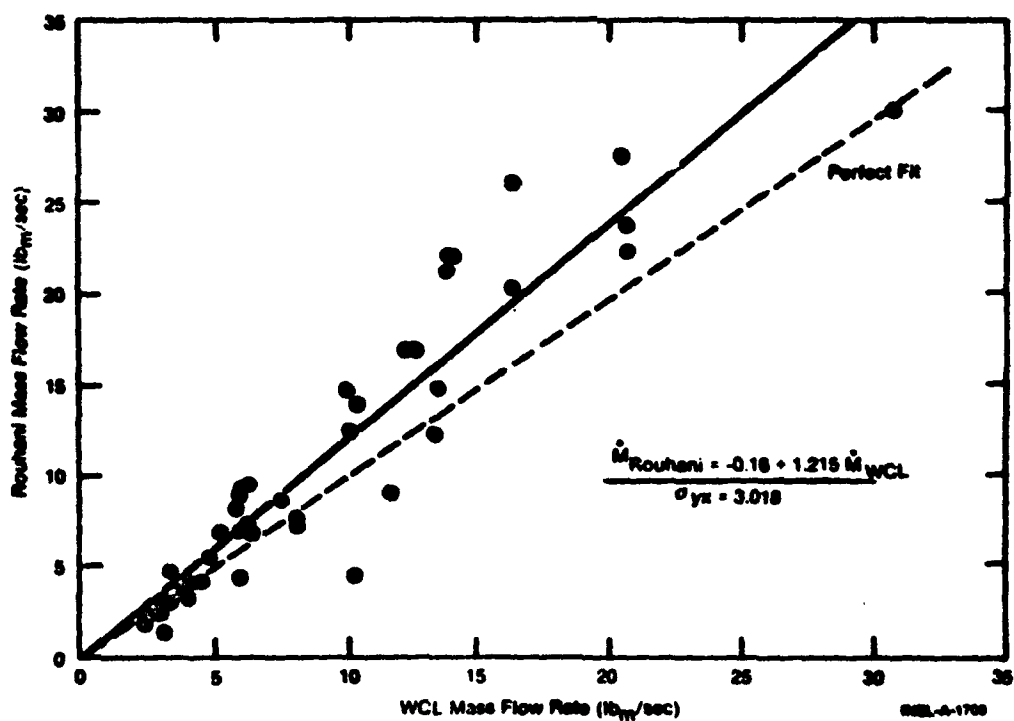


Fig. 6 Predicted versus experimental mass flow rate from the Rouhani model.

I.5-139
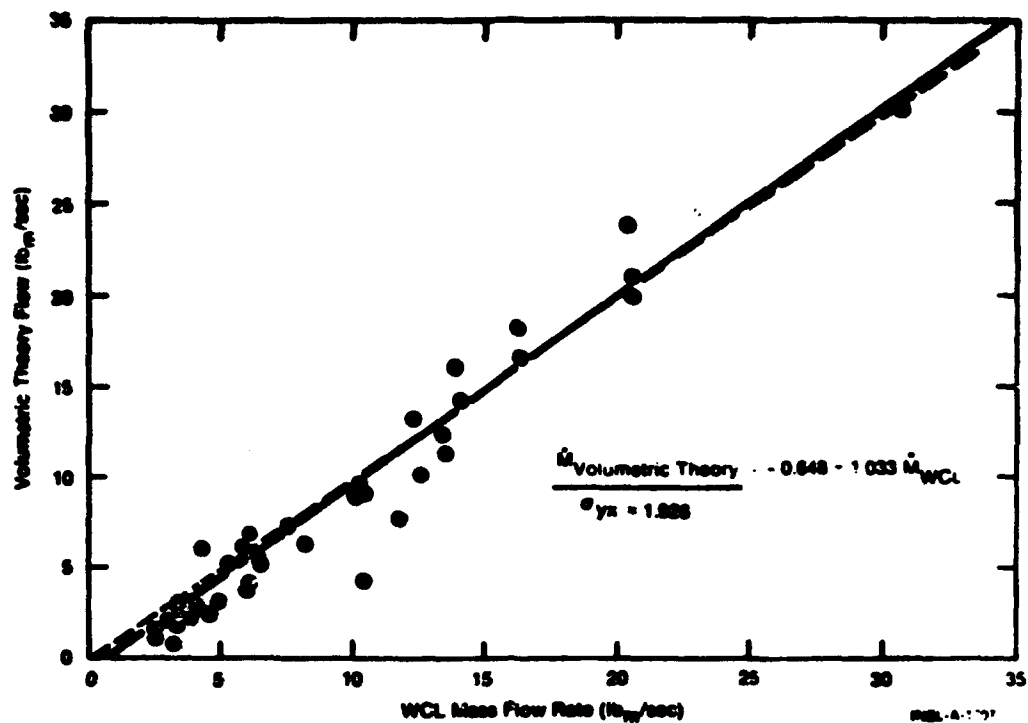
Fig. 7 Predicted versus experimental mass flow rate from the volumetric flow model.
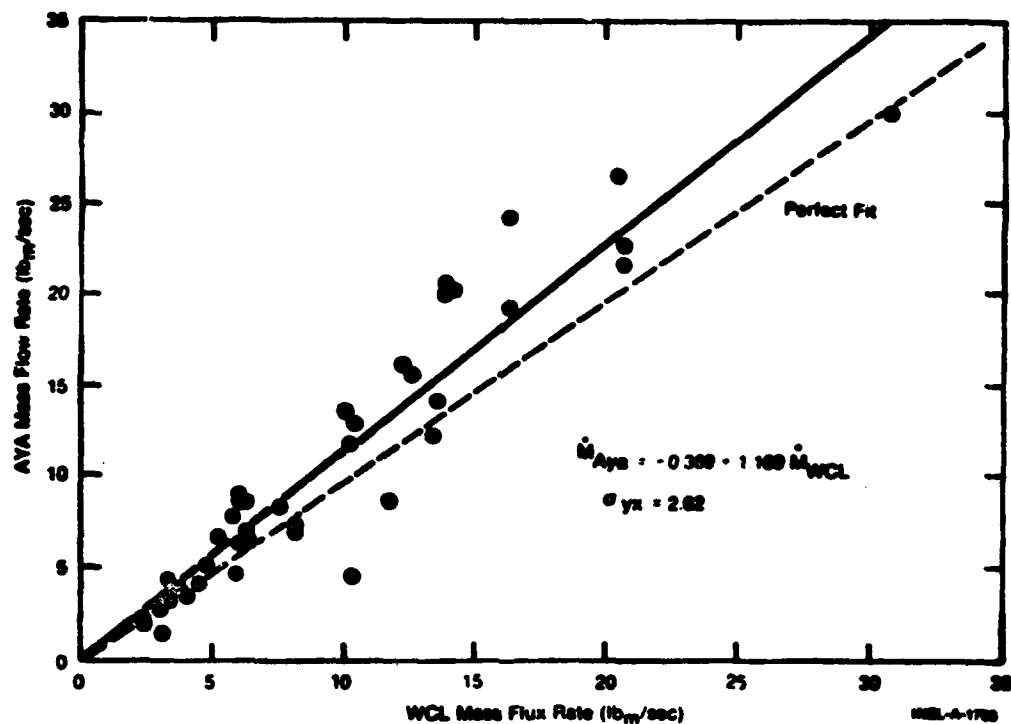


Fig. 8 Predicted versus experimental mass flow rate from the Aya model.

respectively. The data from these figures and from the full flow tests are summarized in Table II.

## TABLE II

RESULTS FROM THE THREE TURBINE MODELS
FORWARD FLOW WITH DRAG-DISC UPSTREAM

| Model | $C_0$ [a] | $C_1$ [a] | Test Configuration | $\sigma_{yx}$ [b] | e, % = $\dfrac{2\sigma_{yx} \times 100}{30.6}$ [c] |
|---|---|---|---|---|---|
| Rouhani | - 0.186 | 1.215 | Free Field | 3.02 | 9.9 |
| Volumetric Flow | - 0.648 | 1.033 | Free Field | 1.93 | 6.3 |
| Aya | - 0.369 | 1.169 | Free Field | 2.62 | 8.6 |
| Rouhani | 0.033 | 0.913 | Full Flow | 0.216 | --- |
| Volumetric FLow | - 0.028 | 0.761 | Full FLow | 0.311 | --- |
| Aya | 0.036 | 0.870 | Full Flow | 0.198 | --- |

[a] $\dot{m}_{model} = C_0 + C_1 \dot{m}_{MCL}$, lbm/sec

[b] The estimated standard deviation of y on x is $\sigma_{yx}$.

[c] The quantity 30.6 is the maximum flow rate for the free field tests.

For the free field tests, the agreement between the predicted and measured mass flow rates is surprisingly good for all three models. However, the mass flow rate predicted from the volumetric flow model agrees best with the experimentally measured mass flow rate. This is evidenced by the closeness of the $C_1$ coefficient to 1.0 and the smallness of $\sigma_{yx}$.

For the full flow tests, Aya's and Rouhani's models agree with each other very closely and both agree better with the experimental data than does the volumetric flow model.

I.5-141

An examination of the results shows that for the free field the errors in mass flow rate are ±9.9, ±6.3, and ±8.6% of test range for the Rouhani, volumetric flow, and Aya models, respectively

## 8. CONCLUSIONS

The three turbine models all predict mass flow rates which are in surprisingly good agreement with the measured rates. For the purposes of the LOFT experiments, the free field tests are more representative. For these tests, best results were obtained using the volumetric flow model.

Presently, work is continuing with the models. From preliminary data it appears that the Rouhani and Aya models correlate the liquid velocity and steam velocity better than the volumetric flow model.

Linear extrapolation of the predicted mass flow data from the WCL to LOFT size piping indicates that large errors may occur.

From the above it is seen that none of the models appear to be significantly more accurate than the others and that caution should be utilized in applying the turbine models to large pipes.

## 9. REFERENCES

1.  S. Silverman, LOFT Drag Disk Turbine Uncertainty Analysis, Supplement No. 13 to LTR 141-39, EG&G Idaho, Inc. (November 1975).

2.  I. Aya, A Model to Calculate Mass Flow Rates and Other Quantities of Two Phase Flow in a Pipe with a Densitometer, a Drag Disc, and a Turbine Meter, ORNL TM-47591 (November 1975).

3.  Z. Rouhani, <u>Application of the Turbine Type Flowmeters in the Measurement of Steam Quality and Void</u>, Symposium on In-Core Instrumentation, Oslo (June 15-19, 1964), Paper D-6, p 3, (CONF-640607) Institute for Atomerergi, Halden, Norway.

4.  S. Silverman, <u>Principles of Operation and Data Reduction Techniques for the LOFT Drag Disc Turbine Transducer</u>, TREE-1109, EG&G Idaho, Inc. (February 1977).

5.  H. W. Heiselmann, A. E. Arave, L. D. Goodrich, L. C. Worley, <u>Design, Development, and Testing Status of the LOFT Drag Disk Turbine Transducer</u>, Aeroject Nuclear Company, LTR 141-14, (August 1974).

6.  M. M. El-Wakil, <u>Nuclear Heat Transport</u>, Scranton, PA: International Textbook, (1971).

7.  <u>1967 ASME Steam Tables</u>, American Society of Mechanical Engineers, Second Edition, New York.

8.  J. R. S. Thom, "Prediction of Pressure Drop During Forced Circulation Boiling of Water," <u>INT. J. Heat Mass Transfer, 7</u> (1964), pp 709-724.

## SURVEY OF FACILITIES FOR TWO-PHASE FLOW INSTRUMENT TESTING

1.  **Categories of Two-Phase Flow Instrument Tests**

    A limited review is being conducted of facilities, in the United States and abroad, which have capabilities for testing the flow instruments used in water reactor safety experiments. Such experiments require flow instruments which determine the mass flows of each fluid phase (steam and water) and a flow regime characterizing variable, such as void fraction. Because mass storage effects are significant, flow instruments are required at several locations in a typical safety experiment. At each location, a number of measurements of differing principle must be made to define the mass flows and void fraction; the number corresponds to the number of unknowns. Thus, a flow "instrument" which is to be tested, may actually consist of several measuring devices, from which individual phase mass flows and regime can be inferred.

    Testing such instruments requires facilities have a variety of characteristics. The variety derives from the scope of the tests needed to develop and calibrate a flow instrument. The tests are as follows:

    a.  **Conventional Calibration Tests**

        All of the individual measurement devices making up a flow instrument, whether the instrument is the first of a kind or a follow-on unit, must be subjected to limited (conventional) calibration testing. These "production calibration" tests establish the "meter factors" of the measurement devices by observing the response under flow conditions where the nature of the response is well understood (usually single phase flow). Separate tests in both gas and liquid phases may be necessary to characterize a device fully. For example, large liquid phase flows may be needed to achieve rated momentum flux while small gas phase flows may be needed to characterize minimum velocity measuring capability (turn-down). "Meter factors" established in this manner are used as parameters in the equations which model the responses in two-phase flow.

        In addition to measuring meter factors, conventional calibration tests are needed to check the repeatability, linearity, and accuracy of each sensing device manufactured.

1.6-1

In order to combine outputs of measuring devices to calculate the parameters of two-phase flow in engineering units, an analytical or, possibly, an empirical model of the response of each measuring device in two-phase flow is essential. Usually, a plausible model can be postulated on theoretical bases. The accuracy of the model must then be examined by an extensive series of tests with a prototype flow instrument. In outline, the test procedure consists of:

(1) Observing the response of the measuring devices of the prototype flow instrument over the full range of hydraulic conditions expected in service.

(2) Calculating phase mass flows and other flow parameters of interest from these responses again, over the full hydraulic range.

(3) Comparing the flow parameters calculated from the  ..    ; of the instrument under test with the same flow param       4e-termined by independent means. The independent r.    ..  are flow measuring standards of known precision for the conditions of measurement. Typically the standards will include measurements of the individual phase flows upstream of a mixing device, since no two-phase flow measurement standard exists.

Correlation tests are of the nature of a calibration test for a prototype instrument under two-phase flow conditions. However, not all of the conditions of the ultimate instrument installation may be duplicated simultaneously (i.e., in a single test). On the contrary, the calibration testing of the prototype instrument will in general require the separation of effects which may alter instrument response, e.g., it is desirable to examine the effect of temperature and hydraulic conditions separately.

Correlation testing may also be used as an adjunct to the design of the instrument itself. For example, an analytical model of an instrument may assume a spatially uniform distribution of phases over the flow cross section (though not necessarily equal velocities). The correlation testing might be used to select a means for homogenizing the flow to obtain spatial uniformity.

The products of correlation testing of prototype instruments are:

(1) An experimentally confirmed mathematical correlation whereby the flow parameters of interest can be calculated from measured instrument responses, for all thermal and hydraulic conditions of the experiment in which the instrument is ultimately to be used.

(2) Quantitative estimates of the uncertainty in the flow parameters, as established via the correlation, for the range of thermal and hydraulic conditions of the experiment.

I.6-2

(3) Quantitative modifiers to individual measuring device calibrations (or "meter factors") for use in two-phase experiments. These modifiers alter calibrations from those measured under the "production calibration" conditions of (a) above and are determined by the correlation testing to be appropriate for the two-phase flow conditions.

c. **Mechanical Development and Proof Testing**

In addition to providing interpretable outputs under the thermal and hydraulic conditions of the experiments in which they are used, flow instruments must withstand the mechanical loadings imposed by the experiment and must endure, without malfunction, for a time period determined by the length of the experiment and the accessibility of the instruments for maintenance following it. The capability of the instruments to withstand the experimental environment must be demonstrated by testing in facilities which duplicate that environment.

d. **Scaling Tests**

Calibration and correlation tests normally require that all of the flow be directed through the measuring instrument. This procedure minimizes uncertainties when the flow parameters computed by the instrument are compared against those determined via the standards. The intended use of the flow instrument, however, may involve only the sampling of a large flow field with a small instrument (as with the LOFT drag disc turbine transducer). Testing may be required to establish procedures whereby the phase flows sampled by the instrument can be extrapolated to infer phase flows for the pipe as a whole. The product of such tests is a set of scaling factors for the instrument-computed local flows, and/or a quantitative estimate of the uncertainties in the total flows inferred from small samples. Additionally, the physical location of a flow-sampling instrument could be selected in a scaling test.

Another form of scaling test could arise, if a small model flowmeter were built for correlation testing, but a larger version of the same meter were intended for the safety experiment. In this situation, full scale single-phase (production) calibration testing would undoubtedly be necessary.

e. **Transient Tests**

Many of the water reactor safety experiments which require two-phase flow instruments are of a transient nature -- flow changes, sometimes rapid, are inherent in the experiment. For this reason,

I.6-3

an understanding is needed of the factors affecting the transient responses of the devices making up the flow instrument. This knowledge can, in certain instances, be used to infer actual flows more accurately from instrument indications; in others, the uncertainties associated with the transient measurement can be bounded.

An understanding of instrument transient response requires a dynamic model for each element. The objectives of transient tests are:

(1)  To confirm the form of the model.

(2)  To determine the numerical value of certain constants of the model which are operative only in transient (e.g., effective rotary inertia of a flow turbine).

## 2.  Facility Requirements

Facility requirements depend on the specific category of a test to be performed; no single facility is likely to satisfy the requirements of all categories. Also it does not appear that one, unique unalterable set of facilities must be found; there will generally be several combinations of facilities capable of filling testing requirements. For example, it appears desirable to do much of the correlation and prototype calibration testing in gas/water loops, but some of this testing might be done (albeit with more difficulty) in a well designed steam water loop.

The types and characteristics of facilities which can satisfy the requirements of each testing category are outlined below:

### a.  Conventional Calibration Test Facilities

A water loop and a separate gas loop are needed to exercise an instrument over the full range of velocities, mixture densities, and momentum fluxes it may see in service. The experimental set up should be full flow; that is, the fluid flowing through the instrument should have passed entirely through the standards against which the instrument is compared. The capability to determine quantitatively the effects of temperature on instrument calibration is also needed; this can be obtained if the water loop can be operated at temperatures up to the maximum expected in service. Standards against which the measuring devices are compared should be of high quality (absolute accuracy better than $\pm$ 1%) and traceable to NBS, to reduce insofar as possible the uncertainties due to this source. Some or all of the production test facilities might be located at the instrument manufacturer.

I.6-4

## b. Correlation (Prototype Calibration) Test Facilities

As has been indicated, the separation of temperature from hydraulic effects makes desirable the use of gas/water loops in developing calibrations of a set of measuring devices in two-phase flow. To duplicate hydraulic phenomena fully, the following characteristics are needed in gas/water calibration loops:

(1) The ability to generate, simultaneously, phase velocities and qualities which duplicate those expected in service. The locus of velocities and qualities will depend, of course, on the expected instrument location. A limiting example for a LOFT broken loop is shown in Figure 1. In this figure, the ordinate is the approximate velocity of each phase. (In the broken loop, phase velocities are expected to remain nearly equal throughout the blowdown, because of the high velocity of the dominant phase.)

(2) The ability to generate, simultaneously, momentum fluxes and qualities similar to those expected in service. As with velocity, this locus will depend on specifics of instrument location and experiment; a limiting example for a LOFT broken loop is shown in this figure. In this figure, one ordinate is void fraction-weighted momentum flux

$$[\overline{\rho V}^2 = \alpha \rho_G V_G^2 + (1-\alpha) \rho_L V_L^2]$$

This parameter is believed to govern the response of drag-measuring devices in two-phase flow. A second ordinate is the void fraction, which with quality, is necessary to characterize the two-phase mixture spatially.

These capabilities infer the selection of a gas with a density ratio relative to water similar to that which will be encountered in service. While useful testing can be accomplished with air water mixtures at pressures near atmospheric, full range coverage requires pressurization to about 30 atmospheres, or, alternatively, use of a heavier gas.

The use of a gas such as air, rather than steam for this phase of testing does not only derive from the need to separate temperature-induced effects. It also permits a visual examination of the flow regime seen by the instrument since pipe walls can be made transparent. This examination may be useful not only in characterizing instrument response as a function of regime, but also in determining the effectiveness of homogenizing devices in obtaining a spatially uniform phase distribution. A homogenizer is often necessary to a repeatable and predictable instrument response, and is an important part of instrument development.

Depending on the ultimate application of the instrument, capability
to mock-up hydraulic conditions may be necessary. If the instrument
under test is intended for an experiment in which it measures full flow,
then duplication of bends and other hydraulic features, upstream and
immediately downstream, is necessary to ensure that the distortions
of velocity and void fraction profiles which these features will bring
about in service are duplicated in the calibration. Duplication of
gravitational forces may also be important in some two-phase flow
situations. This requires that:

(1) Bends and other hydraulic features, as well as the flow element
    itself, be oriented relative to the earth's surface as they will be
    in the experiment,

(2) Scaling of the instruments and hydraulics be full; extrapolation of
    the two dominant flow field forces, inertial and gravitational, to
    another scale requires preservation of the Froude number, but
    maintaining Froude number is not consistent with maintaining
    fluid velocity and momentum flux up to the ratings of the sensing
    instruments.

The impact of temperature on the calibration of many flow instruments
is, generally speaking, the result of changes in instrument dimensions
owing to thermal expansion of individual parts and of the instrument as
a whole. Calibrations of readout devices, particularly strain gages,can
also be affected by temperature. In these situations, the evaluation of
temperature effects can be carried out in single-phase fluid, operating
over the temperature range of interest.

If, however, the physical phenomena  to which a measuring element
responds is sensitive to temperature, testing in two phases at elevated
temperature may be necessary. In any case, elevated temperature
tests in two phases can be a desirable confirmatory adjunct to other
calibration testing. Such tests might be performed in conjunction with
mechanical tests discussed in the next paragraph.

c.  Mechanical Development and Proof Testing Facilities

Obviously, tests carried out for purposes of calibration (categories a
and b, above) also serve to a degree, to test the capability of an in-
strument to withstand the mechanical loadings to which it will be sub-
jected. However, conclusive proof testing requires the simultaneous
imposition of mechanical loads and thermal effects. This leads to
the requirement that final proof testing be carried out in a facility
capable of supplying steam water mixtures at pressures, temperatures,
flows and qualities spanning the expected service range. The capability
for mixed phases is particularly important, since the random, rapid
variations in void/liquid distributions characteristic of steam water

I.6-6

mixtures can result in very severe vibratory loads on bearings and other mechanical parts. As with calibration tests, mechanical proof tests require the facility to supply phase velocities and momentum fluxes up to the maximum capacity of the instrument, but not more. If an instrument samples a flow field (as does the LOFT DTT), this means that proof testing could be accomplished in a facility with the capability to supply that fraction of the total mass and volume fluxes seen by the instrument itself. It is considered that the mechanical design of the supporting strut for such an instrument can be made sufficiently conservative to eliminate the need for testing in a two-phase facility (though such tests would remain desirable).

d. **Scaling Test Facilities**

If a small flow instrument is used to measure a large flow field (as in LOFT), scaling tests may be desirable. The principle questions to be answered by such scaling tests relate to the interplay of inertial and gravitational forces on the phase velocity profiles and on the distribution of voids [for most water reactor experiments viscous forces are believed to play a minor role]. Many of these questions are best answered visually -- by high speed photography or similar techniques. The force field and the ability to measure it can best be achieved by a large scale gas/water facility (as opposed to a steam water facility). In addition, detailed void maps and other flow field information may be obtainable by laser or hot wire anemometry, minature conductivity probes and similar instruments, all of which can be readily applied in gas/water experiments but are difficult to use in steam and water.

The scaling test facility must have the capability of operating with gas/water density ratios similar to those expected in the safety experiment. It must also be adaptable with respect to hydraulic geometry; individual tests duplicating the hydraulics of each instrument location may be needed.

Although some measurements of individual phase flows prior to mixing are necessary to ensure the conditions of the experiment have been duplicated, great precision in these measurements is probably unnecessary. Operation of the flow instrument itself in the scaling experiment while desirable may not be necessary.

e. **Transient Test Facilities**

Because of the time response of the measuring devices is likely to be a function of void fraction, the transient test facility must be capable of operating with mixed (two-phase) flows. Again a gas/water facility appears better able to satisfy requirements than a steam-water facility The capacity of the facility should be sufficient to supply maximum gas and liquid phase flows to the flow instrument, proper. (Transient testing of a sampling type of instrument in a full size pipe is not considered necessary.) A key feature of a transient test facility is the

I.6-7

ability to generate rapid changes in the rate of flow of either phase. Theoretical determination of instrument responses to step flow changes is usually straightforward; it is accordingly desirable to measure responses in experiments which come close to duplicating steps. Furthermore, accurate determination of instrument response means that one must measure the flow disturbance with a standard much more rapid than the instrument. But the responses of the measuring devices making up the instrument may be extremely rapid -- a few milliseconds, and finding standards sufficiently fast will be difficult. Consequently, the most feasible way to produce a known, rapid flow change is by means of a quick acting valve. The fluid system arrangement must be such that the change in phase flow does not necessarily proceed to a zero final value; instrument response characteristics may be sensitive to initial and final phase flow values.

3. **Facility Survey (Preliminary Status)**

The approach to the survey of facilities is to:

(a) Identify by literature search and other means, candidate facilities for various test categories.

(b) By telephone conversation, establish a preliminary set of facility characteristics including:

 (1) Willingness to do "contract calibration" work, contractual requirements, and costing rates.

 (2) Fluids employed [e.g., gas, water, gas/water, steam, steam/water]

 (3) Maximum operating pressure and temperature

 (4) Nominal size of loop and materials of construction

 (5) Maximum capacities of loop in terms of phase mass flow rates, velocities, and apparent momentum flux, versus quality

 (6) Type and accuracy of standards including turn-down range

 (7) Interface requirements between the device under test and the loop (e.g., acceptable methods of closure, support facilities available)

 (8) Schedule lead time and notification requirements

 (9) Capability to change hydraulic geometry; cost and schedular impact of such changes

I.6-8

(10) Capability to construct ad hoc hydraulic models (e.g., reactor vessel outlet plenum and nozzles)

(c) In selected cases confirm facility characteristics and capabilities by visit or other contact.

Most of the work under item (a), above has been completed, and work under item (b) has begun. Preliminary results of the survey are shown in the matrix of figure 3, which defines, in qualitiative terms, the types of facility best suited for each category of instrument test. Also shown are the names of facilities which have been identified as possessing some or all of the characteristics required. All of the needs of a particular category may not be filled by the indicated facility; if however, it appears that a significant fraction of the designated testing can be accomplished, the facility has been included. For example, the ability of the ORNL and INEL air water loops to operate at elevated pressure is believed limited; nonetheless, these loops may be useful (and in the case of the ORNL loop, have been useful) in development of instrument correlations and two-phase calibrations. From the preliminary information concerning the facilities on the matrix of requirements, the following tentative conclusions may be drawn:

(1) There have not been a large number of (single phase) gas loops identified. This need is however not considered crucial, since generally the gas/water loops of the 4th row can be operated in a single phase mode. Also, it is believed that additional facilities not yet identified may exist (used in calibration of meters for gas pipelines).

(2) The ability to operate existing small gas/water loops at high pressure appears limited; this is a significant gap in two-phase calibration capabilities.

(3) No large size gas/water loops, suitable for scaling studies have been identified. This may be a significant deficiency for programs such as LOFT.

(4) There are no obvious requirements for large scale steam/water loops, though such loops might in some instances be used in scaling tests. (If this is done, however, instrumenting will be difficult, expenses high, and results more limited than a comparable test in air/water.)

An argument might be advanced in favor of large steam/water loops to the effect that they constitute final "proof-of-the-pudding" calibration of the two-phase instrument. Because of profile effects, however, such calibrations are of little real use, unless upstream and downstream hydraulic geometry is duplicated. In effect, the calibration facility will come to resemble the safety experiment itself. A more effective final test of the instrument is considered to be accomplished in the safety experiment. Here the instrument can be checked against others of similar types if redundancy in instrumenting is employed, and by mass balances using fluid level and other instruments.
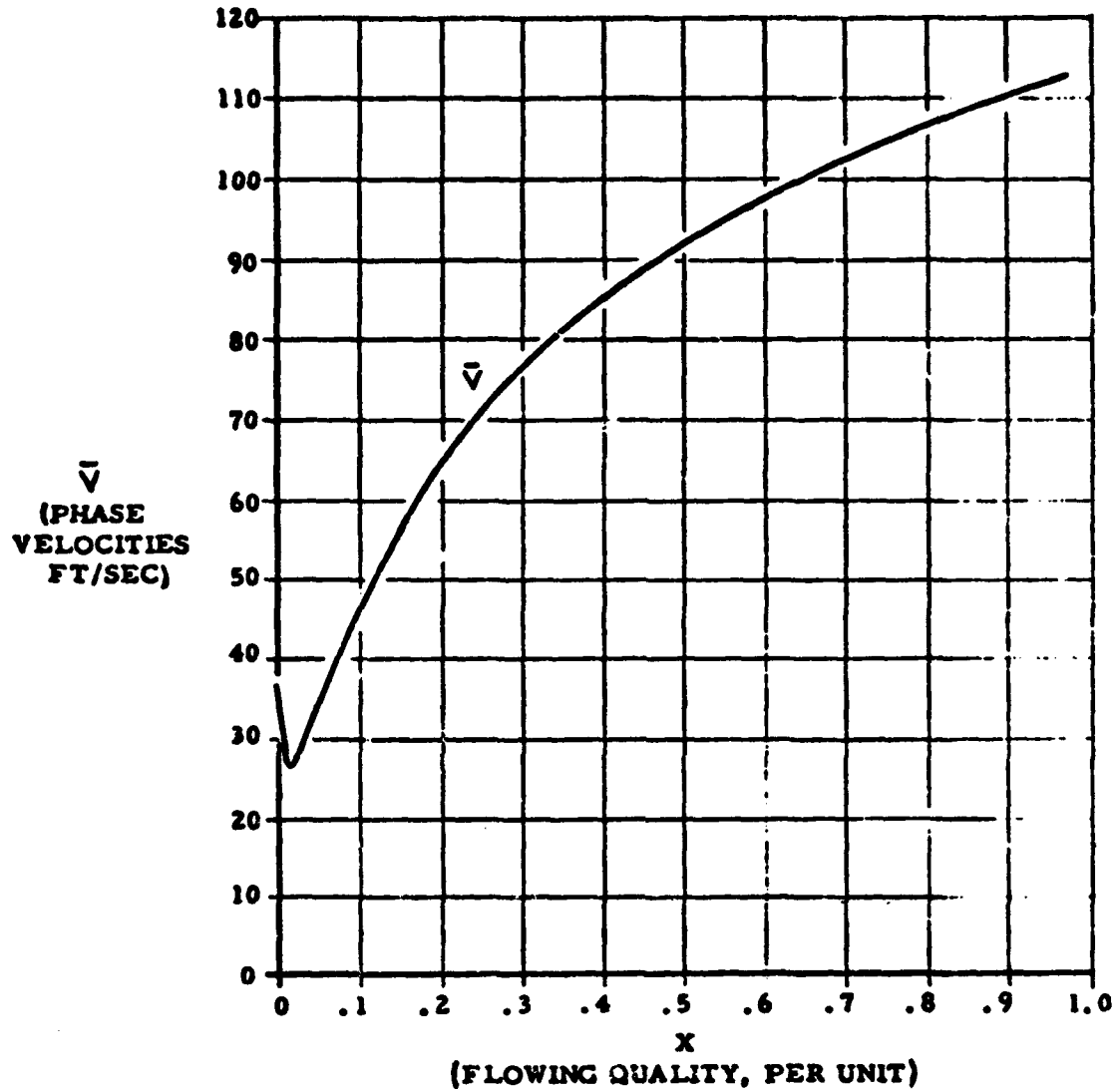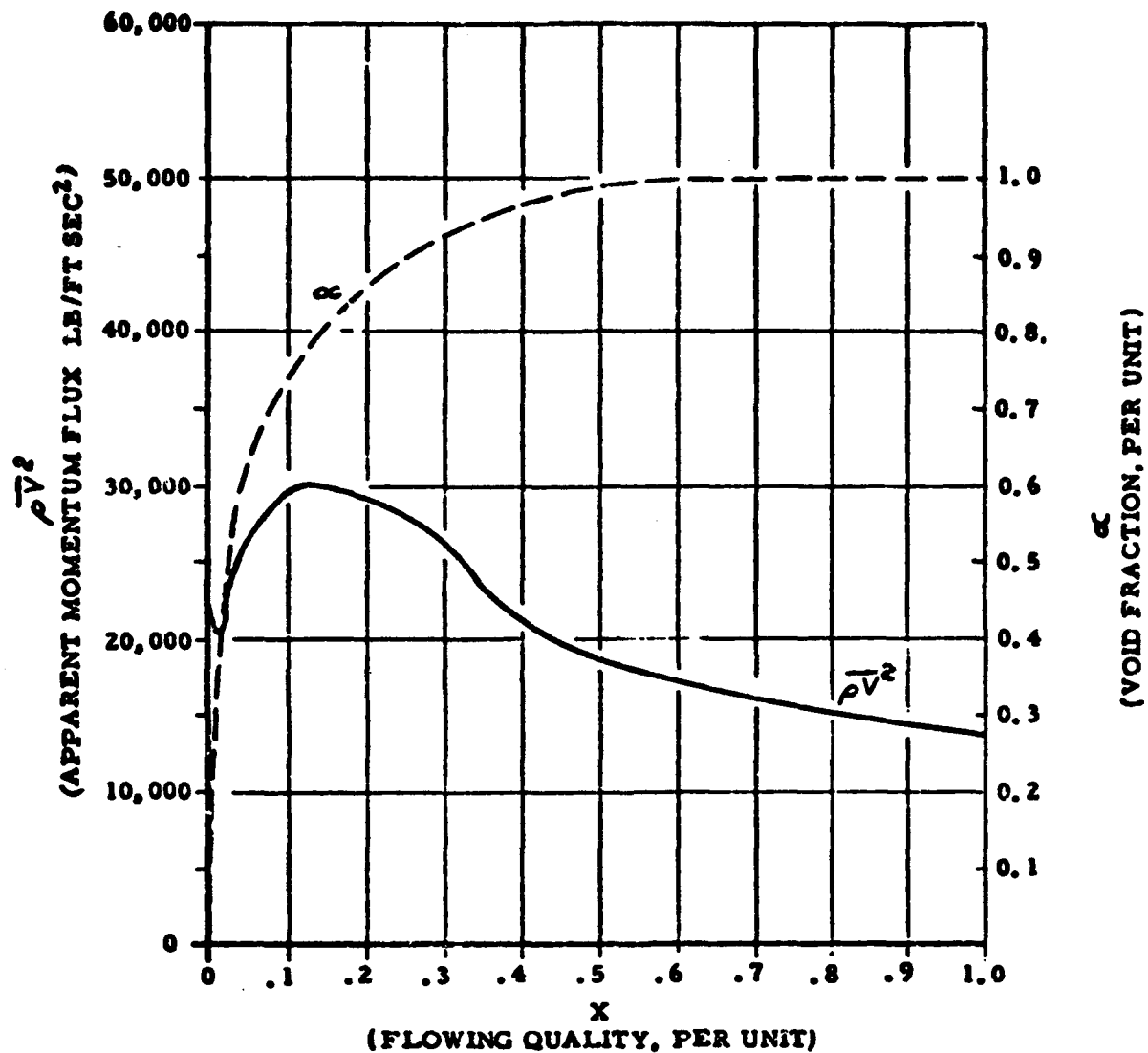
APPROXIMATE VELOCITY REQUIREMENTS
COLD LEG BREAK
BROKEN LEG LOCATION

FIGURE 1

I.6-10

$\bullet \ X = \dot{M}_G / (\dot{M}_G + \dot{M}_L)$

$\bullet \ \overline{\rho V^2} = \alpha \rho_G V_G^2 + (1-\alpha) \rho_L V_L^2$

APPROXIMATE APPARENT MOMENTUM FLUX REQUIREMENTS
COLD LEG BREAK
BROKEN LEG LOCATION

FIGURE 2

I.6-11

FIGURE 3

Calibration Facility Matrix

| Required Facility | a. Conventional Calibration | b. Correlative Development Prototype Calibration | c. Mechanical Proof Tests | d. Scaling Tests | e. Transient Tests | Candidate Facilities |
|---|---|---|---|---|---|---|
| Small[1], low temperature water | required | | | | | Numerous, (e.g., Alden Lab, Wyle, Daniel, Foxboro, BIF) |
| Small, low pressure gas | required | | | | | Colorado Engrg Exp Station |
| Small, high temperature water | required | required | | | | Columbia U; Exxon, Richland; CE |
| Small, high pressure[2] gas/water | | required | optional | required[4] | required[5] | GE, San Jose; ORNL; INEL; Karlsruhe; Whiteshell, AECL |
| Small, high pressure/ temperature steam/ water[3] | | optional | required | | | Karlsruhe; W Canada; CE; ISPRA; AECL Dry Lab |
| Large, high pressure gas/water | | | optional[4] | required[4] | | |
| Large, high pressure/ temperature steam/ water | | | | optional[4] | | B&W Alliance; GE San Jose; CISE |

NOTES:
(1) Small loops are defined as less than 6 inches in nominal diameter.
(2) Pressure capability to 30 atm desired.
(3) Pressure/temperature capability to 1800 psi/620° F desired.
(4) Applicable only to "sampling" flow instruments.
(5) Quick acting valves or other transient inducing capabilities required.